MUD VOLCANOES AND THE BEHAVIOUR OF OVERPRESSURED CLAYS AND SILTS

by

Najwa A. Yassir

A thesis submitted to the University of London for the Degree of Doctor of Philosophy in Geological Sciences

March, 1989

Department of Geological Sciences,
University College London,
Gower St.,
London WC1E 6BT,
U. K.

To Palestine

ABSTRACT

Mud volcanoes are a poorly understood phenomenon whereby overpressured, fine-grained sediments extrude to the surface from depths of up to several kilometres. They are observed worldwide, usually in areas of tectonic compression and thick, rapidly-deposited sedimentary sequences. This research is aimed at achieving a better understanding of the type of sediment behaviour leading to mud volcanoes. The study combines a geological investigation of the origin of mud volcanoes with a geotechnical investigation of their behaviour.

As part of the geological study, the mud volcano examples around the world are described, and possible mechanisms of overpressuring and extrusion are investigated. Particular attention is paid to the field description and the subsurface geology of the mud volcano areas visited in South Trinidad and Southwest Taiwan. The results of laboratory analyses on the muds sampled in the field, mineralogy, particle size and shapes, Atterberg limits and, where possible, micropalaeontology, are presented. These are aimed at understanding the origin of the clay and establishing any characteristics unique to mud volcanoes.

The geotechnical investigation concentrates on the undrained shear behaviour of mud volcano clays, which originate in an environment where thick, low permeability sedimentary sequences are subjected to tectonic compression. The experiments were conducted in a high pressure triaxial cell, using confining pressures of 5 to 50 MPa. Particular attention is paid to the effects of consolidation path, stress magnitude and material properties on the behaviour of mud volcano clays.

The results of the experiments are discussed in the light of the geological study, and equivalent testing results from low pressure soil mechanics studies. The discussion concentrates on the role of tectonic activity in the formation of mud volcanoes.

ACKNOWLEDGEMENTS

I would like to thank all the people who have helped me in my three years of research. It is impossible to name them all, but the following deserve particular mention.

Of the many individuals who have given me good support and advice, I would like to thank Dr. H. Shaw, and Mr. R. Giddens, Geology Department, Imperial College London; Professor D. Brunsden, Geography Department, King's College London; Dr. A. Barber, Geology Department, New College, London; Drs. N. Kenyon and R. Belderson, Institute of Oceanographic Sciences, and Drs. R. Channon and S. Hall, B.P., U.K. Harry Shaw has given me very good advice on mineralogical aspects of my research and has allowed me access to departmental facilities such as the Scanning Electron Microscope, and Denys Brunsden bravely attempted to cross treacherous country to visit the New Zealand mud volcanoes. I thank both.

My sincerest thanks to those who have assisted me directly in my study areas, Taiwan and Trinidad. In Taiwan, these include Professor C. Ho, Professor, Dr. J. Chou and Professor S. Wang; Professor Wang was kind enough to take me to the mud volcano area in southwest Taiwan. I am grateful to my Chinese colleagues for their kind hospitality.

I am also indebted to the Trinidad oil company geologists, who allowed me access to some company data and provided me with field assistants to the mud volcano areas. The companies include Trinidad and Tobago Oil Co. Ltd. (TRINTOC), who kindly covered the cost of shipping my samples back from Trinidad, Trinidad Marine Operations (TRINMAR) and Trinidad and Tobago Petroleum Co. Ltd. (TRINTOPEC). I would particularly like to thank the following people for their help: Mr. W. Bertrand, Mr. B. Carr- Brown, Ms. K. Merrick and Mr. W. Sumadh (TRINTOC); Mr. K. Birchwood, Dr. J. Frampton and Mr. W. Ali (TRINMAR); and Mr. M. Lutchman, Mr. H. Marcus and Ms. C. Telemaque (TRINTOPEC). Also, my thanks to the Ministry of Energy and to Mr. G. Rohr, Amoco Trinidad Oil Co. for the assistance offered. Particular mention should be made to John Frampton and Barry Carr-Brown whose hospitality and help made my trip to Trinidad both enjoyable and productive. John is duly acknowledged for welcoming an extremely muddy geologist into his home! Finally, I would like to thank two of the pioneer workers on sedimentary volcanism in Trinidad, Mr. J. Saunders, Natural History Museum, Basel, and Mr. G. Higgins for their help. George Higgins paved the way for my visit to Trinidad, and continued to give me valuable advice on my work.

Part of my research was undertaken at the Soil Mechanics Laboratory, Imperial College London. My special thanks go to the technical staff, Steve Ackerley, Alan Bolsher, Eileen Gibbs, Roger Hare, Graham Keefe, and Lou Spall, and the section secretary, Cathy Evans. I am particularly grateful to Lou Spall and Steve Ackerley for their continuous help and support, especially in times of a crisis, which were very frequent! My fellow researchers at the Soils Laboratory have proved to be good friends and teachers. They have all been bombarded at one time or another with one of my obvious questions;

their patience with me has been admirable. Many thanks to Andrew Bond, Luiz Bressani, Mike Crilly, Robert Day, George Dounias, Dave French, Teta Georgiannou, Jan Hellings, Barry Lehane, Mahmoud Mahmoud, Chris Menkiti, Dalmas Nyaoro, Nicholas Ninis, Efrain Ovando-Shelley, Andrew Ridley, Denys Schreiner, Satoru Shibuya, Phil Smith, Theodora Tika and Dave Toll. Luiz Bressani and Dave Toll deserve particular mention for solving my never-ending computing problems. Dave Toll also set up the datalogging system for me at University College London; thank you!

My time in the Soils Laboratory was a good education and I would like to thank the Head of Section, Professor J. Burland for giving me the opportunity to work there. Special thanks also go to the academic staff, Dr. R. Chandler, Professor J. Hutchinson, Dr. R. Jardine, Dr. S. Leroueil (visiting academic from University of Laval), Dr. D. Potts, Professor A. Skempton, and particularly Dr. A. Skinner and Professor P. Vaughan for their illuminating discussions.

The main part of my research was undertaken at the Department of Geological Sciences, University College London. I would particularly like to thank the technical staff there for doing "last minute" jobs for me; these include John Bowles, Jim Davy, Ron Dudman, Mike Gray, Sean Houlding, Tony Osborn and Peter Woods. Thanks also to the Head of Department, Professor M. Audley-Charles, and Dr. J. Milsom for sparking off my interest in mud volcanoes. The crystallography and micropalaeontology groups kindly gave me access to their facilities. Professor Banner in micropalaeontology also analysed a number of Trinidad mud volcano samples for microfossils. I am very grateful to them. Steve Kaye and Ron Harris sampled mud volcano clays for me from areas I was not able to visit and their help is duly acknowledged.

I would also like to thank my friends Khaled Kamhawi, Civil Engineering Department, UCL, Zeinab Othman, Bartlet School of Architecture, UCL, Ann Leddra and Melina Xenakis-Axiotis for their help and support.

My friends and colleagues at the Reservoir Dynamics Laboratory, UCL, deserve special mention in these acknowledgements, because without them, none of this work would have been possible. Tony Addis patiently taught me the "rudiments" of high pressure soil mechanics testing and has given me useful help and advice throughout my research. He is also responsible for deleting numerous brackets in the text. Hongey Chen introduced the group to his beautiful country, Taiwan, and provided me with the opportunity to visit the mud volcanoes there. Tony Goldsmith patiently assembled the high pressure triaxial apparatus for my use, and was always helpful during machine breakdowns and leaks; Tony has saved me months of labour and I am very grateful to him. Mike Leddra has been a good friend and support throughout my university years, despite his occasional lapses into vintage aircraft jargon.

I would like to thank my supervisor, Dr. Mervyn Jones for his help and advice during my research; it was he who encouraged me to approach the subject of sedimentary volcanism from a geotechnical point of view and this has proved to be a very challenging prospect.

Last, but not least, I wish to express my gratitude to my dear family, Salma, Nada and Alia, and especially my parents, for their love and support. I cannot thank them enough.

LIST OF CONTENTS

LIST OF TABLES

LIST OF FIGURES

LIST OF PLATES

CHAPTER 1

INTRODUCTION

"Buried rocks saturated with gas, oil or water under pressure carry a latent energy capable of producing geological phenomena similar to those caused by magmatic intrusions and eruptions."

Kugler (1933)

Plate 1.1 Lagon Bouffe mud volcano, Trinidad

1.1. BACKGROUND

In 1931, the Waimata Valley mud volcano in New Zealand erupted, extruding 150,000 metric tons of mud (Strong, 1931). In 1936, the Sayncha mud volcano in the Apsheron Peninsula, USSR, extruded 100,000 m^3 of mud; this covered an the area of 112 ha, reaching a maximum thickness of about 60m (Jakubov et al, 1976). In 1964, an island appeared off the southern coast of Trinidad, reaching a height of 2m above sea level in two days. The Chatham Island mud volcano, as it was called, was estimated at 255,000m^3 of mud and rock (Higgins and Saunders, 1964). Although not always so spectacular, this type of phenomenon is widespread, occurring in areas such as Azerbaijan, U.S.S.R. (Jakubov et al, 1976), Greenland (Henderson, 1976), Italy (Higgins and Saunders, 1974), New Zealand (Ridd, 1970), Timor (Barber et al, 1986), Tanimbar (Kaye, pers. comm., 1987) Malaysia, (McManus and Tate, 1986), Taiwan (Shih, 1967), Trinidad (Higgins and Saunders, 1974), Venezuela (Gansser, 1960), Columbia (Gansser, 1960), and Mexico (Humphrey, 1963), (fig. 1.1; see also table 1.2 below).

Some of the earliest known research on the subject was undertaken in Trinidad by Lavaysee (1813) who assumed an igneous origin for the "volcanoes" there. However, in the early twentieth century, with the advent of oil exploration, the igneous origin was generally ruled out in favour of a sedimentary origin. One of the best known early researchers in this field is Kugler (1933, 1965, 1978), who coined the term "sedimentary volcanism" for these features. Today, several types of sedimentary volcanism are recognised, the most important being mud volcanoes, shale/mud diapirs, and mud lumps; these range in scale from a few centimetres to several kilometres across.

The phenomenon of sedimentary volcanism is usually associated with thick overpressured argillaceous sequences, found in both tectonically active areas such as accretionary complexes and in tectonically passive areas such as major river deltas. Although sedimentary volcanism is more common in the former type of environment, it is also observed in the latter (table 1.1). Sedimentary volcanism is also occasionally found in association with areas of volcanic activity such as Lake City Hot Springs, California (White, 1955; table 1.1).

ENVIRONMENT	MUD VOLCANOES	MUD/SHALE DIAPIRS	MUDLUMPS	SAND VOLCANOES	SAND DYKES
Passive Tectonic	shallow	deep	shallow	shallow	-
Active Tectonic	deep	deep	-	?	shallow
Volcanic	shallow	-	-	-	-
shallow = near-surface up to a few hundred metres; ductile overburden. deep = generally 500m - 5000m; brittle overburden.					

Table 1.1. Types of Sedimentary Volcanism in Different Environments

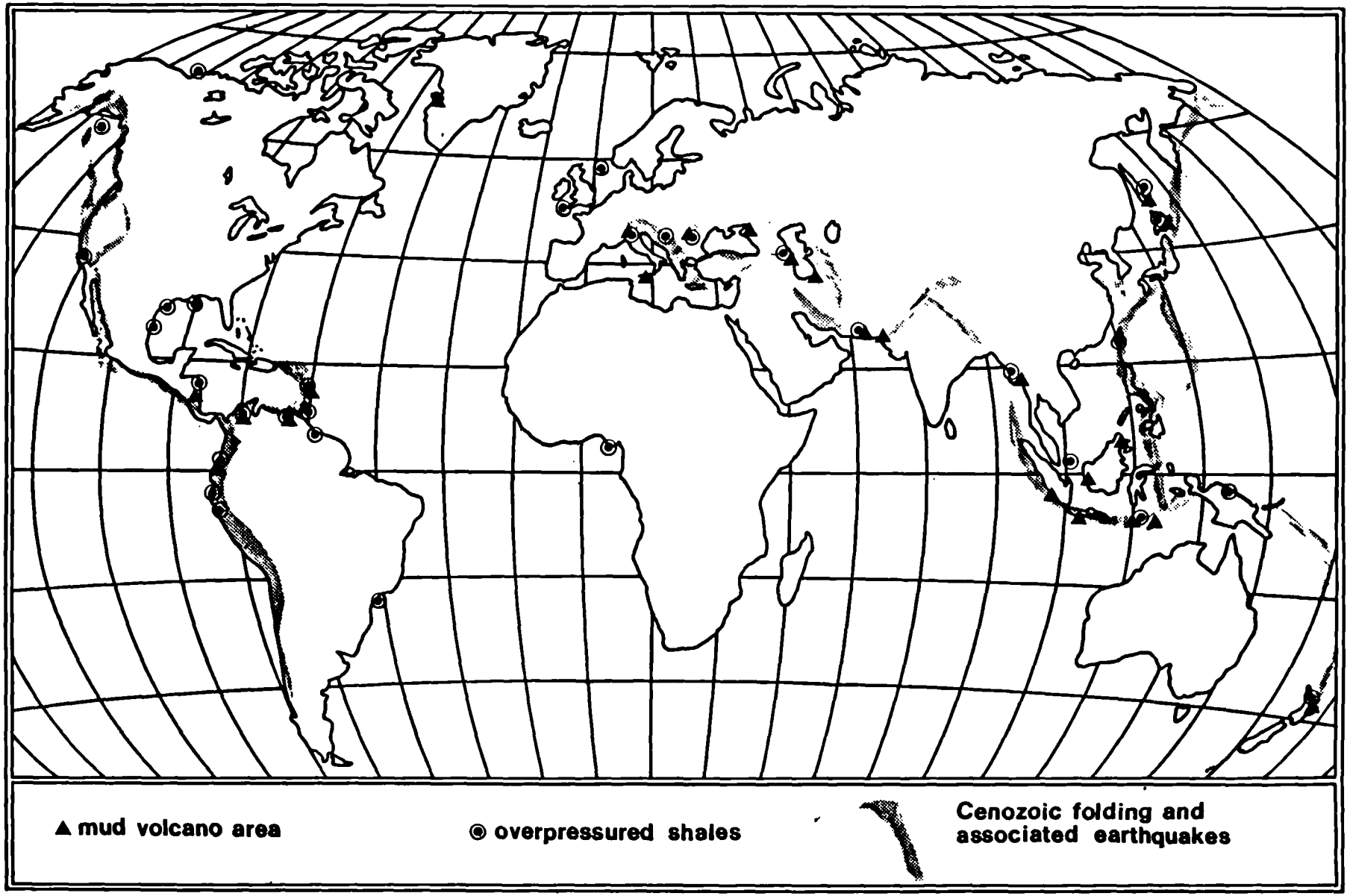

Fig. 1.1 Map of mud volcano occurrences, overpressured shales and Cenozoic fold belts (compiled from Higgins and Saunders, 1974; Shih, 1965 and Fertl, 1976 - see also Chapters 1 and 2).

What, then, is this "latent energy" referred to by Kugler (1933) which produces sedimentary volcanism? Opinions differ, particularly on the driving forces responsible for the deep- seated examples (table 1.1), varying from dynamic causes, like subsurface gas under pressure and tectonic activity, to passive processes like density inversion. Despite the fact that a great deal of research has been undertaken on the subject of sedimentary volcanism, very little is known of the mechanical behaviour of the sediments undergoing this type of deformation. Sedimentary volcanism is not only an important process of sedimentation active today, it also provides vital clues about the deformation of sediments at depth.

This study will be chiefly concerned with the origin of deep-seated sedimentary volcanism from both a geological and a geotechnical point of view, with particular reference to mud volcanoes. Mud volcanoes from the islands of Trinidad and Taiwan were studied in the field and sampled for further laboratory work. Before the objectives of this research are more fully explained, a brief description of the main features of mud volcanoes will be presented to give the reader an introduction to the nature of the phenomenon being investigated.

1.2. GENERAL FEATURES OF MUD VOLCANOES

The best examples of mud volcano occurrences are found in the areas listed in the previous section (fig. 1.1). These exhibit several distinctive features, listed in table 1.2..

1.2.1. Sedimentology and Stratigraphy

Mud volcanoes are always associated with thick, overpressured, regressive clay sequences (Gansser, 1960; O'Brien, 1968; Chapman, 1974), (fig. 1.1). The clays are of Tertiary age in most areas, including Azerbaijan, Trinidad, Venezuela, Columbia, Taiwan and New Zealand (table 1.2). However, important exceptions are known. Although most of the Azerbaijan mud volcanoes seem to originate from Tertiary clays, some can be traced back to the Cretaceous (Jakubov et al, 1976). Barber et al (1986) date the Timor examples as Permian, disagreeing with the Pliocene age proposed by Audley-Charles (1968).

The source clays are often thought to be of olistostromal origin due to the presence of exotic blocks in the matrix (Audley- Charles, 1968; Higgins and Saunders, 1974; McManus and Tate, 1984). These can be older than the clay. Other workers (eg. Barber et al, 1986; Brown, pers. comm., 1986) believe that the blocks are overburden material incorporated into the mud. The blocks were used by Russian workers (Jakubov et al, 1976) to date the mud volcanoes; this may explain the pre-Tertiary age they ascribe to their examples. Others use the fossils in the matrix (Saunders, pers. comm., 1987; Lin, 1965).

Where the pore pressures in thick regressive Tertiary clay sequences have been measured, they have been found to be abnormally high, i.e. above the hydrostatic gradient (Fertl, 1976; section 2.2). For example, in Trinidad, these pore pressures reach 80% of geostatic load at depths of just over 1km (Chapman, 1983); in North Taiwan, pore pressures again reach 0.185 kg cm^{-2} m^{-1} (Chan, 1964), which is approximately 80% of geostatic load; also the Maikop Formation, which is thought to be the origin

AREA	STRUCTURAL ASSOCIATION	SEDIMENTOLOGY & STRATIGRAPHY	AGE OF PARENT BED	MAX. THICK.	MAX. DEPTH	CHARACTER OF MUD	EXOTICS	FLUIDS	TEMP	OTHER
Azerbaijan, USSR (Jakubov et al, 1976)	V.strong with synclinorium, anticlines, faults, thrusts & diapirs. Sometimes none.	Maikop Fm. clays	Oligocene& younger. Some root to Cret.& Jurassic	<1800m		Bluish-white, fine consistency, plastic.	<10% U.Cret. & L.Tert. Some striated	Brines & gas (mostly methane)	✓	Dating fm. exotics.
B.C. Columbia (Ganssser, 1960; Humphrey, 1963)	Sharp Tertiary folds. One on normal fault.	Finely-bedded marine sandy shale	Tertiary			Dark grey, viscous mud.		Methane-rich, usually no oil.	-	Some explosive. Some assctd w facies changes
Iran - Baluchistan, (Harrison, 1944; Ganssser,	Earthquakes		Miocene						some	Dramatic subsidence
East Mexico - El-Coquito NW (Humphrey, 1963)	On anticline plunging NE to deepest part of basin.		U.Oligocene matrix	Tert.= 5750m		Light grey, very liquid.	Late Miocene	Methane and oil.	-	
New Zealand - E & NE of N.Island (Ridd, 1970)	High angle reverse faults. Sometimes earthquakes.	Bentonitic beds	L.Tertiary		3000m	Bluish-white, fine plastic. mud.	U.Cret. & U.Tert 10% of	Mostly methane. No oil.	-	diapirs fm. U.Cret & L.Tert.
Pakistan - Baluchistan (Snead, 1964) Makran Coast (Humphrey, 1963)	Faults, shale squeezes along them. None observed								-	
Sabah, East Malaysia McManus & Tate, 1986)	E: Random W: NE structural trend, parallel to shear zone	Chaotic deposits - blocks in clay matrix	Tertiary			Blue grey,	Tertiary	Mostly N + O, oil (no methane in E. Sab	50°C	Islands form after earth-quakes
Taiwan (Shih, 1967)	Thrust faults. Underlying diapir?	Gutingkeng Fm. - clay	Plio-Pliocene	5000m		Dark grey, viscous,		Methane and oil.	-	
Trinidad Higgins and Saunders, 1974)	Lines on folds, thrust and wrench faults.	Herive, Karamat & L.Cruse-Lengua clays	Neogene	3000m		Light grey, runny. Clayey to sandy.	Rounded Cret. & angular younger.	Methane and oil; pH 8.1-9.4.	-	Mud islands offshore.
Timor (Audley-Charles, 1968; Barber et al, 1987)	Lines on wrench faults	Saboneru Scaly Clay	Pliocene (MAC) OR M.Triassic (B et al)	3000m	3000m	Grey, runny.		Methane, black oil slicks	-	Diapirs offshore
E. Venezuela - Paria Coast (Ganssser, 1960)	NW's in row on Pedernas anticline core.	Clays	L.Miocene				Oily Oligocene SS blocks.		-	Large gravity minimum.

Table 1.2. Typical mud volcano features

of most of the Azerbaijan mud volcanoes (table 1.2), is highly overpressured and has been reported to have localised pore pressures greater than geostatic pressures (Fertl, 1971).

1.2.2. Structure

Mud volcanoes usually have a very clear structural association. They are found in areas of Cenozoic folding (Higgins and Saunders, 1974; fig. 1.1); they occur along fold axes (Gansser, 1960) and/or faults and they often erupt in association with major earthquakes (eg. New Zealand - Ridd, 1970; fig. 1.1). The faults with which mud volcanoes are associated are compressional. Barber et al (1986) suggest a genetic relationship between mud volcanoes and wrench faults. This certainly seems to be true for Timor, and some examples in U.S.S.R and Trinidad. However, mud volcanoes and diapirs are often observed along thrust faults (Jakubov et al, 1976 - Azerbaijan, U.S.S.R.; Biju-Duval et al, 1982; Mascle et al, 1973, 1979 - Barbados Ridge Complex; Breen et al, 1986 - Sumba, Indonesia). Similarly, the New Zealand mud volcanoes occur on high angle reverse faults (Ridd, 1970). Rare examples, however, do not apparently show an association with structure, such as those on the Makran Coast of Pakistan (Humphrey, 1963).

Mud volcano eruptions often correlate with earthquake activity, for example in New Zealand (Ridd, 1970), East Malaysia (McManus and Tate, 1986) and U.S.S.R. (Jakubov et al, 1976). In the Kobystan region, U.S.S.R., earthquake-associated activity is observed every 14 years or so, after periods of quiescence (Jakubov et al, 1976).

The association with clay diapirs is also important. Chapman (1983) states that "most mud volcanoes can be considered as mudstone diapirs that have reached the surface." Ridd (1970) and Barber et al (1986) seem to agree with Chapman; both use this relationship to explain the presence of exotic blocks in mud volcano areas.

1.2.3. Parent Bed Thickness

Mud volcanoes always occur in areas of thick overpressured argillaceous sequences which are assumed to be the source of the material. The thickness of these sequences is related to rapid deposition associated with the tectonic environments where the mud volcanoes are found. Where the thickness is recorded, it is generally over 500m, reaching values of up to 5000m in Taiwan (table 1.2).

1.2.4. Parent Bed Depth

There is conflicting evidence on the maximum limiting depth allowing diapiric behaviour. Chapman (1974) approximates this at 3000m, stating that clay compacts too much below that depth. Deeper diapirs than this are, however, known in deltaic environments (see section 2.3.3). Gilreath (1968) and Musgrave and Hicks (1968) show seismic sections from the Texas and Louisiana Gulf Coast where shale diapirs seem to originate from depths of up to 5000m or more; Musgrave and Hicks distinguish between the shale and salt masses by using velocity data. Cross sections of mud volcano regions in New Zealand (Ridd, 1970) and Timor (Barber et al, 1986) depict parent bed depths of up to 3000m. The

depth is obviously dependent on the area, but where it is mentioned, it tends to be at least several hundred metres. Parent beds at depths in the order of 100m are known in areas such as the Mississippi Delta (Morgan, 1961) but these occur in Recent sediments and sedimentary volcanism is easily explained by the small thickness and ductility of the overburden material. As this study is concentrated on deep-seated mud volcanoes, the shllower examples are not considered further here.

1.2.5. Character of the Mud

The term "mud volcano" is possibly misleading as the ejected material often contains considerable amounts of silt and sometimes sand (Higgins and Saunders, 1974; Shih, 1967; see also section 4.2 in this study). The character of the mud varies from area to area depending on water content and particle size distribution. On the whole, however, the muds are considerably less viscous than those of mud diapirs. As mentioned above, many workers believe that mud volcanoes are often the surface expression of a diapir, where the most mobile elements in the diapir are extruded to the surface.

1.2.6. Fluids in the Mud

All mud volcanoes emit saline waters and hydrocarbons. Jakubov et al (1976) found that the Azerbaijan mud volcanoes varied in water composition, containing alkaline waters in the northern region and calcite-rich waters in the southern region. They also observed that all the mud volcanoes contained elements/compounds like iodine, bromine, ammonia and naphtenic acid which, to them, indicated the unity of geochemical conditions for the mud volcanoes in the area. The Timor and Trinidad waters were found to be alkaline, the pH ranging between 7 and 9 for Timor (Santoso, 1976) and 8 and 9 for Trinidad (Higgins and Saunders, 1974); oilfield waters in the latter were approximately 8.4. In Taiwan, the pH varied, so that it had a value of 8-9 in the south-west mud volcanoes, and 5-6 in the south-east. Henderson (1976) also notes the high alkalinity of the mud volcanoes in West Greenland. It is difficult to compare the salinity of the mud volcano waters with formation waters with any degree of reliability due to possible contamination by surface and overburden waters. No description is made of the sampling procedure and its timing; this should take account of seasonal fluctuations in the water table, and water chemistry.

Where extruded gases have been analysed, methane was always present, making up over 90% of the gaseous emission of the mud volcano (Shih, 1967; Higgins and Saunders, 1974; Jakubov et al, 1976; Brown, pers. comm., 1986). Liquid hydrocarbons are often present (table 1.2). Brown used seismic data to study sedimentary volcanism offshore Barbados, and makes the distinction between mud volcanoes and diapirs by the presence of methane in the former. The mud volcanoes in his classification look like diapirs, with the same dimensions, but form cones on the sea floor.

1.2.7. Shape and Size

Mud volcanoes vary greatly in shape and size. A typical active mud volcano onshore occurs in a "tassik" (Higgins and Saunders, 1974), which is a circular clearance in the vegetation caused by the high salinity of the muds (plate 1.1). Surrounding vegetation (where present) is typical of beach environments; for

a.

b.

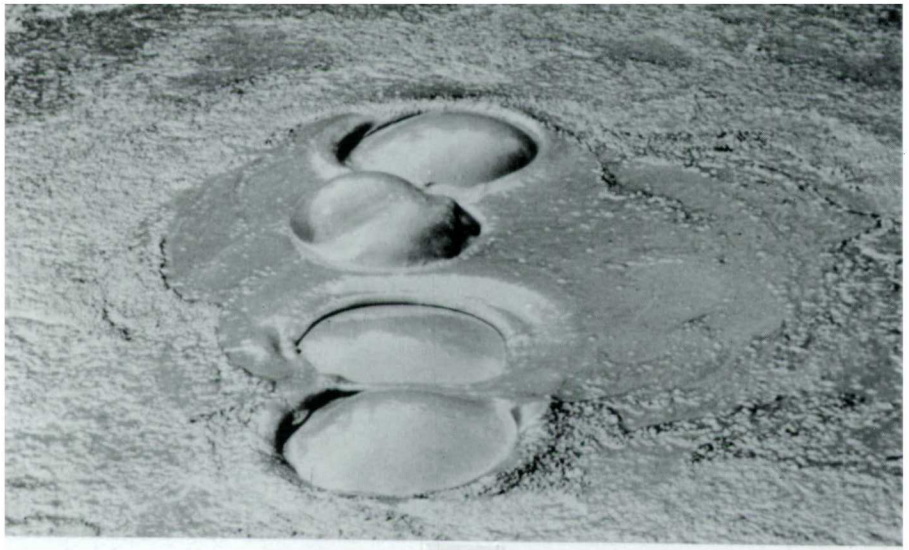

c.

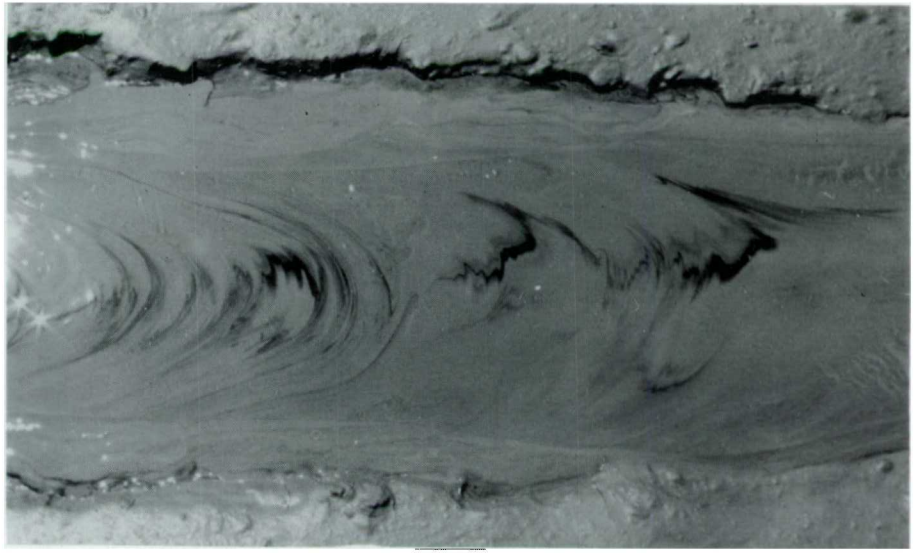

d.

Plate 1.2 Typical mud volcano features : a. a circular "tassik" with several centres of activity, Devil's Woodyard, Trinidad; b. an active mud volcano cone, with exploding methane bubble and viscous mud flowing from the vent, Wushanting, Taiwan; c. methane bubbles bursting through a mud volcano pool, Palo Seco, Trinidad; d. liquid hydrocarbons in the mud, Aoshenshui, Taiwan.

example, mangroves are commonly found around mud volcanoes. The tassik normally contains several centres of activity in the shape of cones and/or pools of mud.

The most extensive field description of mud volcanoes was undertaken by Shih (1967) who classified the Taiwan examples according to their shape and size. The five categories used by him were:

- **A: Cone - inclination of sides $>20^{\circ}$, crater diameter tens of centimetres.**
- **B: Shield - inclination of sides 5-20°, crater diameter tens of centimetres.**
- **C:Maar - inclination of sides $<5^{\circ}$, crater diameter several centimetres to 2 metres.**
- **D: Basin - crater diameter several metres, some with parasitic volcanoes.**
- **O: Hole - crater diameter few centimetres.**

Higgins and Saunders (1974) used Shih's classification for the Trinidad mud volcanoes but had difficulty with some examples. Indeed, some of the mud volcanoes in Azerbaijan (Jakubov et al, 1976) and Pakistan (Freeman, 1968) would fit the shape of an A cone but their size is in the range of hundreds of metres. The effect of size seems to be a direct function of rainfall: for the same quantity of mud ejected, the largest cone would develop in a more arid environment.

Mention should be made here of the massive (up to 10km diameter) structures observed offshore such as those to the east of Barbados and Trinidad and south of Timor. Westbrook et al (1984) and Brown and Westbrook (1987) refer to the Barbados examples as mud volcanoes as they form cones on the ocean bottom (section 1.2.6). As mentioned in section 1.2.2 above, these are very closely associated with the phenomena observed onshore.

1.2.8. Duration

It is difficult to estimate the duration of mud volcano activity as fossil records are exceedingly rare. The massive size of some mud volcanoes in areas of low rainfall (section 1.2.7) implies an age of an individual cone of at least several thousand years. However, individual centres of activity within a tassik may not last for very long, regularly changing their position (Gansser, 1960; section 3.2.5).

The only definite mention of the age of a mud volcano was given by Langseth et al (1988). The large mud volcano/diapir studied occurs offshore to the east of Barbados. The west flank of the cone was dated by acoustic stratigraphy at 20-30,000 years and the east flank was dated at less than 300,000 years.

The duration of a mud volcano must be dependent on various factors. Naturally, the thickness of the parent bed will control the maximum amount of material extruded; also, the mud will only continue to rise to the surface in the presence of an abnormal pressure gradient. The third factor is overburden

tensile strength; if this increases for any reason, it could prevent the mud from squeezing upwards (Chapter 7).

1.2.9. Speed of Extrusion

Again, it is difficult to estimate the speed of extrusion without regular geophysical work on a mud volcano area. The speed must be dependent on the rheology of the material. Langseth et al (1988) quote a vertical flux of interstitial fluids present in the above-mentioned offshore mud volcano of less than 10 cm/year. Reports of very rapid extrusion are known, such as the overnight appearance of Chatham Island mud volcano south of Trinidad (Birchwood, 1965). Workers like Kugler (1933) and Freeman (1968) favour the idea of rapid extrusion to explain the presence of exotic blocks in mud volcano areas. Others, such as Barber et al (1986) believe that the blocks are brought up by underlying more viscous diapirs.

1.2.10. Temperature

Mud volcanoes are usually a low temperature phenomenon (see Table 1.2), their temperature being ambient. However, some of the USSR examples are associated with high temperatures (Jakubov et al, 1976; Ovatanov and Tamarazian, 1970). High heat flow (four times the average basin value) was also recorded by Langseth et al (1988) on the large mud volcano/diapir they investigated offshore east of Barbados. As mentioned above, some mud volcanoes are associated with volcanic activity, which seems to drive them, such as the mud volcanoes in Lake City Hot Springs, California (White, 1955). Examples of this type are not considered in this work as they are assumed to be driven by volcanic heat.

1.2.11. Geophysical Characteristics

The main geophysical feature of mud volcanoes is their association with low gravity anomalies, which are attributed to the abnormally low density of the material (Nettleton, 1949). Assuming that mud volcanoes are also associated with overpres sured shale masses, the following geophysical characteristics should also apply (Musgrave and Hicks, 1968; Herring, 1973; Fertl, 1976),

- **low velocity sound transmission (2,000-2,600 m/sec.) and very little increase in velocity with depth.**
- **low density (2.1-2.3 g/cc).**
- **low resistivity (0.5 ohm-m).**
- **high fluid pressure.**
- **Gilreath (1968) adds dipmeter surveys to distinguish diapiric clay from overpressured clay in-situ; as a diapir is approached from above, dips increase until the shale is penetrated, then the dips remain constant. This seems unusual, as diapiric shale would be expected to have random dips.**

1.2.12. Summary

It can be seen that deep-seated mud volcanoes have the following features in common,

- **They are generally associated with thick, rapidly deposited, overpressured Tertiary argillaceous sequences.**
- **They have a very strong structural association.**
- **They extrude muds, brines and hydrocarbons.**
- **Most eruptive centres consist of several volcanic cones; shallow and steep-sided cones can be present together.**
- **Rock fragments are commonly present in the mud, usually originating from older strata.**
- **Diapiric zones with mud volcanoes generally coincide with areas of negative gravity anomaly.**

1.3. AIMS OF THE STUDY

As mentioned in section 1.1, this work is aimed at achieving a better geological and geotechnical understanding of the phenomenon of deep-seated sedimentary volcanism, with particular reference to mud volcanoes. Using field examples from the islands of Trinidad and Taiwan, the following aspects will be investigated,

- **the type of sediment extruded and its origin;**
- **possible causes of overpressuring in fine grained sediments, and mechanisms of extrusion; and**
- **the geotechnical behaviour of the materials involved in deep-seated sedimentary volcanism.**

1.4. STRUCTURE OF THE THESIS

The thesis is divided into eight chapters, defining four parts: an introduction and literature review, a field and laboratory geological investigation of mud volcanoes, an experimental study of the behaviour of mud volcano materials at high pressure, and the discussion and conclusions.

Chapter 2 reviews the literature on overpressuring in fine-grained sediments - a feature common to all mud volcano areas - and the mechanisms of intrusion/extrusion of these sediments.

Chapters 3 and 4 describe the geological investigation undertaken of mud volcano examples from two areas: Taiwan and Trinidad. Chapter 3 sketches out the general stratigraphy and structure of the areas and a field description of the volcanoes visited. Chapter 4 includes the laboratory description and classification work on the samples collected. This includes particle size distribution, clay mineralogy, microscope description of the coarser fraction, including micropalaeontology where possible, and Atterberg Limits (parameters used by engineers to classify the physical state of a soil in terms of general grain size and moisture content). The work is aimed at understanding the nature of the material extruded, its origin, and the possibility of contamination by the overburden. Comparisons are made with published results on the same type of material.

Chapters 5, 6 and 7 are an investigation of the geotechnical behaviour of the mud volcano materials. Mud volcanoes are associated with both rapidly deposited, underconsolidated clays and with tectonic activity. These two factors are both thought to be vital to the formation of the mud volcanoes studied. The experimental programme was therefore aimed at understanding the consolidation and undrained shear behaviour of the clays sampled; the tests were performed in a high pressure triaxial cell. Chapter 5 describes the soil mechanics principles underlying the experimental approach, Chapter 6 presents the experimental data and Chapter 7 discusses these data in the light of relevant published literature on high pressure and low pressure soil mechanics. Chapter 7 also incorporates the observations made in previous chapters into a general discussion on mud volcanoes and their origin.

Chapter 8 presents the conclusions of the study.

CHAPTER 2

THE ORIGIN OF MUD VOLCANOES - A LITERATURE REVIEW

2.1. INTRODUCTION

"Throughout the world, wherever mud volcanoes are found, there has been rapid Tertiary and/or Late Cretaceous sedimentation: and where evidence is available, pore fluid pressures are abnormally high" (Fertl, 1976). It would seem reasonable to assume that overpressuring is a prerequisite for the formation of mud volcanoes. However, overpressuring alone cannot account for the phenomenon, as mud volcanoes are not common to all overpressured clay formations (fig. 1.1, Fertl, 1972; Rehm, 1972). In order to understand the origin of mud volcanoes, it is therefore important to study not only the causes of overpressuring in mud volcano areas, but also to understand the processes leading to the failure and extrusion of these clays.

In the first part of this chapter, mechanisms of overpressuring of fine-grained sediments will be reviewed and discussed. The second part of this chapter will briefly discuss mechanisms of intrusion/extrusion of the clays. Within this latter review, which concentrates mainly on diapirism, it is assumed, for simplicity, that mud volcanoes are the surface expression of a near-surface diapir. As mentioned in section 1.2, this assumption has been made by workers like Ridd (1970), Fertl (1976) and Barber et al (1986).

2.2. CAUSES OF OVERPRESSURING

Rocks or sediments with pore fluid pressures exceeding the hydrostatic gradient (the weight of a continuous overlying column of water) are termed "overpressured" (fig. 2.1). This is common in thick clay sequences where pore pressure dissipation is slow due to the low permeability of the material. Overpressured clays occur in many different types of environment, varying from passive deltaic to active compressional regimes. They have several features in common (Fertl, 1976, fig. 2.1):

- **They are mostly thick (up to several kilometres), rapidly-deposited, clay sequences.**
- **They are mostly Tertiary in age, but Mesozoic examples are known.**
- **They are almost always regressive marine sequences.**
- **They are usually low density clays.**
- **They are usually associated with an increase in the temperature gradient.**
- **Their salinities are usually anomalously low.**


Image removed due to third party copyright

- **They are associated with hydrocarbons.**

- **They have the same geophysical properties (see section 1.2.11)**

There are numerous theories on the origin of overpressuring in clays. Many reviews have been published on the different mechanisms (Tkhostov, 1963; Hanshaw et al, 1965, 1968; Bredehoeft and Hanshaw, 1968; Rieke and Chilingarian, 1974; Fertl, 1976; Pritchett, 1978; Plumley, 1980; Chapman, 1983; Isaac and Shaw, 1984; Gretener, 1985). The main ideas can be divided into three categories:

1) Rapid loading:
  a) sedimentary.
  b) tectonic.
2) Fluid generation and migration during burial:
  a) smectite dehydration.
  b) methane generation.
  c) osmosis.
3) Aquathermal pressuring.

All workers agree that a number of different factors may be the cause of abnormally high pore fluid pressures, and that the origin of overpressuring will vary from area to area.

2.2.1. Rapid Loading

a) Sedimentary Loading and Undercompaction

Most workers believe that overpressuring in clays is the result of rapid sedimentary loading (Dickinson, 1953; Rubey and Hubbert, 1959; Bredehoeft and Hanshaw, 1968; Magara, 1968; Harkins and Baugher, 1969; Bishop, 1978; Chapman, 1983). There can be no doubt that this mechanism plays a very important role in overpressuring clay-rich strata.

In order to understand the causes of overpressuring under such conditions, one must first consider the consolidation behaviour of clays.

i) The Consolidation of Clays
The theory of consolidation of saturated clays was developed by Terzaghi (1943). He illustrated his theory by considering a water-filled cylindrical vessel containing a number of plates with very small perforations (representing permeability) separated by springs (representing the compressibility of the soil skeleton), (fig. 2.2). When a load is applied to the top plate, the springs remain intact initially because of the low "permeability". At that point, the whole load is taken up by the water, so that the system is 100% overpressured. After a while, however, the water begins to escape and the height of the

springs decreases. With increasing "consolidation" the lower springs take up more of the load until the water pressure is restored to its pre-loading level.

This is analogous to the mechanism whereby a clay compacts after the addition of a load. Initially, the whole weight is taken up by the pore fluids, but as compaction progresses, the load is shared by the water and clay particles until all the excess water has been expelled and the load is totally supported by the clay.

The above-mentioned model is too simplistic in terms of geological stresses and materials, but it illustrates the concept that a load is shared partly by the soil skeleton and partly by the pore fluids; this was formulated by Terzaghi into the theory of effective stress. The effective stress acting on an element (σ') is the difference between the total load (σ) and the pore pressures in the element (u),

$$\sigma' = \sigma - u \qquad 2.1$$

ii) Underconsolidation in Thick Clay Sequences

If a clay is allowed to dissipate its excess pore fluids as it is buried, it compacts and the pore pressure gradient remains hydrostatic. When complete pore pressure dissipation is impeded, the clay becomes underconsolidated, with an abnormally high porosity for its depth of burial[1]. The high pore pressures are preserved and increase with increasing load.

Underconsolidation occurs in areas of rapid deposition where great thicknesses of clay are buried to depths of several kilometres in relatively short periods of time. For example, Bruce (1973) describes the Texas Gulf Coast where normally consolidated sandstones are rapidly deposited over low permeability, low density overpressured clays. How rapid does loading need to be to hinder consolidation? This, of course, is a function of several variables. If we consider the simple case of one-dimensional consolidation (Terzaghi, 1943), the rate of change of effective stress ($d\sigma' / dt$) is expressed by the equation,

$$-d\sigma' / dt = C_v \, d^2u / dz^2 \qquad 2.2$$

where,
dz = increment of thickness, m,
C_v = coefficient of consolidation (equation 2.3), $m^2 s^{-1}$

$$C_v = k / M_v \gamma_w \qquad 2.3$$

where,
k = coefficient of permeability, $m s^{-1}$,

1 *It can be problematic to look at porosity-depth relationships when assessing overpressuring.* It is *more reliable to relate porosity to changes in effective stress, because the latter does not necessarily increase linearly with depth, as is assumed by the porosity-depth relationship.*

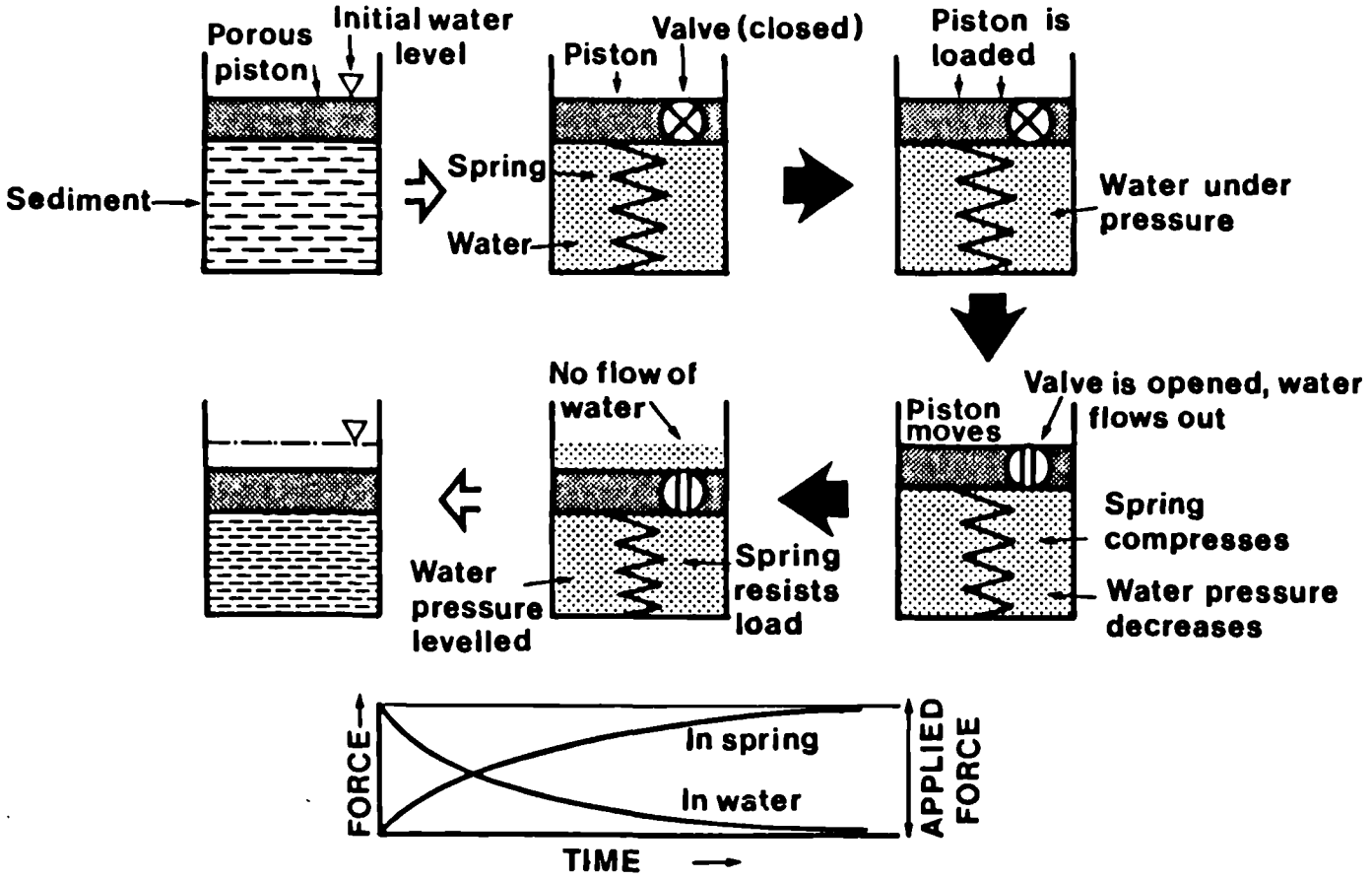

Fig. 2.2 Schematic illustration of consolidation. The spring represents the compressibility of the mineral skeleton, the water represents the pore fluid and the valve represents the permeability of the sediment.

M_v = coefficient of compressibility (vertical stress/vertical strain), MPa^{-1}
y_w = unit weight of water.

From work undertaken by Gibson (1958), Skempton (1970) has shown that for a sediment to reach 95% consolidation with a uniform rate of deposition (r), C_v / rh must be greater than 10, h being the thickness of the layer. Skempton (1970) uses this to estimate consolidation conditions in different depositional environments. Holocene clays with a rate of deposition of 2m / 1000 years would be fully consolidated. The Orinoco delta Holocene clays, however, have been deposited at a rate of 8m / 1000 years, with overpressures of 0.5 kg / cm^2 at 30-50m (Kidwell and Hunt, 1958). In the Mississippi delta, McClelland (1967) reported a rate of deposition of Holocene clays of 120m / 1000 years, so that very little consolidation is taking place. Rapid sedimentary loading is also very important in areas of convergent tectonics. Moore (pers. comm., 1988) reports depositional rates of 10m / 1000 years in the Caribbean.

Rubey and Hubbert (1959) applied the principle of effective stress to overpressuring by rapid loading and underconsolidation; they express the degree of overpressuring using the ratio λ,

$$\lambda = u / \sigma v \qquad 2.4$$

where u = pore pressure, MPa,
and O_v = total vertical stress, MPa.

The greater the overpressuring, the nearer the value of λ to 1, i.e. the overburden weight becomes increasingly supported by the fluid in the clay.
Rubey and Hubbert (1959) also introduced a term to indicate underconsolidation: "equilibrium depth" (z_e); this is the maximum depth at which a sediment has existed in a normally consolidated state.

$$z_e = (Y_{bw} z - p) / (Y_{bw} - Y_w) \qquad 2.5$$

where z = depth, m
Y_{bw} = mean specific weight of water-saturated rock, and
Y_w = specific weight of pore water, $kg\ cm^{-2}$
p = pore fluid pressure (same as u), MPa.

Chapman (1972) re-expresses (z_e) as a function of λ (equ. 2.4),

$$z_e = [(1 - \lambda) / (1 - \lambda_e)]z \qquad 2.6$$

where λ_e = equilibrium value of λ.

When normal consolidation has occurred, equilibrium depth is equal to actual depth; when no consolidation has occurred, on the other hand, it is equal to zero.

iii) The Transition Zone

As mentioned above, overpressured clays occur in regressive sequences which, by definition, coarsen upwards. The top part of the clay unit is a drainage boundary with the overlying coarser sediment; this allows it to consolidate more fully than the middle of the unit, so that it can act as a seal to part of the clay. If the bottom boundary of the clay unit is also drained, that too would be preferentially consolidated.

The "transition zone" is the boundary zone to an overpressured sequence where the pore pressure gradient is much steeper than the geostatic gradient (Smith, 1973; Chapman, 1972) - (fig. 2.3.a).

The shape of the pore pressure and equilibrium depth curves (fig. 2.3. a & b) implies that overpressuring begins at depth, which is the idea proposed by workers favouring mechanisms such as a fluid source at depth or a temperature increase (see below). Fig. 2.3.b shows a sudden decrease in z_e with depth. Chapman (1972) states that if abnormality begins at depth, reverse consolidation must take place, which, he argues, is impossible[2]. He therefore suggests that overpressuring must begin at very shallow depths (fig. 2.3.c). The abnormality of pore pressures is attributed to loss of permeability, which would have to increase with increasing burial depth or sedimentation rate to maintain hydrostatic conditions (Magara, 1971; Chapman, 1972). Overpressures at relatively shallow depths have been observed by several workers, e.g. Spinks (1970).

iv) Clay Fabrics, Diagenesis and the Underconsolidation Model

As Isaac and Shaw (1984) point out, not many workers give enough importance to the clay fabrics produced in different environments of deposition. Martin (1972), for example, related the fabrics directly to overpressuring in the Oligocene of South Texas. Using the data by Bennet et al (1977), Isaac and Shaw (1984) expect clay fabrics in underconsolidated sediments to be randomly oriented if the clay is truly underconsolidated. Interestingly, McGregor et al (1979) find evidence of bioturbation during early burial of continental slope mudrocks near Baltimore Canyon. The bioturbation was observed to make the clay particle orientation random, thus increasing the porosity and disturbing the mechanical compaction process.

Equally, diagenesis plays an important role in the consolidation of clays and must have an effect on overpressuring. It is thought that diagenesis can obliterate early burial characteristics by a depth of about 1000m (Isaac and Shaw, 1984). This must depend on the effective stresses in the sediment. Cementation can be an indication that underconsolidation is not responsible for overpressuring. Many examples of high density, overpressured clays are known. Certainly, in the Viking Graben in the North Sea, λ ratios of 0.8 are known at depths of 4000m in low porosity, cemented shales of Jurassic age (Lindberg et al, 1980; Carstens and Dypvik, 1981). Also, the Karamat Formation in southern Trinidad (thought to be the source of some of the mud volcanoes) has yielded highly overpressured mudrocks of high densities (Higgins, 1987, pers. comm.). In such cases, overpressuring must have occurred at depth, which would explain the high density of the sediment. It is therefore vital to understand the

2 *Although Chapman's suggestion seems valid, it should be said that consolidation of clays is partly reversible, provided a decrease in effective stress occurs (Chapter 5)*

Fig. 2.3 Abnormal pressures and equilibrium depth in the transition zone (after Chapman, 1972). a. pore pressure - depth curve; b. equilibrium depth - depth curve; c. Chapman's explanation for the evolution of the equilibrium depth curve.

relationship between sediment fabrics, diagenesis and overpressuring - a relationship which is as yet relatively unexplored.

b) Tectonic Loading

Tectonic loading is a very important active process in mud volcano areas. It has been deemed at least partly responsible for abnormal pressures by many workers (Hubbert and Rubey, 1959; Wilson and Birchwood, 1965; Hottman et al, 1979; Berry, 1973; Higgins and Saunders, 1974; Biju-Duval et al, 1982; Westbrook and Smith, 1983; Barber et al, 1986).

Although most workers appreciate the importance of tectonic loading, very little work has been undertaken to understand pore pressure response in sediments undergoing tectonic deformation. With the exception of Hubbert and Rubey (1959) and Rubey and Hubbert (1959), the only quantitative work on mechanical aspects of overpressuring that has been considered by geologists has been on simple models whereby a sediment is vertically loaded and horizontally constrained, similar to the water vessel-spring model described in the previous section (2.2.1.a). The stress system in most geological settings of overpressured clay sequences is far from being that simple. Certainly, in an area of tectonic compression, the greatest principal stress is most likely to be horizontal. Even in a passive deltaic environment, this stress may not be vertical. In both types of environment, and especially in the former, very large shear stresses develop which profoundly affect the pore pressures in the sediment.

Hubbert and Rubey (1959) argue that tectonic loading produces much greater deformational stresses than sedimentary loading, and is therefore a more effective mechanism for producing overpressures. Whereas in the case of sedimentary loading, λ can only approach 1 when the sediment is almost totally undercompacted (see equations 2.1 and 2.2), in the presence of lateral compression, the pore pressure can increase without this constraint. In low pressure soil mechanics studies, shear stress is known to cause the generation of excess pore pressures if the material is normally consolidated and undrained (see for example Schofield and Wroth, 1968). Undrained conditions are expected in thick, low permeability sediments, and, provided they have not experienced uplift, the sediments can be regarded as normally consolidated (even if they are underconsolidated). This is illustrated in Chapters 5 and 6, and discussed in Chapter 7.

There are numerous examples of tectonically-induced overpressuring (Rieke and Chilingarian, 1974). In the California Coast Ranges, Berry (1973) reports a thick clay sequence of Jurassic to Cretaceous age, overlain by up to 3000m of Tertiary sediments, all undergoing tectonic deformation. The area affected is bound to the west and north by the San Andreas Fault and to the east and south by granite. Berry suggested that the high fluid pressures are caused by the squeezing of this belt of highly compressible shales east of the San Andreas by relatively incompressible granite. Several workers associate the overpressuring in Trinidad with tectonic loading (e.g. Suter, 1954; Higgins and Saunders, 1974). Values of λ of 0.8 are reported at depths of just over 1 km.

Overpressuring is particularly closely associated with thrust faulting in tectonically active environments. Geophysical work undertaken in the Barbados accretionary complex (Westbrook et al, 1983) shows that a thick complex of sediments is accreted against a plate while much less deformed sediments are underthrust beneath it, remaining almost intact for a distance of 80km. The "undeformed" zone,

Fig. 2.4 Overpressuring and horizontal compression. a. abnormal pore fluid pressures in the Barbados accretionary complex (after Westbrook and Smith, 1983); b. the onset of abnormal pore fluid pressures and compressional structures with depth, offshore, Gulf of Alaska (from Hottman et al, 1978).

approximately 2300m thick, is thought to be overpressured by the load thrust on top of it (fig. 2.4.a); its pore pressures are estimated to carry 90% of that load (λ = 0.9). In the Gulf of Alaska, abnormal pore pressures are observed at just over 2000m, reaching λ values of 0.85 at 4000m (Hottman et al, 1979). The overpressured zone is associated with compressional faults (fig. 2.4.b). Barber et al (1986) state that tectonic loading is responsible for overpressuring sediments in Timor dating as far back as the Permian. Barber (1988, pers. comm.) suggests that the overpressuring occurred when thick sedimentary sequences were thrust over these sediments.

2.2.2. Fluid Generation and Migration During Burial

a) Clay Diagenesis

Work done on the clay-rich sediments in the Texas Gulf Coast has revealed that the transformation of smectite (montmorillonite) to illite can cause overpressuring (Powers, 1967; Hanshaw and Bredehoeft, 1968; Bruce, 1973, 1984).

Powers (1967) introduced the idea that when intermolecular water in the smectite is released to become intergranular water it takes up an extra 40% of its original volume, thus causing overpressuring. The minimum depth at which excess pore pressures start is given as approximately 1800m. Burst (1969) suggests that the density of interlayer water is 1, and involves a volume increase of approximately 12% during smectite dehydration.

There is some evidence that overpressuring is associated with smectite dehydration in the Gulf Coast, as mentioned above, but the evidence is not always conclusive. Bruce (1984) compared Tertiary shales from a) the Brazos Colorado River system in Texas, b) the Mississippi River shale in Louisiana and c) the Niger Delta. In the first two, he found a relationship between high pore pressures and the smectite-illite transformation: in the Gulf Coast, this occurs at around 600m. Temperatures were found to vary: "the threshold temperature required to initiate diagenesis ranges from about 71°C in the Mississippi River to 150°C in the Niger Delta". The mineralogy also varied: in the Brazos Colorado River, montmorillonite constituted 40% of the clay with 20% kaolinite, whereas in the Niger, montmorillonite was only 15% with 60-70% kaolinite.

Magara (1975, 1978) disagrees with the clay diagenesis theory because he cannot see how consolidated material can "rebound" after the release of intermolecular water and because he finds that the volume of water released is not sufficient to explain the low density of the overpressured clay. Isaac and Shaw (1984) disagree with Magara's "rebound" objection. They find it plausible that a secondary porosity can be created by the dehydration of smectite. As mentioned in section 2.2.1.b, a clay can rebound if the effective stresses are reduced (by an increase in pore pressure in this case). If it is uncemented and therefore plastic in behaviour, the clay will swell by a small amount (Chapter 5). If the clay is cemented, the reduction in effective stress would cause an elastic rebound and therefore a volume gain equivalent to volume loss for that effective stress increment.

Isaac and Shaw (1984) consider two problems with this theory, however: a) the illite-smectite transition zone does not always coincide with the much narrower pore pressure transition zone, and b) as implied by Bruce (1984), this is very dependent on mineralogy and chemical conditions. The experimental work of Hall et al (1985) on pressure and temperature effects on the smectite dehydration process agrees with the second point. They found that very high temperatures and pressures had no effect on the clay in the absence of the right chemical conditions.

The latter point is important. There is no real evidence for smectite dehydration in any of the prime mud volcano areas. Indeed, in the New Zealand examples, the source bed is a smectite-rich clay (Ridd, 1970) at depths of up to 3000m. The Taiwan mud volcanoes, on the other hand, seem to have no smectite in the clay (Shih, 1967; section 4.3). It could be argued that all the smectite has transformed to illite in Taiwan, but it is equally feasible that the original bed is smectite-free.

One alternative view of the smectite-illite transformation was proposed by Plumley (1980), who does not find any evidence of density change in the intermolecular water after it is released. Plumley suggests that it is the collapse of the smectite structure which transfers a greater proportion of the total stress from the clay structure to the interlayer water than under pre-clay transformation conditions, causing an increase in pore pressures. This does not require a density difference between interlayer and pore water and, therefore, the total porosity does not change. Similar structural collapse effects on pore fluid pressures are discussed in Chapter 7.

b) Hydrocarbon Generation

A few workers attribute overpressures to the generation of hydrocarbons (e.g. Hedberg, 1974; Jones, 1980; Meissner, 1980, 1982; McIver, 1982). The main idea, presented by Hedberg (1974), is that because organic matter constitutes a substantial part of freshly deposited muds, biochemical activity can produce large volumes of methane. This gas is thought to further accentuate or even create the overpressures in a clay sequence by building up additional interstitial pressure.

There is some evidence of an association between overpressuring and hydrocarbons. Milliken et al (1981) and Swanson (1984) note this in the Gulf Coast. The latter found that the Gulf Coast overpressured formations encountered by 12 test wells all showed that formation waters were gas-"saturated". Jones (1980) and Meissner (1982) studied the increase in volume involved in the kerogen-hydrocarbon transformation as a possible cause of overpressuring. However, although Goff (1983) conducted similar studies, he still favoured the undercompaction model.

Gas hydrates are another proposed mechanism of overpressuring sediments. McIver (1982) states that gas hydrates are formed by "hydrocarbon gases at or near saturation in the interstitial waters of the near bottom sediments". They can store enormous volumes of gas and water in semi-solid form in the ocean bottom. If the equilibrium conditions are disturbed in any way, the solid gas and water matrix decomposes, releasing gas and water in volumes exceeding those occupied by the gas hydrates. This can not only decrease the density of the sediment, but also increase the pore fluid pressure (this would, again, be dependent on the above-mentioned conditions). McIver visualises this as a potential mechanism for the formation of mud volcanoes and diapirs. Gas hydrates become more unstable with increasing depth and temperature (Kvenvolden, 1985). Instability occurs at relatively shallow depths,

and hydrates are therefore largely irrelevant to the deep-seated mud volcanoes under investigation here. The evidence presented for gas hydrates is mainly geophysical, but cores containing hydrates were encountered in several offshore locations (e.g. the Black Sea, Yefremova and Zhizhchenko, 1975).

This raises an interesting question on overpressuring by gaseous hydrocarbons. Because of the high compressibility of gas, its sudden release, especially into already overpressured formation waters, will cause it to dissolve, as observed by Swanson (1984), so that formation pressures only increase when sufficient volumes of gas have been released to "oversaturate" formation waters. This is further discussed in section 7.4.2,

Kalinko (1967) studied hydrocarbon regions in the Caucasus and Central Asia and found that, as a rule, no major gas deposits were present at the source of the mud volcanoes there. Also, in Trinidad, the hydrocarbons are now thought by many workers to originate from the Cretaceous because of the low geothermal gradient of the area, which does not allow hydrocarbon maturation in Upper Tertiary and younger sediments (Leonard, 1983; Rodrigues, 1985); the only area where hydrocarbon generation was possible in the Middle and Lower Tertiary is in the south-west peninsula; this excludes many mud volcano areas on the island (see fig. 3.4). If this is the case, then hydrocarbons cannot be regarded as a mechanism of "in-situ" overpressuring in many of the Tertiary sequences on the island. However, most of the mud volcano examples around the world, listed in table 1.2, are associated with at least methane, and sometimes liquid hydrocarbons. Hydrocarbon generation may therefore be a potential mechanism of overpressuring in mud volcano areas. The mechanism is probably only secondary, however, as it is only effective while hydrocarbons are being generated.

c) Osmosis

Some workers propose osmosis as a possible mechanism of overpressuring (eg. Hanshaw and Zen, 1965; Young and Low, 1965; Fertl, 1976). This stems from the idea that clays can act as a semi-permeable membrane so that less saline waters can move through them to more saline waters. However, osmosis would generally cause the expulsion of water from overpressured clays because they usually have abnormally low salinities (Rieke and Chilingarian, 1974; Magara, 1978).

2.2.3. Aquathermal Pressuring

The relationship between overpressuring and temperature has been studied by various workers (Barker, 1972; Magara, 1975; Barker et al, 1982; Daines, 1982; Sharp, 1983).

Barker (1972), Magara (1975) and Barker et al (1982) propose that overpressuring is caused by temperature gradients. Barker uses the pressure-temperature-density diagram for water to show that for any geothermal gradient greater than 15°C/km, the pressure in an isolated volume increases with increasing temperature, to such an extent, that it can exceed geostatic pressures (fig. 2.5). He therefore assumes that the clay unit will be completely isolated, and uses the abrupt change in pore pressure and salinity in an overpressured clay unit to support his view. Three conditions for this mechanism are that

Fig. 2.5 Illustration of aquathermal pressuring. a. pressure- temperature-density diagram for water with superimposed geothermal gradients of 25°C, showing overpressuring after isolation occurs at point A; b. increase in excess pore pressure after isolation at two temperature gradients, for pure water (AB, AB') and for 30% NaCl solution (AC, AC'); (from Barker, 1972).

the material retains a constant volume, is totally isolated from its surroundings, and that isolation has occurred at lower temperatures than present.

Many workers oppose Barker's ideas. Chapman (1980, 1982) argues against the idea of aquathermal pressuring for several reasons including,

a) The hypothesis requires that the seal is perfect, so that pore pressure gradients in adjacent beds are hydrostatic. The pore pressures in the transition zone increase gradually, which implies an imperfect seal.

b) Abnormally pressured shales are more common in Tertiary sediments than in Mesozoic or older sediments.

c) Using the maximum geothermal gradient in the Gulf Coast region (36°C/km), Chapman calculates a maximum rate of expansion of the pore fluid of 5% / m.y. Chapman therefore concludes that this rate of thermal expansion can be easily dissipated in the absence of a perfect seal. He further argues that the porosity increase in the transition zone would be associated with an increase in permeability.

Daines (1982) also finds the expansion of fluids unfeasible because they are dissipated by hydraulic conductivity. Using the above-mentioned pressure-temperature-density relationship, Daines calculates that the smallest degree of permeability in the surrounding rocks will be enough to dissipate overpressures created by normal geothermal gradients. Daines does say, however, that aquathermal pressuring could be significant in areas of high geothermal gradients. Sharp (1983) questions Daines' deductions and argues that it is theoretically possible to maintain thermally produced abnormal pore pressures with the Gulf Coast permeabilities. (The reader is referred to the papers by Daines and Sharp for a mathematical treatment of the subject).

Is there any evidence of aquathermal pressuring in mud volcano areas? Mud volcanoes usually have an ambient temperature at the surface (table 1.2), but there are exceptions. Ovnatanov and Tamarazyan (1970) observe temperatures higher than the local geothermal gradient near a mud volcano in Apsheron Peninsula, U.S.S.R.: 40°C is measured near the mud volcano at a depth of 430 - 500m, whereas, further away, such a temperature is found at 600 - 700m or more. Langseth et al (1988) also detect high heat flow from a mud volcano offshore Barbados. Neither team suggest that the high temperature is solely responsible for the overpressure, however. In Trinidad, the average geothermal gradient is very low (1°F/100' or 20°C/km), Rodrigues (1985), which tends to argue against aquathermal pressuring in that area.

2.2.4. Discussion

As can be seen, there is conflicting evidence on the origin of overpressuring in fine-grained sediments. Of course, none of the workers suggest that one mechanism is operational in all areas. Each example has to be studied on its own merit, depending on the conditions of the area and their variation with depth. In an oil-producing sedimentary basin where rapid deposition has taken place it is difficult to separate underconsolidation from hydrocarbon generation. Equally, in a tectonically active area with high geothermal gradients, one cannot ignore the potential roles of both tectonic activity and temperature.

What evidence can we see from mud volcano areas in particular? They are all associated with rapidly deposited thick argillaceous sequences but, as mentioned above, not all overpressured formations in mud volcano areas are underconsolidated. They are all associated with active tectonics and structures, which seem to play a vital role in overpressuring the sediments. Smectite dehydration is difficult to prove without a very close examination of each example. As mentioned above, and further discussed in Chapter 4, the muds often contain appreciable amounts of smectite (Ridd, 1970; Higgins and Saunders, 1974). Hydrocarbons, particularly methane, are always present. Whether these play a role in overpressuring the sediments is not certain, but the possibility cannot be ignored. Finally, temperature. This is not common to all the examples at the surface, but may be of importance in some areas.

Mechanisms of overpressuring are briefly reviewed again in Chapter 7 in relation to changes in effective stress and sediment behaviour.

2.3. CAUSES OF DIAPIRISM

As mentioned in section 1.1, mud volcanoes and diapirs seem to be closely related. Since the early studies by Kugler (1933, 1938) no work has been done on extrusion mechanisms of mud volcanoes specifically, but a great deal has been published on diapirism. Some aspects of the extrusion of clays will be briefly discussed here.

Reviews on the origin of sedimentary diapirism (Kugler, 1933; O'Brien, 1968; Coward, 1981; Chapman, 1983) indicate that several factors are involved in the process,

- **Regional stress system (compression / extension) and related structure.**
- **Density and rheology of source bed and overburden.**
- **Thickness of source bed and overburden.**
- **Hydrocarbon generation.**
- **Temperature.**
- **Depositional history.**

2.3.1. Regional Stresses and Geological Structure

How important is the regional tectonic framework for diapir formation? Mud diapirs are found in both compressional and extensional environments (although deep-seated mud volcanoes are only found in the former).

a) Compression

Mud volcanoes and diapirs are now acknowledged as being a major process in the evolution of modern accretionary wedges such as 8 3 those east of Barbados (Biju-Duval et al, 1982; Westbrook and Smith, 1983; Williams et al, 1984) and south of Timor (Barber et al, 1986). These workers all believe that compression causes the sedimentary volcanism, whether directly, by squeezing the clays out, or indirectly, by sudden loading due to overthrusting (Westbrook and Smith, 1983; Barber et al, 1986; section 2.2.1.b.; fig. 2.4).

Mud volcanoes and diapirs are also closely associated with compressive structures such as lateral faults, thrust faults and overfolds, which are believed to cause their extrusion. Kugler (1933) was the first to suggest that faulting is directly responsible for mud volcanoes. As mentioned in section 1.2.2, Barber et al (1986) suggest a direct relationship between mud volcanoes, diapirs and lateral faults, whereby the fault triggers off the movement of the overpressured clay. Compressive structures in extensional environments, such as overthrusts at the toe of a delta, are also found in association with clay diapirism (Chapman, 1974 and Dailly, 1976).

b) Extension

The most famous extensional regimes where clay diapirs and mudlumps are found are the deltas of major rivers such as the Mississippi, Niger and McKenzie (Dailly, 1976). In a river delta, major regressive sequences form where a wedge of underconsolidated clay is trapped under an ever-thickening, consolidated sandy layer. As more sediment is added on top, the clay begins to form diapirs at the toe of the wedge (fig. 2.6). Many workers believe that this type of sediment progradation is responsible for diapirism (Morgan et al, 1968; Dailly, 1976; Bishop, 1978) as it creates a pressure gradient causing the flow of the underconsolidated clay. Ward et al (1955) presented their work on the excess pore pressure generation and swelling in a peat layer caused by building an embankment; they found that consolidation of the layer underneath the embankment led to the swelling of this layer at the toe, forming a structure very similar to those observed at the toe of a delta (fig. 2.6). Underconsolidation is still necessary, so that it is easier for the pore fluid pressures to dissipate laterally into the toe of the delta rather than upwards through a low permeability boundary with the overburden; this creates overpressures at the toe and the clay swells in response to this increase in pore pressure. Diapirism in deltaic environments is closely associated with both extensional (Dailly, 1976) and compressional faults (Morgan et al, 1968).

Tanner and Williams (1968) conducted some model experiments to simulate tension-induced diapirism in salt. They placed asphalt in a drawer with a clay "overburden". The sides of the drawer were drawn apart for 4 hours, then the clay was removed to study the structures in the asphalt. They found that a

Fig. 2.6 Diapirism in a deltaic sequence (after Morgan et al, 1968).

field of domes and/or ridges had formed perpendicular to the tensional deformation; this was related to the greater plasticity of the asphalt, so that it flows into points of weakness created by the tension of the overburden. Although the result is very interesting, it is felt that this type of modelling is very misleading as there is little control on the parameters involved. Bishop (1978) disagrees that tension induces diapirism, arguing that only 53 out of the 126 salt domes studied by Tanner and Williams are associated with regional extensional faulting.

2.3.2. Density and Rheology of the Source Bed and Overburden

The stress regime may not be enough to induce diapirism if the source bed does not have the appropriate rheological characteristics. A prerequisite for sedimentary volcanism is overpressuring. As discussed in section 2.2, overpressuring usually (but not necessarily) implies low densities. Some workers therefore believe that diapirism is caused by density inversion (eg. Morgan at al, 1968) in much the same way as salt diapirism. This is particularly the case in deltaic environments where the overburden is relatively ductile.

A good deal of theoretical work has been conducted on the density inversion hypothesis (Biot and Ode, 1965; Ramberg, 1972; Berner et al, 1972; Dixon, 1975; Shcwerdtner et al, 1978; Zelikson, 1987).

Biot and Ode (1965) and Berner et al (1972) worked on finite element models of diapirism. They showed that the models were very dependent on viscosity ratio, thickness ratio and relative density. Tanner and Williams (1968), however, state that source bed plasticity rather than density differential is the critical factor to consider in a study of diapirism.

The overburden is assumed to be plastic by the density inversion models. This was observed not to be the case in a real situation by Bishop (1978) who demonstrated that the overburden must have some shear strength to develop faults (which are observed in areas of sedimentary volcanism). This led him to the conclusion that, in the presence of a rigid overburden, diapirism cannot be a simple buoyancy problem.

2.3.3. Source Bed and Overburden Thickness

All modelling work undertaken on diapirism naturally takes layer thicknesses into account (eg. Biot and Ode, 1965; Ramberg, 1972). Chapman (1974) gives an upper limit of overburden thickness allowing diapirism as approximately 3000m. Bishop (1978) agrees with this, stating that "the shale density inversion may disappear as the overburden accumulates and the shale compacts". If undercompaction is the cause of overpressuring, it is difficult to see how an underconsolidated clay begins to compact purely because it has reached a certain depth. Also, as mentioned in section 1.2.5, thicknesses of over 5km are known in the Gulf Coast.

Source bed thickness is important in the overpressuring process itself (see section 2.2) and it must control the size and duration of the mud volcano or diapir.

2.3.4. Hydrocarbon Generation

Kugler (1933) regarded methane as the driving mechanism for all sedimentary volcanism. Freeman (1968) agrees with this, stating that methane gives the explosive energy to transport the muds and blocks upwards. Hedberg (1974) and McIver (1982) also favour the idea of methane as a driving mechanism (see section 2.2.2.b.). Mud volcanoes are always associated with methane. Diapirs, however, are not (Brown, pers. comm., 1986). If one favours the idea that mud volcanoes are usually underlain by diapirs, then methane cannot be the driving mechanism of the latter. It is highly likely that mud volcanoes represent the escape of the most mobile elements at the top of a diapir to the surface (Barber, pers. comm., 1986).

2.3.5. Temperature

High temperatures used to be thought of as the cause of mud volcanoes and diapirs. Early Russian workers proposed that high temperatures were responsible for sedimentary volcanism in the U.S.S.R. (eg. Abikh, 1848). As mentioned in section 2.2.3, high heat flow is associated with some mud volcanoes, but is never suggested as the driving mechanism. Temperature can enhance diapirism, however, by affecting the pressure and viscosity of the source bed.

2.3.6. Depositional Environment

Bishop (1978) mentions the importance of depositional history in the formation of diapirs, the speed of deposition being a control of diapir movement and shape: "slow sedimentation rates produce small, discrete diapirs with vertical sides whereas rapid sedimentation rates produce larger, less discrete diapirs commonly having non-vertical sides." (see also section 2.2.1.a.iv.).

2.3.7. Discussion

Several factors should therefore be considered when studying mechanisms of extrusion of diapirs:

- **compression and related geological structures,**
- **tension and related geological structures,**

- **density inversion,**
- **hydrocarbon generation, and**
- **temperature.**

It is immediately obvious that not only can these factors be closely interrelated, but they overlap with factors common to mud volcanoes (section 1.2) and overpressuring in fine-grained sediments (section 2.2). The ideas of tension and density inversion will be disregarded here as mechanisms of extrusion, as mud volcanoes occur in areas of compression in the presence of a rigid overburden. Temperature can enhance overpressuring, but it is now generally accepted that it cannot be a mechanism of extrusion. Hydrocarbons may well provide the mobility for the muds, especially in the more explosive examples (eg. Ridd, 1970). The author believes, however, that tectonic activity and related structures are responsible for the extrusion of the majority of known deep-seated mud volcanoes. This will be further studied and discussed in Chapter 7.

CHAPTER 3

THE MUD VOLCANO AREAS: A FIELD STUDY

3.1. INTRODUCTION

This chapter will describe the two mud volcano areas visited: Trinidad and Taiwan. It includes a brief summary of the geological history of the two islands with particular reference to the stratigraphy and structure associated with the mud volcanoes, and a field description of the mud volcanoes visited. This is aimed at establishing the relationship between the mud volcanoes and the local stratigraphy and structure. Where possible, an attempt is made to correlate surface data with subsurface data.

3.2. TRINIDAD

The following information has been collated from key references on the geology of Trinidad (Kugler, 1953; Barr and Saunders, 1968; Higgins and Saunders, 1974; Saunders, 1974; Carr-Brown and Frampton, 1979).

3.2.1. Morphology

Trinidad can be regarded as the eastward extension of Venezuela. It was characterised by tectonic activity, particularly during the Tertiary, which interrupted and profoundly modified the sedimentation, resulting in several local facies which have no direct counterparts in eastern Venezuela (Barr and Saunders, 1968). Trinidad is divided into five morphological units (figs. 3.1 and 3.2); from north to south, these are,

- **The Northern Range is a mountainous region of metamorphic rocks with an east-west tectonic trend.**
- **The Caroni Plains are a synclinal basin infilled with Tertiary deposits and covered with terraces, alluvial plains and swamp deposits.**
- **The Central Range is an area of low hills trending northeast- southwest.**
- **The Naparima and Southern Lowlands. The Naparima Lowlands are underlain by folded clays and sands of mainly Oligocene and Lower Miocene age. The Southern Lowlands have developed on a major synclinal feature (the Erin-Siparia-Ortoire Basin) infilled with Tertiary and Quaternary deposits and spanning the width of the island. The rims of the basin are folded and faulted, forming the oil producing structures of south Trinidad. The famous Pitch Lake is found on one of the folds.**
- **The Southern Range has the lowest relief in the island, the maximum height being 275m in Trinity Hills. It developed on anticlinal features.**

Image removed due to third party copyright

Fig. 3.1 Geological map of Trinidad After Barr & Saunders (1965)

Image removed due to third party copyright

Fig. 3.2 Schematic cross section through Trinidad (from Barr and Saunders, 1965)

The mud volcanoes in Trinidad are seen in the last two areas, particularly the Southern Range, where the best examples are found.

3.2.2. Stratigraphy

The stratigraphy of Trinidad is illustrated in figs. 3.1 and 3.3.

a) Jurassic and Cretaceous

The oldest known formations in Trinidad are of Upper Jurassic age, found in the Northern Range. They are composed mainly of low grade metamorphosed phyllites, quartzites and recrystallised limestone. The Upper Cretaceous outcrops mainly in Southern Trinidad with a predominant lithology of silicified siltstone/claystone forming, in part, the Naparima Hill Formation. Some Upper Cretaceous shales and sandstones can also be found in the Northern Range. The general lithology reflects quiescent conditions during the Upper Cretaceous. It passes downwards transitionally into the dark calcareous shales of the underlying Gautier Formation. The uppermost Cretaceous shows the reversion to the uniform dark calcareous shale of the Guayaguayare Formation (fig. 3.3).

Movements initiated in the Late Cretaceous persisted throughout the Tertiary and resulted in the separation of the Northern and Southern Basins.

b) Tertiary

i) Palaeocene
During the Palaeocene, a transgression occurred, which formed two formations: the non-calcareous marine shales and subordinate sandstones of the Chaudiere Formation in the Central Range, and the calcareous shales of the Lizard Springs Formation in the Southern Range (fig. 3.3).

There is evidence of tectonic activity during the deposition of these formations. This resulted in conglomerates with exotic blocks and slip masses from Cretaceous formations, including ones not found in outcrop. These deposits were first recognised by Kugler (1953) who refers to them as "wildflysch", as do Barr and Saunders (1965). The same deposits are termed "olistostrome" by Higgins and Saunders (1974) and Carr-Brown and Frampton (1979). They are the first of several examples of this enigmatic type of deposit found in the Tertiary (see Higgins and Saunders, 1974, for definitions of "wildflysch" and "olistostrome").

ii) Eocene
In the south, the Lower and Middle Eocene is characte rised by the foram-rich marls and calcareous shales of the Navet Formation, indicating a quiet depositional environment. It has a thickness of 400m (Kugler, 1953). In the old Central Range, it is represented by the Pointe-a-Pierre Formation which is composed of flysch deposits with evidence of turbidity current action. Kugler (1953) assigns the Pointe-a-Pierre Formation to the Palaeocene, and gives it a thickness of at least 200m. In the Upper

Fig. 3.3 Stratigraphy of Trinidad (from Barr and Saunders, 1965)

Eocene, earth movements resulted in uplift, erosion and the deposition of the shallow water sediments (coarse clastics and conglomerates) of the San Fernando Formation (fig. 3.3).

iii) Oligocene

Earth movements continued into Oligocene times and there was rapid subsidence, resulting in the deep water calcareous clays and marls of the lower part of the Cipero Formation in the Southern Basin (fig. 3.3). The Cipero Formation attains a maximum thickness of 2700m in southern Trinidad (Kugler, 1953).

At about this time, The Central Range Uplift was active, forming a barrier between the northern and southern depositional basins. This renewed movement caused a second cycle of olistostrome deposition contemporaneous with the Nariva Formation. This is restricted to the Central Range. Olistoliths include many large slip masses of older formations and recycled components of Palaeocene olistostrome.

The Cipero and Nariva Formations pass without break into the Miocene.

iv) Miocene

Four Lower Miocene facies can be found; these are, from north to south,

- Cunapo Formation on the southern flank of the Northern Basin - conglomerates that formed during the uplift of the Northern Range and continued into the Pliocene.
- Brasso Formation in the Central Range (fig. 3.3). This intergrades with the Cunapo, forming calcareous clays and silts with rare conglomerate facies. Fauna indicate an outer neritic environment of deposition. This has a thickness of 1800m (Kugler, 1953).
- Upper Cipero Formation. Deep water calcareous clays and marls.

This formation contains important oil-producing sands, the Retrench sands (Lower Miocene) and the Herrera sands (Middle Miocene), (fig. 3.2).

- Nariva Formation. This interdigitates with the Brasso and Upper Cipero Formations (fig. 3.3). Although it is first seen in the Oligocene, the Nariva is predominantly a Miocene formation (Barr and Saunders, 1968). It contains benthonic, mainly arenaceous fauna and its planktonics suggest deposition in a turbid deep water environment (Carr-Brown and Frampton, 1979). The sands in the Nariva form the oldest major oil reservoirs in Trinidad. Kugler (1953) gives it a maximum thickness of 2000m, whereas Higgins and Saunders estimate its thickness at 3000m. Three mud volcanoes are associated with the Nariva Formation (Higgins and Saunders, 1974), including Piparo (section 3.2.5).

Overlying the Cipero Formation are the Karamat and Lengua Formations (fig. 3.3). The Karamat is formed of non-calcareous clays with some sands and seems to mark the third instance of Tertiary olistostrome deposition (Carr-Brown and Frampton, 1979). These authors use the evidence that it "contains distinctive arenaceous foraminiferal fauna, sometimes accompanied by calcareous benthonic and planktonic species" to prove its chaotic depositional environment. Olistoliths range in age between Upper Cretaceous and Lower Miocene. (The Karamat Formation is thought to be of Upper Oligocene age by Kugler (1953)). In the Rock Dome area (fig. 3.1), the Karamat has a maximum thickness of 1200m on the flank of the structure and a minimum thickness of 150m in the syncline to the north. This is attributed to "flow" by Higgins and Saunders (1974), who associate the formation with some mud volcanoes. The Karamat Formation is known to be highly overpressured and to cause drilling problems; some cores sampled from the formation shattered into small pieces upon removal, revealing shiny shear surfaces (Higgins, pers. comm., 1986).

The Lengua Formation is formed of calcareous clays, indicating outer neritic conditions. It is thought by Barr and Saunders (1965) that it was deposited during the folding phase in the upper part of the Lower Miocene. The thickness is estimated at 600m (Kugler, 1953). Its equivalent in the Central Range is the Tamana Formation with shallower marine clays. The Lengua clays, together with the overlying Lower Cruse clays (fig. 3.3), are associated with many of the southernmost mud volcanoes in Trinidad (Higgins and Saunders, 1964, 1974), including Palo Seco (fig. 3.1; section 3.2.5).

In the Central Range, reefal limestones, marine clays, silts and glauconitic sands formed during late Lower to Middle Miocene times. By this time, the Central Range acted as a barrier between the northern and southern depositional basins.

In the Northern Basin, the Tamana clays were followed by the silty San Jose member of the Manzanilla Formation and the Telemaque member (sandstones and clays), (fig. 3.3). The Manzanilla sequence indicates an infilling and shallowing of the Northern Basin.

In the Southern Basin, the Lengua Formation was followed by shallower sediments. The whole period saw a series of transgressions and regressions, ultimately leading to the infilling of the basin. Following Lengua, the Cruse, Forest and Morne L'Enfer Formations (fig. 3.3) each starts with a clay member then becomes very sandy towards the end of the phase (the first two contain submarine slump deposits). The Lower Cruse clays have a thickness of 1200m; they are described as "the last of the major submarine turbidity deposits" by Kugler (1953). The Middle and Upper Cruse, the Forest and the Morne l'Enfer Formations have maximum thicknesses of 750m, 600m and 500m respectively. They are the main oil-producing formations in Trinidad.

Kugler (1933, 1953) mentions the Moruga Formation (fig. 3.1), with a maximum thickness of 3000m, which "seemingly embraces the entire Miocene above the Lower Cruse clay". It is a graded silt with thick sand beds. Kugler (1933) associates the deposition of the Moruga with almost uninterrupted activity of sedimentary volcanism. He describes "great masses of mudflow interbedded between the Moruga beds" and "numerous dykes along or parallel to cross-faults or irregularly injected into shattered zones".

Shallow water deposition continued into the Lower Pliocene in the Southern Basin.

v) Pliocene

The Lower Pliocene marks the final infill stages of the Northern and Southern Basins. The two have completely different lithofacies. The final stages of the Andean orogeny took place during the Middle Pliocene, ending a long depositional history which had continued, almost uninterrupted since the Palaeocene. From the Upper Pliocene onwards, there were several periods of uplift, erosion and the formation of terraces and flood plain deposits.

In the Northern Basin, the shallow water Springvale Formation is overlain unconformably by the Talparo formation (clays and some sand - 1000m thick). In the Southern basin, a minor unconformity

separates the Lower Pliocene sandy Erin Formation and the underlying Morne l'Enfer Formation, although it is difficult to distinguish between the two (fig. 3.3).

By the Middle Pliocene, the Northern and Southern Basins were completely infilled. The Northern Basin is now composed of approximately 4500m of shallow water sediments of Upper Miocene and younger age overlying the Lower Tertiary. The Naparima Fold Belt contains a folded succession of Lower Tertiary and Oligo- Miocene beds with a thickness of around 5000m. The Southern Basin (Erin-Siparia-Ortoire Syncline) contains approximately 5500m of Lower Tertiary to Pliocene sediments (Higgins and Saunders, 1974).

3.2.3. Structure

Trinidad is situated at the junction between the North and South American plates, and the westward-subducting Atlantic ocean floor (Bertrand and Bertrand, 1985). The structure of the area is therefore continuously affected by the tectonics of the region. The five morphological divisions of Trinidad are related to structure. The major folding systems are the uplift of the Northern Range, the Northern Basin syncline, the Central Range uplift, the foothills of the Naparima Belt, the synclinal Southern Basin and the anticlinal Southern Range (figs. 3.2 and 3.4).

The Northern Range has a southward dip of 30-40°. The southern margin is related to the famous El Pilar fault system (right lateral wrench fault). The contact between the metamorphics and the Tertiary cannot be seen, but a very large scale fault is suspected with a downthrow to the south.

The general structure south of the Northern Range has a southward trend of overfolding and in some cases, overthrusting of structures (fig. 3.2; Barr and Saunders, 1968). There are, in addition to fold-associated faults, a series of younger, mostly wrench faults. Some are thought to relate to regional systems.

The Northern Basin (Caroni Syncline) occurs south of the Northern range and is obscured by terraces, swamps and alluvial systems. The unconformity with the Northern Range is exposed, however, and so is the north-dipping southern limb of the syncline. The Central Range uplift occurs south of this structure, showing an unconformity between the Lower Eocene and Upper Tertiary. The southern flank of the anticline is severely faulted by a complex combination of thrusts and possibly wrench faults.

The Naparima Fold Belt occurs immediately south of the Central Range; this is a steeply northward-dipping and in part strongly folded succession of Oligocene and Lower Tertiary beds. They have little structural character, however, as the structures are small and discontinuous. The "wildflysch" lithology is common. It was initially attributed to tectonic origins but was later observed to be sedimentary (Kugler, 1953). The edge of the Southern Basin in marked by folding (figs. 3.2 and 3.4).

The southernmost onshore structures are the Siparia-Ortoire Syncline and Southern Range Anticline (figs. 3.2 and 3.4). The syncline is a very well-defined structure spanning the width of the island. The "anticline" lies south of that and is, in fact, a series of folds with a very regular northern flank, but a heavily faulted and southward-thrust southern flank. This dies away to the east where a series of

After Higgins & Saunders (1974)

Fig. 3.4 Map of Trinidad mud volcanoes and associated structures

en-echelon folds become dominant. Just south of those are the tightly folded, "diapiroid" structures. These lie between Guayaguayare and Moruga and have associated mud volcanoes. The southern limb of the anticline is thought to flank a syncline 10 - 12km offshore, as suggested by geophysical data.

A major right-lateral wrench fault, the Los Bajos fault, offsets the structure of southwestern Trinidad (fig. 3.4). The maximum displacement along the fault is thought to be about 10 km (Wilson, 1965). It has been extensively studied offshore to the west where important oil prospecting takes place.

The structural history of Trinidad was summarised by Persad (1985) into Middle Mesozoic rifting, Late Cretaceous orogeny, observed in the Central Range, and Pliocene to Recent strike-slip faulting.

3.2.4. Mud Volcano Occurrences and Associated Geology

Higgins and Saunders (1974) report 26 active mud volcano areas in Trinidad and 4 fossil ones. They also list some examples which may well be mud volcanoes offshore, but have not been investigated further. The mud volcanoes are found south of the Central Range (fig. 3.4). Three are associated with the Naparima Fold Belt and the rest are found in the Southern Basin and Southern Range Anticline. The East Venezuelan mud volcanoes lie on the same structural trends extending westwards from Trinidad (fig. 3.4).

As mentioned above, the mud volcanoes are associated with mid- Tertiary, thick clay sequences: the Nariva, Karamat and Lower Cruse-Lengua Formations (Higgins and Saunders, 1974). The Nariva and Karamat Formations are both known to cause drilling problems, where mud weights were sometimes needed to prevent formation clays from flowing into the well; the former occasionally oozed out like toothpaste, while the latter has been known to shatter into small pieces, as mentioned above. Higgins (1959) published some well log data from wells drilled adjacent to mud volcano areas in south Trinidad, Barrackpore well 345, south of Digity mud volcano (fig. 3.5.a), Morne Diablo well 34 (fig. 3.5.b), near Morne Diablo mud volcano and Moruga well 15 (fig. 3.5.c), near Moruga Bouffe mud volcano (for positions, see fig. 3.4). The first shows a thick regressive Tertiary sequence, the clay unit (1km of Lower Cruse) occurring at a depth of approximately 1.7km. This is associated with a slight decrease in velocity, which may be an indicator of overpressuring (section 1.2.11). Well Morne Diablo 34 shows a very thick shale sequence associated with relatively low densities and velocities between 1.2 and 1.8km (Karamat-Lower Cruse). The Moruga 15 well also shows a thick shale sequence. Low densities and velocities are encountered at 700m - 1km (Palaeocene and Oligocene); these, however, are interpreted as being the result of thrust faulting. The author had access to confidential sub-surface data in the mud volcano areas which tends to show similar features. A well drilled near Piparo mud volcano (no. 1, fig. 3.4) penetrated a very thick sequence of thrusted, slickensided shales; the Nariva formation, thought to be the source of Piparo, is encountered at a depth of over 2000m. Similarly, wells drilled west of the Anglais Point mud volcano area (no. 5, fig. 3.4) penetrated thick sequences of Lower Cruse clays and shales. Also, in the Palo Seco area (no. 4, fig. 3.4), one well showed "mixed fauna clays", which are thought to be diapiric clays, at approximately 2000m depth (Sumadh, pers. comm., 1986). This evidence therefore supports Higgins and Saunders' (1974) views on the depth of the source beds.

Fig. 3.5 Three well logs from Southern Trinidad. a. Barrackpore Well no.345; b. Morne Diablo Well no. 34; c. Moruga Well no. 15; (from Higgins, 1959).

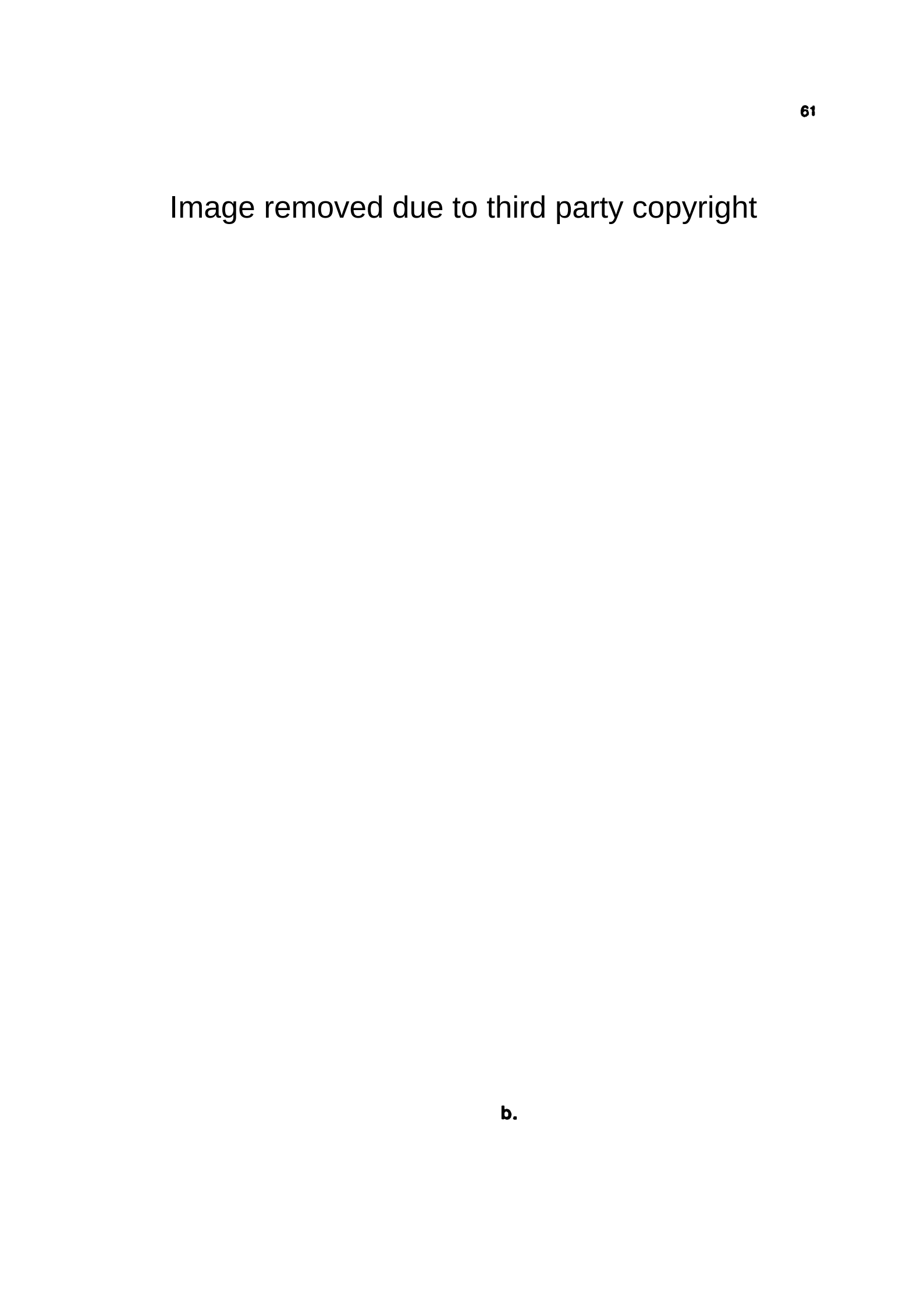

b.

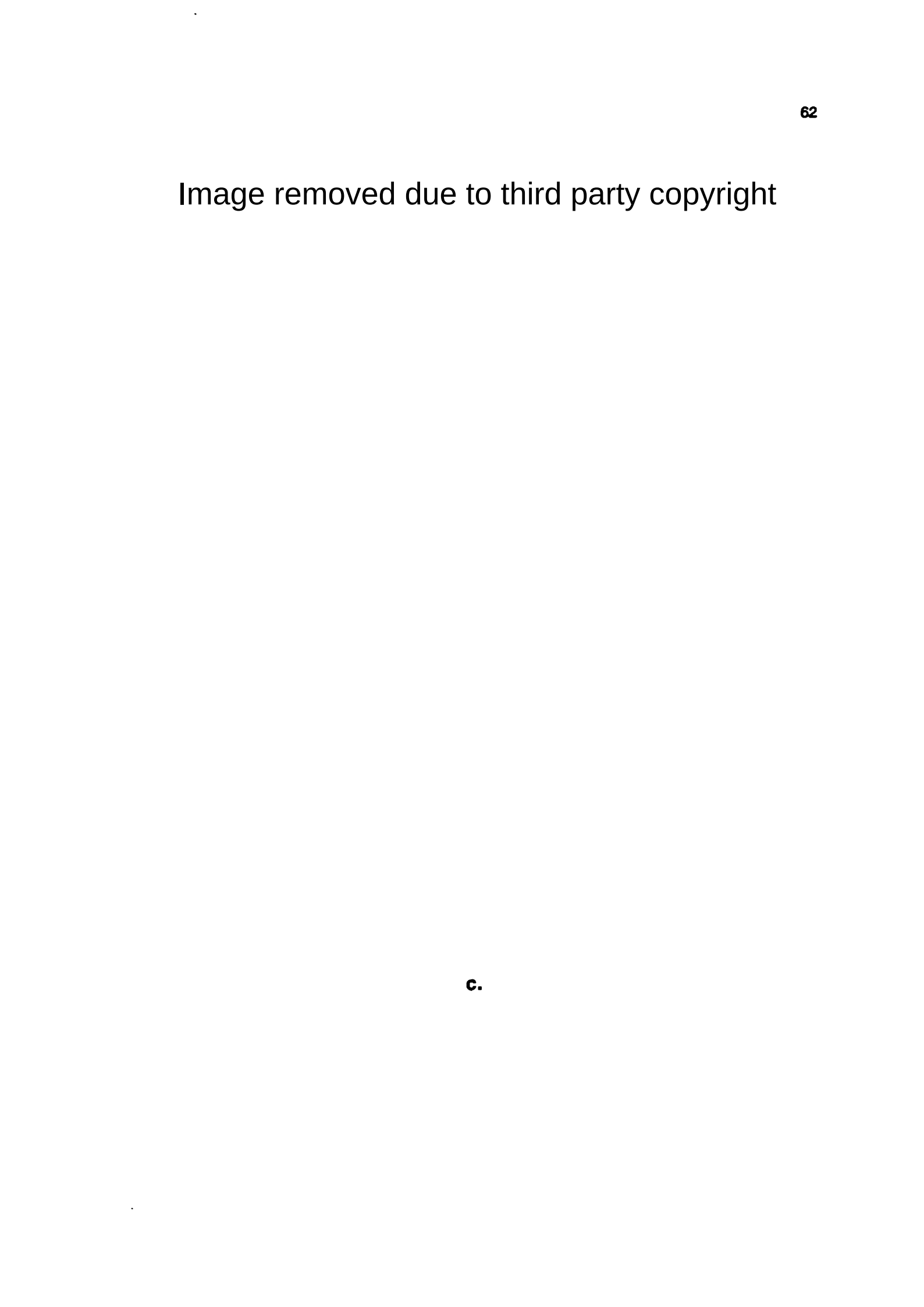

c.

More evidence on the source of the Trinidad mud volcanoes is provided by offshore seismic sections. Fig. 3.6. shows the edge of a very large offshore diapir south of Trinidad. A well drilled nearby indicates that the clays were originating from the Lower Cruse at approximately 3650m, or possibly from the deeper Lower Cruse-Lengua at approximately 3800m; the latter contained re- worked older formation material (Birchwood, pers. comm., 1988). (No pore pressure data could be obtained for the Trinidad formations; the only published data known to the author are in Chapman (1983), where pressure-depth plots of shallow oil reservoirs show λ values of 0.8 at approximately 1km.)

There is a distinct association between structure and mud volcanoes in Trinidad (fig. 3.4). A study of the map compiled by Kugler (1959), and a later, tectonic, map compiled by Persad (1985) shows this association very clearly. The majority of the mud volcanoes occur in the Southern Range Anticline area, which extends offshore into Erin Bay to the south west of the island. Very good examples of mud volcano islands have been reported in that area in association with the axis of the anticline (Arnold and Macready, 1956; Birchwood, 1965; Higgins and Saunders, 1964; see no. 9, fig. 3.4). Two or three mud volcanoes are associated with the Los Bajos Fault onshore (fig. 3.4). Large scale mud flows/diapirs have been observed along this fault, as well as other wrench faults in seismic sections offshore, to the west of Trinidad (Frampton pers. comm., 1986). Fig. 3.6 shows a diapiric structure offshore, south of Trinidad. Mud volcanoes are almost always seen to extrude in the area of a thrust fault, such as Lagon Bouffe (6), Moruga Bouffe (7), Devil's Woodyard (3) and Piparo (1) or a strike-slip fault, such as Palo Seco (4) and Anglais Point (5), (fig. 3.4; Kugler, 1959).

3.2.5. Field Description of Mud Volcanoes

The author visited six active mud volcano areas in Trinidad: Piparo (1), Digity (2), Devil's Woodyard (3), Palo Seco (4), Anglais Point (5) and Lagon Bouffe (6), fig. 3.4. Three other important examples of sedimentary volcanism in Trinidad are also described: Moruga Bouffe mud volcano (7), Forest Reserve Field fossil mud volcano (8) and the mud volcano islands offshore to the south of Trinidad (9), fig. 3.4. A full field description of all the known examples of mud volcanism on the island can be found in Higgins and Saunders (1974).

1) Piparo

A small very muddy pool was found by the side of Piparo Road. This was circular, with a diameter of 50cm and a "depth" of 1m (plate 3.1.a). It bubbled gas continuously and was filled with saline water. The sample labelled (PIP) was taken from this volcano. Higgins and Saunders (1974) studied the area more fully and they reported the abundance of exotic blocks - not around the centre of activity, but within the mud flow area which covers an area of 180 hectares. The volcano is known to have changed size over the years, according to the intensity of activity. It is also known to be violently eruptive. The last violent eruption occurred in 1969, when the ground moved sufficiently to damage houses 60m away. It was not felt beyond 90m.

Fig. 3.6 Seismic section offshore Trinidad showing the edge of a large clay diapir (courtesy of TRINTOC Ltd., Trinidad)

a.

b.

c.

d.

Plate 3.1 Trinidad mud volcanoes: a. mud volcano pool, Piparo; b. mud volcano cone, Digity (1); c. mud volcano cone with active mudflow, Devil's Woodyard; d. exotic blocks in the mud, Devil's Woodyard

2) Digity

This is a classical cone-shaped volcano (plate 3.1.b). It is 4m high with a base diameter of 4-5m and a crater diameter of 40cm. The sides are inclined at an angle of 32° and appear quite rubbly, possibly due to ejected exotic blocks in periods of more violent activity. Two basin-shaped mud volcanoes can be found less than a 100m to the west of this. These are 3-4m in diameter. Sample (DIG1) was taken from the cone and (DIG2) from one of the pools. The area of the mudflow is estimated by Higgins and Saunders to be 180m by 75m.

Wells drilled in the Digity area encountered significant drilling problems due to overpressures (Sumadh, pers. comm., 1986).

3) Devil's Woodyard

This was the best example of a "tassik" seen by the author (plate 1.2.a), (although a more dramatic, larger scale equivalent, Moruga Bouffe, is known to be the most spectacular mud volcano area in Trinidad - see text below). The first violent eruption was reported in 1852 by Wall and Sawkins (1860). Another was reported by Cunningham-Craig (1905) which occurred in either 1888 or 1889. Cunningham-Craig visited the site in 1905 and found it almost completely overgrown. In 1906, another major eruption occurred which formed a "crater" 90m in diameter and 2m high with small cones in the centre. Kugler (1933) describes this eruption: "an area of 15 to 20 acres of forest were blown down and covered with 15 to 20 ft. of very viscous mud.....500,000 cubic yards were extruded in less than 20 minutes. " The margins of the mud were said to have stood almost vertical. The temperature was 30°C, the ambient temperature.

Higgins and Saunders visited Devil's Woodyard just before and after a major eruption in 1969 and witnessed notable changes. They found the surface to be hummocky - very similar to the textures seen on the mud volcano islands (Wilson and Birchwood, 1965; Higgins and Saunders, 1964). The ground had risen a further 2.5m and 3 weeks later, by a further 60cm. A block of Lengua clay was found in the soft mud. The area ended up as a circular tassik, 115m in diameter. The shape was shield-like (Shih, 1967) with small steep cones in the centre. This suggests that the tassik is the site of an underlying, more solid diapir, as suggested by Barber (1986) for the Timor mud volcanoes and Ridd (1970) for the New Zealand examples. Higgins and Saunders (1974) estimate the mudflow area at 900 by 750m.

When the author visited the area in November, 1986, it was a flat, circular tassik, 80-90m in diameter, with several active cones. The old edges of the tassik were visible but overgrown with grass. The cones were less than 1m high, the sides varying in steepness between 15 and 30° (plate 1.2.a). Sample (DW) was taken from one of these cones (plate 3.1.c). Flatter cones to basin-type mud volcanoes were observed at the northern edge of the tassik. Exotic blocks were found in abundance in the ground (plate 3.1.d) These were never observed in the act of coming up in the mud, although some of the cones contained blocks embedded in their sides. The blocks were generally small - less than 20cm; this size, however, could be due to breakdown of larger blocks. These were identified as grey Herrera sands, Cretaceous chert (very rounded), red Pointe-a-Pierre sandstone/siltstone, and soft green Lengua clay (also rounded), (Carr-Brown and Frampton, pers. comm., 1986). See Chapter 4 for a more detailed description of the clasts.

4) Palo Seco

This is a large mud volcano area. Higgins and Saunders estimate its active aerial extent at 0.5 hectares, but ascribe 24 hectares to the total surrounding mudflow area. It has no obvious tassik, but numerous small clearings in the jungle where individual volcanoes are found. The shapes vary from small steep cones, to flattish "shields", to the predominant basins which can have a diameter of up to 10m. Palo Seco 1 (PS1) was such a basin, with prominent gassing near the centre and obvious oil slicks on the surface (plate 3.2.a). The volcano had a strong oily smell. 5m to the east of this, Palo Seco 2 (PS2), a 1.2m high cone with 50 steep sides, was found. The path led southwards to several small pools 1-3m in diameter, until a small clearing, 8m in diameter was reached. This contained two low shields, less than 50cm high, with sides inclined at 15°. The sample labelled Palo Seco 3 (PS3) was obtained here. Not all the centres of activity could be visited as they were numerous and some were inaccessible. No exotic blocks were found.

5) Anglais Point

This is a spectacular mud volcano on the southern coast of Trinidad. It is a low dome-shaped volcano with a diameter of 60m (plate 3.2.b). It is particularly interesting because of the "glacier" of mud extending southwards from it into the sea, the length of which is estimated at 260m. The volcano itself has a rough surface with very small low angle cones a few centimetres high (no more than 15cm). Gas escapes from cracks in the mud. The mud, unlike all the other muds sampled by the author (AP), contained a large proportion of solid grey fragments of mudstone (APC). These were found to have identical mineralogy to the wet mud (section 4.3). In fact, Anglais Point extrudes very large blocks (up to 1m) visible in the hummocky surface of the landslip (plate 3.2.c); Kugler (1933) describes very large individual blocks of Eocene age of up to 42 m^3, and a block of Cretaceous silicified shale of approximately 4.5 m^3). At the toe, the blocks form a semi-circular pattern, convex seawards. Some were collected and are described in Chapter 4. Note that Palo Seco is very close by, but showed no evidence of exotic blocks.

Higgins and Saunders (1974) suggest that Anglais Point experiences "paroxysmal eruptions with periods of several years between each". The first recorded eruption occurred in 1900 (Cunningham-Craig, 1905). A later eruption (1906) "was said to have been heard for more than 1500m distance" (Higgins and Saunders, 1974). The volcano was then 75m wide and the flow was 230m long. C. C. Wilson reported (verbally) that the eruption in 1960 raised the volcano by 2m. The firm mud moved slowly towards the sea. The volcano was not particularly active at the time it was visited by the author.

As suggested for Devil's Woodyard (plate 1.2.a), it is possible that Anglais Point is a diapir, because of its rounded top and general circular outline (plate 3.2.b). The presence of exotic blocks in both could suggest transport in a viscous diapiric matrix (Barber et al, 1986), but it could also be due to explosive eruptions such as those described in section 1.1.

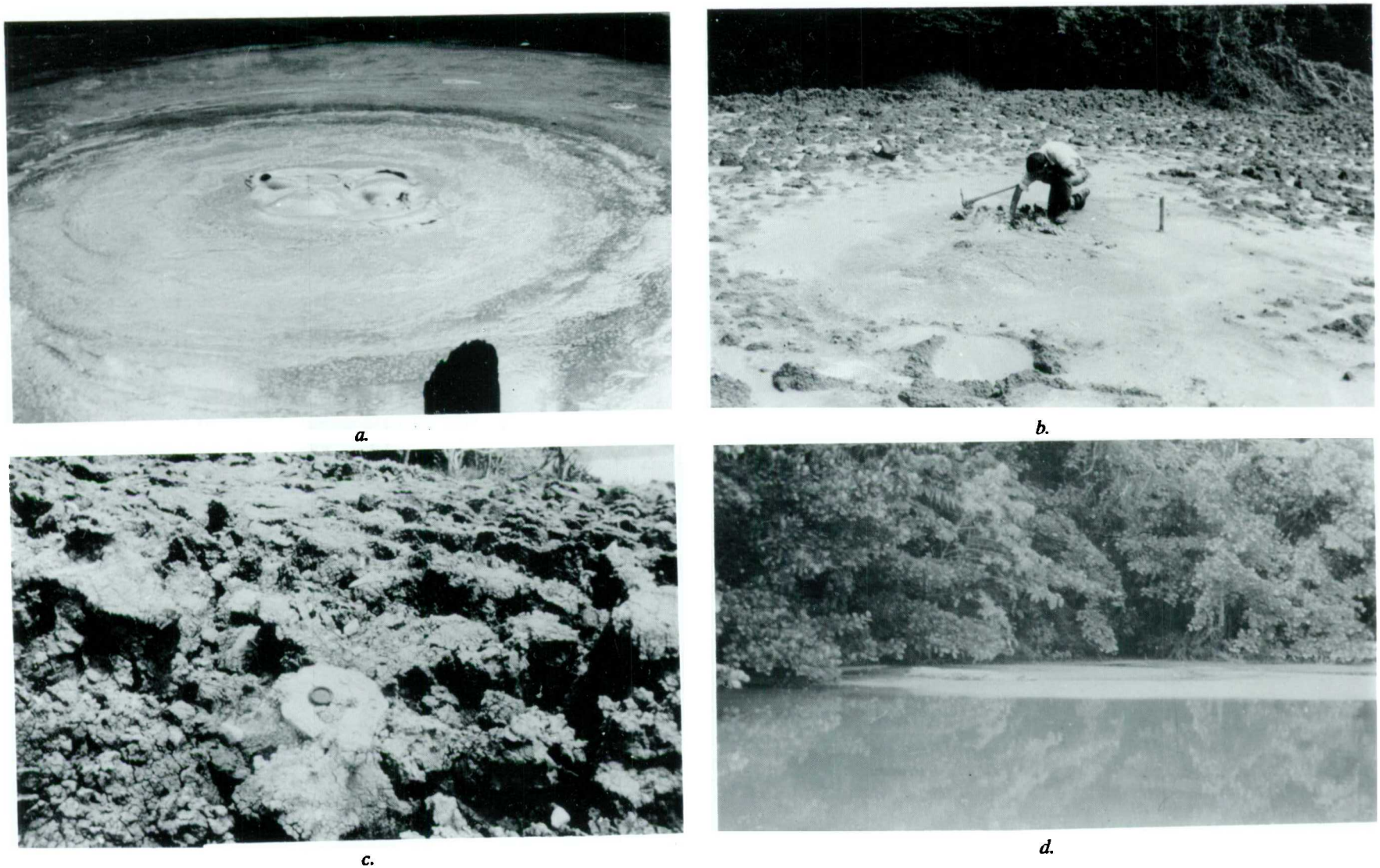

Plate 3.2 Trinidad mud volcanoes (continued): a. mud volcano pool, showing methane and oil, Palo Seco (1); b. Anglais Point mud volcano, with two small eruptive centres in the middle; c. Anglais Point mudflow, showing exotic blocks embedded in the mud; d. Lagon Bouffe mud volcano, a large lake with several eruptive centres, one of which is seen in the background.

(Oddly, the Anglais Point area is associated with a weak positive gravity anomaly (Hofman, 1949) - opposite to the generally observed negative anomalies associated mud volcanoes (section 1.2.11); this, however, could be the effect of local geology).

6) Lagon Bouffe

This is another unique mud volcano in that most of it is covered by a large lake (plates 1.1 and 3.2.d). The tassik is oval in shape, 175m by 110m. Several centres of gassing activity could be seen in the northeast and northwest sides of the lake, but the area of most activity was in the southwestern corner. This was 15m in diameter and slightly elevated above the water. The southwestern bank was very sandy. The bottom of the lake was soft and muddy; some kind of base could be felt at a depth of 1m near the edge, but this was still very soft. The area smelt strongly of oil. No blocks were observed.

Higgins and Saunders (1974) report basin-type volcanoes (5.5m diameter) and very low cones (1.5m in diameter) in the southwestern edge of Lagon Bouffe. These were presumably observed in the dry season, when more of the volcano is visible. In 1970, a period of exceptional activity saw the formation of a prominent low angle cone in the northeastern corner, which is usually under water.

Kugler (1933) associates this volcano with the Moruga Formation. He mentions that Lagon Bouffe was the only active mud volcano in Trinidad at that time. Lagon Bouffe is associated with a weak negative gravity anomaly (Hofman, 1949).

7) Moruga Bouffe

The author attempted to visit this tassik, but rainy conditions and thick vegetation made access very hazardous and the attempt was abandoned. As it is the best mud volcano example in Trinidad, however, it will be given brief mention. The tassik trends in a north-south direction, with an area of 2 hectares and a width of 120m. It is flat to slightly domed with mainly steeply-sided cones up to 2m high. The presence of extinct cones in the surrounding jungle suggests that the tassik area was much larger in the past. A company report counts a total of over 600 cones altogether (Higgins and Saunders, 1974). Moruga Bouffe is associated with faults which are thought to control the alignment of the cones and with mud dykes (Kugler, 1933). It is also the area of a substantial negative gravity anomaly of -2.5 mgals (Nettleton, 1949; Hofman, 1949).

8) Forest Reserve Field Fossil Mud Volcano

This is a rare example of a fossil mud volcano, with mud flows interbedded with, and injected into, Miocene sediments of the Forest Reserve field in Southern Trinidad (Bower, 1951; figs. 3.5 and 3.6). The "volcano" is approximately 1200m in diameter and in maximum thickness (Bower, 1965). The material is composed of clay with large angular blocks (up to 30cm length) ranging in composition from the matrix materials to younger lithological units. The matrix is dated at Upper Oligocene, which, in the near vicinity of the volcano, occurs under a Miocene cover of approximately 1500m - 2400m. Signs of post-Miocene activity, if it occurred, have been removed by erosion. The Forest Reserve Field mud

volcano is thought to have erupted in association with tectonic activity, although no clear evidence of an original structural weakness (Bower, 1951) can be shown.

9) Mud Volcano Islands

Several mud islands have also appeared south of Trinidad in 1911 (Beeby-Thomson, 1910), 1929 (Arnold and Macready, 1956) and 1964 (Higgins and Saunders, 1964; Birchwood, 1965; Wilson and Birchwood, 1965) - fig. 3.5. They were all explosive eruptions associated with large volumes of gas. The last, Chatham Island mud volcano, was formed of Lower Cruse-Lengua silty clay with blocks of Moruga Sandstone (Higgins and Saunders, 1964). No salt water was observed and the mud was highly striated. From the photographs in the report, it appears that the mud had a lower moisture content than those observed in the onshore examples, but the mud extruded in the 1906 eruption of Devil's Woodyard (described above) may have had a similar consistency. Again, this eruption could be classed as a diapir as opposed to a mud volcano, judging by its shape and the consistency of the mud. The islands were totally eroded away in a matter of months.

3.3. TAIWAN

The following information has been collated from key references on the area by Ho (1975, 1982) and Chou (1971, 1973, 1980).

3.3.1. Morphology

- **"The main island of Taiwan has been the site of geosynclinal deposition on a metamorphic basement filled with Tertiary sediments to a thickness of more than 10000 metres" (Ho, 1975). All formations in the island occur in belts parallel to the axis which trends approximately north-south (fig. 3.7). Taiwan can be divided into three major provinces (fig. 3.8). From west to east, these are,**

- **The Western Foothills: This is the best-studied province in Taiwan as extensive mineral exploration is undertaken there. It is composed of Neogene deposits. These are sandstones and shales with some limestone and tuff lenses, reaching a thickness of at least 8000m.**

- **The Central Range: This is the "backbone" of the island. All pre-Tertiary metamorphics and Tertiary sub-metamorphics are found in this province. It is bound to the east by the eastern longitudinal valley, and to the west by a major boundary fault, the Chuchih (Laonung) Fault.**

After Ho (1975)

Fig. 3.7 Geological map of Taiwan

Fig. 3.8 Structural map of Taiwan showing the two mud volcano areas

After Ho, 1982

- The Coastal Range: This too is underlain by Neogene sediments, but they are of different character to those found to the west. They are generally abundant in volcanic derivatives, including poorly sorted clastics and melanges.

3.3.2. Stratigraphy

The stratigraphy of Taiwan is illustrated in figs. 3.7 and 3.9; it was not possible to obtain a stratigraphic table for the whole island, and fig. 3.9 illustrates only the Neogene sediments of Western Taiwan - the area of interest in this study.

a) Pre-Tertiary Metamorphic Complex

This is found mainly in the eastern part of the Central Range. It is 200km long, with an average width of 20km. The metavolcanics, schists and metamorphosed limestones are all grouped under the name, Tannano Schist. The oldest date corresponds to the Permian (fig. 3.7).

b) Tertiary Submetamorphic Rocks

The western part of the Central Range is composed of metamorphosed argillaceous Tertiary sediments. It is called the argillite slate belt, 330 km long and 50 km wide. The rocks are more metamorphosed to the east, ranging in age from Eocene to Late Miocene.

i) Eocene
The dark grey slate and phyllites of this age form the highest peak in Taiwan (4000m).

ii) Eocene to Oligocene
This is represented by the Szeleng sandstone - quartzitic sandstone, dark grey slate and carbonaceous shale with a maximum thickness of 500m. It is exposed in north-central and central Taiwan.

iii) Oligocene to Miocene
Three formations have been identified: the Kanko Formation the Tantungshan Formation and the Aoti Formation (in ascending order). The first is shale and slate ranging in thickness between 600 and 1200m. The second is also a dark shale with sandy and silty interbeds. The Aoti Formation is a carbonaceous coal- bearing sequence of fine sandstone and dark grey shale.

iv) Miocene
The Lushan Formation is made up of argillite and slate of mainly Lower Miocene age.

Fig. 3.9 Miocene to Recent stratigraphy of Western Taiwan (from Ho, 1975)

c) Tertiary Non-metamorphic Rocks: The Western Foothills

i) Miocene

"A continuous sequence of Miocene clastic sediments was deposited in the western geosynclinal trough with only minor depositional breaks" (Ho, 1975). The rocks are mostly sandstones and shales, reaching a maximum thickness of 5500m. The lowest part of the Miocene is found in the northern part and is composed of arenaceous and carbonaceous rocks. This is followed by three cycles of deposition, starting with a coal-bearing unit (300- 700m) and ending with a marine unit (500-700m). From north to south, the sequence becomes thicker and more shaly.

Early Miocene: This is named the Yehliu Group, composed mainly of calcareous sandstones. The group is divided into the Wuchihshan, Mushan and Taliao Formations (in ascending order), which achieve a maximum thickness of 1450m between them (fig. 3.9).

Middle Miocene: This is named the Juifang Group, and is divided into the Shihti Formation and the Nankang Formation (fig. 3.9). The Shihti Formation is the best coal-bearing unit in Taiwan, and is composed of sandstones, siltstones and shales. The Nankang Formation is composed of fine-grained calcareous sandstone in the north, becoming more shaly to the south, and achieving a thickness of at least 800m.

Late Miocene: This is named the Sanshia Group, which is divided into the lower Nanchuang Formation and the upper Kueichulin Formation (fig. 3.9). The first is a coal-bearing formation - thick sandstones which merge into a more shaly sequence southwards. The equivalent of the Nanchuang Formation. In the south, the Changchihkeng Formation may reach up to 1600m thickness. The Kueichulin Formation is again composed of sandstones and shales in the north, again becoming finer and thicker southwards (800m to 1500m).

ii) Pliocene

These are marine clastic sediments 2000m thick in the north, and reaching a thickness of 5000m in the south (Tainan area). The series used to be referred to as the Gutingkeng Formation (Shih, 1967). It is composed of dark grey mudstone with some sandstone interbeds. Two formations in the Pliocene have been recognised. The first is the Chinshui Shale which increases in thickness from 100m in Central Taiwan to at least 1000m in the south, and is associated with olistostromes and sand pipes (Chou, 1973). The second is the Cholan Formation which is sandy in the north and shaly in the south, becoming 2500m thick. Chou (1973) states that, in the Tainan-Kaohsiung area, which is associated with mud volcanoes, it reaches 3500m.

iii) Plio-Pleistocene

Four stratigraphic units belong to this age, but only one of these, the Toukoshan Formation (fig. 3.9) is found in the western Foothills. It is a conglomerate, 1000-1500m thick, lying unconformably over the Pliocene Cholan Formation.

d) Tertiary Non-metamorphic Rocks: The Coastal Range

The most interesting sedimentary feature of the Coastal Range is the predominance of melanges. The Miocene and Pliocene attain a combined thickness of 6000-7000m. Five units can be recognised here,

i) a Miocene igneous complex,

ii) the Tuluanshan agglomerate series, also of Miocene age. This is 1500m thick,

iii) a marine clastic formation of Upper Miocene to Pliocene age; this is dark grey shale, 3000m thick, and showing turbidity features,

iv) a chaotic melange of Plio-Pleistocene age. This is called the Lichi Formation - a sheared argillaceous matrix with enclosed ophiolite and sandstone blocks, found in the southern part of the Coastal Range. It is at least 1600m thick. Chou (1973) relates it to olistostromes.

v) the Pinanshan Conglomerate in the southern part of the Coastal Range, also of Plio-Pleistocene age; it reaches a thickness of 1400m.

Chou (1973) states that the rate of deposition in the Middle Pliocene to the Pleistocene was slightly greater than the rate of subsidence.

3.3.3. Structure

Taiwan is an island arc/continent collision zone on the western border of the Pacific Ocean. The arc is convex to the east, and the structural pattern of the island contradicts this pattern, showing convexity to the west. The main structural patterns are as follows (fig. 3.8),

a) The Western Coastal Plain is underlain by Neogene beds, tilting gently eastwards without marked folding. To the east and north of this plain, younger Neogene and early Pleistocene beds are gently folded, breaking off to the east along thrust faults.

b) The Western Foothills are found to the east of these thrust faults. The strata here are heavily folded and faulted. The folds are asymmetric, the axial planes dipping steeply to the southeast; most are broken off by faults. Many of the faults are low angle thrusts, moving sheets to the northwest.

c) The mountains of the Central Range occur to the east of the Western Foothills. The western part consists of an argillaceous sub-metamorphic belt. Here, open and tight folds are found, traversed by longitudinal thrust faults. The eastern part is composed of highly deformed crystalline metamorphics. The structure here is difficult to resolve due to repeated deformation.

d) The Central Range is separated from the Coastal Range by what is referred to as a rift valley, the East Taiwan Rift, although it is bordered by two active thrusts with a left-lateral wrench movement,

the Central Range Fault and the Coastal Range Fault. Recent earthquake activity has been associated with movement along these faults. The origin of the valley is therefore thought to be compressive.

e) The Coastal Range has a faulted pyroclastic core covered by Neogene sediments. These have been involved in large scale gravity sliding and low angle nappes. A feature of major interest is the predominance of allocthonous materials, thought to be related to the tectonic activity of the region.

All the major provinces are separated by long, usually upthrust, faults extending the whole length of the island, and dipping east. Some have a wrench component. Fig. 3.10 shows a cross section through southwestern Taiwan, just north of Tainan (fig. 3.8). Taiwan is also an area of continuous seismic activity (fig. 3.11).

3.3.4. Mud Volcano Occurrences and Associated Geology

There are 17 mud volcano areas in Taiwan and 64 active individual volcanoes within these areas (Shih, 1967). They occur to the southeast of Taiwan (north of Taitung) and to the southwest (southeast of Tainan) - fig. 3.8. The majority are situated in the latter area (fig. 3.12).

The mud volcanoes in the southeast are associated with the Lichi Formation (Plio-Pleistocene). In the southwest, they are associated with the Gutingkeng Formation, of Pliocene age (Shih, 1967) - see fig. 3.12 and section 3.3.2. As with Trinidad, both formations are associated with melange-type deposits. The Gutingkeng Formation attains a thickness in the south of up to 5000m. Well log data in the general area indicates several kilometres of almost uninterrupted argillaceous sediments (Chou, 1971). Two wells were abandoned at 3946m and 5151m, due to the caving in of very thick shales (Hsieh, 1972). No oil or gas were encountered.

The structural association with mud volcanoes is again evident here (fig. 3.12). Shih (1967) associates the areas of mud volcanoes in Taiwan with fault lines parallel to anticlines. Fig. 3.10 shows this association. Shih (1987, pers. comm.) has stated that these are reverse faults parallel to the regional structure of Taiwan, the movement being in a northwestern direction. The southeast mud volcano region also occurs in a region of seismic activity (fig. 3.11).

Two diapiric structures are known to occur a few kilometres to the west-northwest of the Tainan mud volcano area (Hsieh, 1972). These are both elongate and parallel with the structural trend of the area (approximately northeast-southwest), fig. 3.13. They are composed of a minimum thickness of 3500m of Lower Gutingkeng mudstone. They show no seismic reflections and irregular core dips, as would be expected from a diapiric structure; however, the Bouger gravity anomaly over them is positive (max. +22 mgal), indicating high density (fig. 3.13). This figure also shows that the mud volcano area is associated with a negative gravity anomaly (minimum of -15 mgal). The two diapirs are now fully consolidated, as suggested by the densities of 2.6 g/cc as opposed to L. Gutingkeng outcrop densities of 2.1-2.3 g/cc (Hsieh, 1972). It is possible, therefore, that activity has shifted towards the southeast (fig. 3.13). Hsieh (1972) interprets the structures bordering these diapirs as normal faults; this could be explained by the downward movement of the surrounding sediments as the diapirs were emplaced.

Fig. 3.10 Cross section through southwest Taiwan (from Shih, 1965)

Fig. 3.11 Seismic epicentres of Taiwan (from Ho, 1982)

After Liu (1969)

Fig. 3.12 Geologic map of Tainan mud volcano area, Taiwan

Fig. 3.13 Bouger gravity map of Tainan area, Taiwan (after Hsieh, 1972). The shaded area is the mud volcano area and line A - A' marks the westward extent of the Gutingkeng formation outcrop.

3.3.5. Field Description of Mud Volcanoes

Four mud volcano areas were visited by the author: Aoshenshui (1,2), Wushanting (3), Chienchuliao (4), and Hsiaokungshui (5,6), fig. 3.12. These are all found in the Tainan area. For a full description of all the known occurrences of mud volcanoes in Taiwan, see Shih (1967).

1) Aoshenshui

Two mud volcanoes were found in this area. The first, T-1, looked like two interconnected basins, 10m in diameter. Two centres of activity were observed in the watery mud, from which gas bubbled noisily and continuously. Oil was observed on the surface of the water. T-1 is Shih's Ao 3D (1967), as indicated by its position and the photograph (plate 3.3.a). A few hundred metres north- northeast, T-2 was found. Here, a long 20m channel of mud was found coming from an elevation (to the east) and trickling into the valley below (to the west). The source of the channel was found to be a steep cone (T-2), 1m across and 1m high, the crater diameter being 10cm. Very watery mud was pouring out of this volcano, as though it was also the vent for a spring. Shih (1967) mentions two cones and a basin in the area. T-2 is thought to be one of the cones (Shih's Ao 1A).

2) Wushanting

This is a classic "tassik" 150-200m wide and 150m across. It contains three main steep cones (labelled T-3-1, T-3-2 and T-3-3) and two smaller, shield-type cones. T-3-1 (Ting 4A, Shih, 1967) is inactive; Shih mentions that in the 60's, its periods of activity were very intermittent. It is 2m high with a 45° inclination of the sides. The top of the cone is 30cm wide. It is very silty, also containing small rounded pebbles. T-3-2 (Ting 2A, Shih, 1967) is approximately 1m high, and 50cm wide at the top. The sides are inclined at an angle of 25° or so near the base, increasing upwards to 45°. It is highly active, erupting vigorously every 3 minutes. The mud is dark and viscous, forming tongue-shaped flows (plate 1.2.b). From the 1967 photographs, it seems to have decreased in size. T-3-3 (Ting 3A, Shih, 1967) is 3m high. The top of the cone is 50cm in diameter and the sides are inclined at an angle of 45° (plate 3.3.b). This too is highly active, with gas bubbles bursting continuously through the mud (reminiscent of Digity in Trinidad). One of the two other cones in the area is possibly Shih's Ting 1A. Shih (1967) also mentions Ting 5D - a basin type mud volcano 100m away. As with Devil's Woodyard in Trinidad, the tassik appears to have been larger in the past as it is surrounded by an unwooded, yet grassy flat area.

3) Chienchuliao

Here, a mud basin with a diameter of 20m was found (T-4). This is Shih's Chien 1D which used to be 15m in diameter (plate 3.3.c). Large quantities of gas bubble out of the centre of the volcano which, when lit, produce a bright orange flame. Oil is also visible on the surface of the watery mud. Shih (1967) describes another two volcanoes in the area, one of which, also a basin, has the highest temperature amongst the volcanoes (41°C). Oil exploration in Chienchuliao in 1908 was unsuccessful. No oil was

a.

b.

c.

d.

Plate 3.3 Taiwan mud volcanoes: a. mud volcano pool with methane bubbles, Aoshenshui (T1); b. mud volcano cone, Wushanting (T3-3); c. mud volcano pool with ignited methane, Chienchuliao (T4); d. mud volcano pool, Hsiaokungshui (T5).

found at 445m where the well was abandoned. However, four natural gas zones were found at less than 200m depth and a water zone was found at 140m.

4) Hsiaokungshui

Two basin type mud volcanoes were found in this area. The first, labelled T-5 (Shih's Hsiao 6D) was approximately 6m in diameter, bubbling gas continuously (plate 3.3.d). This too was lit, producing the same orange flame. Approximately 30m southeast of this, T-6 (Shih's Hsiao 5D) was found. This was 5m in diameter and was not as active as the others. It had a man-made channel in its northwestern side which controlled the mud flow. The "levees" on either side showed the extent and volume of mud ejected. They stretched for tens of metres, showing mud cracks and fossil rain drop marks. Shih (1967) describes both in a similar way, except that they were both 10m in diameter in the 60's. A picture of T-6 (Hsiao 5D) in Shih's paper shows the same channel mentioned above. Within a radius of 1 km of these volcanoes, Shih observed eight mud volcanoes of various sizes and shapes.

3.4. SUMMARY OF MAIN FEATURES OF THE MUD VOLCANO AREAS IN TAIWAN AND TRINIDAD

- **Both areas are tectonically active, and the mud volcanoes are closely associated with structure such as thrust faults in Taiwan and strike-slip faults and anticlines in Trinidad. In Taiwan, one of the mud volcano areas occurs in a region of very high seismicity. Diapirs are also known to occur in both areas; there is some evidence in Trinidad that the tassiks could be the surface outline of an underlying diapir.**

- **The mud volcanoes are associated with thick mid-Tertiary regressive clay sequences. In Taiwan these sequences show considerable fining and thickening (up to 5000m) towards the southwest. In Trinidad, the maximum thickness of an individual formation associated with mud volcanoes is 3000m.**

- **Both areas have undergone a history of rapid sedimentation associated with the tectonic activity, and melanges are mentioned in both areas in association with the parent beds.**

- **Pore fluid pressures of up to 80% of the geostatic load are known in both areas (section 1.2.1).**

- **Both areas are oil-producing (particularly Trinidad) and both suffer considerable drilling problems in the overpressured formations.**

- **The volcanoes in both areas show a similar spread of the varieties.**

CHAPTER 4

CLASSIFICATION AND DESCRIPTION OF MUD VOLCANO CLAYS

4.1. INTRODUCTION

Samples of the mud volcano materials collected were the subject of various laboratory analyses. This chapter describes the results of grain size distribution and mineralogy analyses and presents the microscope description of the coarser fraction of the samples. Where possible, micropalaeontological data is also included. The purpose of these tests is to estimate the age and composition of the material, assess the possibility of contamination of the extruded muds by overburden material and to make comparisons between different mud volcano areas. Finally, the results of Atterberg limits tests on the muds will be presented, and compared with the particle size distribution and the mineralogy. These tests provide an introduction to the geotechnical characteristics of the sampled materials.

The samples tested are collected from the mud volcanoes in Taiwan and Trinidad. A few more samples are used for comparison, from a mud volcano in North Tanimbar, collected by Kaye, University College London, in 1986, and from West Timor, collected by Harris, University College London, in 1987.

4.2. PARTICLE SIZE DISTRIBUTION

4.2.1. Introduction

This is one of the most basic and most useful methods of classifying a sediment. Geologically speaking, the particle size distribution (PSD) can give some idea about the origin of the extruded material; also, comparisons with PSD's of equivalent samples can give an indication of possible contamination by overburden material.

The PSD analysis was carried out using the method described in BS1377 (summarised in Appendix 1). The samples analysed were AP, DIG1, DIG2, DW, LB, PIP, PS1, PS2 AND PS3 from Trinidad, T1, T2, T3-2, T4, T5 and T6 from Taiwan and SK26 from Tanimbar. Unfortunately, due to insufficient material, it was not possible to analyse the Forest Reserve fossil mud volcano core (FRC), T3-3 and the sample from Timor (TIM).

A note should be made here about the coarse (>425u) fraction which was removed from the sample before the analysis. This was done because some of the muds (eg. Piparo and Anglais Point) contained small argillaceous fragments which would have disintegrated during the preparation procedure (Appendix 1), thus biasing the samples towards the finer fraction (Chen, 1987). This particular sieve size was chosen because it separated out these fragments; it is also consistent with the limiting size for the Atterberg limits tests in BS1377 (section 4.5; Appendix 3). As seen from table 4.1, the >425u fraction was very small in most samples.

SAMPLE	<425u (%)	>425u (%)	COMMENTS
TRINIDAD			
AP	92	8	mudstone clasts
DIG1	99	1	organics present
DIG2	100	-	organics present
DW	98	2	
LB	99	1	
PIP	89	11	mudstone clasts
PS1	100	-	
PS2	100	-	
PS3	100	-	
TAIWAN			
T1	96	4	
T2	98	2	
T3	96	4	
T4	100	-	
T5	100	-	
T6	99	1	
TANIMBAR			
SK26	95	5	

Table 4.1 Percentages of the <425u fraction

4.2.2. Results

The PSD results are presented in table 4.2.

SAMPLE	CLAY <2u (%)	SILT 2-63u (%)	SAND >63u (%)
TRINIDAD			
AP	51	41	8
DIG1	57	30	13
DIG2	19	66	15
DW	62	35	3
LB	10	46	44
PIP	66	33	1
PS1	43	46	11
PS2	51	40	9
PS3	34	46	20
TAIWAN			
T1	27	48	25
T2	26	56	18
T3	33	59	8
T4	31	62	7
T5	32	66	2
T6	25	69	6
TANIMBAR			
SK26	47	45	8

Table 4.2. Percentages of the clay, silt and sand in the <425u fraction

4.2.3. Discussion

a) Trinidad

The results show a wide range of PSD's, Piparo being the finest-grained, and Lagon Bouffe being the coarsest (fig. 4.1). PS1, PS2, PS3 and AP, sampled from the neighbouring Palo Seco and Anglais Point, are reasonably similar. Surprisingly, Digity 1 and 2, which are very close to each other, are widely different, the former being much more clay-rich (table 4.2). DIG2 is also anomalous in shape to all the other Trinidad PSD curves (fig. 4.1), which are generally parallel to each other, showing uniform distribution throughout the fine-grained fraction. DIG2 shows a bias towards the silt fraction. The wide range of PSD's is to be expected, as the mud volcanoes occur in different parts of the island and are thought to originate from different formations (section 3.2.4). It is interesting that, despite the great difference in the percentages, the shape and gradient of the curves is similar.

Higgins and Saunders (1974) present the results of five PSD's from Trinidad: Palo Seco, Devil's Woodyard, Moruga Bouffe, Forest Reserve fossil mud volcano and Chatham Island mud volcano (section 3.2.5). Their results for Palo Seco and Devil's Woodyard agree very well with the author's. Chatham Island corresponds to AP and PS2, but the curve is a little steeper, showing 40% clay. Forest Reserve has an anomalous distribution (like DIG2's). No conclusions can be drawn from this as it is an isolated result rather than being a general trend.

Kerr et al (1970) compared the results for Palo Seco and Moruga Bouffe (used by Higgins and Saunders) with formation clays thought to be the origin of the mud volcanoes - two from the Lower Cruse Formation and one from the Nariva Formation. They found that the formation samples contained more clay. Kerr et al (1970) suggest that the higher clay content in the formation clay points to contamination of the mud volcano material, but it is difficult to prove that the formation samples analysed by them were representative of the parent bed. The PSD curves of the formation samples were identical to those for PIP and DW (fig. 4.1), i.e., they fall on the fine-grained end of the PSD range for the Trinidad mud volcanoes.

b) Taiwan

The results are presented in table 4.2 and fig. 4.2. These PSD curves lie much closer together than those for the Trinidad mud volcanoes (fig. 4.1); they are also steeper, showing higher silt contents. The similarity between the different curves is to be expected, as they all occur within the same general area (section 3.3.4). It suggests that they are either from the same or a similar source, with no or equal contamination.

Shih (1967) undertook an extensive PSD analysis of the Taiwan mud volcanoes and his results for the same mud volcanoes agree very well with this study, although other volcanoes analysed by Shih showed widely varied distribution.

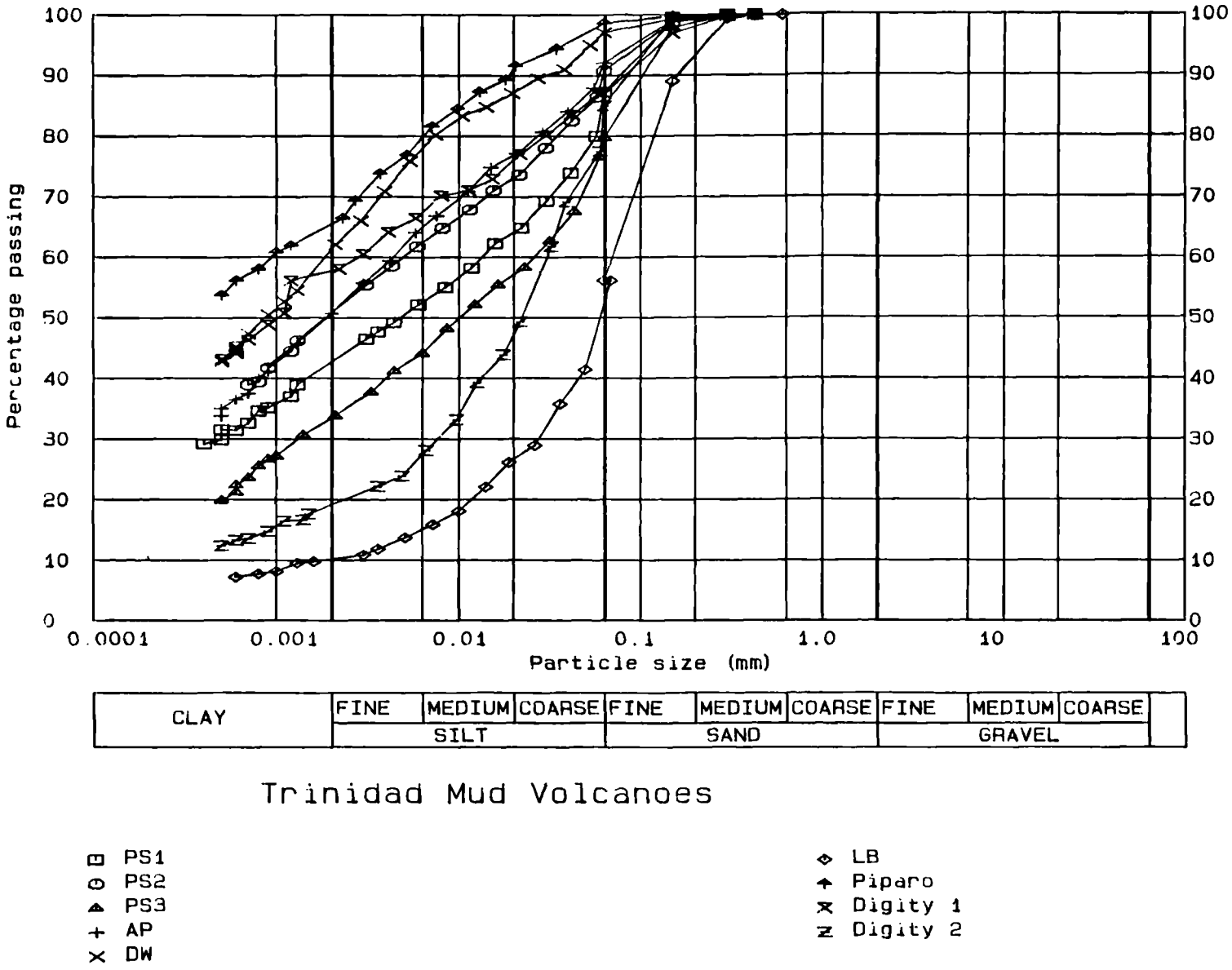

Fig. 4.1 Particle size distribution of the Trinidad mud volcano samples

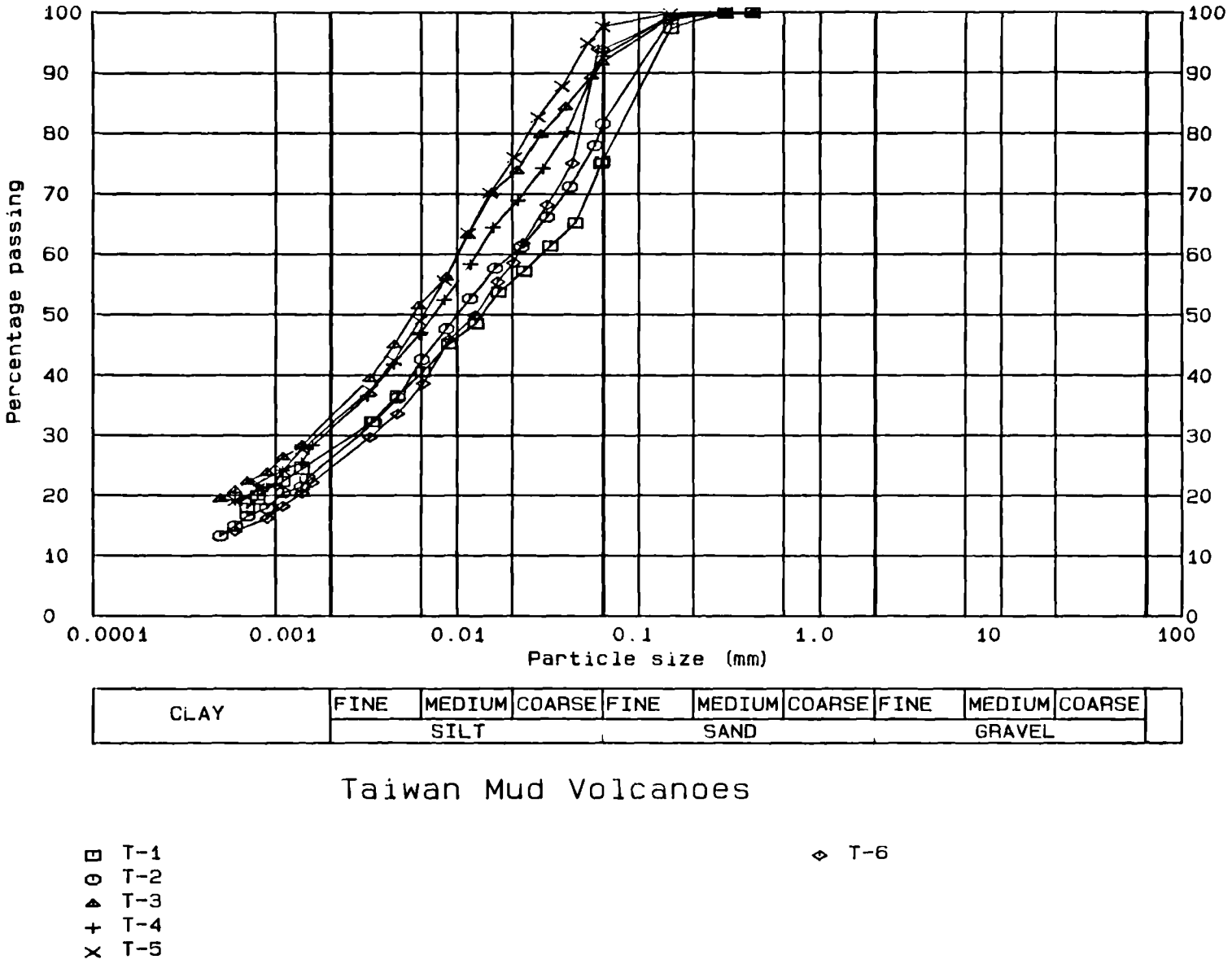

Fig. 4.2 Particle size distribution of the Taiwan mud volcano samples

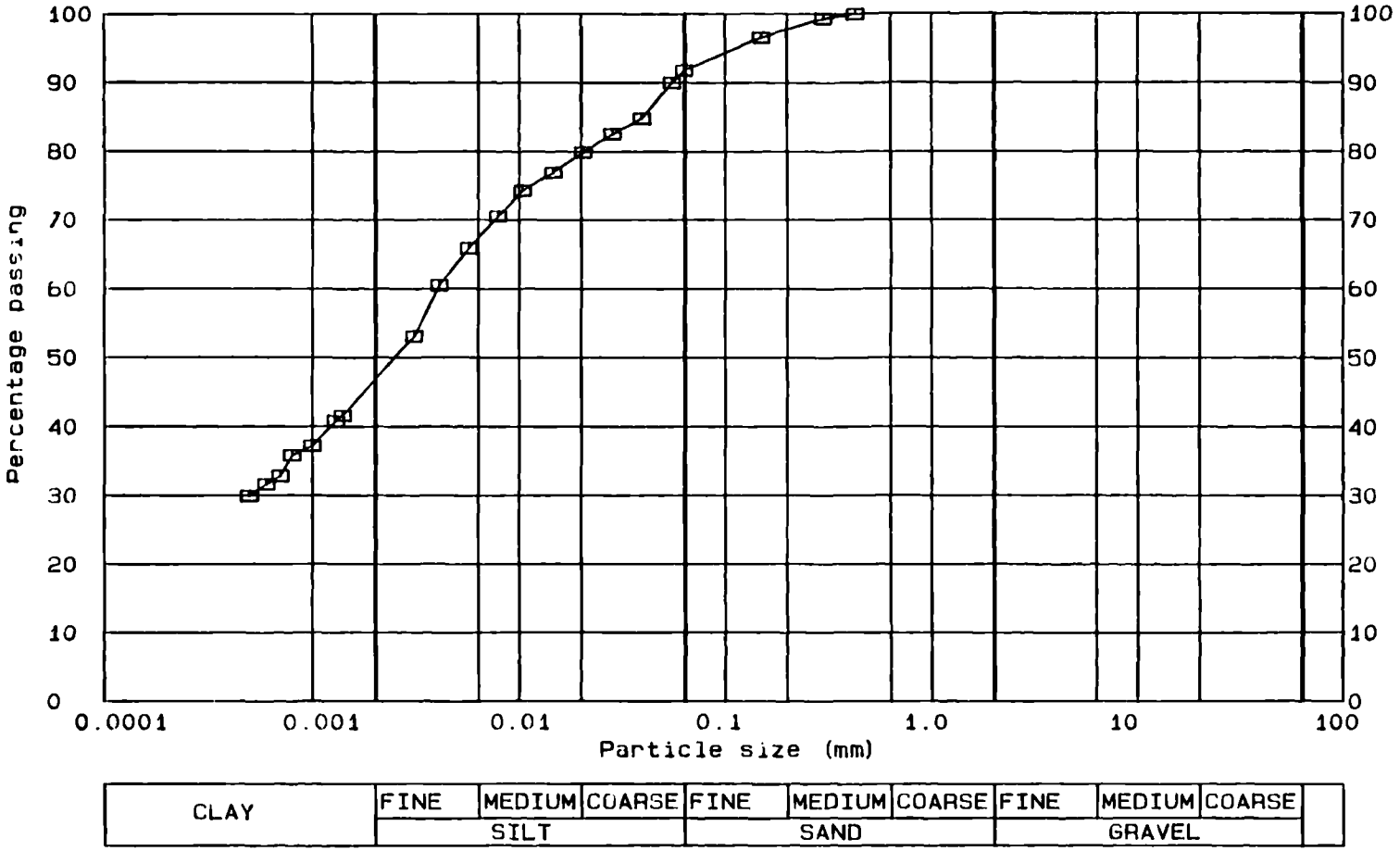

Fig. 4.3 Particle size distribution of the Tanimbar mud volcano sample

c) Tanimbar (SK26)

This contains 48% clay and 12% sand. The PSD curve (fig. 4.3) has the same gradient as the Trinidad volcanoes, and is very similar to PS2.

4.3. CLAY MINERALOGY

4.3.1. Introduction

The muds collected from the volcanoes contain considerable proportions of the clay fraction (section 4.2). It is important to identify the minerals present in that fraction because they could indicate the origin of the mud, and because they have an influence on the behaviour of a sediment (Skempton, 1953).

The most widely used method of identifying clay minerals is X-ray diffraction (XRD). Each mineral has a distinctive atomic structure which diffracts X-rays in a characteristic pattern, indicated by a peak on a trace (Brown, 1961). This relationship is described by the Bragg equation,

$$n\lambda = 2d \sin \Theta \qquad 4.1$$

where,

n = order of reflection,
λ = wavelength of radiation, λ,
d = structural spacing between the mineral layers, Å,
Θ = glancing angle of reflection (1/2 angle between incident and diffracted beams), degrees.

The d-spacing, which identifies the clay mineral, is obtained from the angle of reflection. The reader is referred to the extensive literature on the subject for further details of the basic principles (e.g. Brindley and Brown, 1980).

4.3.2. Methodology

It is generally held that the method of preparation of a clay sample has a great effect on the result of an X-ray diffraction analysis (eg. Brown and Brindley, 1980; Shaw, 1987). The method has to be chosen according to the type of clay being studied. The following points have to be taken into consideration:

a) Separation and Pretreatment of the Clay Fraction

The largest clay grain size is 2 microns; this is used as the uppermost limit in most clay analyses. It is important to separate this fraction out so that the sample analysed contains clay minerals only. Non-clay minerals such as quartz can fall within this size range, but this cannot be avoided. The clay was separated using the method described in Appendix 2. None of the mud volcano clays were carbonate or iron-rich, which would need chemical treatment; they were therefore not subjected to any kind of pretreatment, which might have disturbed their chemistry or structure (Brown and Brindley, 1980).

b) Mounting Technique

Having separated the required clay fraction, there are, again, numerous techniques of mounting this onto a plate or slide for the analysis. The best-known methods are centrifugation, settlement, smear and suction (see review in Shaw, 1987). Gibbs (1965) undertook a quantitative analysis using these four techniques to compare their accuracy. He found that the last two were by far the most accurate as the clay is mounted instantaneously. Any technique depending on settlement of clays will produce a sample that is biased towards the finest minerals which settle last. The centrifugation and suction methods were both used for comparison initially (Appendix 2); the latter was then used throughout.

c) Pretreatment of Slides

In section 4.3.1, it was mentioned that the angle of reflection (indicated by a peak) helps to identify a clay mineral. Some peaks overlap, however, making identification from a single trace very difficult. For example, collapsed smectite has a similar d- spacing to illite, and identification is only possible when the smectite is allowed to swell. Also, kaolinite and chlorite have the same d-spacing and pretreatments are needed to distinguish between them. For most general purposes, therefore, four runs are necessary for clay mineral identification (Shaw, 1987). These include oriented (untreated), glycolated (to expand any expandable clays present), and two heated runs (335 and 550°C) - Appendix 2. The second shifts the smectite peak and destroys the kaolinite; this indicates whether or not chlorite is present. Brown and Brindley (1980) warn, however, that chlorite too can be destroyed at 550°C. The general response of the commonest clay minerals is illustrated in table 4.3. For more detailed information, the reader is referred to Brown and Brindley (1980).

Table 4.3. Effect of some diagnostic treatments on spacing of first low angle spacings in A (from Brown and Brindley, 1980)

d) Quantitative Analysis of the Results

No method has yet been devised which quantifies precisely the clay minerals in a sample. The accuracy of different methods varies; some of the more accurate methods involve using randomly oriented samples (Shaw, 1987), biasing the sample towards different fractions, and the use of internal and external standards (Brindley, 1980). No attempt has been made to undertake such analyses in this study due to time constraints.

Several semi-quantitative methods can be employed using the standard pretreatments (Pierce and Siegel, 1969). Two techniques were used in this analysis. The first compares the areas under the smectite, illite and kaolinite peaks on the glycolated trace, whereas the second compares the change in the illite peak on the oriented and heated traces with the kaolinite peak on the orient ed trace. These are methods 2 and 3, respectively, of Pierce and Siegel (1969); they are described more fully in Appendix 2.

Both methods of calculation are semi-quantitative and only give an approximation of the true values. The advantage of method 2 is that it uses only the glycolated trace so that calculations are not dependent on repeatability of different traces. Any method chosen should be used consistently throughout, so that trends can be reliably observed. For that reason, great care should be taken when comparing results with those of other workers due to variability of methodology.

The samples analysed are listed in tables 4.4 and 4.5. An additional sample from Trinidad is included in the analysis is the Forest Reserve mud volcano core (FRC). Some runs were sometimes repeated for the same sample (eg. DIG1A and DIG1B). The < 40u fraction (whole sample crushed to 40u - see section 4.4.1) produced good results for clays in samples LB and PIP; these were therefore included here for comparison. Three samples not tested for PSD are BSC and AU72 (Bobonaro Scaly Clay; thought to be the origin of the Timor mud volcanoes, Audley-Charles, 1968) and TIM (mud volcano clay). SK24 from Tanimbar is identical to SK26 as it was sampled from the same vent.

4.3.3. Results

The results of the different analyses are presented in tables 4.4 and 4.5, and figs. 4.6 and 4.7.

SAMPLE	PREPARATION METHOD	CALCULATION METHOD	SMECTITE (%)	ILLITE (%)	KAOLINITE + CHLORITE (%)	
AP	suction	2	12.2	37.2	50.6	M
AP	"	3	6.4	43.4	50.2	
AP	centrifuge	2	13.0	51.1	35.9	
AP	"	3	6.0	38.0	56.0	
APC	suction	2	10.7	39.0	50.3	L-M
APC	"	3	15.1	32.1	57.8	
DIG1 A	"	2	17.6	42.4	40.0	v.L
DIG1 A	"	3	unreliable data			
DIG1 B	"	2	17.7	36.2	46.1	
DIG1 B	"	3	10.9	34.4	54.7	
DIG2	"	2	20.0	42.7	37.3	-
DIG2	"	3	12.1	36.2	51.7	
DW	"	2	5.0	48.9	46.1	L-M
DW	"	3	2.0	39.2	58.8	
FRC	"	2	9.6	53.3	37.1	v.L
FRC	"	3	3.8	38.0	58.2	
FRC	centrifuge	2	14.2	42.9	42.9	M
FRC	"	3	3.6	38.0	58.4	
LB	suction	2	8.2	52.5	39.3	L
LB	"	3	11.9	32.6	55.6	
LB 40u	"	2	15.6	53.3	31.1	
PIP	"	2	9.6	48.0	42.4	L
PIP	"	3	18.0	26.0	56.0	
PIP 40u	"	2	14.3	46.6	39.1	
PS1	"	2	17.3	42.0	40.7	L-M
PS1	"	3	13.2	38.2	48.5	
PS1	centrifuge	2	23.0	38.5	38.5	
PS1	"	3	9.1	44.0	43.9	
PS2	suction	2	18.9	43.3	37.8	L-M
PS2	"	3	18.9	32.2	48.9	
PS3	"	2	31.3	36.2	32.5	-
PS3	"	3	24.0	37.3	38.7	

Table 4.4. Clay mineralogy results for the Trinidad mud volcanoes

SAMPLE	PREPARATION METHOD	CALCULATION METHOD	SMECTITE (%)	ILLITE (%)	KAOLINITE + CHLORITE (%)	
TAIWAN						
T1	suction	2	-	63.2	36.8	H
T1	"	3	-	48.6	51.3	
T2	"	2	-	61.5	38.5	H
T2	"	3	-	50.2	49.8	
T3-2	"	2	-	71.9	28.1	H
T3-2	"	3	-	52.3	47.7	
T3-3	"	2	-	66.8	33.2	H
T3-3	"	3	-	53.5	46.5	
T4	"	2	-	65.2	34.8	H
T4	"	3	-	51.1	48.9	
T5	"	2	-	72.7	27.3	H
T5	"	3	-	52.5	47.5	
T6	"	2	2.3	70.5	27.2	H
T6	"	3	-	54.4	45.6	
TIMOR						
AU72	centrifuge	2	46.6	42.2	11.2	v.L
AU72	"	3	unreliable data			
TIM	suction	2	7.7	51.9	40.4	-
TIM	"	3	unreliable data			
BO82	suction	2	45.0	34.8	20.2	L
BO82	"	3	30.5	33.9	35.6	
TANIMBAR						
SK24	centrifuge	2	14.1	39.4	46.5	L-M
SK24	"	3	4.4	30.9	64.7	
SK26	suction	2	8.2	52.5	39.3	L-M
SK26	"	3	0.6	49.1	50.3	

Quantities of chlorite: L = low M = medium H = high

Table 4.5. Clay mineralogy results for the SE Asia mud volcanoes

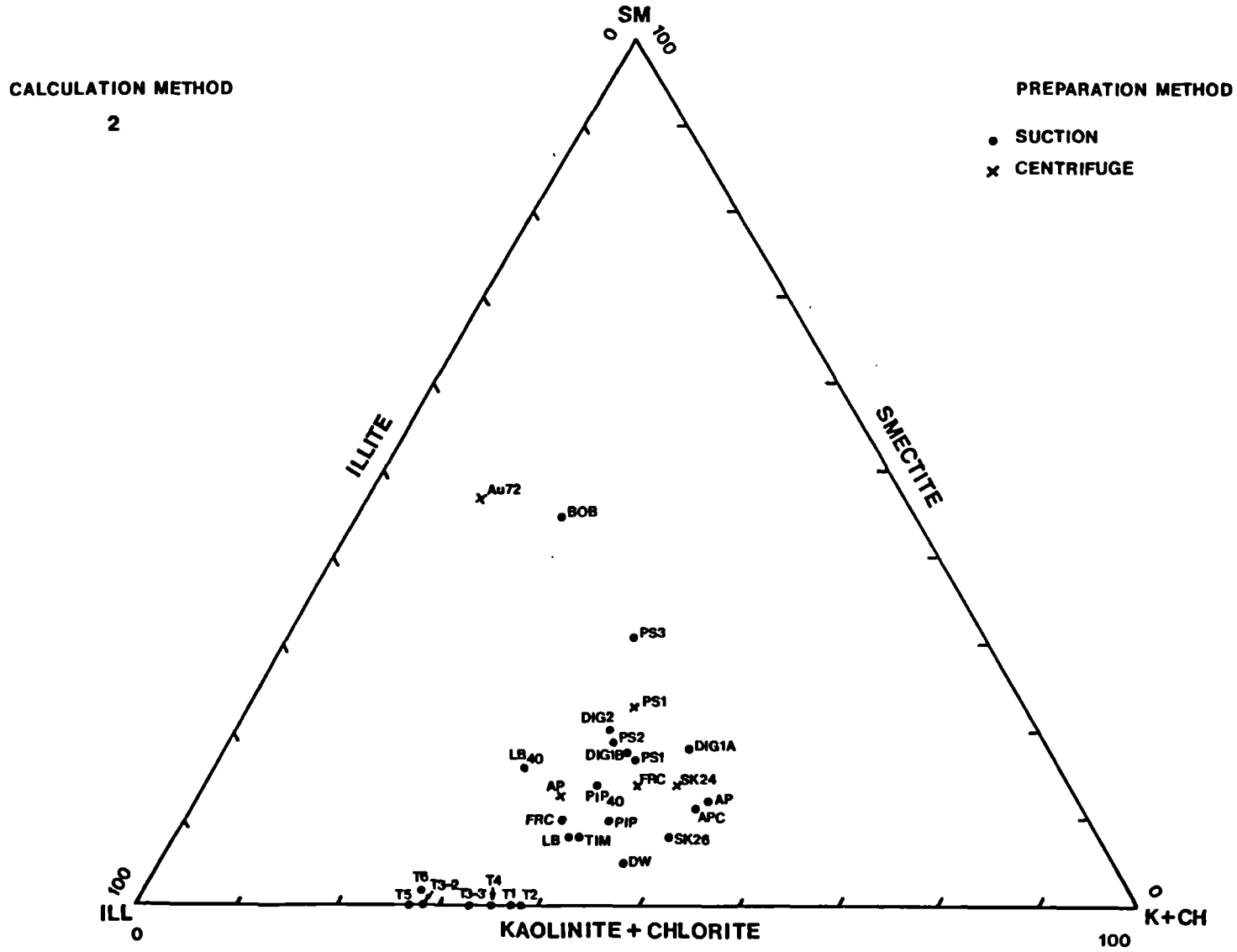

Fig. 4.4 Clay mineralogy of the mud volcanoes, calculation method 2

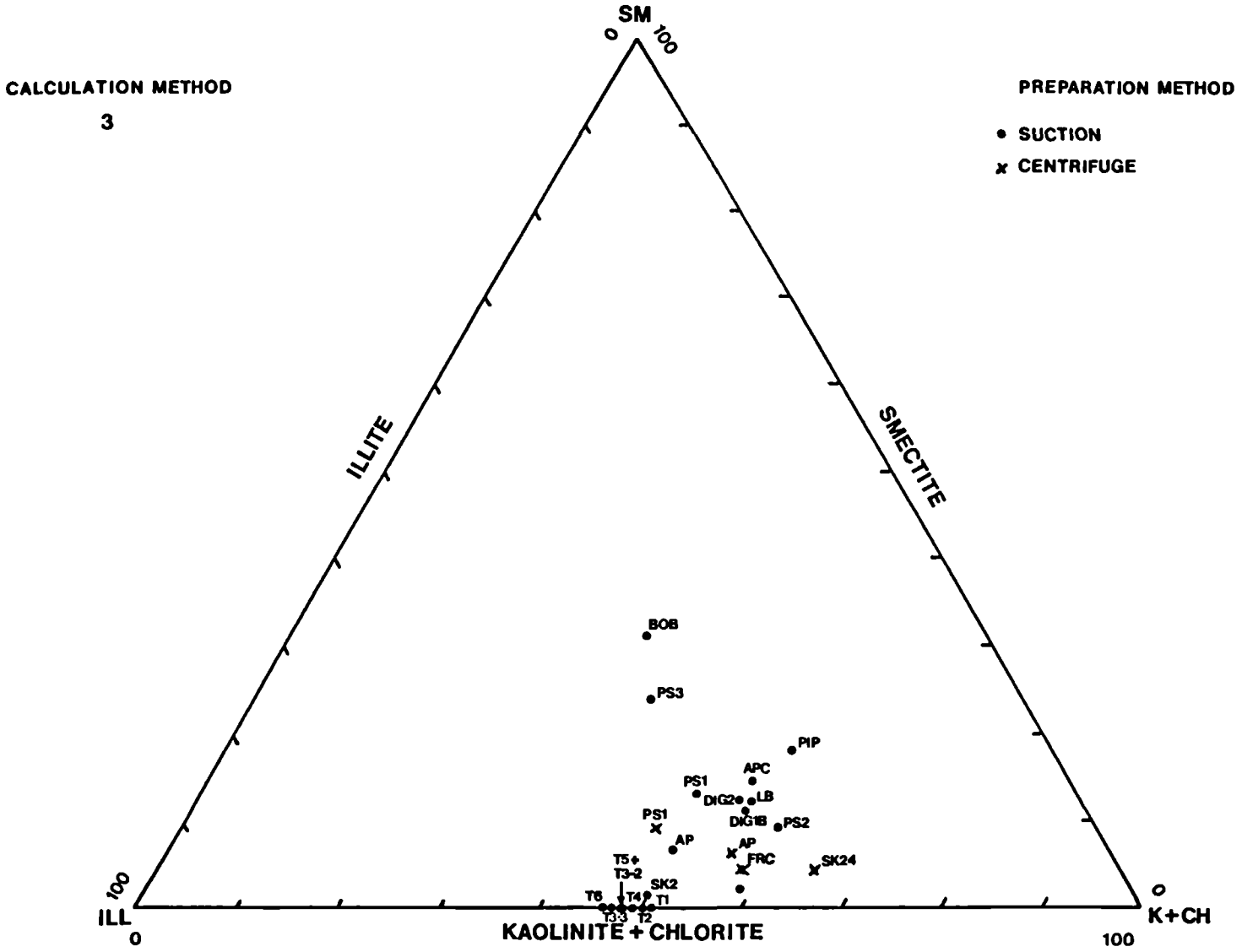

Fig. 4.5 Clay mineralogy of the mud volcanoes, calculation method 3

4.3.4. Discussion

a) Comments on Methodology

Sample Preparation: The results of the two different methods of preparation generally agree with Gibbs' (1965) observation. The centrifuge method is expected to give higher smectite values, which is observed for calculation method 2 on samples PS1 FRC and SK; AP gives similar smectite values for the two preparation methods (table 4.4). This should be treated with reservation, however, as only four samples were tested using both preparation techniques.

Calculation: The results of the two calculation methods are presented in figs. 4.4 and 4.5. Method 3 is expected to give a lower value for the smectite fraction than method 2 (Pierce and Siegel, 1969) due to the fact that peak heights rather than peak areas are used in this method (Appendix 2). This is observed in most of the samples, with the exception of LB, APC, and PIP. More noticeably, method 3 shows stronger trends for both Trinidad and Taiwan. However, method 2 shows much better agreement for mud vents within the same area, e.g. DIG1 and DIG2; AP and APC. (Although PS1 and PS2 are similar, PS3 is anomalous in both figs. 4.4 and 4.5).

As mentioned above, clay mineralogy results are very sensitive to methodology, and one can only use one method of preparation and calculation to compare the results, so that any inherent errors are consistent for all the samples. The suction method and calculation method 2 were chosen as, from the above comments, they seem to be more reliable.

b) Trinidad

From table 4.4 and fig. 4.6, it can be seen that the Trinidad mud volcanoes all contain smectite, illite and kaolinite, with occasional chlorite. A typical trace (PS1) is presented in fig. 4.7. The proportions vary from area to area, but seem to have a general trend towards 20-% for smectite, 40 + % for illite and 40 + % for kaolinite + chlorite. The variation is to be expected, as the mud volcanoes occur in different areas. The percentages do show very good agreement for cones within the same area (see for example Palo Seco (PS1, PS2 and PS3), Digity (DIG1 and DIG2) in table 4.4 and fig. 4.6). The small mudstone fragments (APC) present in the matrix of the Anglais Point mud volcano (AP) have the same mineralogy as the matrix, which suggests that they are from the same source. No particular similarity is observed between Anglais Point and Palo Seco, which are close to each other.

The results seem similar to those obtained by Kerr et al (1970), who analysed the Moruga Bouffe and Palo Seco mud volcanoes, comparing them with samples from the Nariva and Lower Cruse formations (thought to be responsible for some of the Trinidad mud volcanoes - Higgins and Saunders, 1974; table 3.1). The clays in the analysis by Kerr et al were prepared by settling onto a glass slide.

Kerr et al (1970) found the mud volcano traces to contain mixed layer illite and smectite (section 4.3.4.a), and kaolinite - very similar to the above results. The three formation clays were also found to be similar to each other, containing less smectite than in the mud volcano clays. The kaolinite was interpreted as being more ordered than that found in the mud volcano clays due to the fact that it was

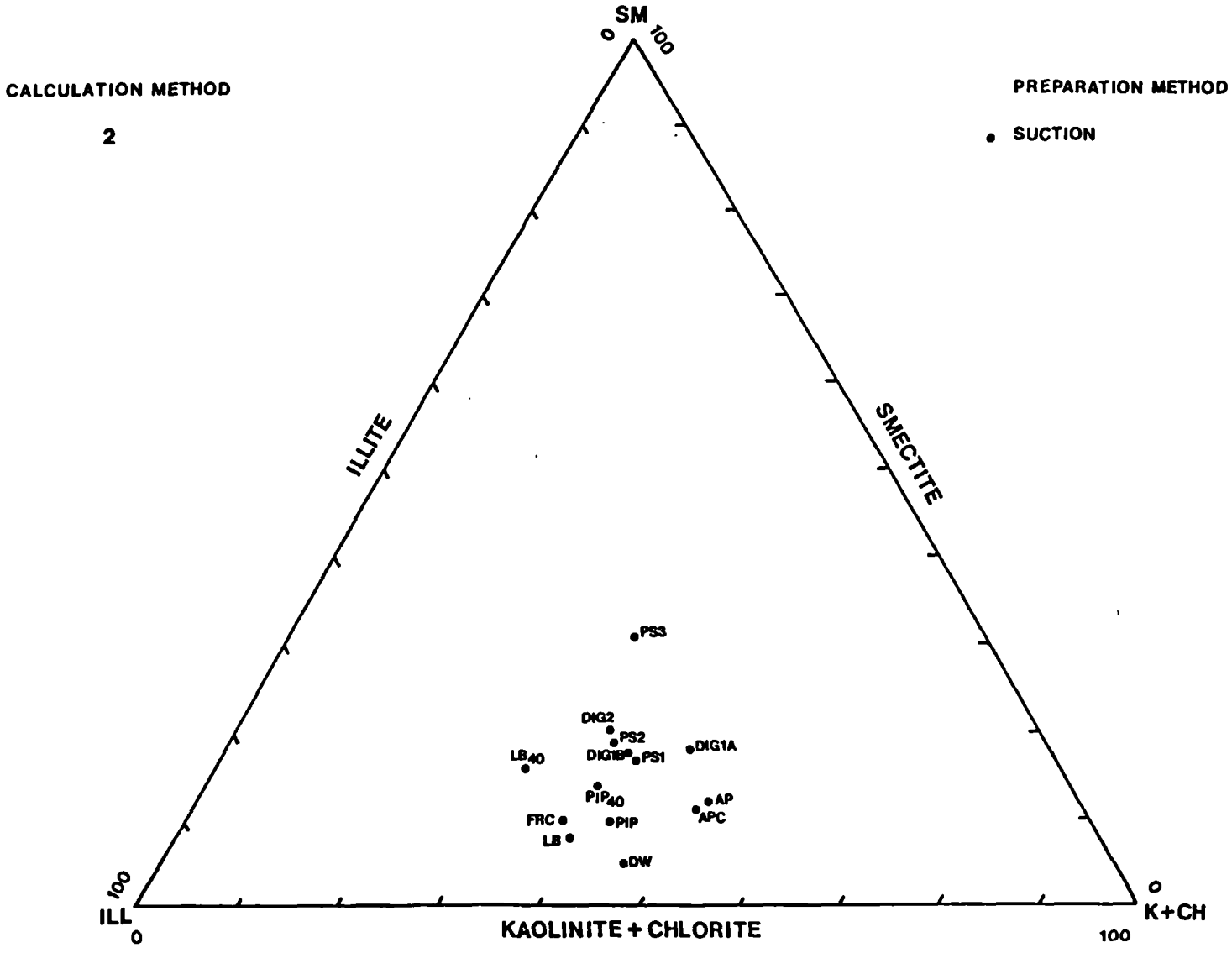

Fig. 4.6 Clay mineralogy of the Trinidad mud volcanoes

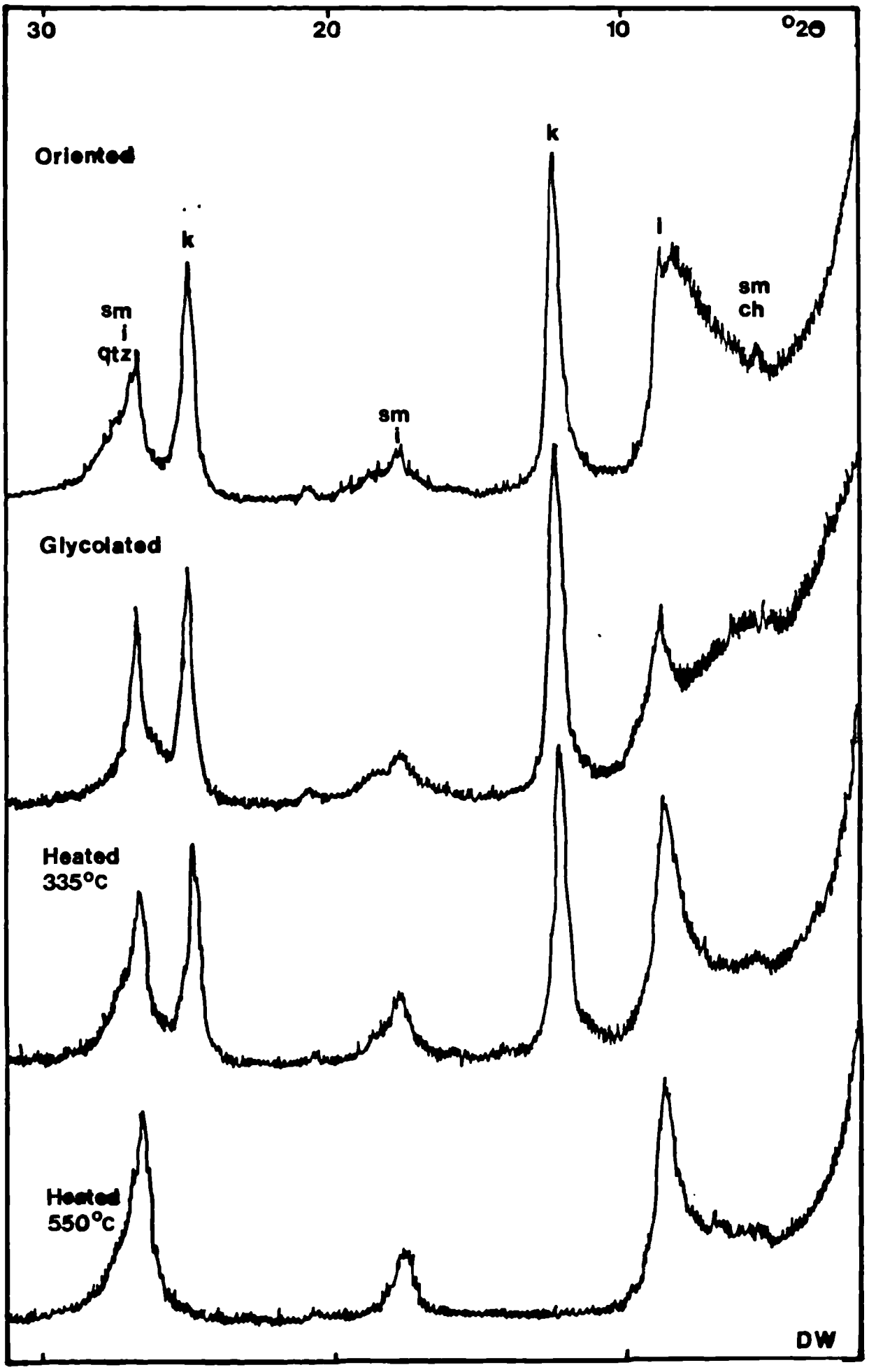

Fig. 4.7 Typical XRD trace for Trinidad mud volcano clay, Devil's Woodyard; sm = smectite; i = illite; k = kaolinite; ch = chlorite; qtz = quartz.

not destroyed by heating at 550° C (Kerr et al, 1970); however, no mention is made of the length of time for heating or method of calculation.

Kerr et al (1970) make the point that the variation between the formation samples and the mud volcano clays is due to contamination by overburden material, supporting the idea with the higher clay content of the formation samples. This is very likely, but, as mentioned in section 4.2.3, the formation samples are not necessarily representative of the parent bed; more samples need to be tested to establish a trend.

No attempt has been made to interpret the results of the mixed layer phase as did Kerr et al (1970) because of the problems inherent in such analyses. Fig. 4.8 shows typical XRD profiles of randomly interstratified mixed layer illite-smectite after glycolation (from Hower, 1981); the Trinidad samples seem to fall between 60 and 80% illite. However, the random interstratification in XRD traces is thought to be an artifact of reconstituting a sample for the analyses, as it is rarely observed in transmission electron microscopy (Shaw, 1987); sample preparation is thought to disaggregate the original material (possibly ordered mixed layer clays) into the constituent minerals (Nadeau et al, 1984). Nadeau et al further demonstrated that, due to interparticle diffraction effects, very thin illite particles could produce XRD data similar to smectite or randomly ordered illite-smectite. This is discussed at length in Shaw (1987).

c) Taiwan

The results for the Taiwan mud volcanoes are presented in table 4.5 and fig. 4.9. A typical run is presented in fig. 4.10. It can be seen that the muds have a similar mineralogy - smectite-free, with an average of 2/3 of illite and 1/3 of kaolinite + chlorite. The chlorite content is considerable as can be seen from the heated traces (fig. 4.10). T-6 (Hsiaokungshui) seems to contain a very small percentage (%) of smectite, indicated by a just-discernible low angle peak in the glycolated trace.

The Taiwan mud volcano results agree well with Shih's (1967). Shih undertook an extensive XRD clay mineralogy investigation, using the centrifuge method to mount the clay onto the plate. He identified the minerals as illite, chlorite, quartz with possible kaolinite (section 4.3.4.b). Shih was probably unable to distinguish between kaolinite and chlorite but the presence of kaolinite is indicated by the disappearance of the 7A peak after heating at 550°C, and by the split of the 3.59A peak (Shaw, 1987, pers. comm.; fig. 4.10).

Aoyagi and Kazama (1969 - in Chou, 1971) studied the clay mineralogy of core and outcrop samples of Neogene mudstones in the Tainan area and found them to contain illite, chlorite and quartz, i.e., their results were similar to Shih's (1967). The illite - chlorite ratio for outcrop samples of the Lower Gutingkeng (most probable source of the mud volcanoes, section 3.3.4) and younger formations taken on either side of the Lungchuan Fault (fig. 3.12) is generally approximately 2/3 illite and 1/3 chlorite, agreeing with the mud volcano results (figs. 4.9); Chou does not indicate the calculation method used. The mud volcano material could therefore originate from anywhere within this sequence (see discussion below - section 4.6). Aoyagi and Kazama (1969) also find trace amounts of smectite (montmorillonite) in some of the muds and assume that the original sediment contained the mineral but has since lost it through diagenesis. This may be true, but it could also be argued that the lack of

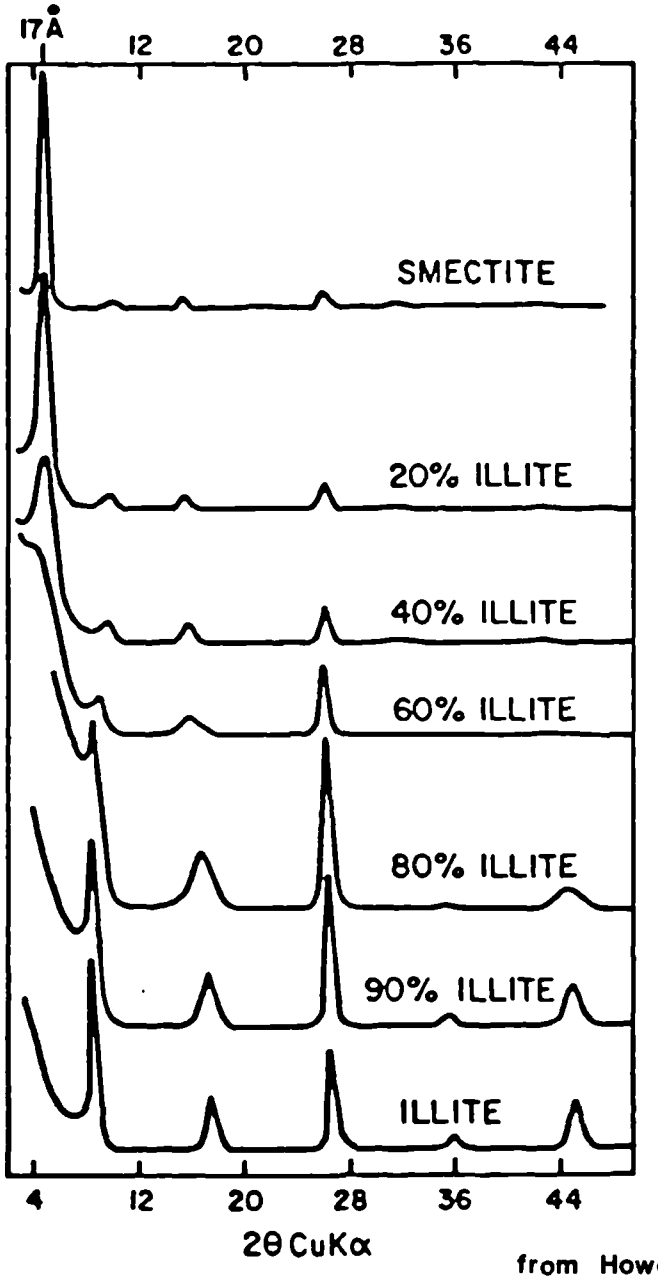

Fig. 4.8 Estimation of mixed layer clay percentages from an XRD trace

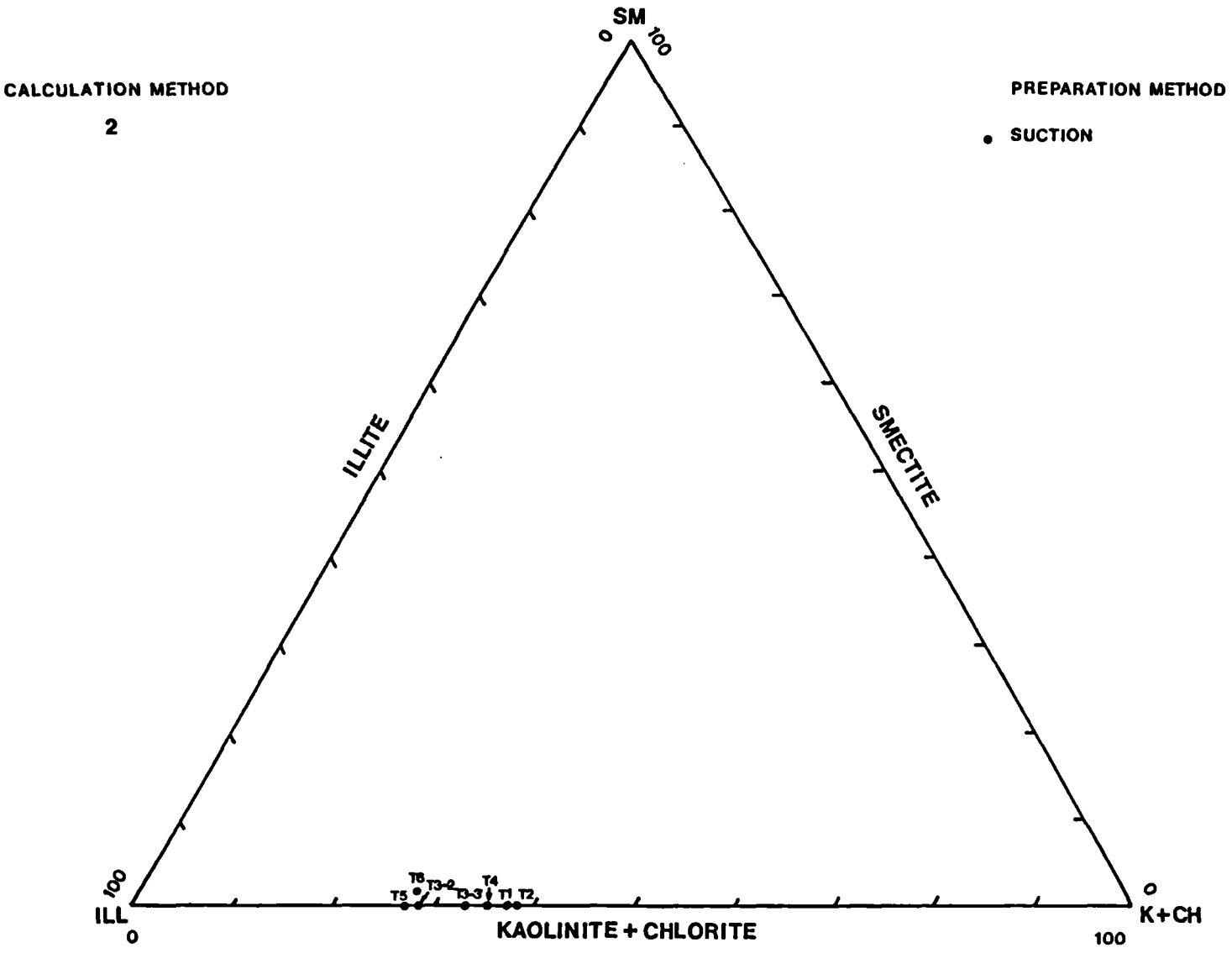

Fig. 4.9 Clay mineralogy of the Taiwan mud volcanoes

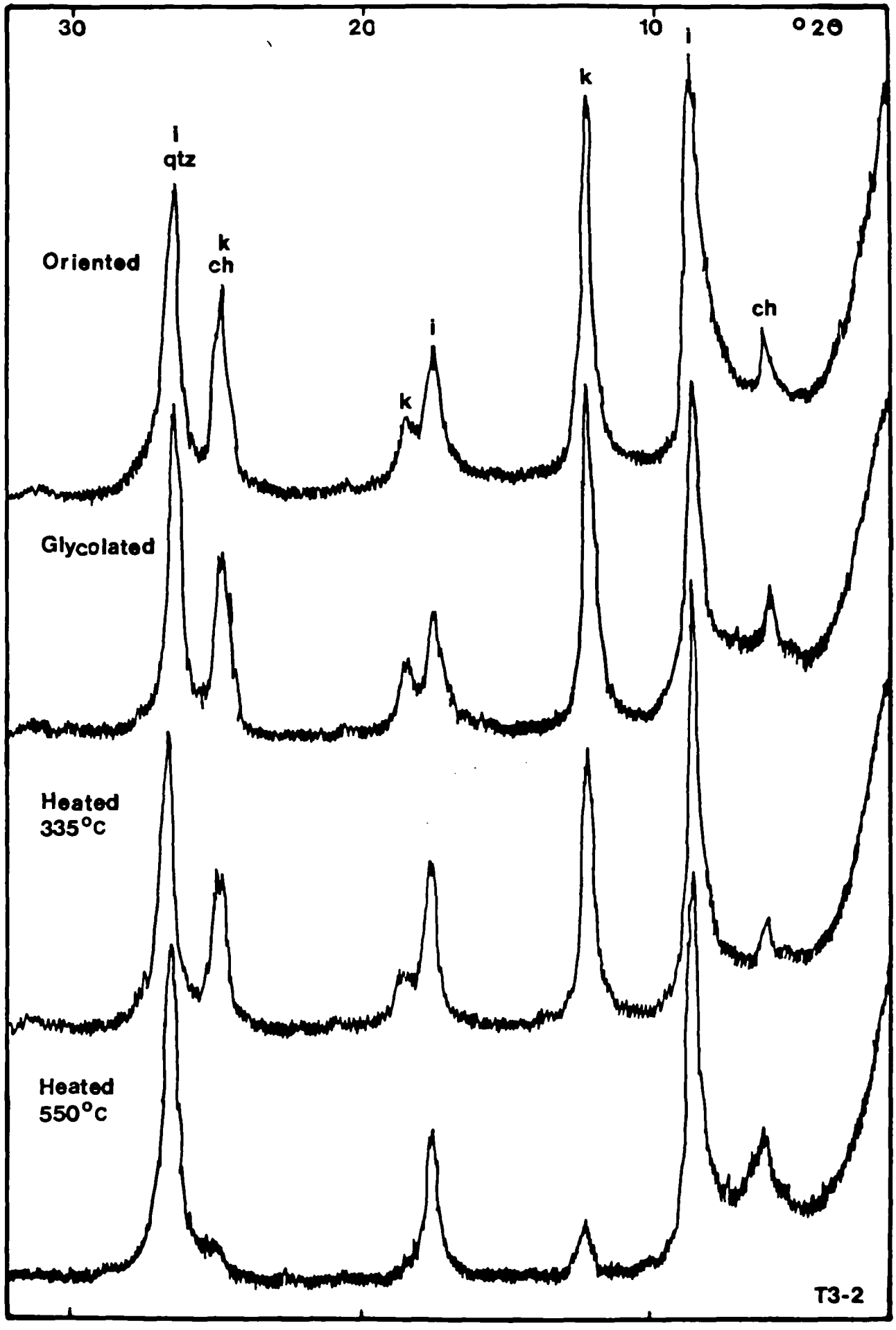

Fig. 4.10 Typical XRD trace for Taiwan mud volcano clay, Wushanting (T3-2); ch = chlorite; i = illite; k = kaolinite; qtz = quartz.

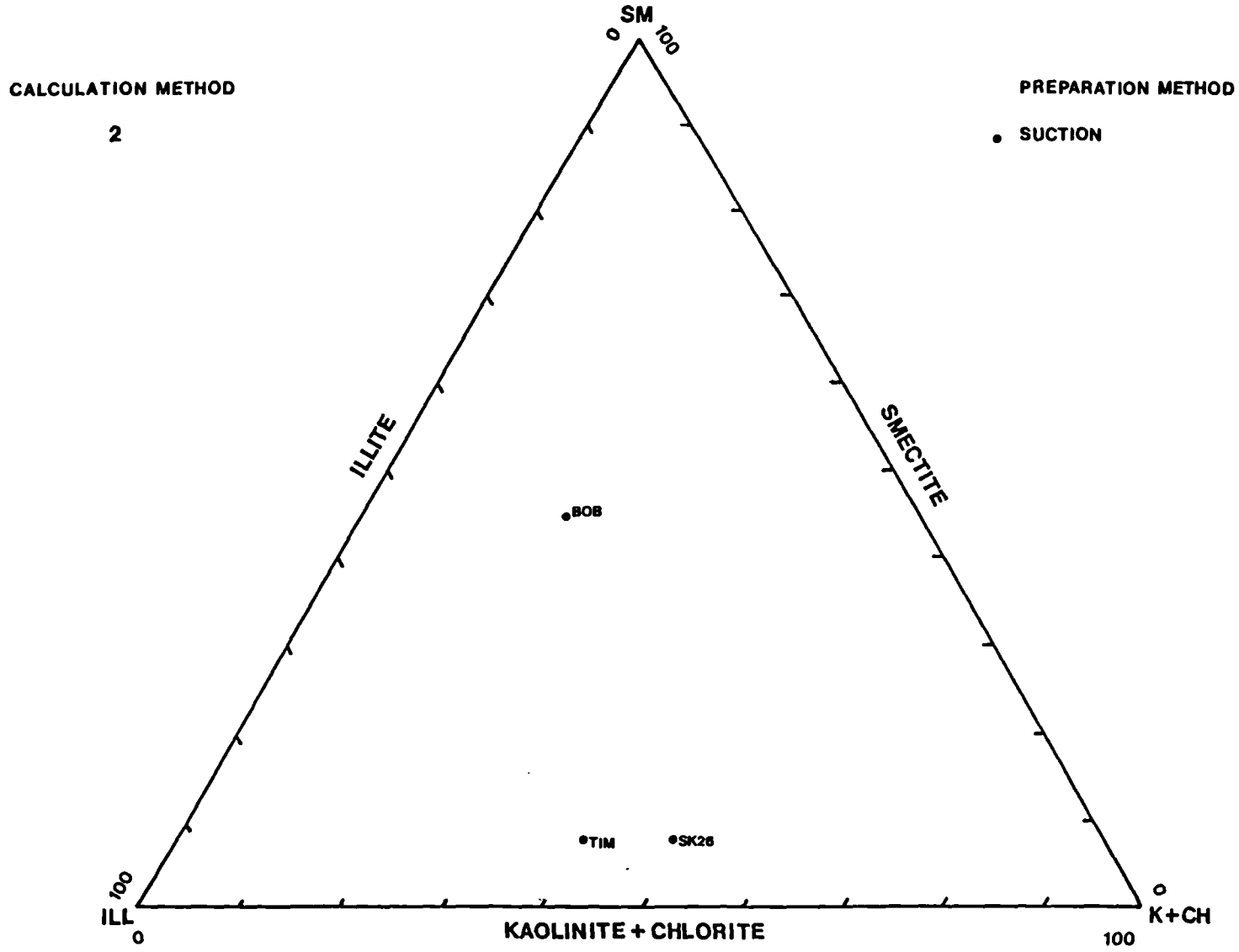

Fig. 4.11 Clay mineralogy of the Timor and Tanimbar mud volcanoes

smectite throughout the sedimentary sequence suggests that the source material was smectite-poor. Section 2.2.2.a presents some evidence of clay diagenesis in the Gulf Coast of Texas, where the smectite within the sequence decreases in amount with depth.

d) Timor and Tanimbar

For Timor, the results are very different. Whereas BOB contains appreciable amounts of smectite (>45%), TIM contains <10% smectite, 50+% illite and 40% kaolinite + chlorite (table 4.5; fig. 4.16). The Tanimbar sample, SK26, has a similar mineralogy to some of the Trinidad mud volcanoes, such as LB, PIP, DW and FRC and the Timor mud volcano, TIM (tables 4.4 and 4.5 and fig. 4.11).

These samples were analysed for comparison with the Trinidad and Taiwan samples. TIM (Timor mud volcano) and SK26 (Tanimbar mud volcano) have comparable compositions to the Trinidad samples. This is not unusual, as the clay minerals found are common in marine sediments. The obvious difference between TIM and BOB suggests that this particular mud volcano did not originate from the Bobonaro Scaly Clay. This supports the work undertaken by Harris (pers. comm., 1988) on the Timor mud volcanoes.

All the muds analysed contained some or all of the commonest clay minerals: smectite, illite, kaolinite and chlorite. None show rare minerals which would have helped as "markers". It is important to remember that these minerals are only a percentage of the <2u fraction, not the whole sample. It is also worth noting that many of the <2u samples seemed to contain some quartz, as indicated by the high secondary illite peak, which corresponds also to a quartz peak (see for example traces in fig. 4.10).

4.4. THE SILT AND COARSER FRACTION

4.4.1. Description of the Non-Clay Fraction of the Matrix

The <425u samples were crushed to <40u to examine the mineralogy of the whole sample. Again, the suction method was used to mount the samples (Appendix 2). The results are not presented here because of their great similarity to the clay results: apart from the presence of clays, large amounts of quartz were indicated on the traces. No other non-clay minerals were found in any appreciable quantities for any of the samples. This implied that the technique employed was inappropriate in that the clays were not separated out (separation of the clay fraction may have possibly produced higher resolution on the coarser fraction). Optical microscope work was therefore undertaken on the silt and sand fraction of the matrix (<425u). No attempt is made to make detailed descriptions of all the samples, but the salient features are summarised below.

The grains of the Trinidad (AP, DIG1, DW, LB, PIP and PS1) and Taiwan (T1 to T6) mud volcanoes are shown in plates 4.1 and 4.2 respectively. Generally, it can be said that they are all very similar, quartz comprising the highest percentage. The samples did show up other minerals, however, such as feldspar (all), occasional biotite and glauconite (LB, PIP, DW, plate 4.1), as well as opaque iron-rich minerals and lithic fragments (all). The grains are generally sub-rounded to angular. Microfossils were scarce, but some were seen in PIP and DW (plate 4.1; see also section 4.4.3.a below). PIP (plate 4.1.f) was the only obviously different sample in that it contained very few fragments coarser than 425u, and these were partly quartz, partly biotite and partly fossiliferous.

Scanning Electron Microscope (SEM) work on the >63u fraction of the matrix (no >425u fraction was available) indicated very high angularity of the grains in all the samples. Unfortunately, due to a faulty camera, only a few results can be shown (plate 4.3). LB is the only sample which contains a few rounded quartz grains (plate 4.3.b).

4.4.2. Description of the Clasts In the Matrix

As mentioned in the previous chapter, clasts were collected from two mud volcano areas in Trinidad: Anglais Point and Devil's Woodyard. None were found in any of the other areas, including Taiwan. These are briefly described below and shown in plates 4.4 to 4.6. (Note that the clast numbers do not refer to particular vents, but to the general area; in the case of Anglais Point, the clasts were collected from the associated mudslide).

Anglais Point
AP1: buff, calcareous clay with calcite veins (plate 4.5.a); angular, 6.5 x 4.5 x 3.5 cm.
AP2: light red-brown silty clay; well-rounded, 5.5 x 5 x 2 cm.
AP3: light grey and buff graded sandstone (identified as Herrera sand, plate 4.5.b); angular, 6 x 3.5 x 3.5 cm.
AP4: buff-brown siltstone with yellow, orange and green stains (plate 4.5.c); angular, 7 x 4.5 x 0.7 cm.
AP5: yellow siltstone fragments, may well be same as AP4.
AP6: light grey fine sandstone - very possibly same as AP3 (plate 4.5.d); angular, 2 x 1 x 1 cm.
AP7: grey beef?-calcite; angular, flat 7 x 3 x 1.8 cm.
AP8: desert rose (gypsum); 6 x 6 x 1 cm.
AP9: white gypsum, fibrous texture; broken off large pebble, 12 x 13 x 9 cm.
AP10: brick-red, weakly calcareous fine clay-siltstone, tightly folded, (plate 4.5.e); angular, 8 x 3 x 1.5 cm.
AP11: light grey fine siltstone; subrounded, 4 x 3 x 2 cm.
AP12: dark brick-red weakly calcareous fine siltstone (AP10?); sub-rounded, 5 x 3 x 2 cm.
AP13: white gypsum, fibrous texture; flattish, folded, 8 x 7 x 3.5 cm.
AP14: very dark grey chert? pebbles with calcite veins (plate 4.5.f); av. 6 x 4 x 1.5 cm.
AP15: buff silty clay - very soft small fragments.

Devil's Woodyard
DW1: orange-red sandstone, calcite-cemented (Pointe-a Pierre sandstone, plate 4.6.a).

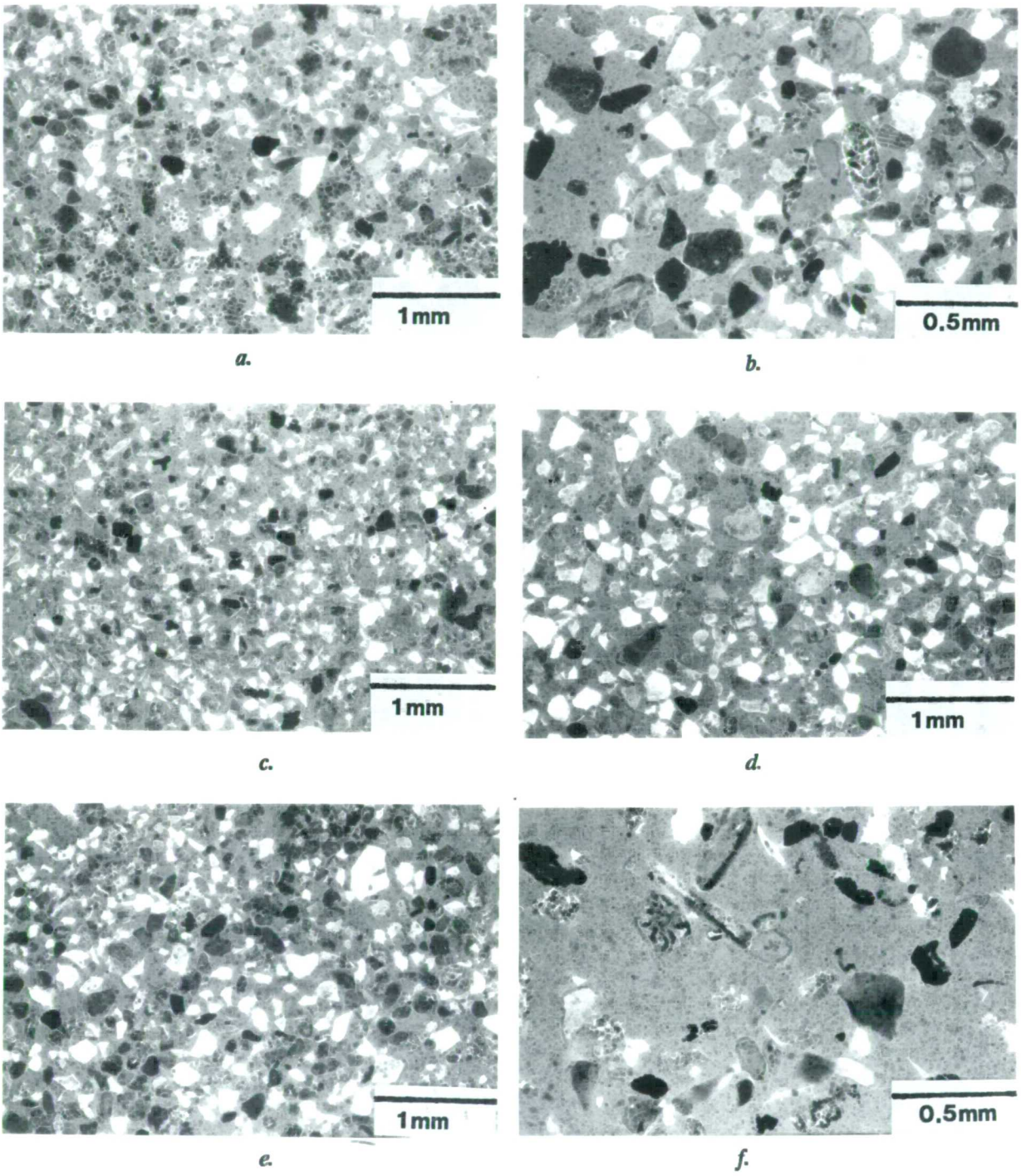

Plate 4.1 Optical microscope photographs of the 63-425u fraction, Trinidad mud volcanoes: a. Anglais Point (magnification x 20); b. Devil's Woodyard, showing microfossils (mag. x 40); c. Digity 2 (mag. x 20); d. Lagon Bouffe (mag. x 20); e. Palo Seco 1 (mag. x 20); f. Piparo, showing microfossils (mag. x 40)

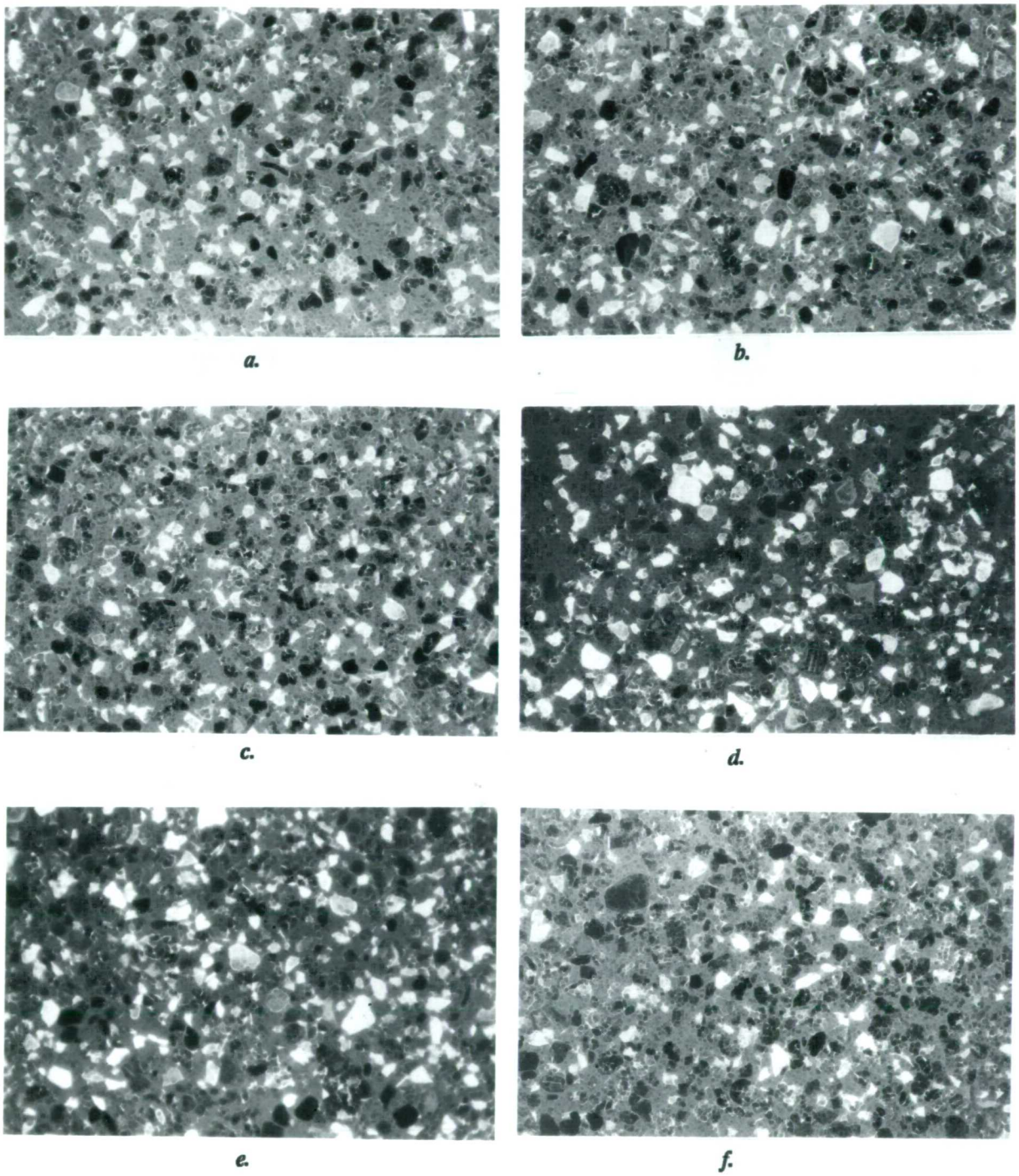

Plate 4.2 Optical microscope photographs of the 63-425u fraction, Taiwan mud volcanoes: a. Aoshenshui (T1); b. Aoshenshui (T2); c. Wushanting (T3-2); d. Chiencuhliao (T4); e. Hsiaokungshui (T5); f. Hsiaokungshui (T6); (magnification x 20).

a.

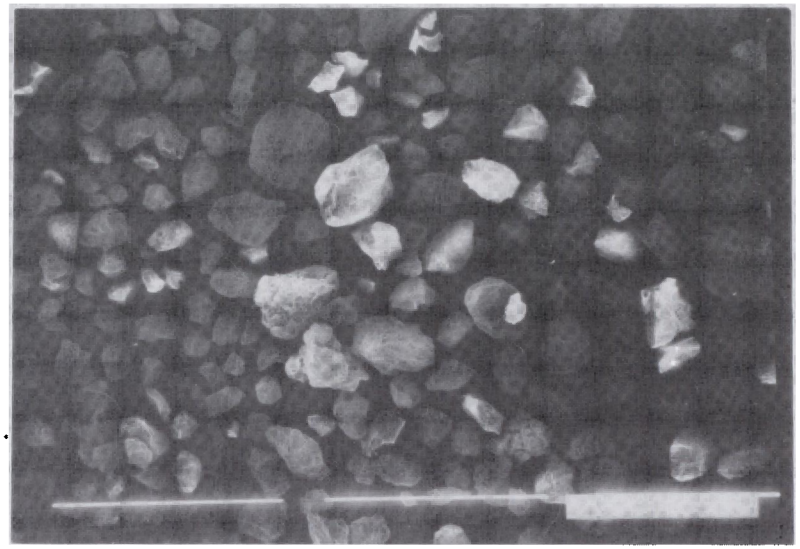

b.

c.

d.

Plate 4.3 Secondary image SEM photographs of the 63-425u fraction showing angularity of grains: a. Anglais Point (scale bar = 1 mm); b. Lagon Bouffe (scale bar = 1 mm); c. Palo Seco 2 (scale bar = 100u); d. Wushanting, T3-2 (scale bar = 1 mm).

a.

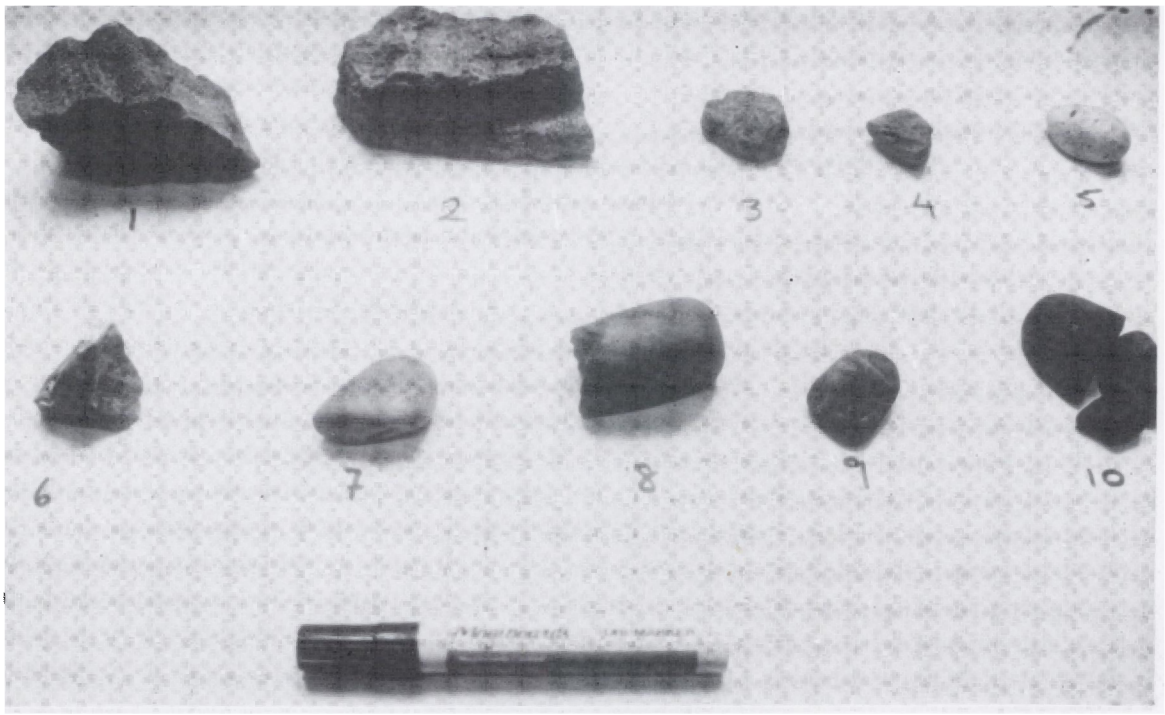

b.

Plate 4.4 Exotic blocks from two Trinidad mud volcanoes: a. Anglais Point; b. Devil's Woodyard.

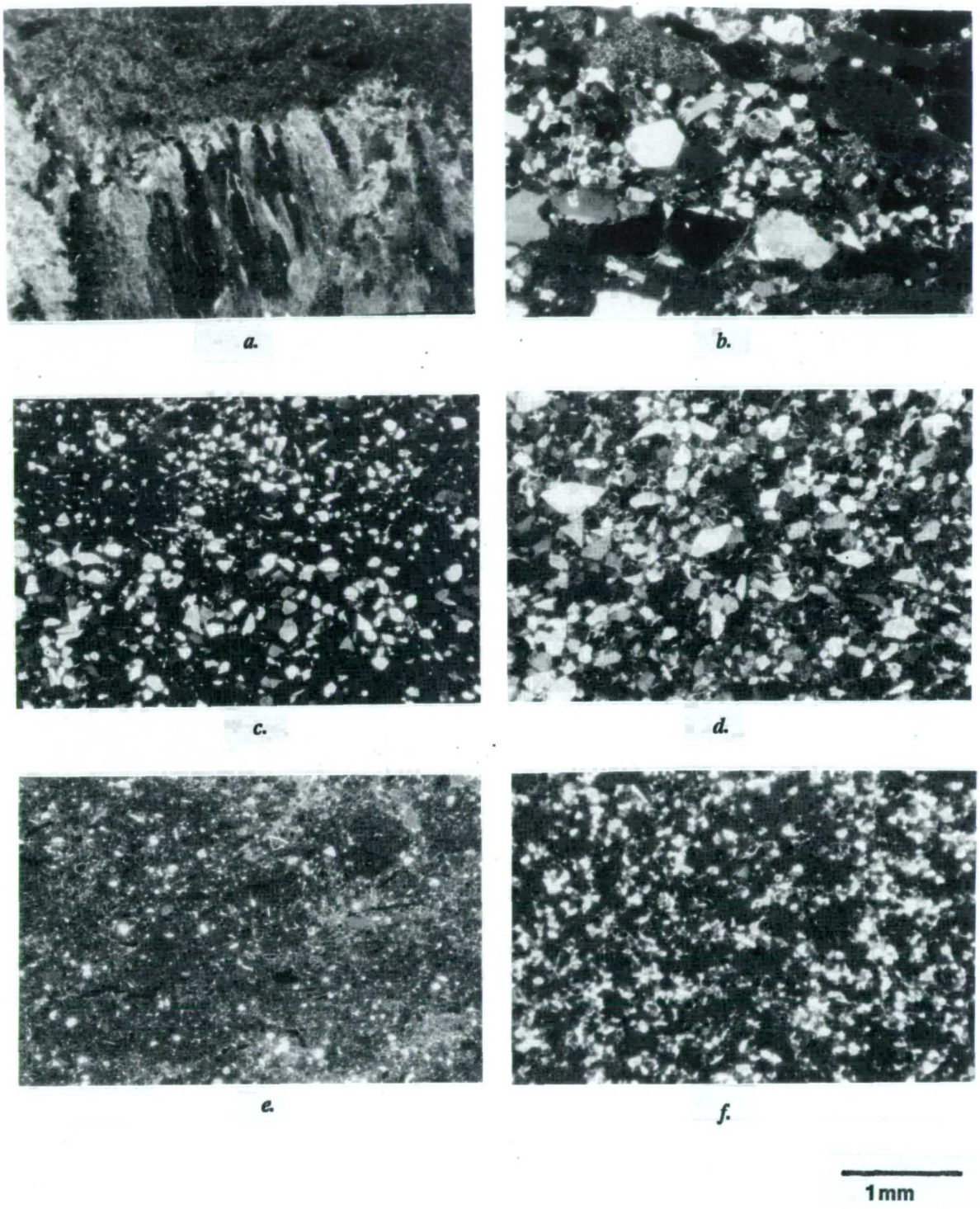

Plate 4.5 Optical microscope photographs of the Anglais Point exotic blocks: a. AP1; b. AP3; c. AP4; d. AP6; e. AP10; f. AP14; (magnification x 20).

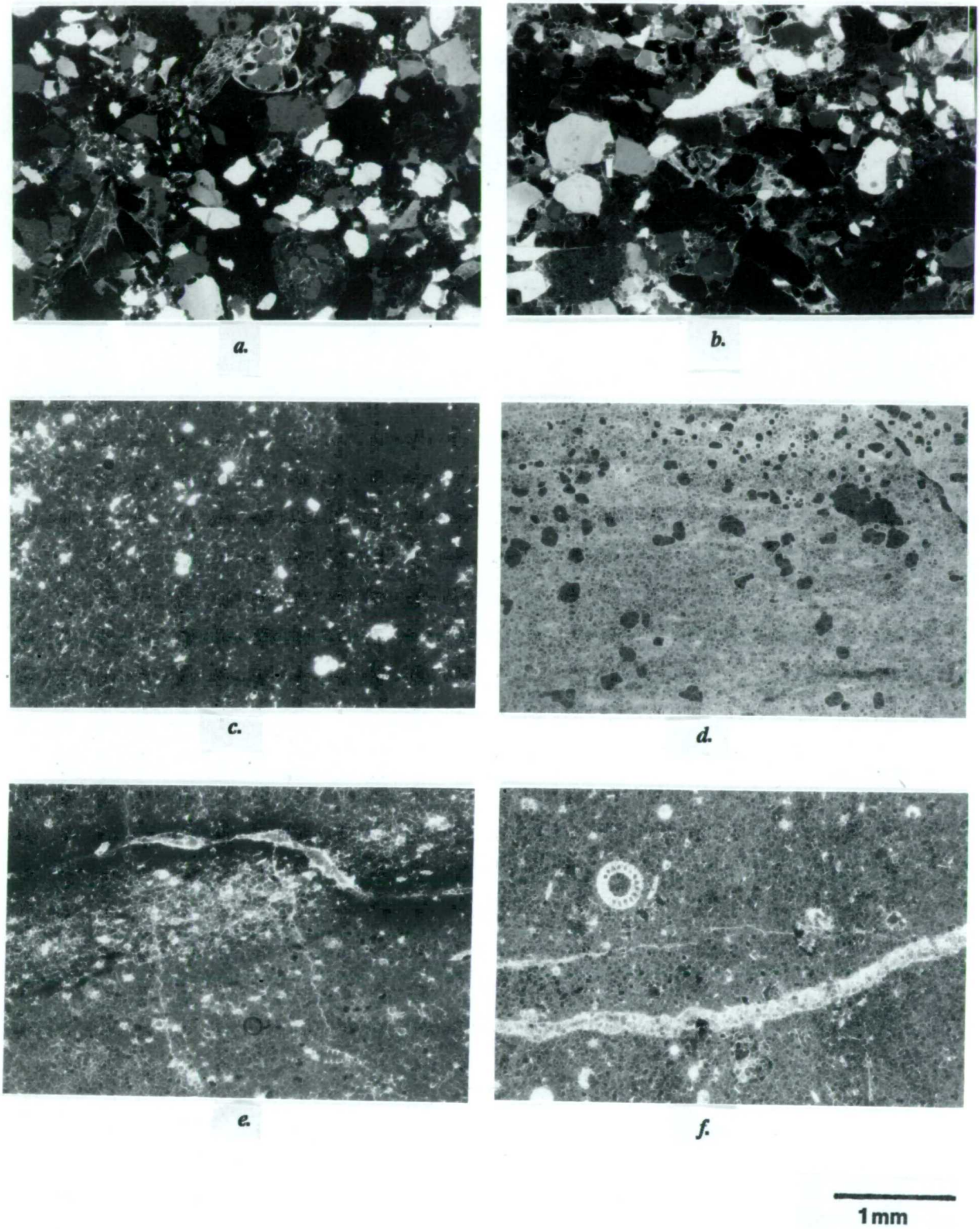

Plate 4.6 Optical microscope photographs of the Devil's Woodyard exotic blocks: a. DW1; b. DW2; c. DW4; d. DW5; e. DW6; f. DW7; (magnification x 20)

DW2: light grey and buff graded sandstone (Herrera Sand, plate 4.6.b); angular, 11 x 6 x 3 cm. (see AP3).
DW3: yellow-orange calcareous siltstone; sub-rounded, 3.5 x 2.5 x 1.5 cm. (see AP5).
DW4: brick-red, weakly calcareous fine claystone?, radiolaria present (plate 4.6.c); angular, 2.5 x 1.5 x 1 cm. (see AP10).
DW5: white pebble, siliceous, dark iron-rich "bands" (plate 4.6.d); 4 x 2.5 x 1.5 cm.
DW6: black fine, non-calcareous (dolomitised?) matrix surrounding more weathered siltstone pebbles (matrix: plate 4.6.e); angular 4 x 2.5 x 2.5 cm.
DW7: light green, weakly calcareous (Cretaceous radiolarian chert?), (plate 4.6.f); pebble, 4.5 x 3 x 1.5 cm.
DW8: dark grey weakly calcareous chert (Cretaceous); pebble, 5 x 3 x 2.5 cm.
DW9: same as DW8; flat pebble, 3.5 x 2.5 x 0.5 cm.
DW10: same as DW8; small pebbles;
Some soft green Lengua clay was also found.

No attempt is made to correlate these blocks with particular formations (except where identifications were made by Trinidad geologists), as the author has little experience with the field geology of the area. From the few identifications made, some of the blocks are Eocene (Pointe-a-Pierre sandstone), Miocene (Herrera sand, Lengua clay) and Cretaceous (chert), section 3.2.2. The cherts were pebbles and are more than likely to have been in younger formations. The angular blocks are very likely to be from the parent bed, or overlying beds, broken off by the "volcanic" activity.

Higgins and Saunders (1974) correlate blocks in the Anglais Point mud volcano with the Karamat, Herrera and Cruse formations, and in Devil's Woodyard with the Lengua, Tamana and Upper Cipero formations.

4.4.3. Micropalaeontology

a) Trinidad

The samples were analysed by Banner (University College London), who found them to be barren, with the exception of the Forest Reserve Core (FRC), Piparo (PIP) and Devil's Woodyard (DW).

Banner (1987, pers. comm.) reported that,

"FRC contains a mixture of foraminifera from various biozones of the Lower Cipero formation: opima opima and younger zones, covering some, at least, of the Oligocene and early Miocene parts of this formation. The microfossils are fresh and show little or no signs of abrasion or erosion."

"Sample labelled Piparo contains foraminifera which all show signs of post-mortem abrasion, surface solution and general wear and tear, as though they had been subjected to transportation....this could have happened by recirculation within the mudflow. Some of the specimens are from the opima opima zone, Oligocene, Lower Cipero formation...They include Paragroborotalia opima opima, Globigerina

angulisuturalis, Catapsydrax unicavus, Globigerina praebulloides, etc. Also present are rare Catapsydrax stainforthi of the Early Miocene part of the Cipero (about the same age as the Globiggerinoides ruber subquadratus present in the FRC sample). So, it is the same general origin for both samples."

"Sample labelled DW....contains rare forams that look as though they have been derived from a white marl and from a ferruginous mudstone. Nothing seen here is older than Early Miocene (i.e., Middle Cipero or younger - Lengua or Cruse." This possibly dates the above-mentioned brick-red clasts at the same age.

Banner points out that there is no trace of Navet or older microfossils and concludes that all the material that he could date was post-Eocene. Higgins and Saunders (1974) conducted micropalaeontological studies on the Trinidad mud volcanoes. Piparo was found to be associated mainly with the Lengua Formation, Digity and Devil's Woodyard with the Upper Cipero and Lengua Formations, Palo Seco and Anglais Point with Lower Cruse and Lengua clays, and Lagon Bouffe with the Eocene. The above result is therefore agreeable with their findings.

b) Taiwan

Unfortunately, it was not possible to conduct a comprehensive study of the microfossils in the Taiwan muds because they yielded very little information (Saunders, pers. comm., 1988). However, this work has been undertaken by a previous worker (Lin, 1965). Lin studied the fossils in the Kunshuiping area (fig. 3.12), and found that the microfossils emitted by the mud volcanoes there were overwhelmingly from the Gutingkeng Formation (section 3.3.2), with a few from the overlying formations. the Gutingkeng formation is also thought by Shih (1967) to be the origin of the southwest Taiwan mud volcanoes.

4.5. ATTERBERG LIMITS

4.5.1. Introduction

A useful method of sediment classification, used by engineers, is the measurement of the Atterberg limits (see Lambe and Whitman, 1979). This is a very simple method of defining the state of clays and silts based on their water content (wc) where,

$$wc = w_w / w_s \,(\%) \qquad 4.2$$

w_w = weight of water , g ,
w_s = weight of solids , g .

The Atterberg limits are based on the concept that a sediment changes from a solid state to a liquid state with increasing water content. When the water content is increased, the material becomes weaker and eventually begins to flow like a liquid. If the water content is decreased, the material strengthens and becomes brittle. The Atterberg Limits are the moisture contents which define the points at which a sediment begins to behave in a liquid fashion, the liquid limit (LL), or a brittle fashion, the plastic limit (PL). These values are very dependent on the grain size of the material - the finer the grains, the greater the surface area, and therefore, the higher the water content needed to weaken this material.

The Atterberg limits were measured for the mud volcano samples (method described in Appendix 3) to get an idea about their general state (strength) at any particular water content and to look for possible trends in different areas. Three related parameters, described below, are also used for general classification purposes,

a) the plasticity index (PI), which is an estimate of the water content range in which the material behaves plastically.

$$PI = LL - PL \qquad 4.3$$

Generally, the finer the grain size, the higher the plasticity.

b) The liquidity index (LI) where,

$$LI = (wc - PL) / PI \qquad 4.4$$

The LI puts the water content of a soil into the context of its plasticity, and thus gives an idea about the state of a sediment for that water content. For example, a very fine clay with a water content of 30% will be in a solid state because its PL is, say, 50%. However, a very sandy material with the same water content (30%), will be in a liquid state if its LL is 25%. Leroueil et al (1983) use values of liquidity index to estimate the undrained shear strength of clays.

c) A third useful parameter related to Atterberg limits is "activity" (A), defined by Skempton (1953).

$$A = PI / \%\ \text{clay (by weight)} \qquad 4.5$$

This is a measure of the attractive forces in a sediment: because of the increase in surface area per mass with decreasing particle size, it may be expected that the amount of attracted water will be largely influenced by the amount of clay present in the sediment.

Typical values of activity are presented in table 4.6.

Table 4.6. Soil classification according to activity (from Skempton, 1953)

The Atterberg limits were determined using the techniques described in BS1377 and Appendix 3. It should be stressed here that they are simple standard tests. Although they provide useful information about a sediment in a remoulded state (Appendix 3), they do not take any account of any fabrics in the sediment in its natural state (Lambe and Whitman, 1979).

4.5.2. Results

The results are presented in fig. 4.12 and table 4.7. Fig. 4.12 is a plasticity chart (see Lambe and Whitman, 1979); the A-line separates organic from inorganic soils, which plot below and above the line respectively.

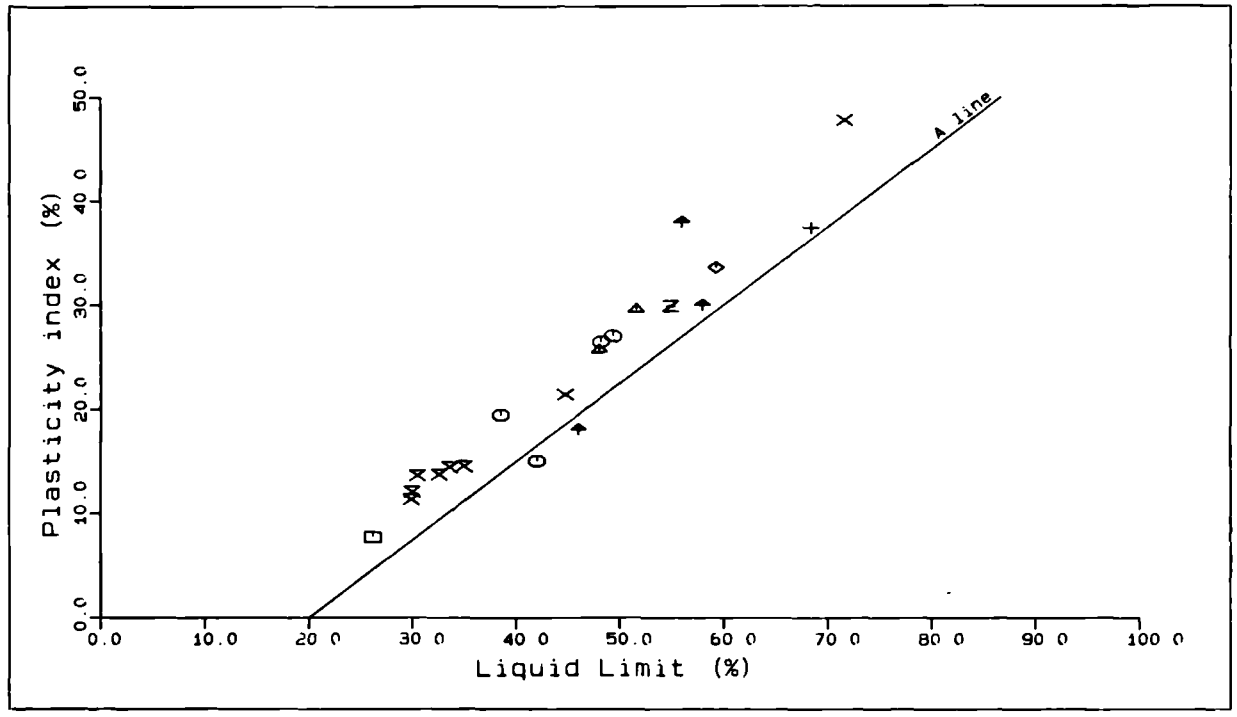

Fig. 4.12 Plasticity chart of the sampled mud volcanoes

SAMPLE	LIQUID LIMIT (%)	PLASTIC LIMIT (%)	PLASTICITY INDEX (%)	WATER CONTENT (%)	LIQUIDITY INDEX	CLAY CONTENT (%)	ACTIVITY
TRINIDAD							
AP1	48.1	22.3	25.8	49.8	1.1	51.0	0.5
AP2	51.7	22.0	29.7	39.8	0.6	51.0	0.6
DIG1	71.6	23.8	47.8	78.9	1.15	57.0	0.8
DIG2	44.7	23.4	21.3	40.8	0.8	19.0	1.1
DW	59.3	25.7	33.6	93.5	2.0	62.0	0.5
LB	26.2	18.5	7.7	25.0	0.9	10.0	0.8
MB*	55.0	23.0	32.0	-	-	34.0	0.9
PIP	68.4	31.0	37.4	67.8	1.0	66.0	0.6
PS1	48.3	21.7	26.5	77.1	2.1	43.0	0.6
PS2	49.4	22.4	27.0	43.8	0.8	51.0	0.5
PS3	38.5	19.1	19.4	40.8	1.1	34.0	0.6
PS*	42.0	27.0	15.0	-	-	43.0	0.4
LCF1*	58.0	28.0	30.0	-	-	69.0	0.4
LCF2*	56.0	18.0	38.0	-	-	55.0	0.7
NAR*	46.0	28.0	18.0	-	-	57.0	0.3
TAIWAN							
T1	30.5	16.9	13.6	92.3	5.	27.0	0.5
T2	30.0	18.0	12.0	48.8	2.6	26.0	0.5
T3-2	29.9	18.6	11.3	51.8	2.9	33.0	0.3
T4	33.6	19.2	14.4	72.3	3.7	31.0	0.5
T5	35.0	20.5	14.5	65.6	3.1	32.0	0.5
T6	32.6	18.9	13.7	58.7	2.9	25.0	0.6
TANIMBAR							
SK26	55.0	25.0	30.0	46.2	0.7	47.0	0.6

* Data from Kerr et al (1970)
Moruga Bouffe (MB); Palo Seco (PS); L. Cruse (5268-5380 ft.) (LC1); L. Cruse (5062-5074 ft.) (LC2); Nariva (NAR)

Table 4.7. Classification of mud volcano clays

4.5.3. Discussion

a) Plasticity Index

The Trinidad samples show a great variation in PI, reflecting the scatter observed for the PSD's (section 4.2.2). Lagon Bouffe, the coarsest material, has a PI of 8%, whereas Piparo, the finest, has a PI of 38%. Digity 1 has the highest plasticity (47.8%). This is explained by the smectite percentage in DIG1 (table 4.4), which was considerably higher than those for PIP. Smectites are the finest of the common clay minerals and their presence in a sediment would increase the plasticity dramatically. The Digity anomaly observed with the PSD's is again seen here: DIG2, the coarser material, also had the lower plasticity. It is not certain why DIG1 and 2 should be so different when they occur in the same area. PS1, PS2, AP1 and AP2, from the same general area, show similar plasticity (around 27%); PS3 has a lower plasticity index (19.4%).

Kerr et al (1970) measured the Atterberg limits of two mud volcano and three formation samples in Trinidad. Their results for Palo Seco (PS) do not agree with the results of this study (table 4.7). Moruga Bouffe (MB) had high Atterberg limits, although it is known to contain a considerable amount of silt (Higgins and Saunders, 1974). The formation samples LCF1, LCF2 and NAR, contain higher clay percentages, but their PI's did not reflect this. NAR (Nariva formation, thought to be the origin of Piparo, yielded a surprisingly low PI despite its high clay content (table 4.7). It is very difficult to compare the results of Kerr et al (1970) with the results of this study as it is not known which methods they used to measure the Atterberg limits, but table 4.7 shows that they are not anomalously higher than the other samples.

The results for Taiwan agree very well, again indicating, as did the PSD and clay mineralogy results, that the mud volcanoes sampled are extruding the same type of material; the Taiwan muds generally have a low plasticity (fig. 4.12).

It is interesting that the general range of plasticities for the mud volcanoes is quite low, considering the high clay content of most of the samples (section 4.2). This is briefly discussed below.

b) Liquidity Index

The values of LI varied considerably, the lowest being 0.6 for AP2 in Trinidad and the highest being 5.5 for T1 in Taiwan. The liquidity indices were generally higher for the Taiwan samples than for the Trinidad samples. The values of liquidity index cannot be used to any reliable degree because the water contents of the samples were very affected by climatic conditions, especially the basin-shaped mud volcanoes which collected a great deal of rain water. Generally, most of the mud volcano material was at or well above its liquid limit. Unfortunately, there is no moisture content data on formation samples for comparisons of liquidity indices (see section d below).

c) Activity

The Activity of the muds varied between 0.5 (AP1, PS2) and 1.1 (DIG2) in Trinidad. In Taiwan, the value was predominantly 0.5, but T3-2 gave a value of 0.3 and T6, a value of 0.6. SK26 from Tanimbar also gave a value of 0.6.

The results of activity are surprising. The majority of the samples fell into Skempton's (1953) A and B categories (table 4.6), which correspond fresh water sediments; the exceptions were the Digity and Lagon Bouffe samples. The parent bed material would be expected to have an activity of 1 (category C) if it is a marine clay. These results could indicate contamination by overburden material, but if this were the case, the Taiwan results would not be expected to be as uniform as they are for all the classification tests. One possible explanation could be in the preparation procedures for PSD and for Atterberg limits tests (Appendix 1 and 3 respectively), which vary. Whereas the clays are disaggregated by a special dispersing agent for the PSD tests, this is not done in the Atterberg limits tests. If the clays are flocculated in the sample, they could behave like a coarser particle and thus give an underestimate of the true value of plasticity index (PI). In this case, the value for activity would also be an underestimate. An example of this was observed in the Lagon Bouffe grains under the SEM, where small particles were cemented together to form a large particle (plate 7.1.b). Another possibility is that the $\overline{<2}$ fraction is not composed purely of clays, but also of crushed granular material, which explains the unusually low plasticities, despite the high clay content of most of the samples. This was observed to a certain extent in the XRD traces, where the secondary illite peak was usually quite high, indicating the presence of quartz; however, only a small quantity of quartz would bias an XRD trace. The crushing and fining of granular materials by shear is discussed in Chapter 7.

A note should be made here about the salinity and hydrocarbon content of the material which would be expected to affect its behaviour and the Atterberg limit values. These were not removed from the samples (Appendix 3).

4.6. GENERAL DISCUSSION

The tests conducted on the mud volcano samples have yielded interesting information about the material extruded. The data collected are combined in this discussion to explore any possible indications of the nature and origin of the material.

4.6.1. The Origin of the Mud Volcano Clays

The only method of identifying the source of a mud volcano is by a close study of borehole and geophysical data, combined with extensive analyses of core materials for comparison with the extruded material. Unfortunately, this was not possible, because subsurface data was confidential in both areas.

However, it is still necessary to study the properties of the materials extruded, in the likelihood that unusual characteristics unique to a certain bed could be seen; also, it was possible to make some comparisons with published data.

The main clues on the age of the mud volcanoes was provided by the micropalaeontology data and the clasts in the matrix (Trinidad). These should be treated with caution as they could indicate the age of contaminants only. For Trinidad, the few microfossils identified were traced to the Cipero Formation for Forest Reserve, Piparo and Devil's Woodyard, and possibly Lengua for the last (section 3.2.2). The Cipero Formation is a deep- water calcareous clay, reaching a thickness of 2700m in south Trinidad; it is also contemporaneous with the Nariva Formation (section 3.2.2). The Lower Cruse-Lengua Formation has been identified as a diapiric source offshore Trinidad (section 3.2.4). They are therefore both potential source formations. The Taiwan clays can almost without doubt be said to originate from the thick argillaceous Gutingkeng Formation as proven by Lin (1965) for the Kunshuiping mud volcanoes, and as inferred from well log data (Chou 1971, see section 3.3.4). But what of the other classification tests?

The Trinidad results showed no particular trends in any of the properties in that they had a fair scatter in PSD, clay mineralogy and Atterberg limits. They were compared with results for the Nariva and Lower Cruse clays (Kerr et al, 1970) and were found to have similar clay mineralogy (section 4.3.4). The similarity is superficial, however, as the mud volcanoes are scattered around the south of Trinidad and would not be expected to originate from exactly the same formation; also, the clay minerals found are all very common (fig. 4.6). Kerr et al argue that the formation samples are more clay-rich than the mud volcano samples. The clay content of the Piparo sample was compared with the result for the Nariva, which is thought to be the origin of this particular mud volcano. The Piparo result gave a higher clay percentage and plasticity (table 4.6) than the Nariva, but both are clay-rich. The Lower Cruse materials are also clay-rich, but the mud volcanoes of Anglais Point, Digity 1 and Devil's Woodyard have comparable amounts of clay (table 4.6), the rest being coarser; the Atterberg limits of these samples were also comparable. No conclusive evidence could be found to support Kerr et al, but it must be stressed that many more samples are needed to make this type of comparison reliably. Generally, therefore, no clues on the origin of the Trinidad mud volcanoes could be established from the classification tests.

The Taiwan results were more promising, as the muds all had very similar properties, suggesting that they come from the same source. The muds showed a notable lack of smectite, which could have been a useful marker. Unfortunately, the sedimentary sequence in the Tainan area, where the muds were collected, has a similar mineralogy throughout the Pliocene upwards, and the exact origin could not be established.

4.6.2. Contamination by Overburden Material

When the muds come up to the surface, they probably assimilate some the overburden material; if so, can this be detected?

The limitations mentioned above about lack of subsurface data apply again here. However, if no (or equal) contamination is occurring, one would expect mud volcanoes within the same area to extrude the same material. This is observed to some extent in Trinidad, in that the mud volcanoes of Palo Seco and Anglais Point had the same properties, with the exception of PS3; Digity 1 and 2 are different in grain size, but have identical clay mineralogy. The Taiwan samples all occur in the same general area and show more similarity in all their properties, which suggests that they are likely not to have been heavily contaminated.

If contamination is occurring, then one would expect the material at the surface to have coarser grain-size, assuming that the sedimentary sequence is regressive. As mentioned above, from the limited data for Trinidad, this is observed by Kerr et al (1970), based on only five samples. Of course, if clasts from overlying formations are assimilated into the mud, they are very likely to contaminate it. In the experimental work described in Chapter 6, however, it is assumed, for simplicity, that the $<425\,\mu$ components of the muds are representative of the parent bed (Appendix 4).

4.6.3. Mud Volcano Composition

Are there any particular properties unique to mud volcano materials? Unless considerable contamination by the overburden is changing the original composition, the answer is no. Judging by the variation in the grain size, mineralogy and Atterberg limits for all the mud volcanoes sampled, there do not seem to be any. Chapters 6 and 7 explore the effect of composition on the behaviour of three different clays: Lagon Bouffe, Devil's Woodyard and Taiwan.

4.6.4. The Clasts in the Matrix

There is a possibility that some of the clasts in the matrix are part of the parent bed. The small clasts in the Anglais Point samples looked very similar to the matrix. Their clay mineralogy was analysed and was found to be identical. If this is the case, then the material extruded may be a "remoulded" version of the parent bed. Certainly, if the Cipero Formation is responsible for any of the mud volcanoes then there must be a breakdown of the associated calcareous cementation. The calcite cement observed around some of the Lagon Bouffe grains may be another example of this (section 4.5.3). This is discussed further in Chapter 7.

The identified larger clasts in the Trinidad mud volcanoes DW and AP are of various ages, some being older than the assumed age of the matrix. This is not difficult to explain, as extensive thrust faulting occurs in southern Trinidad (observed in some of the well data mentioned in section 3.2.4). The size of the clasts was noted in this work, but it is appreciated that they may well be smaller pieces of much larger clasts, such as those observed in Anglais Point (section 3.2.5).

4.6.5. Mud Volcano Shape

Shih (1967) assessed the effect of the composition of the mud on mud volcano shape. His classification, as mentioned in Chapter 1, was as follows:

- **A: Cone - inclination of sides $>20^{\circ}$, crater diameter dozens of centimetres.**
- **B: Shield - inclination of sides 5-20°, crater diameter dozens of centimetres.**
- **C:Maar -inclination of sides $<5^{\circ}$, crater diameter several centimetres to 2 metres.**
- **D: Basin - crater diameter several metres, some with parasitic volcanoes.**
- **O: Hole - crater diameter few centimetres.**

Shih came to the conclusion that the PSD had a marked effect on shape. He found that the A cones generally contained the highest clay percentage. D cones were found to fall under two categories: silty and clayey, whereas B and C cones generally showed poor sorting (steep curves). This classification does not stand (at least, for the limited available data). PS1 (D), PS2 (A), PS3 (B) and AP (C) have similar distributions. Piparo (D) has the highest clay percentage, whereas Lagon Bouffe (D) has the lowest. Also, Moruga Bouffe clays, which are known to be very silty (Higgins and Saunders, 1974) form A-cones. The Taiwan vents vary between A and D-types, but all show poor sorting with no significant variation. There is enough scatter in Shih's results and the above results to render this classification doubtful.

No correlation was observed by Shih between mud volcano shape and mineralogy. This is confirmed here: the mere difference in the mineralogy of the Trinidad and Taiwan mud volcanoes, despite the similarity in their A, B and D cones, points to this. Also, the Taiwan mud volcanoes all have a very similar mineralogy, despite the differences in shape. This lack of correlation applies to Atterberg limits as well, as they are related to clay mineralogy and PSD.

It is suggested that the differences in mud volcano shape within the same area could be related to the size of the structural weakness along which the mud is being extruded. Another possibility is the liquidity index of the material, which will affect the viscosity and, perhaps, shape. Unfortunately, it was not possible to determine the moisture content reliably, especially in the basin-shaped mud volcanoes, because of contamination by rain water.

4.6.6. Conclusion

In brief conclusion, the classification tests have proved very useful in determining and comparing various properties of mud volcanoes. The Taiwan results are more consistent than the Trinidad results, and they point to a similar origin for the Taiwan mud volcanoes: the thick Gutingkeng Formation. Generally, however, more samples need to be collected from mud volcanoes, outcrop material, and, where possible, core material for better determinations of the origin of the muds. Mud volcanoes should ideally be sampled at regular intervals and at different times of the year to compare the consistency and chemistry of the mud extruded.

The results have shown that the sampled mud volcanoes emit medium to very low plasticity clays, with variable mineralogy. These plasticities are not, however, assumed to be representative of all mud volcanoes; the New Zealand mud volcanoes, for example, emit smectite-rich clays (table 1.2) which would be expected to have very high plasticity. The behaviour of clays of different plasticities is therefore explored in Chapters 6 and 7.

CHAPTER 5

BACKGROUND TO THE EXPERIMENTAL STUDY OF MUD VOLCANOES

5.1. INTRODUCTION

Although a great deal of work has been done on the geological causes of overpressuring and extrusion of mud volcano clays, very little is known about these mechanisms from a geotechnical point of view. Thick clay sequences in a tectonically compressive environment undergo a complex stress history where vertical (overburden) and horizontal (tectonic) loads are acting on the sediment. The behaviour of the clay under various stress conditions is therefore the main factor to be considered when studying these phenomena.

The next three chapters will cover an experimental approach to the problem. This is derived from the science of soil mechanics which models the behaviour of soils under different stress conditions. Although generally studied for soils at the surface, studies in soil mechanics have been applied to higher, geological stresses (Rieke and Chilingarian, 1974; Skinner, 1975; Bishop et al, 1965, 1975; Bishop, 1976; Bishop and Skinner, 1976; Jones and Addis, 1985; Karig, 1987; Addis, 1987).

The principal theories of soil mechanics are based on an extensive experimental investigation of the response of a sediment to an applied stress. The experiments are conducted in different types of apparatus, chosen according to the complexity of the stress conditions. In this study, two different aspects of sediment deformation are under analysis:

1) The compaction characteristics of a sediment, including a) volume loss with time under a constant effective stress (consolidation), using a high pressure oedometer (described in Addis, 1987)[1], and b) volume loss with increasing effective stresses (compression), using the high pressure triaxial cell (described in Appendix 5).

2) The effect of tectonic activity on a thick, effectively undrained, clay layer. The undrained shear deformation and pore pressure response of the mud volcano clays, consolidated at different principal stress ratios, was investigated in the high pressure triaxial cell (Appendix 5).

Naturally, the exact stress conditions in the sediments undergoing overpressuring and volcanism are not known. It is therefore necessary to make some experimental simplifications. In this chapter, some of the main principles and assumptions used in the study will be briefly covered. Section 5.2 describes the major concepts in soil mechanics relevant to this study, beginning with an appraisal of the principle of effective stress at high stresses, then applying this principle to the consolidation and undrained shear of clays. The drained volume change and undrained pore pressure response of sediments under different stress conditions are also described. Finally, these ideas are incorporated into the critical state model for clays (Schofield and Wroth, 1968), which defines the ideal failure conditions of a sediment.

1 *The results of one-dimensional consolidation in the oedometer will not be presented in this thesis due to continuous equipment failure during testing, which rendered the results unreliable. The analysis was aimed at exploring permeability controls on consolidation/underconsolidation, using the one-dimensional consolidation equations described in Chapter 2 (equations 2.2 and 2.3). This is not dealt with in this work.*

Section 5.2 is collated from key soil mechanics textbooks (eg. Schofield and Wroth, 1968; Atkinson and Bransby, 1978; Lambe and Whitman, 1979). The applications of this theory to the experimental study is discussed more rigorously in Chapter 7. The basic methodology of the experiments is described in section 5.3 (see also Appendix 6).

5.2. ASPECTS OF SOIL MECHANICS USED IN THE EXPERIMENTAL STUDY

5.2.1. The Principle of Effective Stress

The main assumption made in the experimental study is that the principle of effective stress, as defined by Terzaghi (1943), holds. As mentioned previously (equation 2.1), the effective stress acting on a sediment is the total applied stress (σ) minus the pore fluid pressure (u),

$$\sigma' = \sigma - u \qquad 5.1$$

A sediment will only consolidate in response to changes in effective stress (Terzaghi, 1943). If the pore fluid pressure goes up by the same amount as the total stress, the sediment will not feel any changes in effective stress. This principle facilitates the simulation of the effective consolidation stress acting on a sediment without using the same magnitudes of total stress and pore pressure occurring in nature.

Certain assumptions are made in the formulation of equation 5.1,
a) the soil is homogeneous,
b) the soil is fully saturated,
c) the pore fluid is incompressible, and
d) the grains are incompressible;
otherwise, the equation becomes more complex to account for these variables.

Various workers have assessed the validity of the principle of effective stress at low and high stresses.

Bishop (1953) revised the effective stress equation to take account of grain compressibility,

$$\sigma' = (\sigma - u) + (C_s / C)\, u \qquad 5.2$$

where,

C_s = compressibility of solid material forming grains, and
C = bulk soil compressibility for relevant stress range.

C_s, however, has been found to be very low for clays for stresses up to 62.1 MPa (Bishop et al, 1975).

Bishop and Skinner (1976) conducted high pressure tests on different materials and found that the effective stress equation is valid up to 70 MPa. From their conclusions, it seems reasonable to assume that the principle of effective stress is valid in the experiments conducted in this study, especially as the materials tested are uncemented and fully saturated (Appendix 4). It will be kept in mind, however, that real sediments at depth will deviate from the norm. It is impossible to attain a homogeneous 3km layer of sediment. Full saturation is likely, except in the presence of gas, like methane, as a pore fluid; this would serve to make the soil highly compressible, unless it has already gone into solution in the presence of high pore fluid pressures (section 2.2.2.b). The behaviour of partly saturated sediments is not investigated in this work. At high geological stresses, one must also consider the compressibility of water (brine) and water-oil mixtures. In addition, the sediment is very likely to be cemented.

5.2.2 Presentation of Stresses

The stress state in a sediment and its pore volume will be presented using the two standard effective stress path axes, p' (mean effective stress) and q (deviatoric stress), and e (voids ratio) or porosity (n) respectively where,

$$p' = (\sigma_1' + 2\sigma_3') / 3 \qquad 5.3$$

$$q = \sigma_1' - \sigma_3' \text{ and,} \qquad 5.4$$

$$e = n / (1 - n) \qquad 5.5$$

These axes are the most commonly used in soil mechanics to present the stress history or stress path of a sediment (see below).

Note: σ_1', σ_2' and σ_3' are the three principal effective stresses. σ_1', the greatest principal stress, is vertical in the experiments, although it is appreciated that it can be horizontal in nature, particularly in an area of tectonic compression (Chapter 7).

5.2.3. Isotropic Consolidation of Clays

When an effective stress is applied to a sediment, the sediment experiences volume loss due to the expulsion of excess pore fluids. It has been found that when clays consolidate isotropically (i.e. under equal all-round stresses), there is a unique relationship between volume change and mean effective stress (fig. 5.1),

$$v = N - x \ln p' \qquad 5.6$$

where,

$v = 1 + e$ (v = specific volume)

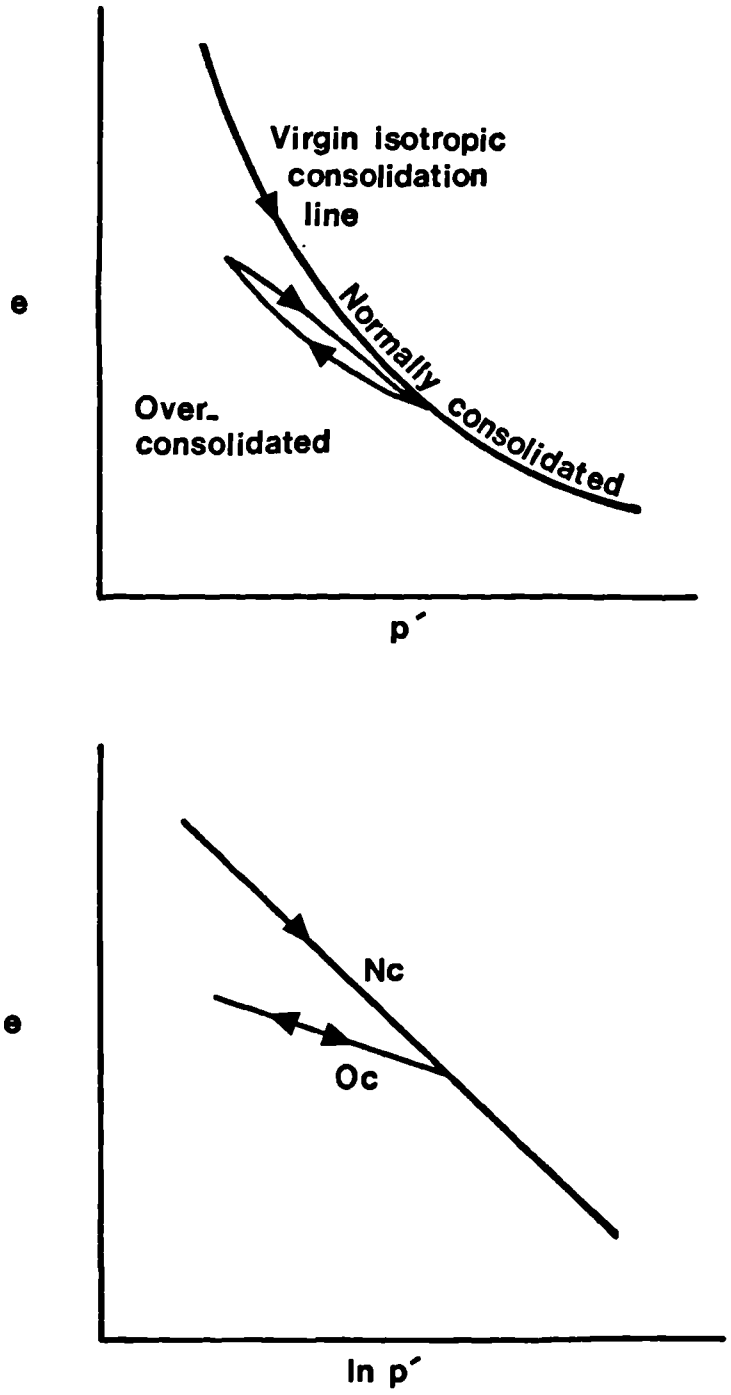

Fig. 5.1 Voids ratio (e) - mean effective stress (p') relationships for an isotropically consolidated material, showing overconsolidated behaviour during unloading and reloading.

N = specific volume of soil consolidated to 1 MPa and,
x = slope of isotropic consolidation line in v - ln p' space.

When the effective stresses are reduced in a drained state, the material regains some volume in a defined manner (fig. 5.1). It then becomes overconsolidated, i.e., it is at a lower effective stress than it had experienced in the past, and its behaviour is different to a normally consolidated material (section 5.2.7). This is mentioned because the term "overconsolidation" is frequently used to denote sediments consolidated to great depth in geology. If they have not experienced uplift, then they are still normally consolidated. The exception to this is if the pore fluid pressures increase, causing a decrease in effective stress.

5.2.4. Anisotropic Consolidation of Clays

In the natural state, the principal effective stresses acting on a sediment will not be equal, and the sediment will be subjected to deviatoric stresses. The lower the ratio between the horizontal and vertical effective stresses (termed the K-ratio), the higher the shear stress, and the lower the voids ratio for the same mean effective stress (fig. 5.2). K_o consolidation is consolidation with zero lateral deformation (i.e. one dimensional consolidation), as would be expected in a passive sedimentary basin. A typical value of K_o for normally consolidated clays is 0.7. K_o is related to the stresses in a soil by the relationship,

$$q / p' = 3(1 - K_o) / (1 + 2K_o) \qquad 5.7$$

It has been found by experimentation that anisotropic consolidation lines are parallel to the isotropic consolidation line in v - ln p' space.

5.2.5. Undrained Shear Behaviour of Clays

When a normally consolidated clay is sheared in an undrained state, the pore pressures increase; this phenomenon is related to pore fluid loss during drained shear (fig. 5.3). Generally, the fluid pressure increases with increasing deviatoric stress until a maximum strength is reached, beyond which failure occurs; this is termed the undrained shear strength (C_u) of a soil. C_u is not a constant; it is very dependent on various factors, including,
a) the initial structure of the soil,
b) the stress path followed during consolidation,
c) the stress path followed during undrained shear (compression, extension, cyclic), and
d) under high effective stresses, the effects of the sediment "skeleton" and its pore fluids.

These effects on C_u and pore pressure generation in a clay will be investigated in the next two Chapters.

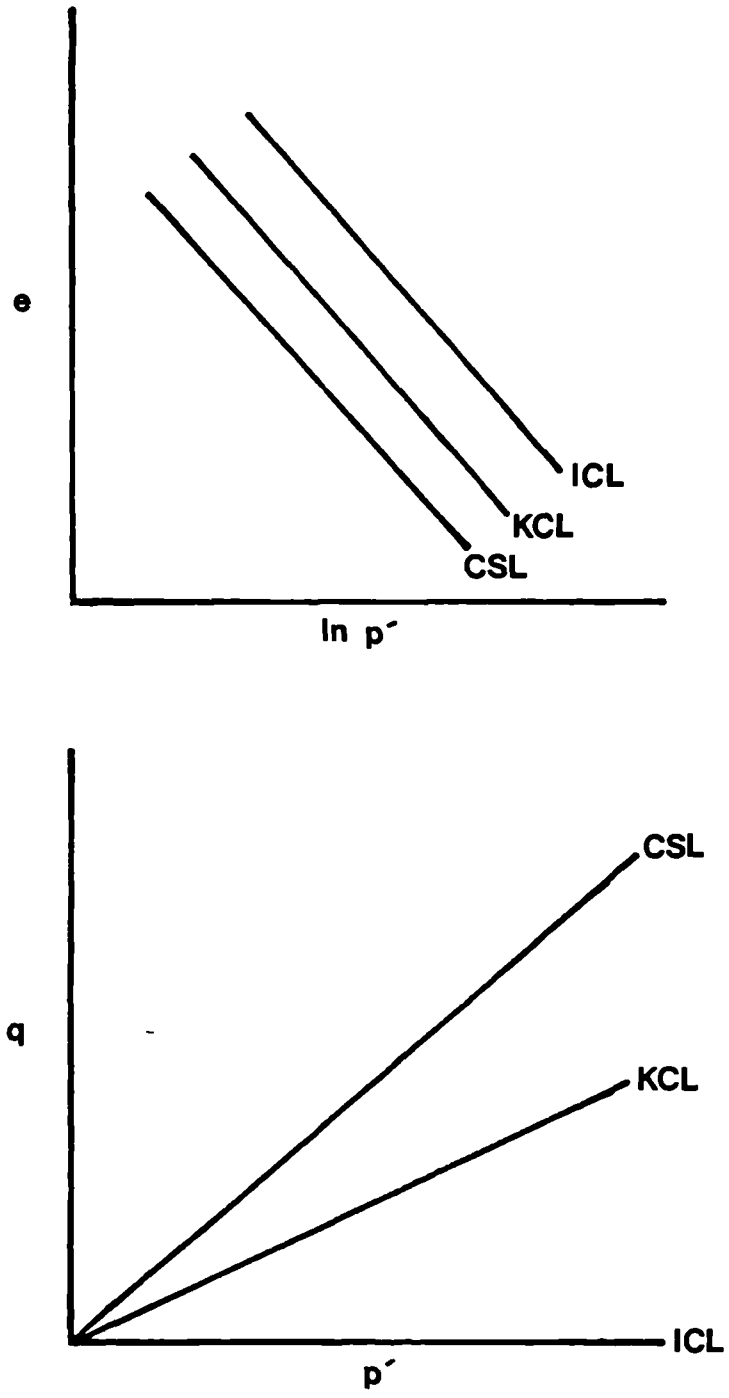

Fig. 5.2 Voids ratio (e) - mean effective stress (p') - deviatoric stress (q) relationships for the isotropic (ICL) and anisotropic (KCL) consolidation lines and the critical state line (CSL).

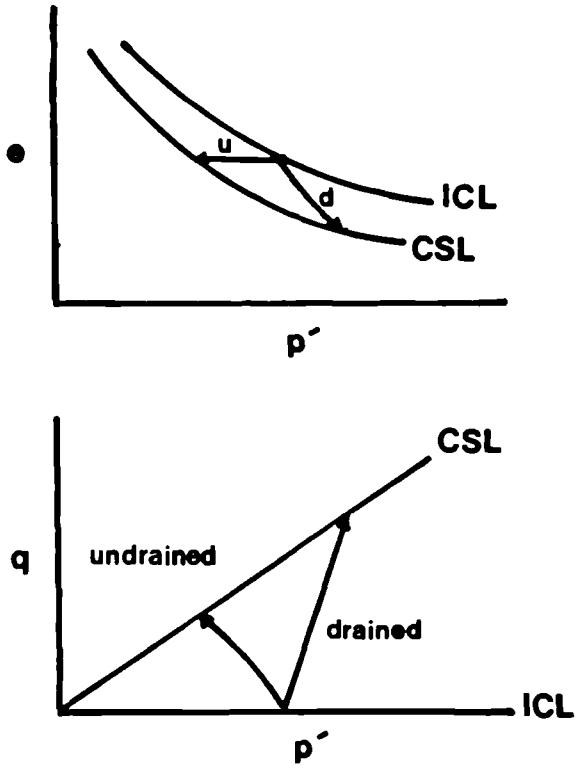

Fig. 5.3 Voids ratio (e) - mean effective stress - deviatoric stress relationships for drained (d) and undrained (u) shear tests

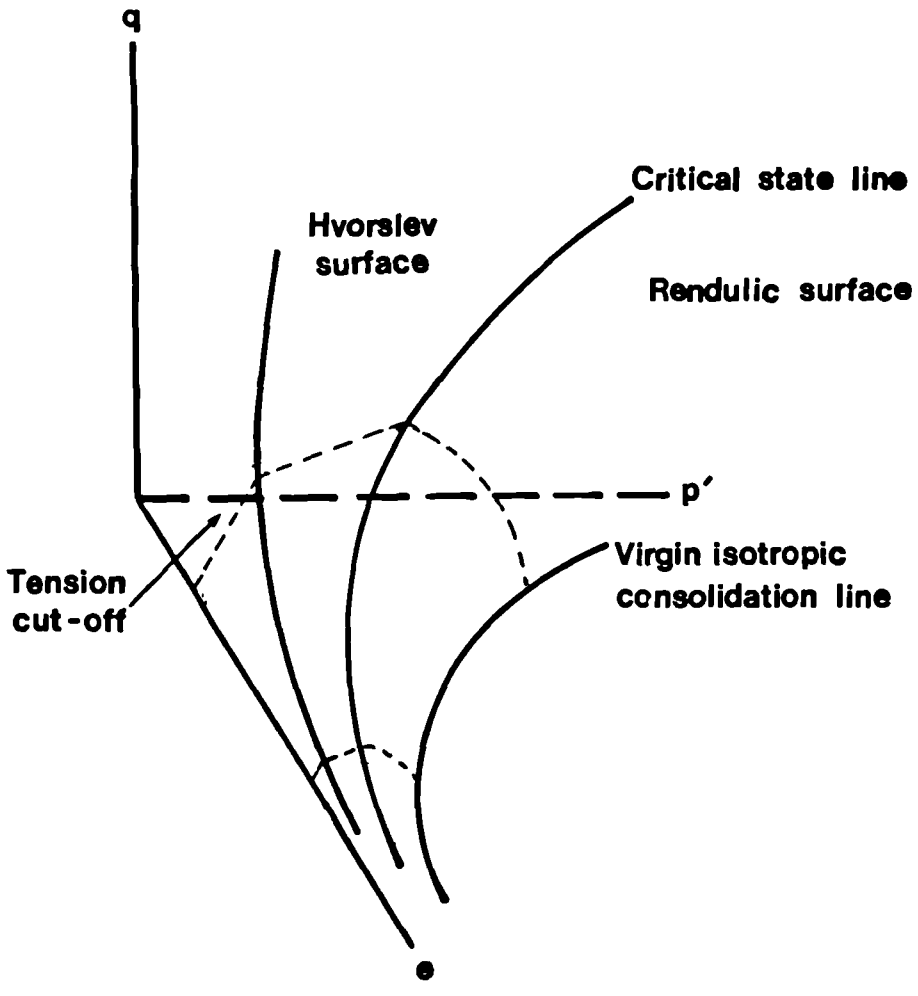

Fig. 5.4 The Critical State model of soil behaviour

5.2.6. Undrained Pore Pressure Response

When a stress is applied to a soil in an undrained state, the pore fluid pressure caused by this increase in stress cannot escape and the soil becomes overpressured. In this section, the relationship between the total stresses and pore pressure response is considered for different loading conditions (Skempton, 1954; Lambe and Whitman, 1979).

a) Pore Pressure Parameter C

When an increment of load is applied in an oedometer, the pore pressure response (C) is,*

$$C = du / d\sigma'_1 = 1 / \{1 + n (C_w / C_{c1})\} \qquad 5.8$$

where,

n = porosity,
C_w = compressibility of water, and
C_{c1} = compressibility of soil skeleton (M_v in equ. 2.3).

Due to the negligible compressibility of water and soil grains at low effective stresses, this value is equal to unity in fully saturated sediments. It is only less than unity in the presence of a third phase (air/gas) or for very stiff materials such as rocks. Deviations from this value at higher stresses have been observed by Addis (1987) for chalk, which produced C-values greater than unity. This was attributed to structural collapse at the near-yield stresses.

b) Pore Pressure Parameter B

When an isotropic increment of stress is applied, the pore pressure response (B) is,

$$B = du / d\sigma = 1 / \{1 + n (C_w / C_{c3})\} \qquad 5.9$$

where,

C_{c3} = increment of volumetric strain / increment of isotropic effective stress.

The B and C pore pressure parameters are very related. As for the C-value, this value is equal to unity for fully saturated, highly compressible sediments (Bishop, 1976; Mesri et al, 1976); it is only less than unity in the presence of a third phase and for stiff materials. Deviations from this value at higher stresses were observed in preliminary tests on weak materials in the high pressure triaxial cell, where B-values in excess of 1.5 were observed.

c) Pore Pressure Parameter A

The pore pressure response caused by undrained axial loading after isotropic consolidation is,

* Note: Equation 5.8 does not account for the effect of the shear stress component - (parameter A).

$$A = du - d\sigma_3 / d\sigma_1 - d\sigma_3 = 1 / \{1 + (C_{c2} / C_{c1})\} \qquad 5.10$$

where C_{c2} = sum of volumetric strains due to changes of σ'_2 and σ_3.

The pore pressure parameter A is not a constant; it varies considerably, depending on the initial sediment structure and subsequent stress history, as will be discussed in Chapter 7.

If the pore fluids are not compressible, equations 5.8 to 5.10 become a function of $du / d\sigma_1$ only, assuming that the cell pressure remains constant during undrained shear.

5.2.7. The Critical State Model

In sections 5.2 to 5.8 above, the basic concepts of the consolidation and undrained shear behaviour of a clay normally consolidated to low effective stresses have been introduced. We shall now briefly look at the general behaviour of a clay for all stress states. The general behaviour of an isotropic soil is explained by the Cam-Clay, or critical state model (Schofield and Wroth, 1968; Roscoe and Burland, 1968).

The behaviour of a clay has been found to fall into two categories: one is normally consolidated to lightly overconsolidated clay and the other is heavily overconsolidated clay (section 5.2.3). The former will contract during shear, producing excess pore pressure (and decreasing p') in an undrained state; the latter, on the other hand, will dilate during shear, developing negative pore pressures in an undrained state (fig. 5.4). Ultimately, the material can reach the critical state where it continues to deform with no further changes in effective stress or volume. The material was further found to shear within a defined surface in stress space, beyond which impossible states would be attained. Normally consolidated to lightly overconsolidated clays are thought to move along the Roscoe surface (more aptly termed the Rendulic surface, Burland, 1987) during shear, until they reach the critical state line; heavily overconsolidated materials follow the Hvorslev surface (fig. 5.4). The critical state line joins the two surfaces in e - p' - q space (fig. 5.4). The slope of the line in p' q space is the constant M; in e - ln p' space, it is parallel to the isotropic and anisotropic consolidation lines (fig. 5.2).

The behaviour of heavily overconsolidated clays will not be covered in this study and, as such, only the Rendulic surface side of the model is considered here.

The model provides a very useful general framework for sediment behaviour. Deviations to the model are observed in low pressure soil mechanics, however, due to material anisotropy; greater deviations may therefore be expected at higher pressures. This is discussed in Chapter 7.

5.3. THE EXPERIMENTAL STUDY

The principles of soil mechanics, briefly described in this Chapter, have been used to investigate the consolidation behaviour of mud volcano clays and their pore pressure response during undrained shear. The clays used for testing were from Devil's Woodyard and Lagon Bouffe in Trinidad and all the Taiwan clays. These clays were already in the remoulded state and had very high liquidity indices (table 4.7). They therefore had to be consolidated to reasonably low moisture contents to facilitate the high pressure testing which was in a p' range of 5 to 60 MPa (Appendix 4).

The triaxial experiments conducted on the mud volcano samples were of three types (Table 5.1):

a) Consolidated (isotropic) undrained shear. This is a simple test where the sample is allowed to consolidate fully under an equal all-around stress then subjected to axial loading in an undrained state at a constant cell pressure (Bishop and Henkel, 1962). Isotropic consolidation is probably unrealistic, geologically speaking, but yields useful data on stress-strain relationships. Undrained shear models tectonic activity on a thick clay sequence which is, in effect, undrained due to its low permeability.

b) Consolidated (anisotropic) undrained shear (Bishop and Henkel, 1962). Here, samples were consolidated anisotropically with a horizontal to vertical stress ratio of 0.6. This is probably more realistic in geological terms. The sample was then sheared in the manner described above.

c) Cyclic loading test, where the sample is loaded-unloaded to simulate the effect of earthquake activity on the clay. Cyclic loading is known to produce high pore fluid pressures in clays (eg. Takahashi, 1981).

As mentioned above, only the triaxial test results are presented in this work (Chapter 6).

SAMPLE	TEST	p' BEFORE US (MPa)	TEST NAME	NOTES
TRINIDAD				
Devil's Woodyard				
DW1	IC.US	10	DW1I10	
DW2	IC.US	50	DW2I50	
DW3	O	40	DW3O40	Unreliable results
Lagon Bouffe				
LB1	IC.US	50	LB1I50	
LB2	KC.US	25	LB2K25	
LB3	KC.US	60	LB3K60	
LB4	KC.US	15	LB4K15	
LB5	KC.US	45	LB5K45	Cell p decreased during US
LB6	IC.US	5	LB6I5	
LB7	O	20	LB7O20	Unreliable results
TAIWAN				
TA	IC.US	50	TAI50	
TB	KC	15	TBK15	Failed
TC	KC.US	50	TCK50	
TD	KC.US	15	TDK15	
TE	KC.US	25	TEK25	
TF	IC.US	5	TFI5	
TG	CYC	30	TGCY30	Loaded-unloaded isotropically and axially

KEY: IC isotropic consolidation
K anisotropic consolidation (K = 0.6)
US undrained shear
O oedometer
CYC cyclic loading

(All tests, apart from those with the letter O, were undertaken in a high pressure triaxial cell and include an undrained shear stage.)

Table 5.1. High pressure tests on mud volcano clays

CHAPTER 6

RESULTS OF THE HIGH PRESSURE DEFORMATION EXPERIMENTS CONDUCTED ON THE MUD VOLCANO CLAYS

6.1. INTRODUCTION

As mentioned in the previous chapter, high pressure experiments were conducted on the mud volcano clays to understand their behaviour during consolidation and undrained shear. This chapter presents the results of the experimental programme. The layout of the chapter is based on the two stages of the stress paths followed in the triaxial tests: consolidation and undrained shear. Section 6.2 describes the consolidation behaviour of the clays, presenting the results of both isotropic and anisotropic consolidation tests. Section 6.3 presents the results of the undrained shear stages of the tests.

Results from the different materials are presented in order of increasing plasticity, i.e. Lagon Bouffe, Taiwan and Devil's Woodyard clays respectively. This is done to compare the general behaviour of mud volcano clays over a range of particle size distributions. The main features of the tests are summarised for discussion in Chapter 7.

6.2. CONSOLIDATION

6.2.1. Introduction

This section will describe several aspects of consolidation of the three mud volcano materials used: a) the relationship between voids ratio and effective stress for the isotropic and anisotropic tests carried out in the triaxial cell; b) the pore pressure parameter B and c) axial stress-strain relationships for anisotropic tests.

6.2.2. Lagon Bouffe

a) Voids Ratio - Effective Stress Relationship

Six samples of Lagon Bouffe materials were tested. They were all consolidated isotropically at 5 MPa. LB1 was further consolidated to 50 MPa. LB2, LB3, LB4 and LB5 were anisotropically consolidated at a K-ratio of 0.6 to mean effective stresses of 25, 15, 62 and 45 MPa respectively. LB6 was not consolidated any further. The initial voids ratios of the Lagon Bouffe samples were not identical, varying between 0.36 and 0.42. This is attributed to the difficulties encountered in sample preparation and measurement of this silty material. It was very friable and difficult to handle and evaporation occurred very quickly; the samples also contained oil (Appendix 1), which may have affected measurement of density and porosity. The change in voids ratio is recorded in table 6.1 and fig. 6.1.

TEST	INITIAL e	FINAL p' (MPa)	FINAL e
LB615	0.361	4.9	0.296
LB3K15	0.400	15.3	0.275
LB2K25	0.420	25.1	0.249
LB5K45	0.380	44.7	0.197
LB1150	0.385	50.1	0.213
LB4K60	0.390	61.5	0.185

Table 6.1. Change in voids ratios for the Lagon Bouffe triaxial tests

The slope of the virgin isotropic consolidation line (x) in e - ln p' space is 0.05 and N, the value of specific volume at 1 MPa is 1.39 (fig. 6.2). LB6, and, indeed, all the other samples were consolidated isotropically to 5 MPa, but the e - ln p' curves are parallel rather than being superimposed (fig. 6.1); this suggests that either the samples are slightly different, or that the initial voids ratio measurements were inaccurate due to the above-mentioned problems. The latter reason is more likely. The value of N may therefore be slightly erroneous. The consolidation line changes slope between 1 and 5 MPa; it is difficult to locate the pre-consolidation pressure as the break in slope is not well-defined. (The pre-consolidation pressure is the maximum pressure the sample had been under before the test - in this case, the maximum consolidation pressure of 2.45 MPa in the small cylinder apparatus, described in Appendix 4).

Fig. 6.3 shows the final voids ratio against mean effective stress, which define a curve in e - p' space. (The voids ratios at failure are also plotted for comparison).

b) Pore Pressure Response

The B-values were measured for the isotropic consolidation stages of all the triaxial tests. The results of LB1150 will be presented here as it was the only test with an isotropic consolidation stage reaching a p' of 50 MPa (table 6.2).

p (MPa)	B_1	B_2	TIME
1.3	0.94*		
2.1	1.00		
3.2	0.96	1.02	3 hr
6.5	0.93	0.95*	1 hr
LEAK			
6.5	0.97*		
13.3	0.83	0.90*	37 min
26.4	0.90	1.04	17 hr
50.8	0.59	0.95	24 hr

B_1 = initial B-value B_2 = final B-value
* = pore pressures not allowed to settle completely

Table 6.2 Average B-values for test LB1150

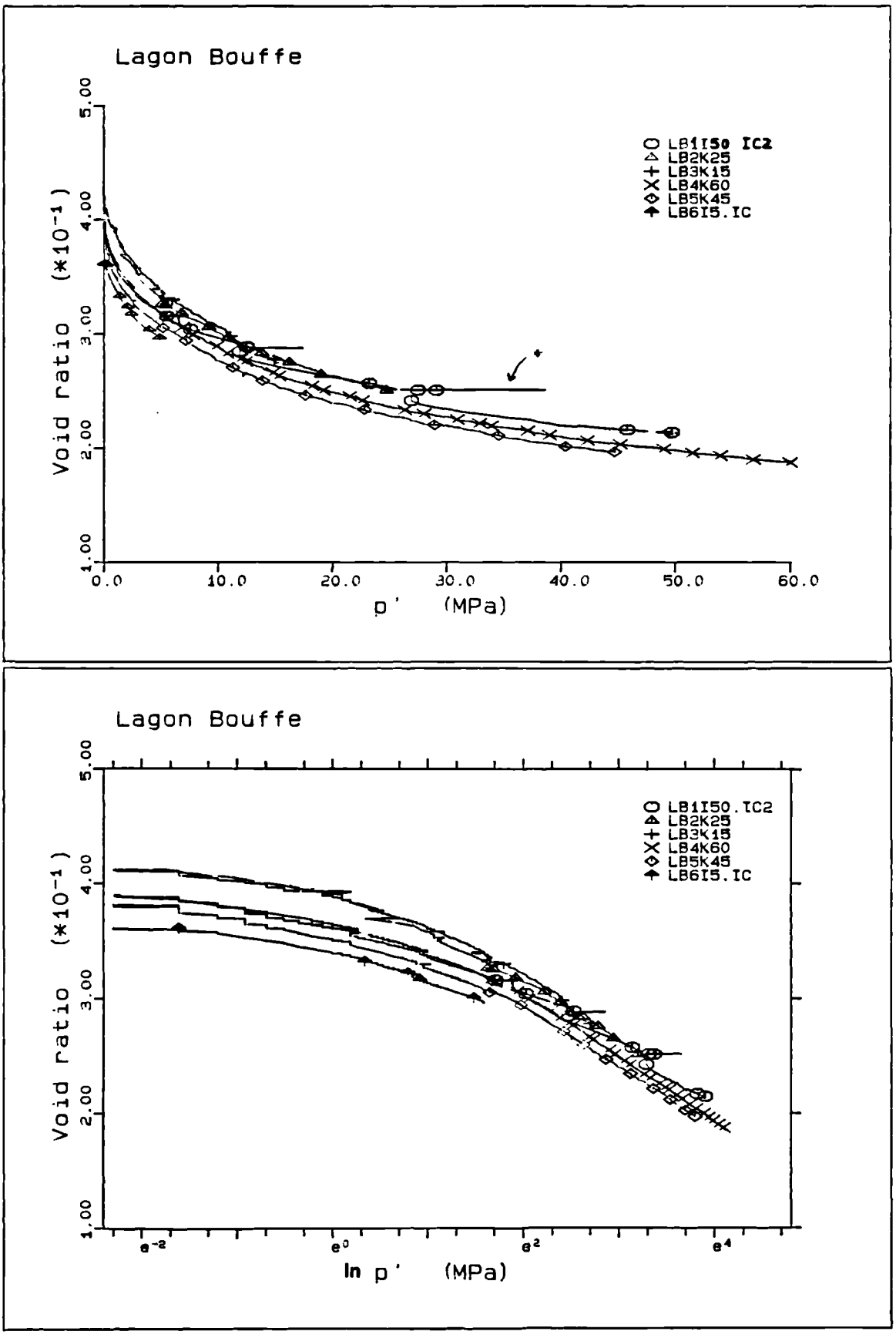

Fig. 6.1 Voids ratio - mean effective stress relationships, Lagon Bouffe series

* These lines are an artefact of experimental procedure

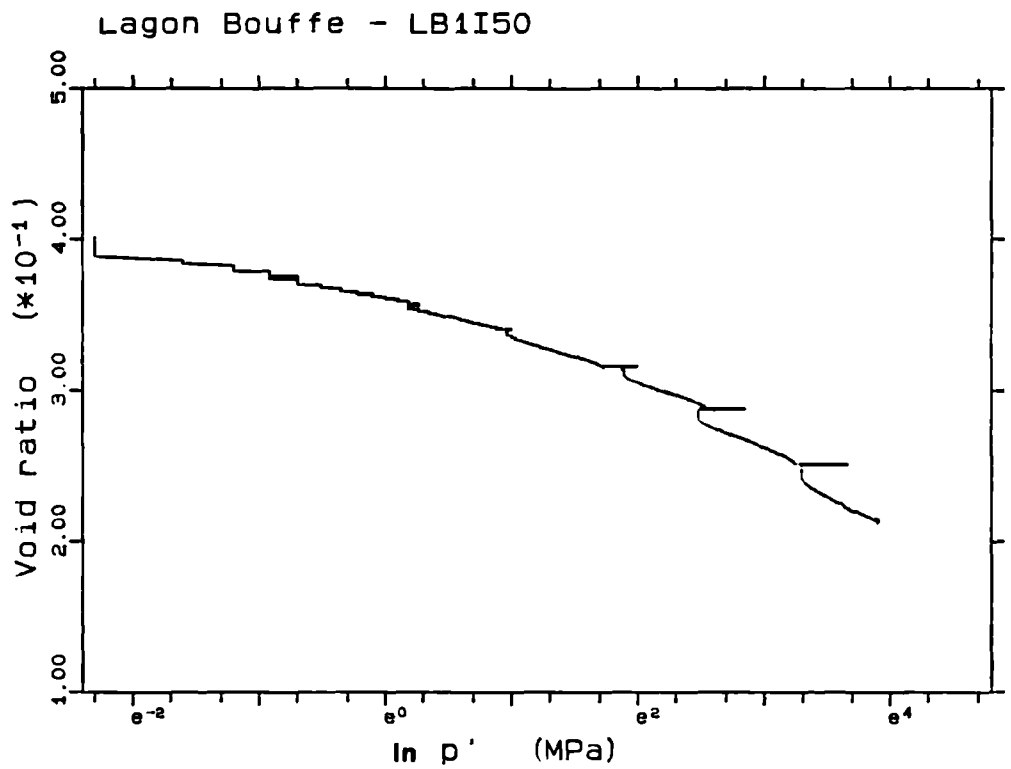

Fig. 6.2 The isotropic consolidation line in e - ln p' space, LB1I50

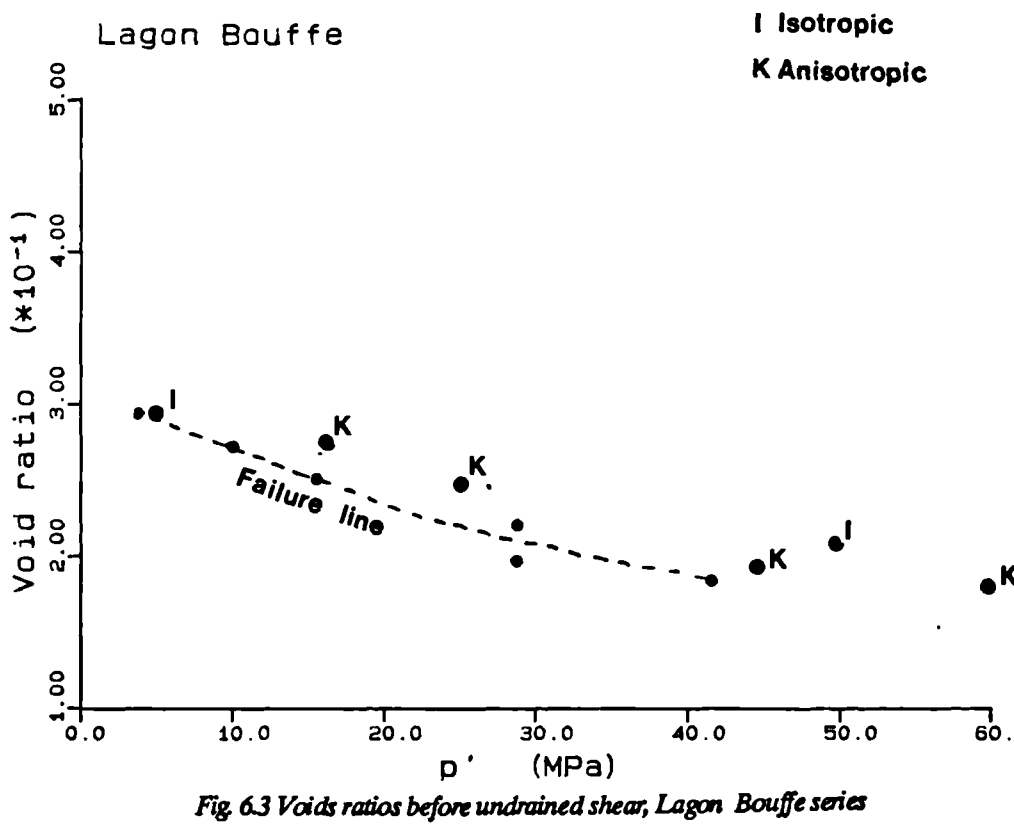

Fig. 6.3 Voids ratios before undrained shear, Lagon Bouffe series

Several points should be noted here. Firstly, the pore pressures took longer to equilibrate as the stress increment increased; this is attributed to the closer packing of the particles, so that the size of the pore throats decreases. The response at the last two increments (p = 26.4 MPa and 50.76 MPa) was not only slow, but inhomogenous across the sample. The top pore pressure responded more slowly than the bottom pore pressure, the initial pressure gradient at p = 50.76 MPa being 6 MPa; the gradient eventually disappeared as the pore pressures equilibrated. Another point to note is that, in test LB4K60, the pore pressure response at p = 6 MPa increased to 1.49 in 24 hours - 0.49 MPa higher than expected. (These B-values do not take account of the compressibility of the material).

c) Stress Strain Relationship During Anisotropic Consolidation

The axial strains during isotropic consolidation could not be measured due to the lack of internal strain gauges (Appendix 6). They could only be directly measured when the ram was in contact with the sample; i.e. during anisotropic consolidation. Fig. 6.4 shows the stress strain relationships for anisotropic consolidation of the Lagon Bouffe clays. The initial break in stress-strain curves is due to change of the ratio of σ_3' to σ_1' (Appendix 6). Beyond that, the value of q continues to rise and the relationship is no longer linear at high stresses; this is again attributed to increased packing of the particles. LB4 and LB5 show this very well.

The values of maximum axial stresses and strains reached before undrained shear are recorded in table 6.3.

SAMPLE	p' (MPa)	q (MPa)	AXIAL STRAIN (%)
LB3	15.3	7.9	3.93
LB2	25.1	12.5	4.66
LB5	44.7	25.4	7.48
LB4	61.5	34.7	9.39

Table 6.3 Values of stress and strain at the end of isotropic consolidation for Lagon Bouffe Clays

6.2.3. Taiwan Clays

a) Voids Ratio - Effective Stress Relationship

All the samples were consolidated isotropically at 5 MPa. TA was further consolidated isotropically to 50 MPa, and the TC, TD and TE were consolidated anisotropically at a K ratio of 0.6 to mean effective stresses of 50, 15 and 25 MPa respectively. TF was not consolidated any further. TG was consolidated isotropically up to a p' of 35 MPa, but has undergone isotropic cyclic loading. After isotropic consolidation at each stress increment, a load was added and removed undrained, causing the generation of excess pore pressures (see table 6.6 below); the sample was not allowed to consolidate after cyclic loading, however, and the stress was immediately increased to the next consolidation increment (Appendix 6).

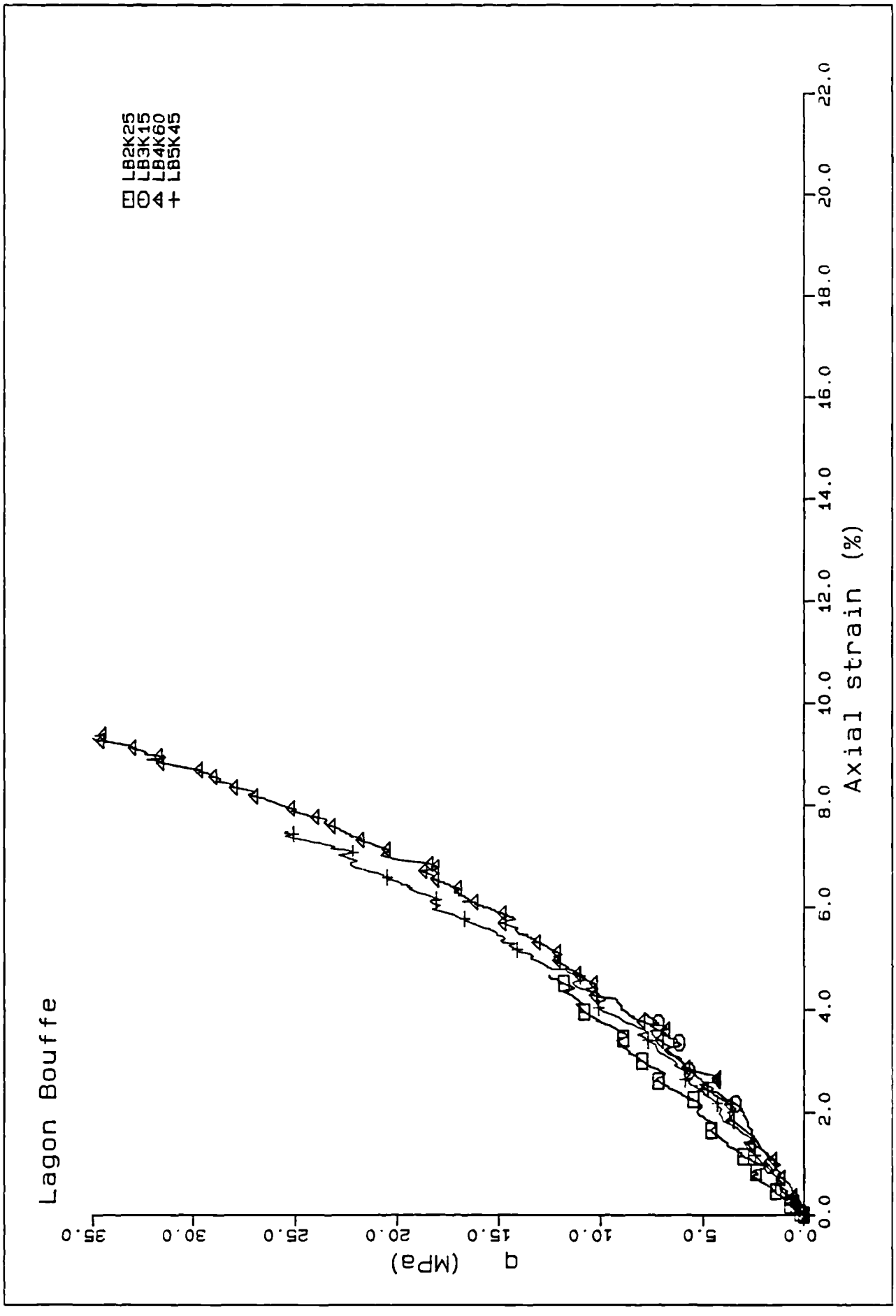

Fig. 6.4 Stress - strain relationships during anisotropic consolidation, Lagon Bouffe series

Unlike the Lagon Bouffe silty clays, the Taiwan samples all had uniform initial voids ratios, lying between 0.44 and 0.45. The change in voids ratio is recorded in table 6.4 (see also fig. 6.5).

TEST	INITIAL e	FINAL p' (MPa)	FINAL e
TF15	0.434	4.8	0.298
TDK15	0.448	14.8	0.249
TEK25	0.442	25.7	0.194
TGCY30	0.450	35	0.170
TAI50	0.440	47.9	0.163
TCK50	0.444	49.4	0.169

Table 6.4. Change in voids ratio for the Taiwan triaxial tests

The slope of the virgin isotropic consolidation line in e - ln p' space (x) is 0.075 and the value of specific volume at 1 MPa (N) is 1.42 (fig. 6.6). The break in the line marks the pre- consolidation pressure, which lies between 1 and 2 MPa for all the samples; the pre-consolidation pressure is 2.45 MPa under K_o conditions (see Appendix 4).

All of the samples follow very similar consolidation paths, although TC, TD and TE have undergone anisotropic consolidation (fig. 6.5). In this case, the K = 0.6 consolidation lines lie very slightly to the right of the isotropic consolidation line.

Fig. 6.7 shows the final voids ratios before undrained shear, which define a curve in e - p' space. (The voids ratios at failure are also plotted for comparison).

b) Pore Pressure Response

Again, the results of TAI50 will be presented here as it was the only test in the series with an isotropic consolidation stage reaching a p' of 50 MPa (table 6.5).

p (MPa)	B_1	B_2	TIME
1.4	0.39	0.84	22 hr
1.8	0.43	1.00	70 min
3.4	0.98		
6.6	0.93	0.98*	20 min
12.8	0.90	0.94*	20 min
25.1	0.84	0.99	2 hr
50.1	0.78	0.95	17 hr

B_1 = initial B-value B_2 = final B-value
* = pore pressures not allowed to settle completely

Table 6.5. B-values for test TAI504

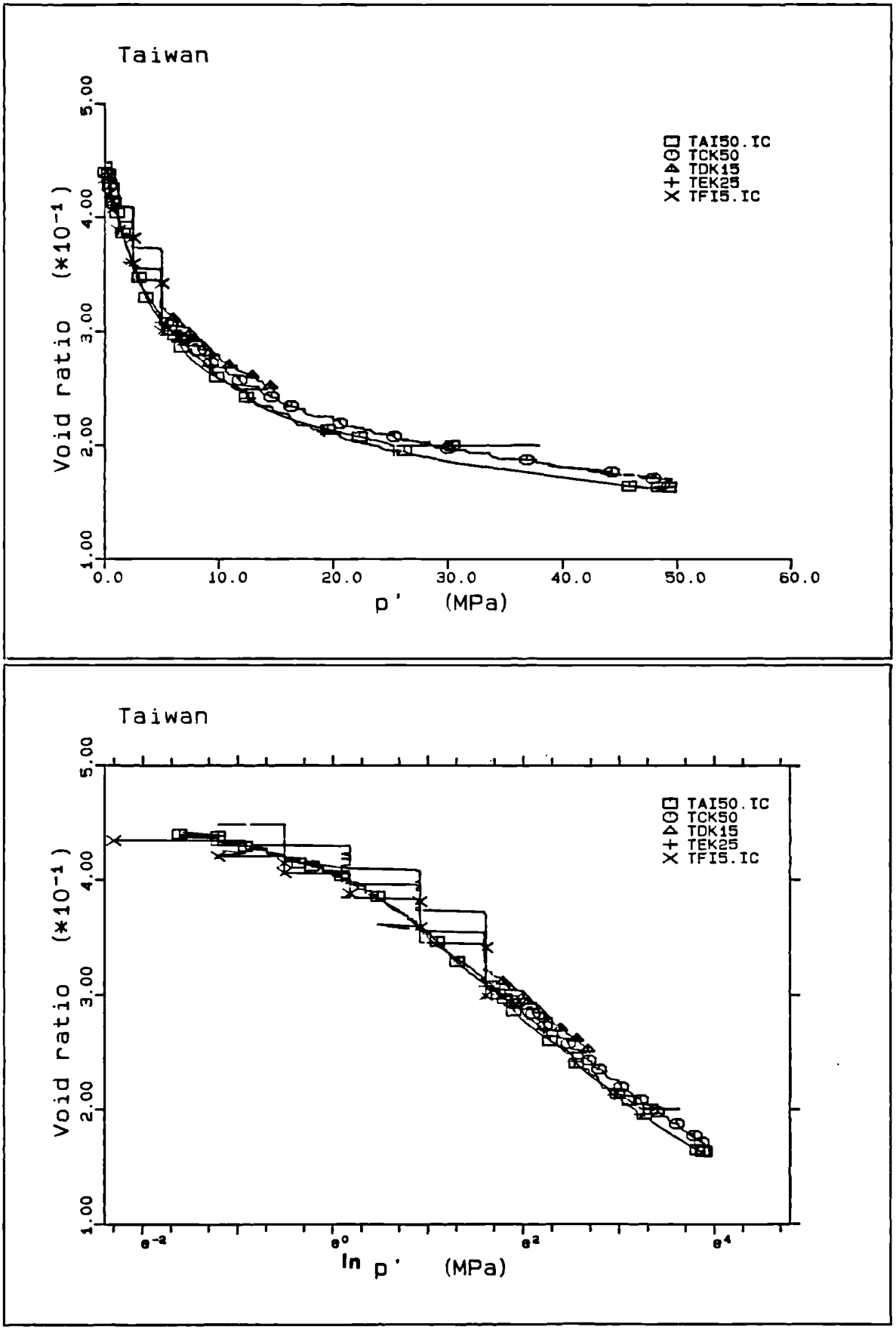

Fig. 6.5 Voids ratio - mean effective stress relationships, Taiwan series

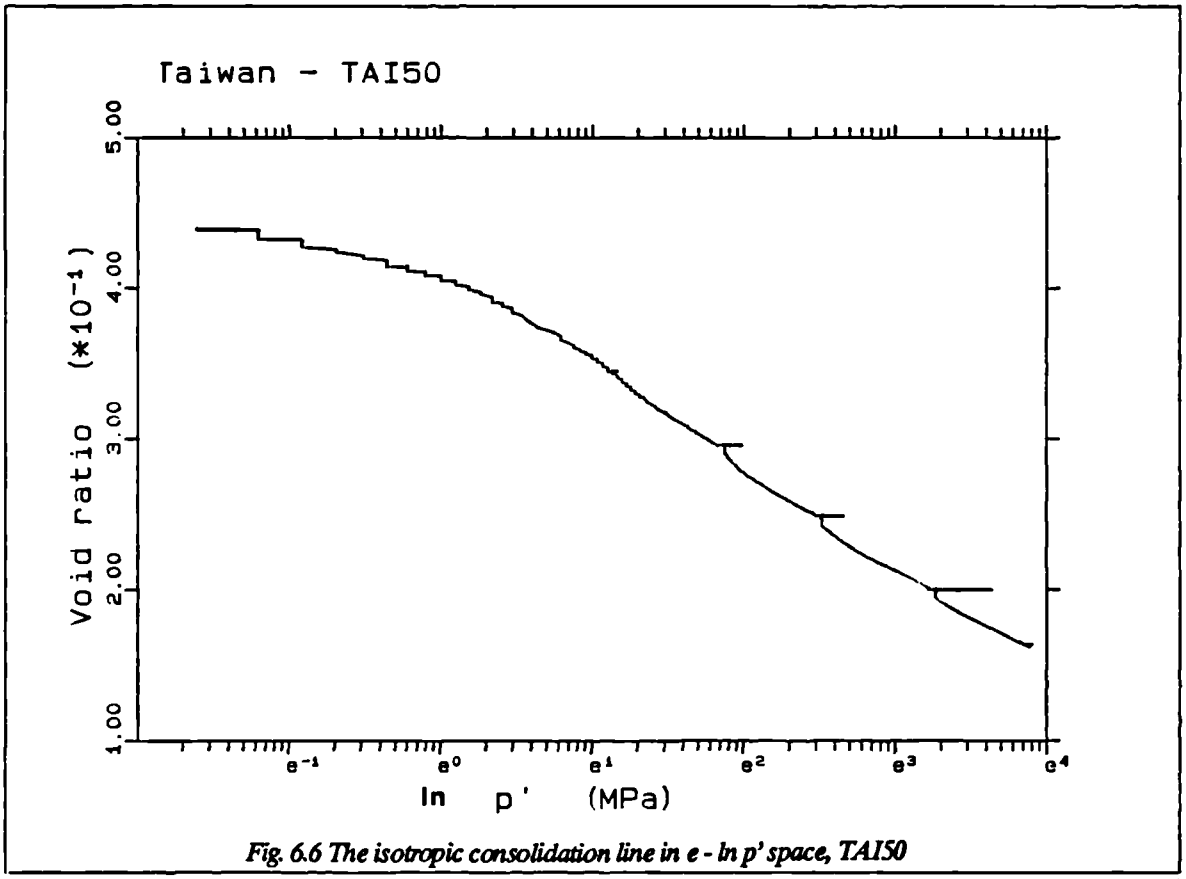

Fig. 6.6 The isotropic consolidation line in e - ln p' space, TAI50

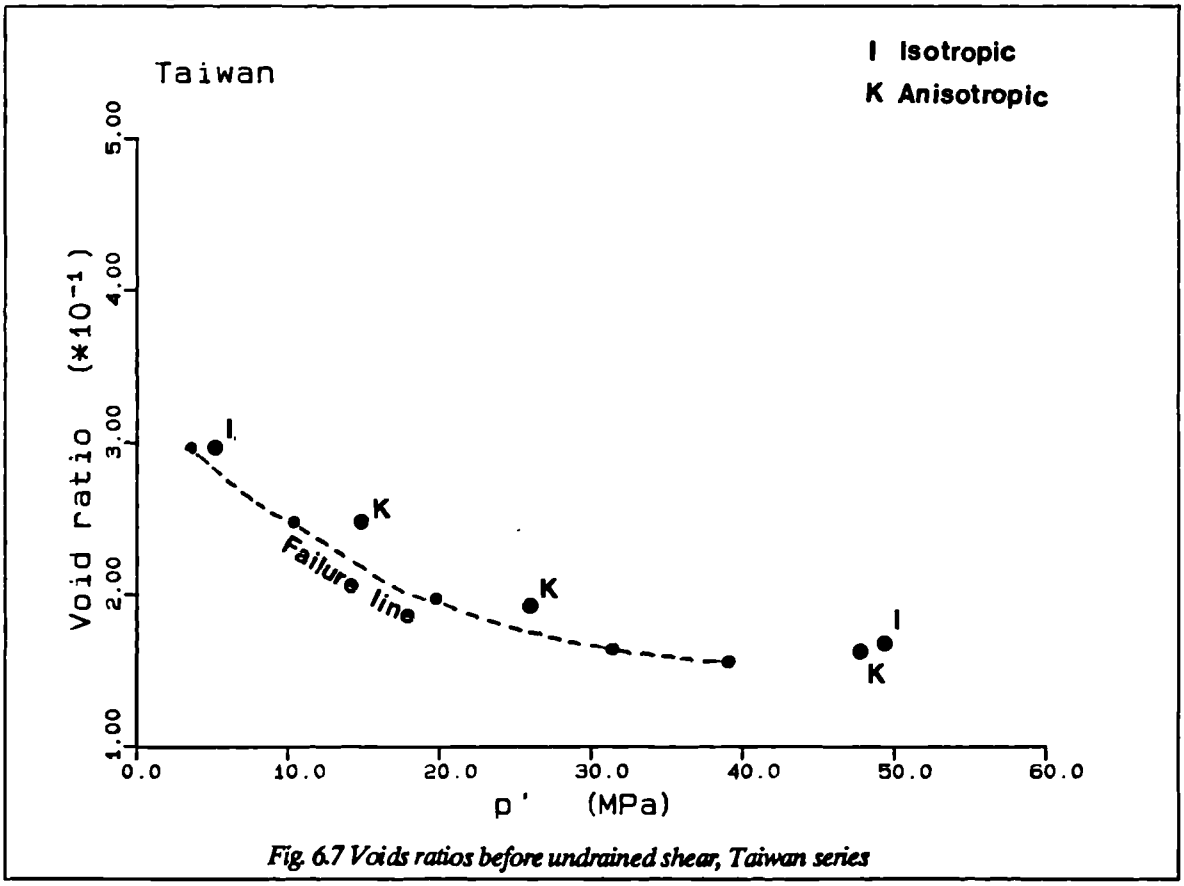

Fig. 6.7 Voids ratios before undrained shear, Taiwan series

The final B-value for the first increment is low, indicating incomplete saturation of the sample. Unlike LB1, TA does not show any pore pressure gradients across the sample at the start of the highest pressure increments, but the delay in attaining a maximum pore pressure response at higher stress increments is again observed here.

TG, the only cyclic loading test performed, produced interesting results on the isotropic cyclic loading. It must be pointed out that this test was not performed under controlled conditions (the sample was initially loaded isotropically by adding and removing an extra pressure increment; the frequency and duration of the cycles varied - Appendix 6). The results must therefore be treated qualitatively (table 6.6).

CONSOLIDATED TO	EXCESS CELL PRESSURE (MPA)	EXCESS u (MPa) (beg. last cycle)	EXCESS u (MPa) (end last cycle)
5	1	1.38	0.44
	2	2.92	0.52
10	5.4	5.8	1.33?
20	11	11.7	2.62?
35	11	13.34	5.93

Table 6.6 Pore Pressure Response for Isotropic Cyclic Loading of Sample TG

The response recorded at both the beginning and end of the last cycle (table 6.6) is after the pore pressures were allowed to settle down. Note that the isotropic cyclic loading produced a permanent excess pore fluid pressure, which finally rose to 5.93 MPa. The excess pressure was not allowed to dissipate before undrained shear.

c) Stress - Strain Relationship During Anisotropic Consolidation

Fig. 6.8 shows the stress strain relationship for the Taiwan materials. Again, this initial break is seen, followed by a gradual increase in the gradient, particularly evident for TC, which is taken up to the highest effective stress.

The values of maximum axial stresses and strains reached before undrained shear are recorded in table 6.7.

SAMPLE	p' (MPa)	q (MPa)	AXIAL STRAIN (%)
TD	14.8	7.1	5.56
TE	25.7	13.2	9.78
TC	59.4	25.5	12.88

Table 6.7. Values of stress and strain at the end of anisotropic consolidation for Taiwan clays

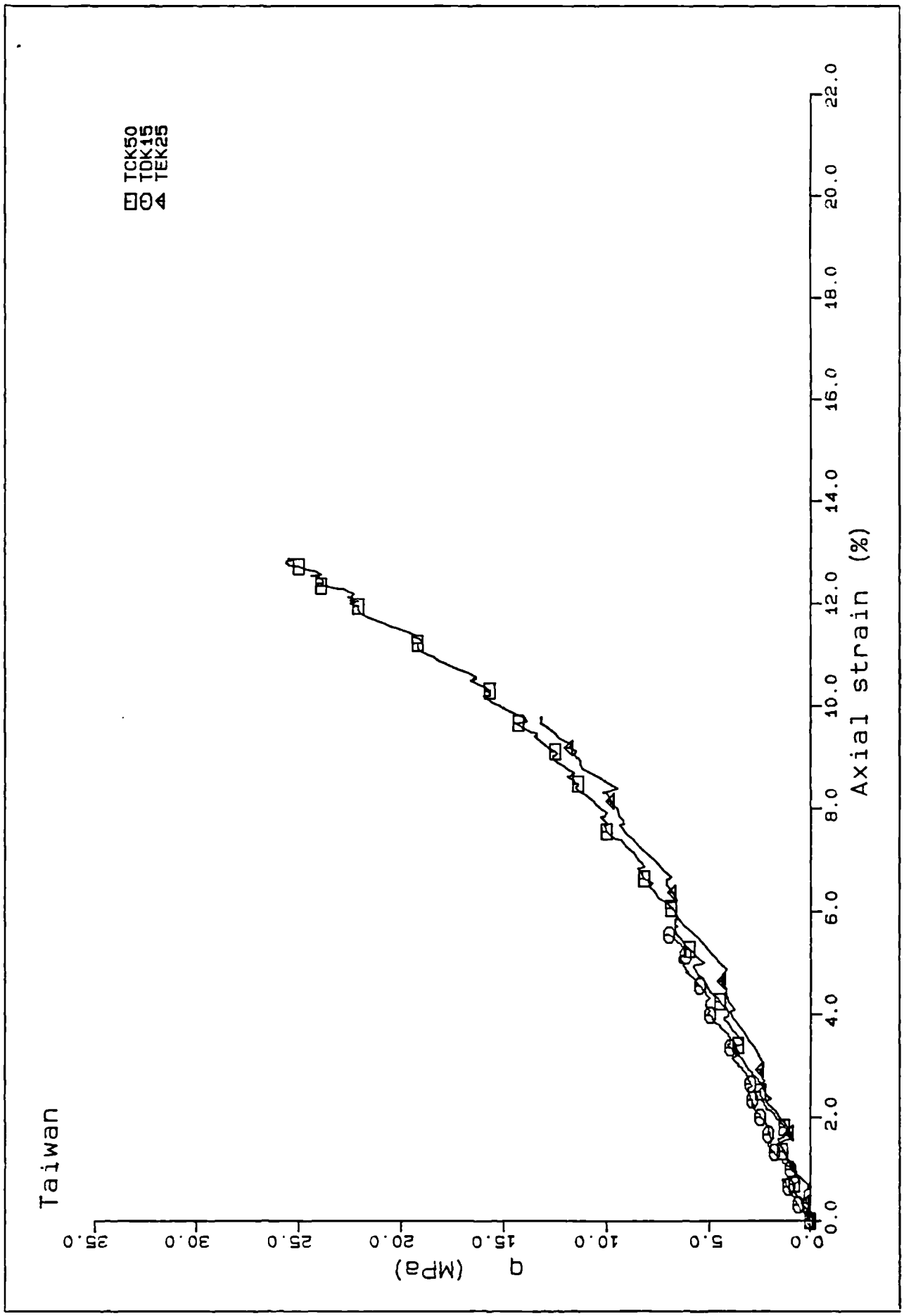

Fig. 6.8 Stress - strain relationships during anisotropic consolidation, Taiwan series

6.2.4. Devil's Woodyard

a) Voids Ratio - Effective Stress Relationship

Two isotropic tests were performed on the Devil's Woodyard clay - one to 9 MPa (DW1) and the other to 50 MPa (DW2). The former, DW1, was the only triaxial sample not to be consolidated in the small cylinder before the test; it had therefore only been consolidated one-dimensionally to 300 kPa (Appendix 4). The e - p' relationship is different for the two (figs. 6.9; table 6.8). Whereas DW1 has an x value of 0.16, DW2 is 0.12; the values for N are 1.94 and 1.87 respectively. This suggests that consolidation in the piston has made the material less compressible, i.e. the material loses less volume for the same effective stress increment. This is to be expected as one- dimensional consolidation up to 2.45 MPa would produce a stronger, less compressible sample.

SAMPLE	INITIAL e	FINAL p' (MPa)	FINAL e
DW1	1.146	8.6	0.529
DW2	0.992	59.5	0.477

Table 6.8. Change in voids ratios for Devil's Woodyard triaxial tests

b) Pore Pressure Response

The pore pressure response for all isotropic stress increments in DW2I50 are listed in table 6.9.

p (MPa)	B_1	B_2	TIME
2.1	0.86	0.9	50 min
3.3	0.99		
6.5	0.83	1.02	2 hr
13.5	0.81	1.07	9 hr
26.1	0.57	1.18	17 hr
51.2	0.74	1.07	17 hr

B_1 = initial B-value B_2 = final B-value

Table 6.9. B-values for test DW2I50

A pore pressure gradient of 1.3 MPa is created across the sample at the beginning of the last increment. The delay in pore pressure response is again observed for the Devil's Woodyard clay.

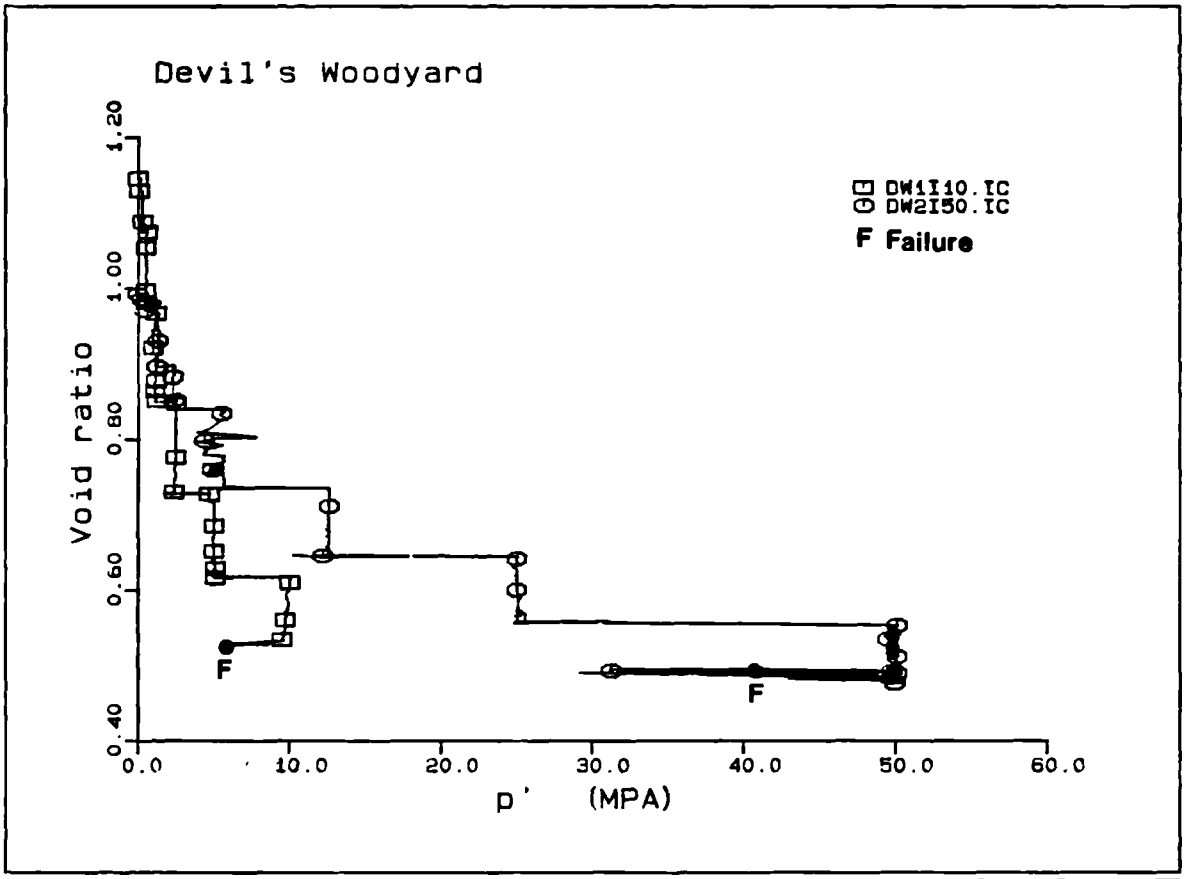

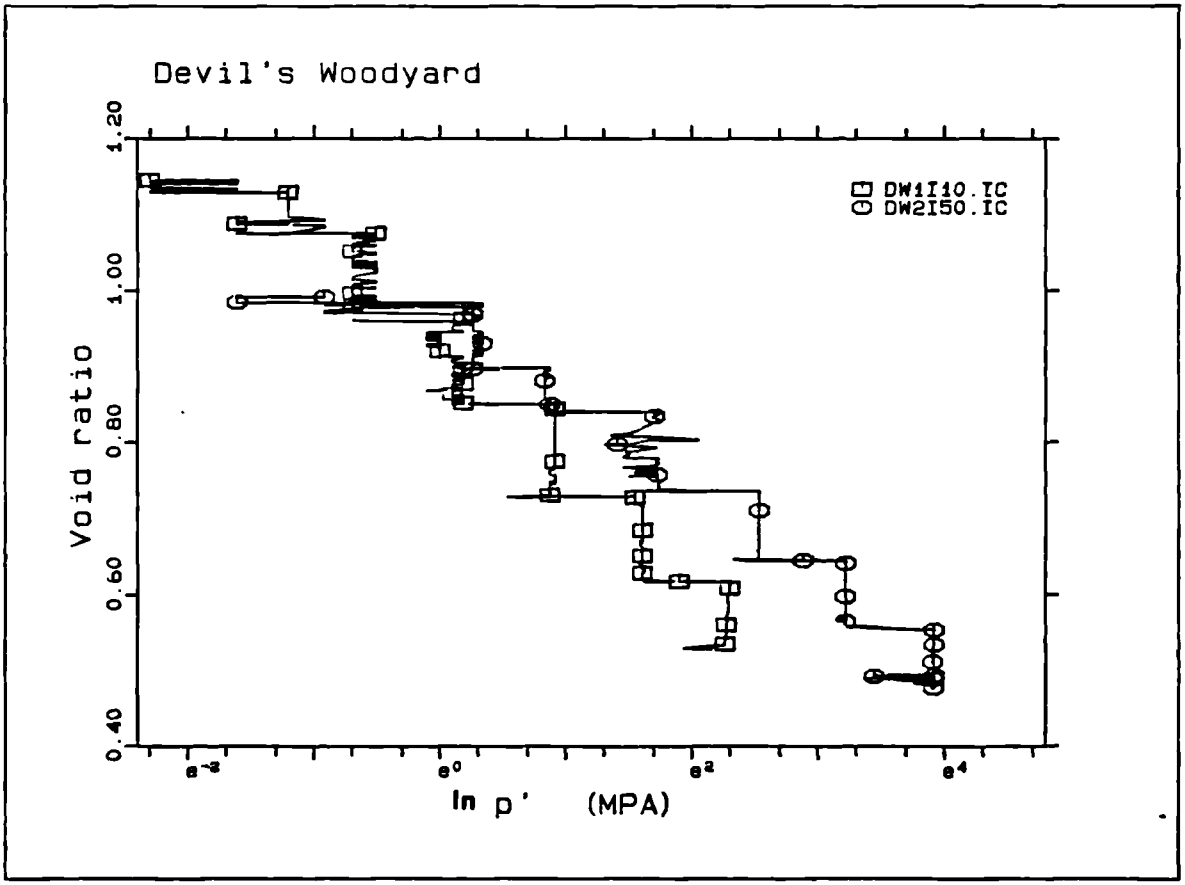

Fig. 6.9 Voids ratio - mean effective stress relationships, Devil's Woodyard series

6.3 UNDRAINED SHEAR AND FAILURE

6.3.1. Introduction

After consolidation was complete at a particular mean effective stress, drainage to the sample was closed and the sample was loaded axially at a constant cell pressure. In this section, the results of the undrained shear experiments will be presented, with particular reference to stress ratios, stress-strain effects and pore pressure response. Failure conditions for each test are defined using these parameters. The results of the three test series, Lagon Bouffe, Taiwan and Devil's Woodyard, are described separately.

6.3.2. Lagon Bouffe

Six undrained shear tests were performed on the Lagon Bouffe materials; LB1 and LB6 were isotropically consolidated to 5 and 50 MPa respectively; LB2, LB3, LB4 and LB5 were anisotropically consolidated at a K ratio of 0.6, to p' values of 25, 15, 60 and 45 MPa respectively.

a) p' - q Relationship

The stress paths of the six undrained shear experiments are presented in fig. 6.10. All six samples show a gradual decrease in p' with increasing q, associated with pore pressure increase. LB1, LB4, LB5 and LB6 all reach a point where they "dilate", or show an increase in p' (due to decreasing pore fluid pressure - see below). LB2 and LB3 are flatter undrained shear curves than the rest, indicating increasing pore pressure with no increase in q (fig. 6.10); they both reach a point where the effective stresses no longer change with increasing axial strain (critical state). Apart from LB6, which dilates, there is a change in behaviour with increasing stress (between LB2 and LB5, fig. 6.10). A line through the origin can be drawn through the points where samples show "dilation" or reach critical state (fig. 6.10).

Note: LB5 experienced a drop in cell pressure during undrained shear; this was recovered and the test was completed.

b) Stress - Strain Relationship

The stress strain curves of these tests are shown in fig. 6.11. The initial values of q in the anisotropic tests are quoted in table 6.3. The figure shows that the two isotropic stress-strain relationships are different from the anisotropic tests, in that the shear stresses begin to "level off" at slightly higher, although still very low, strains; LB6I5 shows strain hardening. LB2 and LB3 show the constant stress at failure and LB4 and LB5 continue to show slight increase in q; the latter recovers its stress-strain

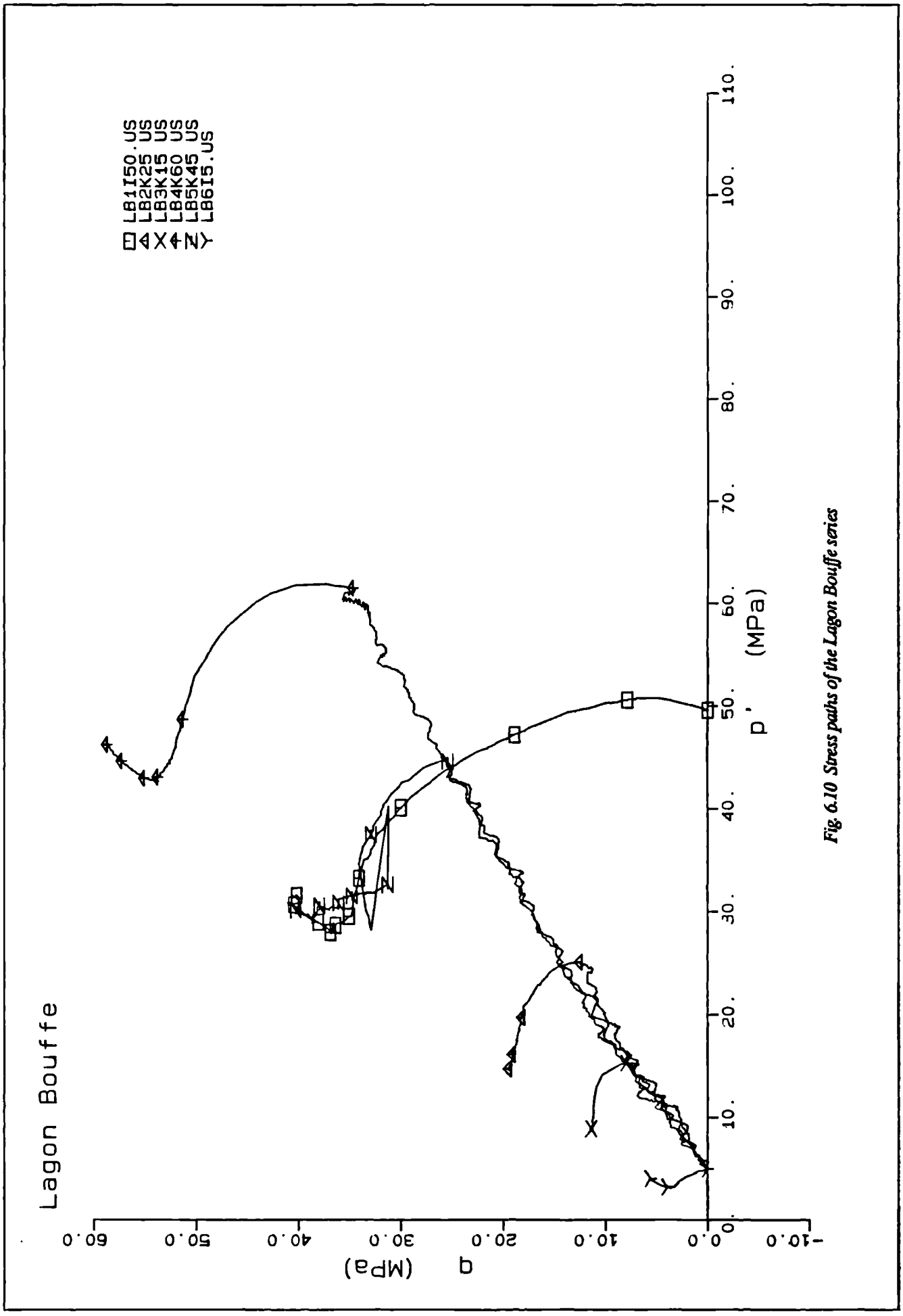

Fig. 6.10 Stress paths of the Lagon Bouffe series

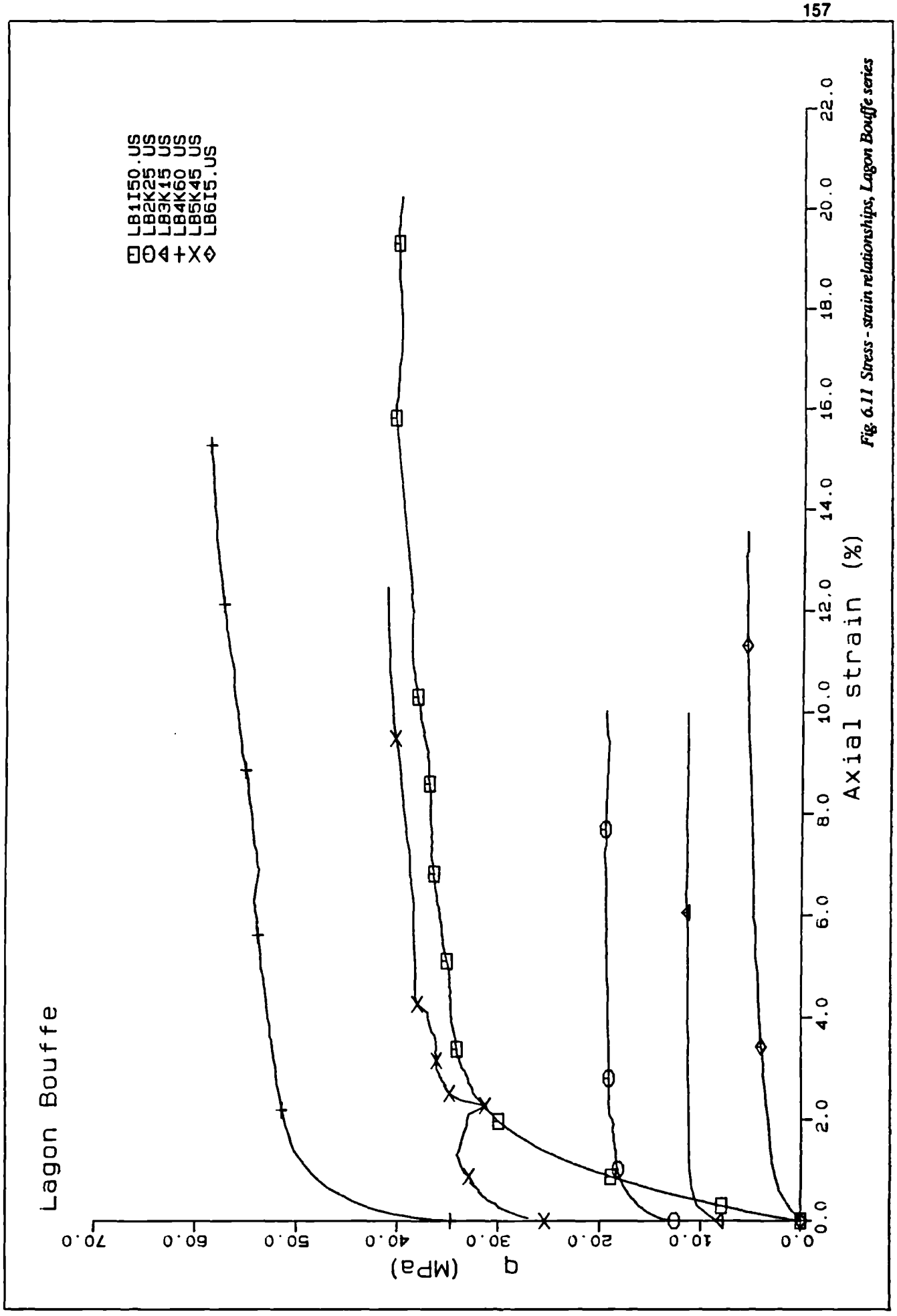

Fig. 6.11 Stress - strain relationships, Lagon Bouffe series

behaviour despite the drop in cell pressure. Values of final stresses and strains are given in table 6.11 below.

c) Pore Pressure -Strain Relationship

The relationship between pore pressure and axial strain is shown in fig. 6.12 and tabulated below. The curves are similar to the stress strain curves in that the pore pressure reaches a maximum value at low strains. Beyond this peak value, LB1, LB4, LB5 and LB6 show a slight drop in u_e, and LB2 and LB3 show no further changes in u_e.

If the curves in fig 6.12 are compared with those in fig. 6.11, it can be seen that q begins to level off at lower axial strains than u_e. LB1 and LB6, the two isotropic tests, show a more rapid rise in q than in excess pore water pressure, whereas the four anisotropic tests, LB2, LB3 LB4 and LB5 show that the pore pressure increment is much greater than an increment of q. Table 6.10 lists the maximum and final values of excess pore pressure and associated stresses and strains for all the tests.

TEST	u_{max} (MPa)	E_a (%)	q (MPa)	u_{fin}	E_a (%) (MPa)	q (MPa)
LB615	3.4	3.7	4.1	3.0	13.5	5.6
LB3K15	7.5	6.7	11.2	7.4	10	11.2
LB2K25	12.9	6.0	19.5	12.1	15.5	18.5
LB5K45	20.3	6.3	38.0	19.6	12.5	41.0
LB1150	33.0	7.5	36.5	31.0	20.0	40.0
LB4K60	25.5	6.0	53.0	23.0	15.2	58.0

Table 6.10. Values of maximum and ultimate excess pore pressures and associated stresses and strains for the Lagon Bouffe test series

d) Failure

From all the tests above, it can be seen that a line going through the origin can be drawn through each series of stress paths beyond which q does not increase (fig. 6.10). This line is used to define failure, as opposed to the maximum shear stress on a stress strain curve (fig. 6.11), because q continues to rise along the line in four out of the six Lagon Bouffe tests.

SAMPLE	p' (MPa)	q (MPa)	AXIAL STRAIN (%)	u_f (MPa)	M
LB615	3.2	3.8	3.14	3.1	1.19
LB3K15	8.9	11.4	7.5	7.5	1.28
LB2K25	14.5	19.2	9.2	13.0	1.32
LB1150	28.0	37.0	8.8	33.5	1.32
LB5K45	29.3	38.8	7.2	19.9	1.32
LB4K60	42.5	54.5	8.1	25.0	1.28

Table 6.11. Failure Conditions of the Lagon Bouffe test series

The failure line also projects as a curve in e - p' space (fig. 6.3).

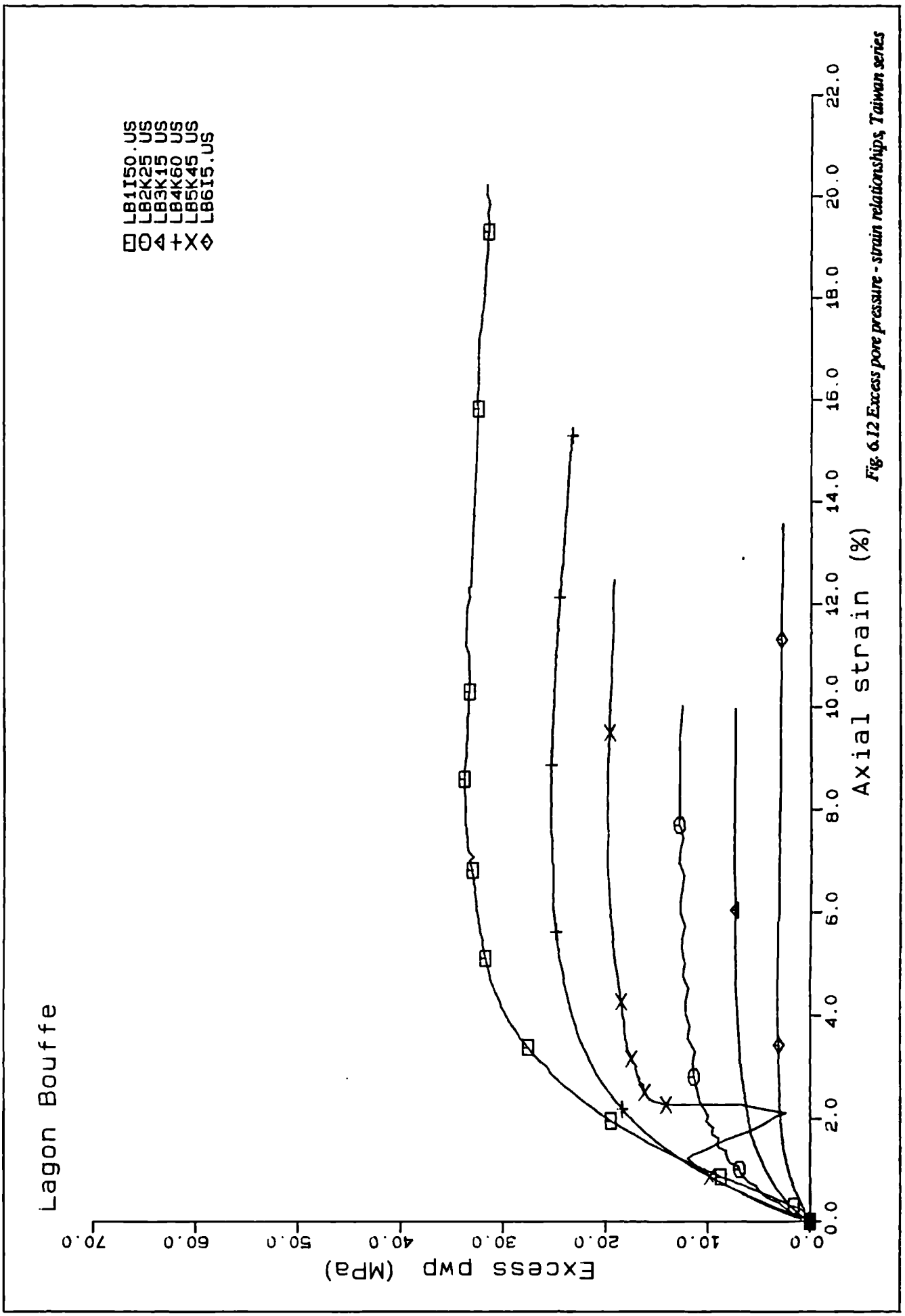

Fig. 6.12 Excess pore pressure - strain relationships, Taiwan series

6.3.3. Taiwan

Five undrained shear tests were performed on the Taiwan material. The sixth, a cyclic undrained loading test, is described separately. As mentioned above, TA and TF were consolidated isotropically to mean effective stresses of 50 and 5 MPa respectively; TC, TD and TE were consolidated anisotropically at a K ratio of 0.6, to mean effective stresses of 50, 15 and 25 MPa respectively.

a) p' - q Relationship

The five tests display a marked variety in undrained shear behaviour (fig. 6.13). The mean effective stress p' decreases steadily with increasing q for all the tests. TC and TE, in fact, show continuing decease in p' with a final decrease in q. The remaining samples, TA, TE and TF seem to reach steady values of p' and q. Whereas the isotropic tests (TA and TF) show steep undrained shear curves, TC, TD and TE are much shallower curves, flattening off towards failure. A line through the origin joins the points of maximum shear stresses for all the tests (fig. 6.13).

b) Stress - Strain Relationship

The stress strain curves of these tests are shown in fig. 6.14. The initial q values for the anisotropic tests are quoted in table 6.7. The two isotropic tests TAI50 and TFI5 have similar stress-strain curves in that the shear stress begins to level off at slightly higher axial strains than for the anisotropic tests; q does not level off completely for the latter. TC and TE show the drop in q, which is more dramatic for TE; TF shows steady stresses at failure.

c) Pore Pressure - Strain Relationship

The relationship between pore pressure and axial strain is shown in fig. 6.15. As for the Lagon Bouffe series, the pore pressure axial strain curves follow a very similar shape to the stress strain curves (compare the curves in figs. 6.14 and 6.15). The pore pressure increment is marginally smaller than the stress increment in the isotropic tests, whereas in the anisotropic tests, the pore pressure increment is greater than an increment of q; also the pore pressure continues to rise after q has reached a steady value. Two tests, TC and TE show a decrease in q with increasing pore pressure (fig. 6.15; table 6.12).

TEST	u_{max} (MPa)	E_a (%)	q (MPa)	u_{fin} (MPa)	E_a (%)	q (MPa)
TFI5	2.7	4.5	3.1	2.7	5.7	3.2
TDK15	5.9	8.5	9.6	5.9	11.1	9.6
TEK25	9.6	9.6	16.3	9.6	17.4	15.2
TAI50	24.5	6.6	29.0	24.5	8.3	29.5
TCK50	15.0	8.5	33.2	15.0	17.4	32.2

Table 6.12. Values of maximum and ultimate excess pore pressures and associated stresses and strains for the Taiwan test series

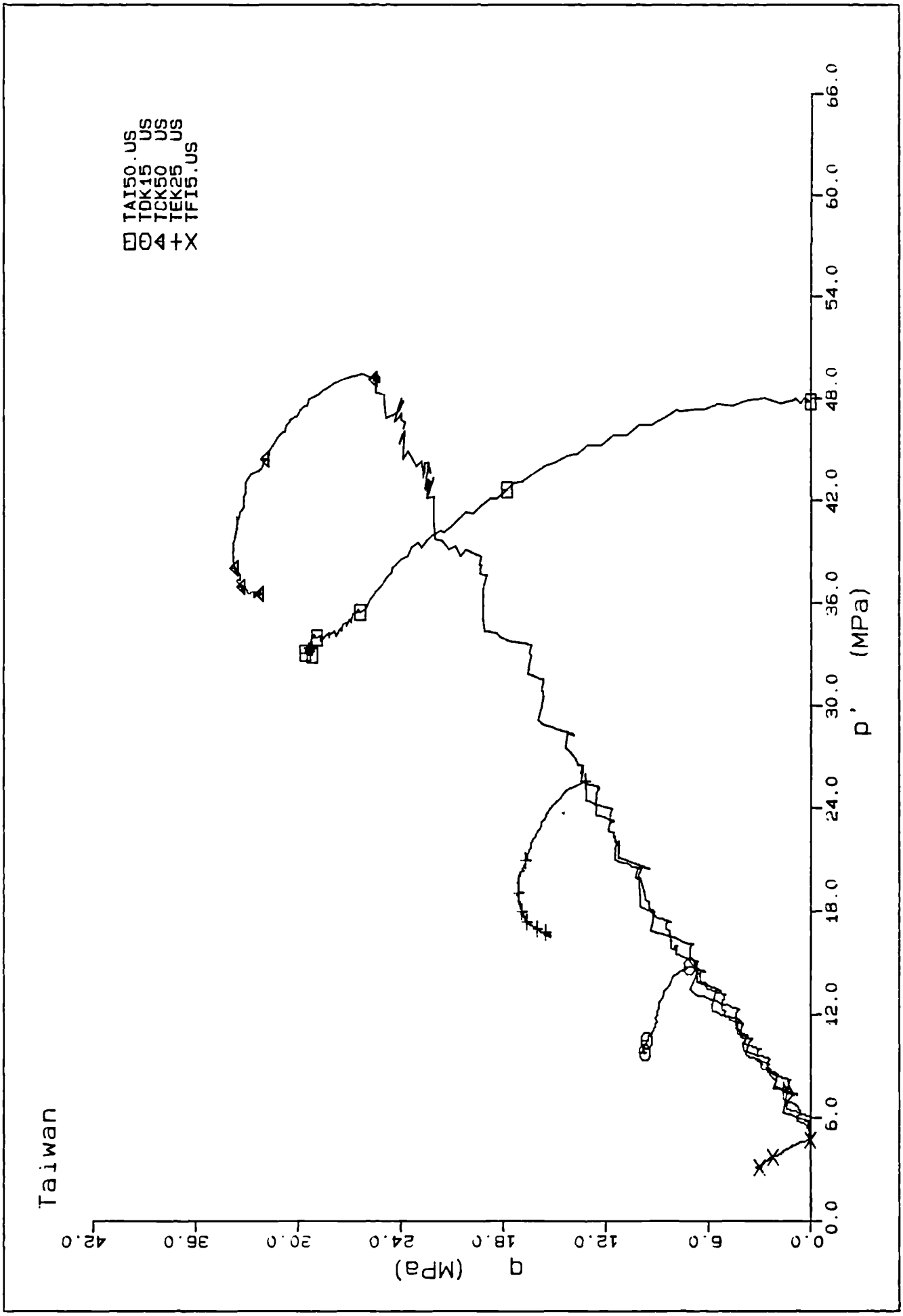

Fig. 6.13 Stress paths of the Taiwan series

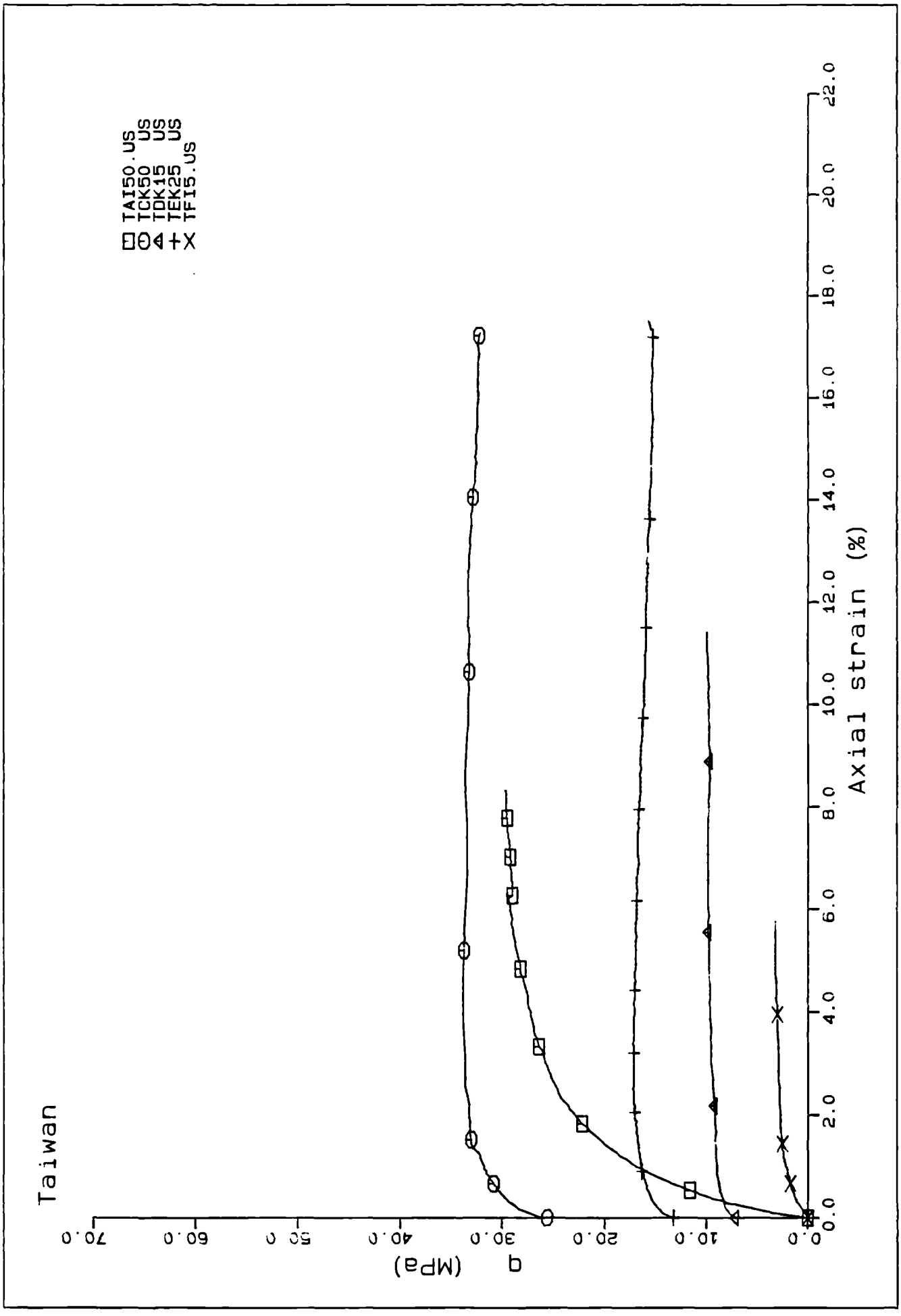

Fig. 6.14 Stress - Strain relationships, Taiwan series

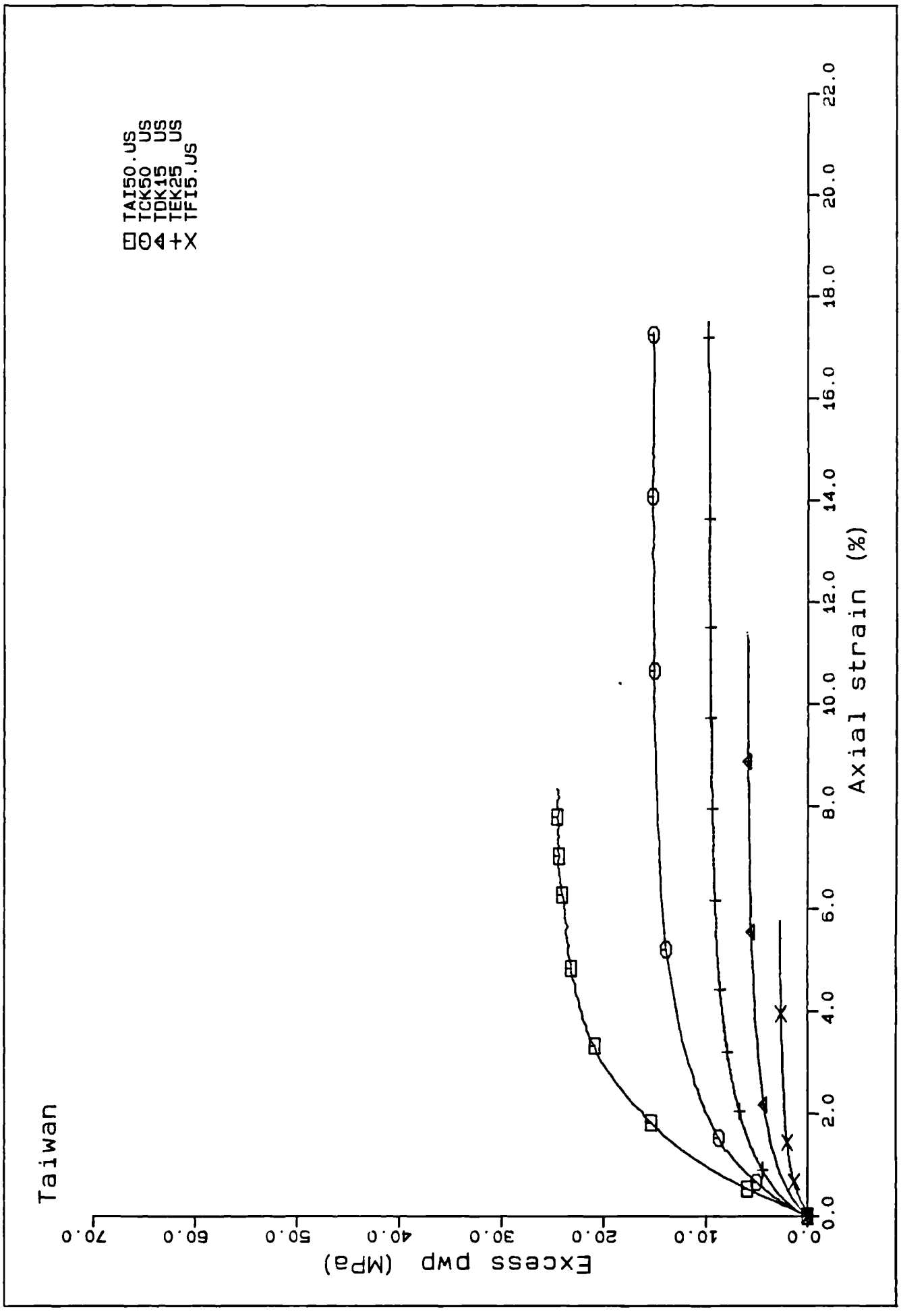

Fig. 6.15 Excess pore pressure - strain relationships, Taiwan series

d) The Cyclic Loading Test

As mentioned above, the conditions for cyclic loading were not controlled. The load was taken up to a certain value of q, then decreased back to zero. The amplitude of the cycles was increased four times; thirty cycles were performed before the sample was sheared undrained (Appendix 6). The stress path is shown in fig. 6.16 The first cycle begins with p' = 28.5 MPa (note that the sample was fully consolidated at 35 MPa but was overpressured by isotropic cycling, and that the cell pressure remained at that pressure throughout the axial loading). q increases with very little change in p' until the top of the cycle (q = 13 MPa); at the end of the unload, p' = 25.5 MPa. p' decreases gradually, although by a smaller degree, with each cycle. Apart from the first cycle, all the cycles show an increase in p' on loading and a decrease on unloading (fig. 6.16). At p' = 22 MPa, the amplitude was increased to 16 MPa, and the first cycle displays the same dramatic decrease in p' by comparison with subsequent cycles. Cycles with amplitudes of 18 and 20 MPa respectively were per formed before undrained shear at a p' of approximately 15.5 MPa. At p' = 19.6 MPa and q = 20 MPa, p' begins to increase more dramatically with increasing q; the test was stopped at p' = 22 MPa and q = 21 MPa.

The stress strain curve (fig. 6.17) gives a qualitative idea about the relationship, but cannot be trusted on the unload, as no measurements of internal strain were taken. The curve shows a steady increase in q to 21 MPa; q begins to level off, reaching a maximum at 21 MPa. After a further 3% strain, q begins to drop.

Again, the pore pressures follow the stress strain relationship fairly well (fig. 6.18). u_e reaches a maximum of 16.2 MPa, drop ping to a steady value of 14 MPa at the same point that q begins to decrease.

e) Failure

In the case of the Taiwan series, the maximum values of q define a line going through the origin (fig. 6.13); this is assumed to be the failure line. Table 6.13 lists the main failure conditions for the Taiwan materials.

SAMPLE	p' (MPa)	q (MPa)	AXIAL STRAIN (%)	u_f (MPa)	M
TF	3.1	3.2	4.5?	2.7	1.03
TD	9.9	9.8	8.2	5.8	1.00
TE	18.6	17.2	3.8	8.3	0.92
TA	32.0	29.0	6.8?	24.5	0.91
TC	38.0	33.5	5.3?	14.0	0.88

Table 6.13. Failure conditions for the Taiwan test series

The failure line also projects as a curve in e - p' space (fig. 6.7).

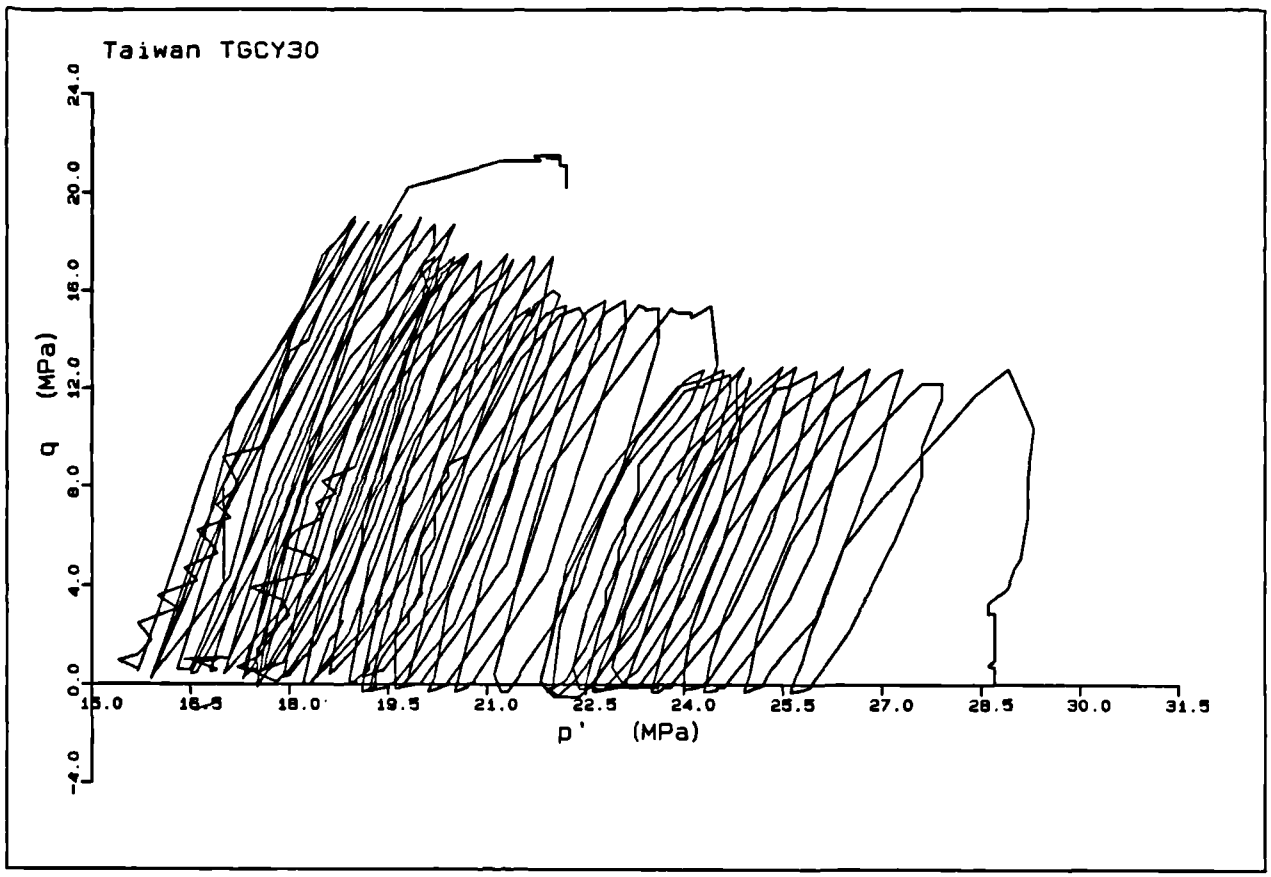

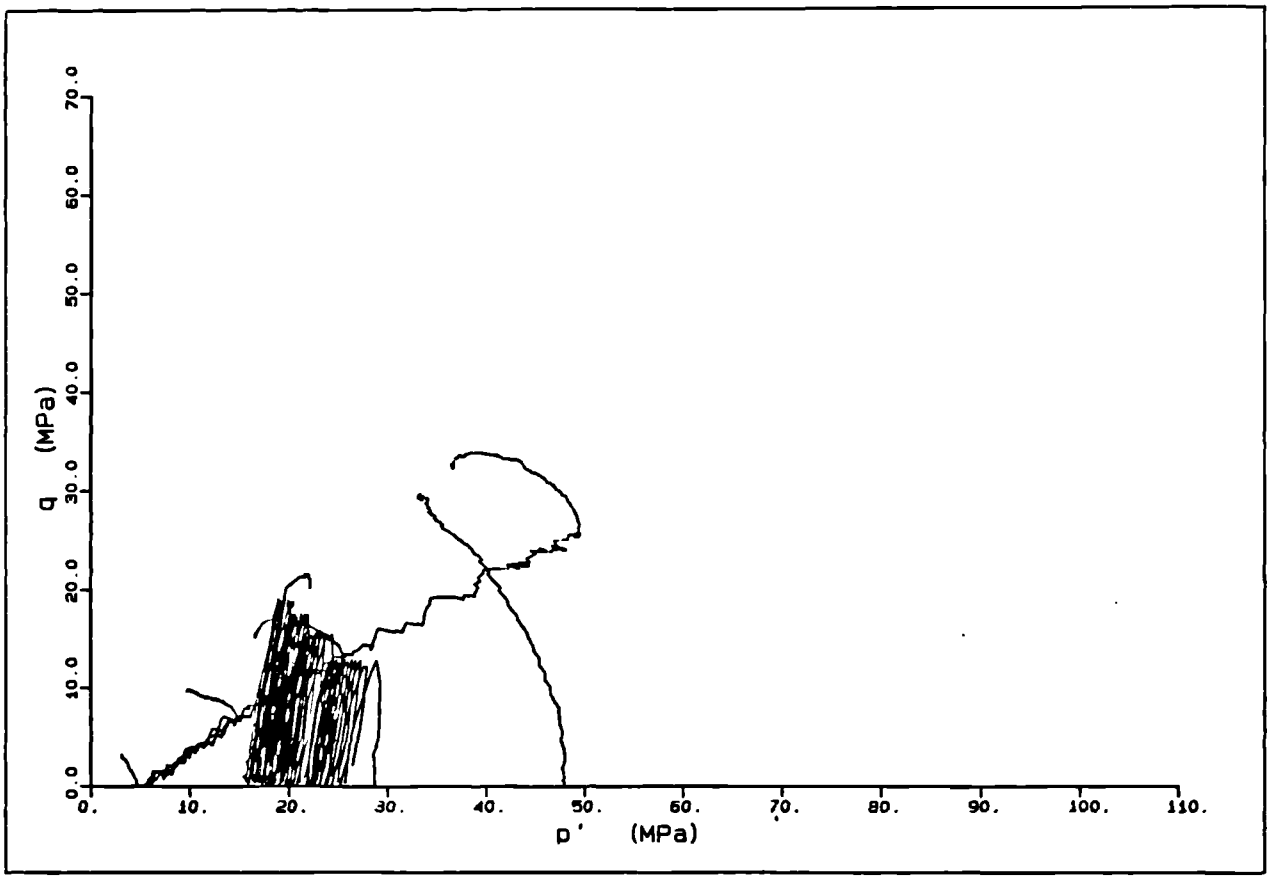

Fig. 6.16 Stress path of the cyclic loading test, TGCY30

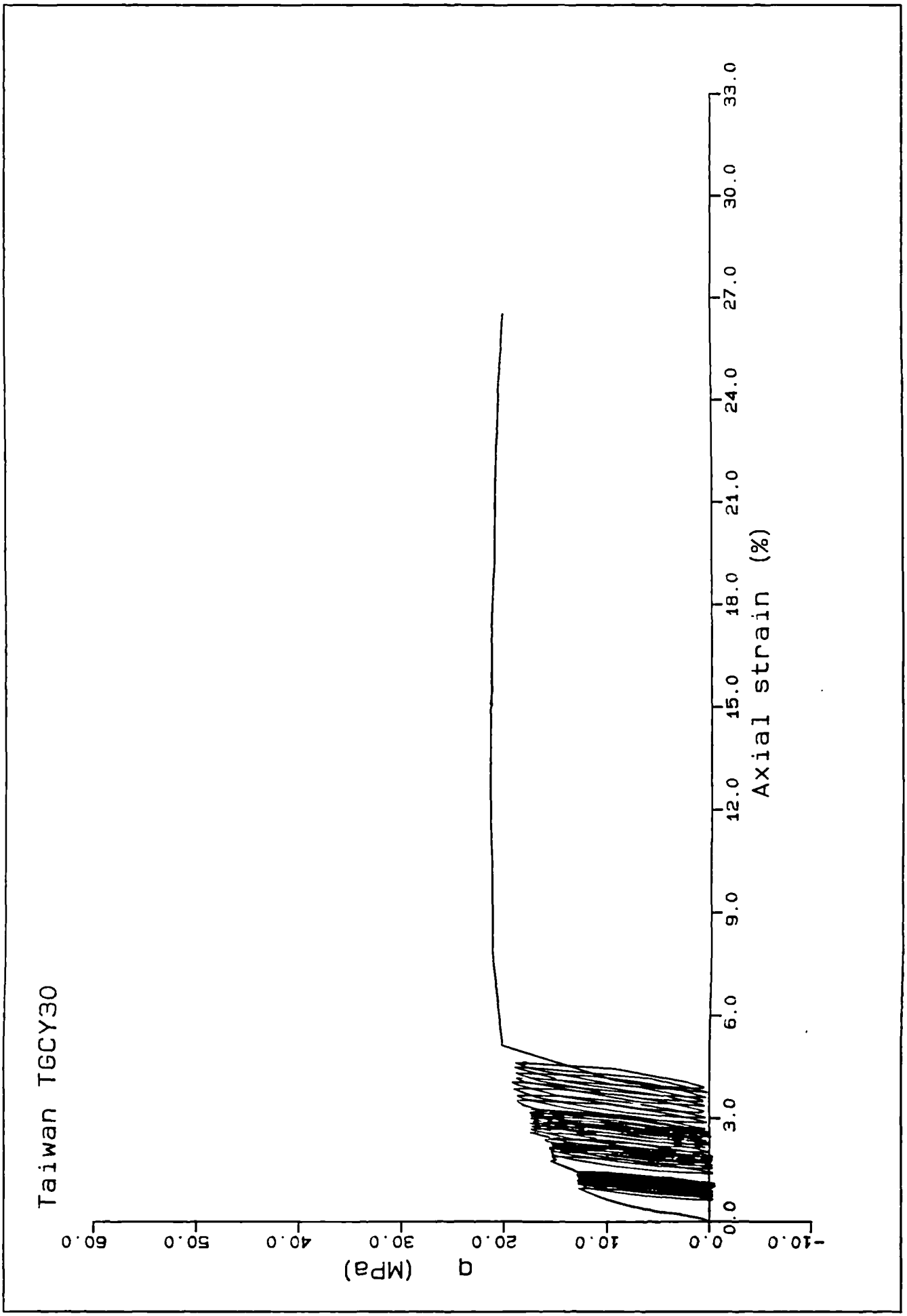

Fig. 6.17 Stress - Strain relationship of the cyclic loading test, TGCY30

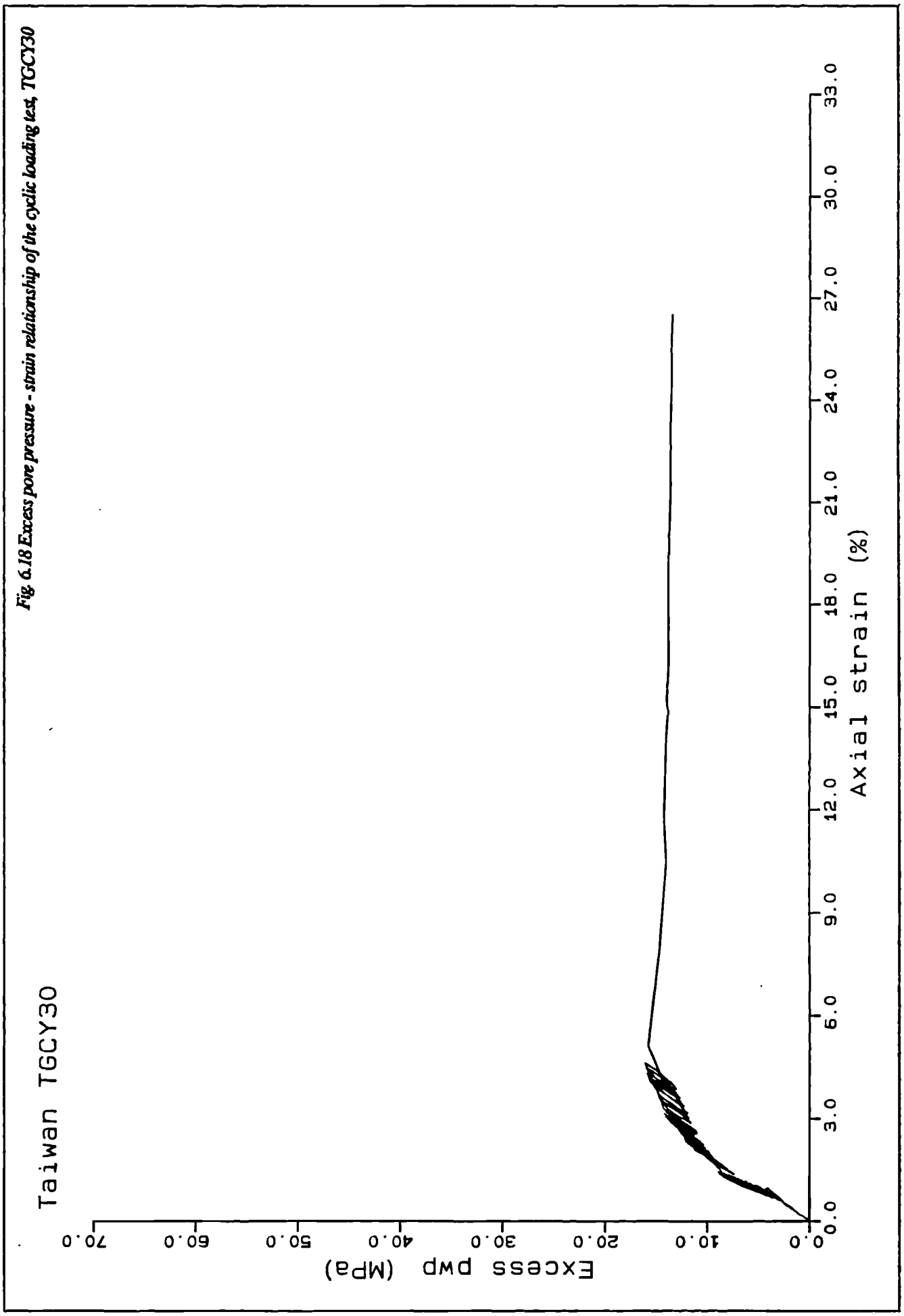

Fig. 6.18 Excess pore pressure - strain relationship of the cyclic loading test, TGCY30

6.3.4. Devil's Woodyard

Two undrained shear tests were performed on the Devil's Woodyard clays - both isotropic. DW1 was consolidated to a p' of 10 MPa and DW2 was consolidated to 50 MPa.

a) p' - q Relationship

The undrained shear behaviour is completely different for the two. (fig. 6.19) shows the stress paths of the two tests. DW1 shows a decrease in p' with increasing q, reaching a point (p' = 5.6 MPa; q = 2.7 MPa) where the effective stresses no longer change. DW2 shows a steady rise in q with little or no decrease in p' until q begins to drop sharply at p' = 41 MPa and q = 22 MPa.

b) Stress - Strain Relationship

The stress strain curves are shown in fig. 6.20. DW1 reaches maximum q at high axial strains, but q levels off. In DW2 shows a dramatic drop in strength at low axial strains.

c) Pore Pressure - Strain Relationship

The relationship between pore pressure and axial strain is shown in fig. 6.21. If the curves are compared with their stress strain equivalents (fig. 6.20), it can be seen that DW1 shows a similar relationship, but the pore fluid pressure rises to a greater value than q. This is not observed for any of the other isotropic tests on other materials. DW2 shows a steady rise in pore pres sure, at a lower rate than q. At high strains, however, the pore pressure value exceeds q (figs. 6.20 and 6.21; table 6.14).

TEST	u_{max} (MPa)	E_a (%)	q (MPa)	u_{fin} (MPa)	E_a (%)	q (MPa)
DW1110	3.5	17.0	2.6	3.4	27.8	2.6
DW2150	16.8	13.4	20.8	16.8	18.0	18.8

Table 6.14. Values of maximum and ultimate excess pore pressures and associated stresses and strains for the Devil's Woodyard test series

d) Failure

As for the Taiwan series, values of maximum q define the failure line of the Devil's Woodyard material, going through the origin (fig. 6.19; table 6.15).

SAMPLE	p' (MPa)	q (MPa)	AXIAL STRAIN (%)	u_f (MPa)	M
DW1	5.6	2.7	9.1	3.4	0.48
DW2	41.0	22.0	6.2	14.5	0.54

Table 6.15. Failure conditions for the Devil's Woodyard test series

Both samples had "slickensided", polished shear planes at the end of the test (plate 6.1).

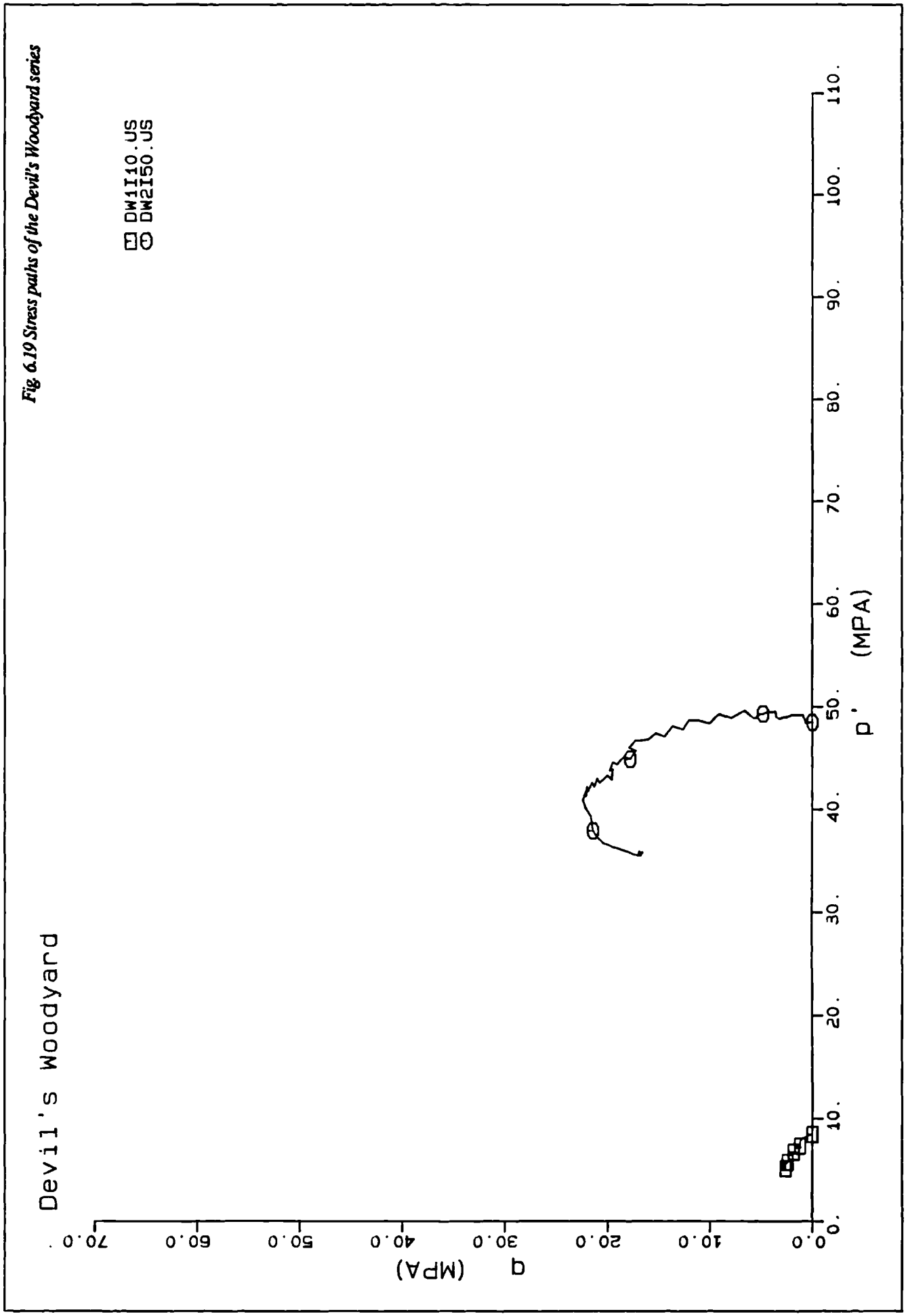

Fig. 6.19 Stress paths of the Devil's Woodyard series

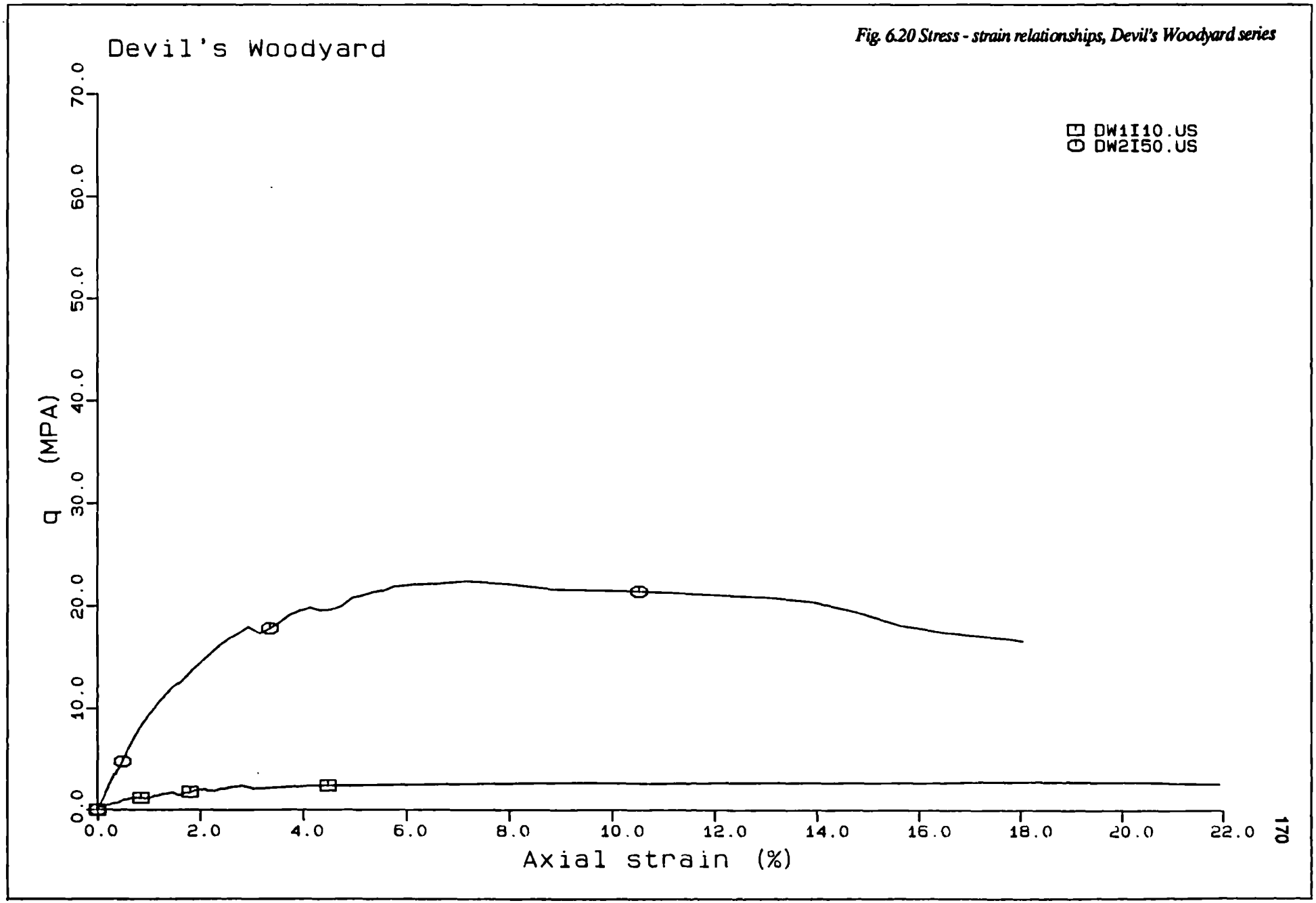

Fig. 6.20 Stress - strain relationships, Devil's Woodyard series

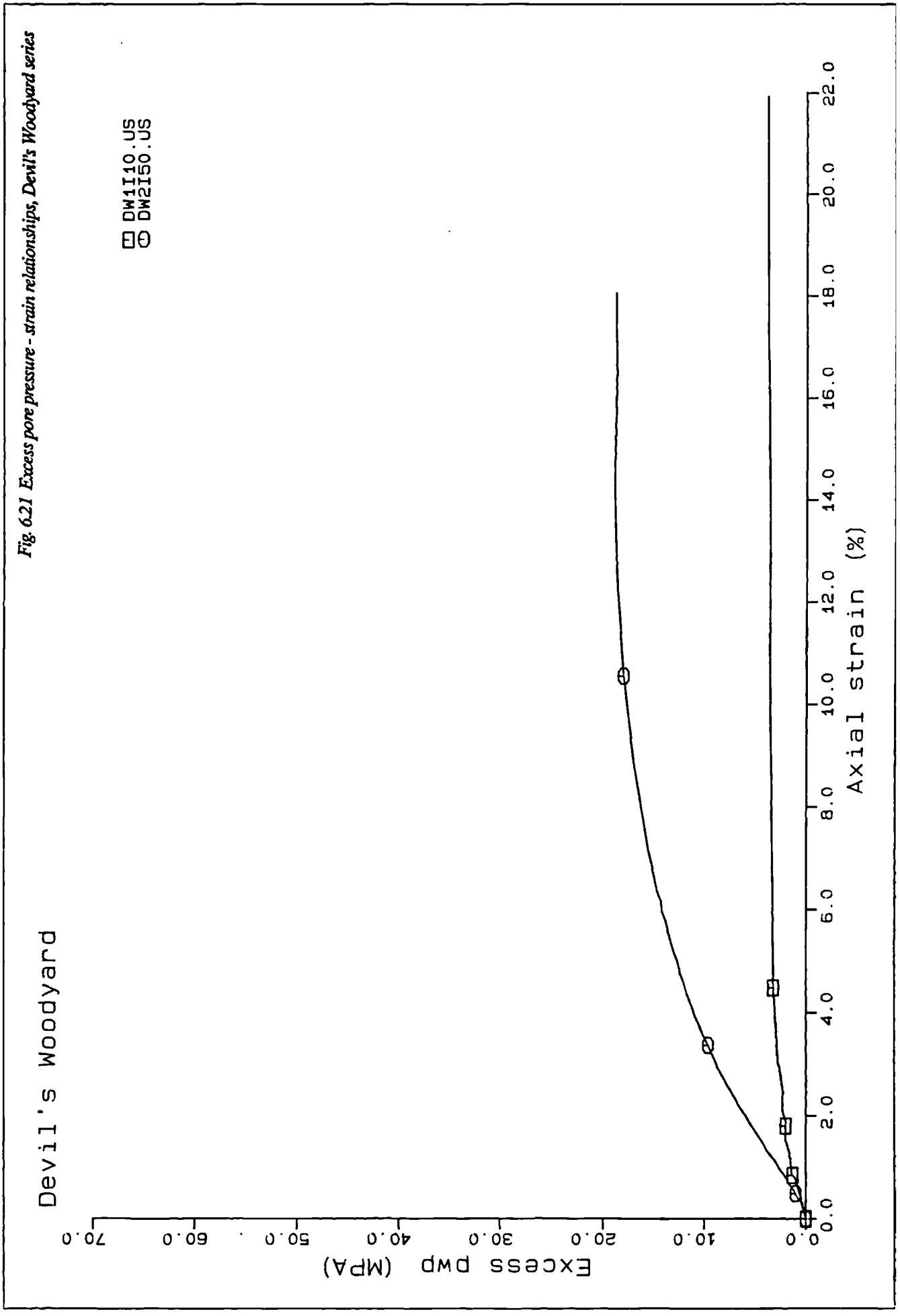

Fig. 6.21 Excess pore pressure - strain relationships, Devil's Woodyard series

a.

b.

Plate 6.1 Polished, striated shear surfaces developed in the two Devil's Woodyard samples after testing: a. DW1I10; b. DW2I50.

6.4. SUMMARY OF THE MAIN RESULTS

6.4.1. Consolidation

The three materials display different consolidation behaviour. The Lagon Bouffe clay is the least compressible material and the Devil's Woodyard clay is the most compressible, as indicated by values of x (fig. 6.22).

The only sample tested without prior consolidation in the piston, DW1, was more compressible than its equivalent, DW2. All the others display a break in the consolidation curve, generally between 1 and 2 MPa, marking the pre-consolidation pressure in the piston. The difference in the value of x for DW1 and DW2 suggests that the preparation procedure has an effect on the manner in which the samples deform subsequently.

It is difficult to make accurate comparisons between different tests within the same test series because of the slight variability of initial voids ratios, particularly for Lagon Bouffe. Generally, however, Lagon Bouffe clays seemed to show more sensitivity to stress path than Taiwan clays. For the former material, the K-line seems to fall to the left of the isotropic consolidation in e - ln p' space (fig. 6.3). For the latter material, however, there seems to be very little effect of stress path on voids ratio.

The pore pressure responses of the three isotropic tests, LB1, TA and DW2 (tables 6.2, 6.5 and 6.9) indicate that the materials are not fully saturated at the beginning of the tests; consolidation at a low effective stress and a high back pressure (Appendix 6), however, ensures saturation. The pore pressures take longer to equilibrate as the material consolidates; this is particularly noticeable for the LB1, although it is the coarsest and would be expected to give the fastest pore pressure response. This is probably related to the pore pressure gradient created across the sample as it was loaded at higher stresses. The delay in B-value is attributed to the high density of the material at higher stresses, so that it takes longer for the additional pressure to be transformed from the grain "skeleton" to the pore fluids after undrained loading.

These points are discussed in greater detail in Chapter 7.

6.4.2. Undrained Shear

Again, the three different materials display different styles of behaviour. All the samples show a decrease in p' with shear, caused by the generation of excess pore fluid pressures. For a sample consolidated to the same p', the siltiest materials (LB) produce the highest pore fluid pressures during shear, and the lowest associated axial strains (compare, for example, LB1I50, TAI50 and DW1I50 in tables 6.10, 6.12 and 6.14 respectively).

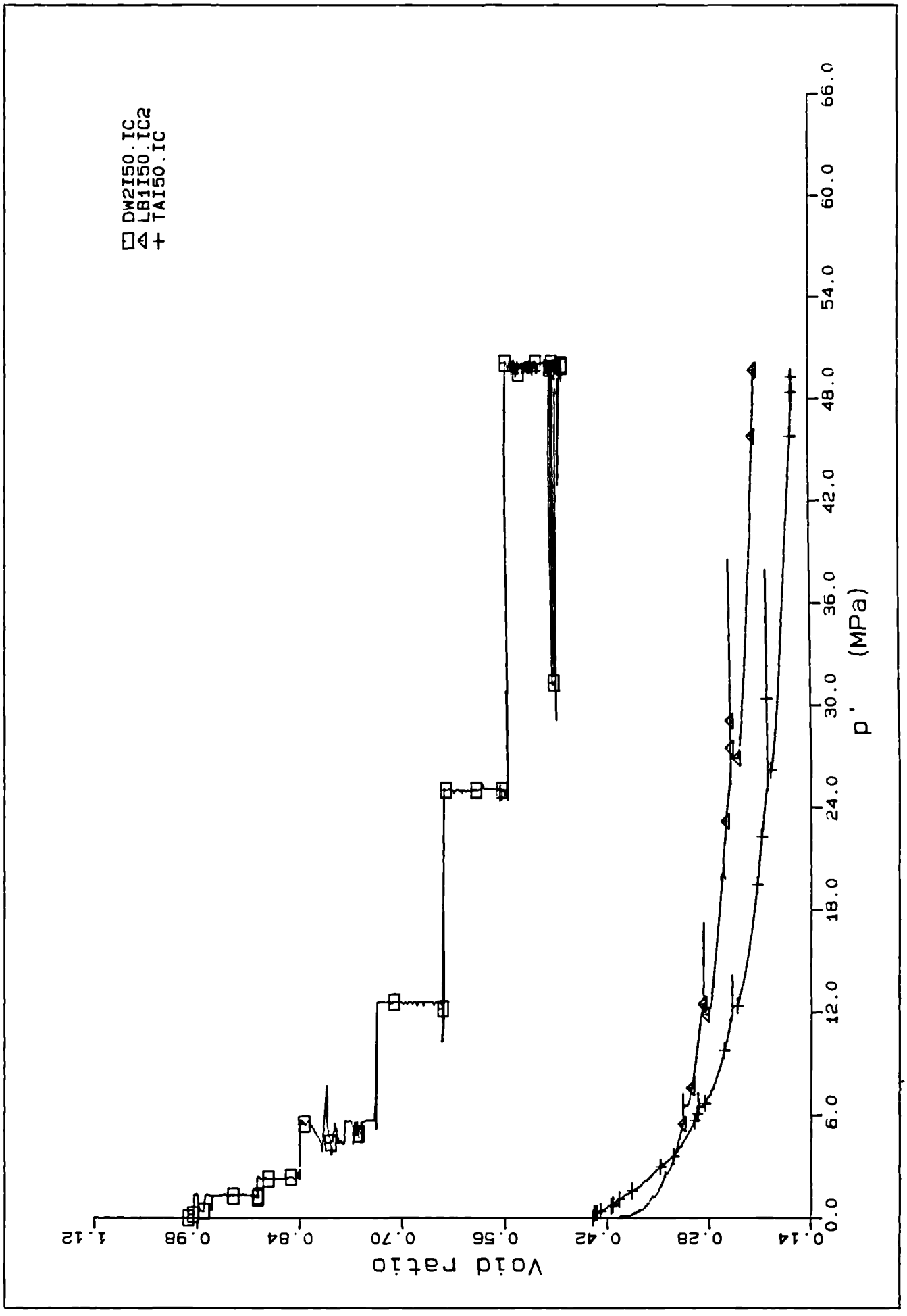

Fig. 6.22 Comparison of the voids ratio - mean effective stress relationships for LB1I50, TAI50 and DW2I50

The pore pressure response is associated with stress path. Comparison between isotropic and anisotropic tests for both the Lagon Bouffe and Taiwan test series shows that the rate of pore pressure generation is greater than the rate of increase of q for anisotropic tests, although DW1, an isotropic test, shows the same phenomenon. For two samples consolidated isotropically and anisotropically to the same voids ratio, the maximum pore pressure value is greater for the isotropically consolidated sample (compare, for example, LB1I50 and LB5K45 in table 6.10); this also applies to isotropic and anisotropic consolidation to the same value of p' (compare, for example, TAI50 and TCK50 in table 6.12).

The mode of failure varies for the three materials. The LB series had the highest strength, and the DW series, the lowest strength, as indicated by the values of M, the slope of the failure line in p' q space (tables 6.11, 6.13 and 6.15). The three series showed two styles of failure: one which can be equated to the "critical state" type of failure described in Chapter 5, where the sample continues to deform with no further changes in effective stresses (LB2, LB3, TA, TD, TF and DW1), and one where the effective stresses continued to change with increasing deformation. The latter type of failure varied for the three materials. The LB series showed increasing effective stresses with deformation, associated with decreasing pore fluid pressures. The Taiwan series showed the opposite, where q began to drop in tests TCK50 and TEK25, with associated increasing pore pressures; this is also observed in DW2, although the drop in q for the latter was much sharper.

The DW samples were the only ones where shear planes developed; the others only bulged and shortened.

These phenomena are discussed in Chapter 7.

CHAPTER 7

DISCUSSION: MUD VOLCANOES AND MUD VOLCANO CLAY BEHAVIOUR

7.1. INTRODUCTION

The objective of the experiments conducted in this study was to understand the geotechnical behaviour of mud volcano clays, with particular reference to the role of tectonic activity in overpressuring and deforming the clays.

The results of this experimental study will be discussed here in the light of theoretical and experimental soil and soft sediment behaviour. Section 7.2 will explore the effect of consolidation history, stress magnitude and material properties on the undrained shear behaviour of the three clays; particular attention is paid to pore pressure generation and failure mechanisms. This is followed by a discussion of a number of factors influencing the undrained shear behaviour of the source material, not (or only briefly) explored in the testing programme (section 7.3); these include the effect of cementation, earthquake activity and the orientation of the principal stresses in a mud volcano environment. The chapter is concluded with a general discussion of the overpressuring and sediment deformation mechanisms leading to mud volcano activity.

7.2. THE UNDRAINED SHEAR BEHAVIOUR OF MUD VOLCANO CLAYS

7.2.1. Introduction

This discussion explores the relationship between the stresses and the pore fluid pressures generated in the mud volcano clays and their different modes of failure during undrained shear. Three main factors regarded as possibly affecting the undrained shear behaviour of the clays at high effective stresses will be investigated, including consolidation path, stress magnitude and material properties. Because of the close interrelation of all aspects of sediment deformation, pore pressure generation and failure mechanisms are discussed within these three main sub-sections, before the main conclusions are summarised at the end of the section. Throughout the discussion, comparisons are made with ideal behaviour, as predicted by soil mechanics theory, and with similar experiments carried out on other soils and sediments at a range of effective stresses.

7.2.2. Effect of Consolidation Path on Undrained Shear Behaviour

a) Comparisons Between Isotropic and Anisotropic Tests

The ratio between the horizontal and vertical effective stresses in a depositional environment will vary according to the tectonic setting of the sedimentary basin. This is significant, because the consolidation

path followed by a sediment can have a very strong influence on the manner in which this sediment behaves during undrained shear. The effect of consolidation path on undrained shear behaviour is explored in the experimental programme by using two different stress ratios: K = 1 (isotropic), and K = 0.6 (anisotropic). It was not possible to explore more complex stress paths due to the limitations of the equipment used. Before the results are compared, the idea behind the comparison is briefly explained here.

Chapter 5 introduced some of the critical state soil mechanics theory on the behaviour of normally consolidated isotropic materials (Schofield and Wroth, 1968; Roscoe and Burland, 1968). Section 5.2.3 described the isotropic normal consolidation behaviour of soils. It was shown that there was a unique relationship between voids ratio and mean effective stress for an isotropic material, defined by a straight line in e - ln p' space (fig. 5.2). Section 5.2.4 showed that an anisotropic stress system affected the consolidation behaviour of an isotropic material, so that a shear stress component acting on an isotropic material causes it to consolidate further; i.e. the lower the K- ratio, the lower the voids ratio for the same mean effective stress (fig. 5.2). Anisotropic consolidation lines were therefore found to plot to the left of the isotropic consolidation line in e - ln p' space, and also to be parallel to it. The theory further predicts that all deformations in a normally consolidated isotropic material can be defined by a surface in stress space called the Roscoe, or Rendulic surface (section 5.2.7; fig. 5.4). This means that all virgin consolidation paths, drained and undrained shear paths follow this surface is stress space (fig. 7.1).

Fig. 7.1 shows that if the same isotropic material was consolidated isotropically and anisotropically to the same voids ratio, it would ideally follow the same stress path during undrained shear; i.e., consolidation path should not affect the undrained shear behaviour. If the theory is taken literally, in geological terms, this would mean that the behaviour of sediments consolidated to a certain porosity in a passive sedimentary basin will be identical to the behaviour of the same material in an active basin. It should be appreciated, however, that this theory is only applicable to isotropic materials, and geological materials are usually far from isotropic.

The basics of the theory are used here to investigate the effect of consolidation path on the behaviour of non-ideal, anisotropic sediments. The two different stress paths are therefore compared for the Lagon Bouffe and Taiwan test series; no anisotropic consolidation tests were performed on the Devil's Woodyard clays.

The Lagon Bouffe sample LB5K45 was anisotropically consolidated to the point of intersection in p' q space with the undrained shear path of the isotropically consolidated sample LB1I50 (fig. 7.2). This point was point X in fig. 7.1. As mentioned in Chapter 6, the cell pressure decreased during undrained shear in test LB5K45 so that it is difficult to make exact comparisons with test LB1I50. The paths prior to the problem with LB5 are fairly similar, however. In fact, the two samples did fail at a similar point, although LB1I50 was slightly stronger (fig. 7.2). It therefore seems that the Lagon Bouffe material is not very sensitive to consolidation path in its undrained shear behaviour.

The same comparison was attempted for the Taiwan material with TAI50 and TCK50. Unfortunately, the latter was consolidated beyond the point of intersection X (fig. 7.1), to the same value of p' as TA; comparison could therefore be made between the two consolidation paths up to the same mean effective stress. The result (fig. 7.3) is interesting. TC has a similar strength to TA, although it was

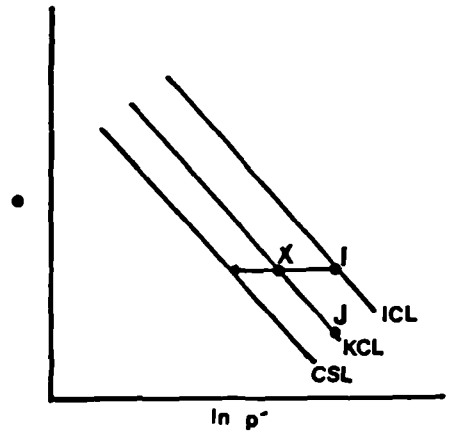

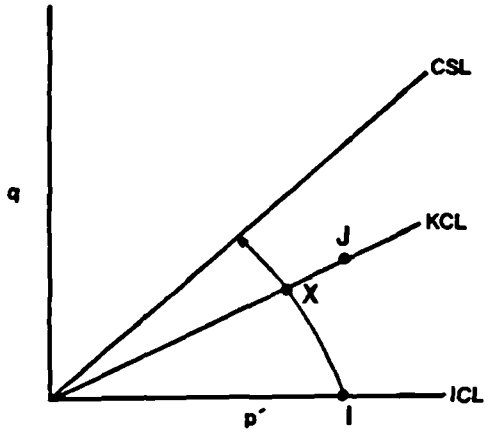

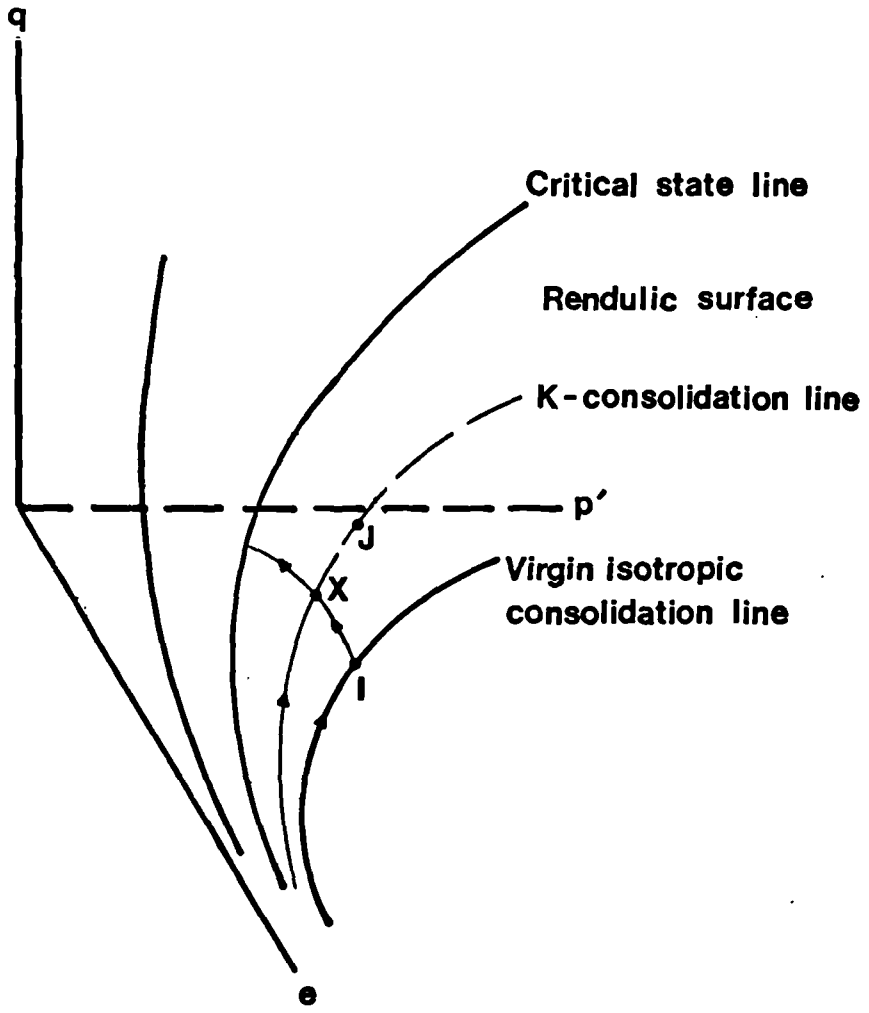

Fig. 7.1 Isotropic and anisotropic consolidation paths and the Rendulic suface.

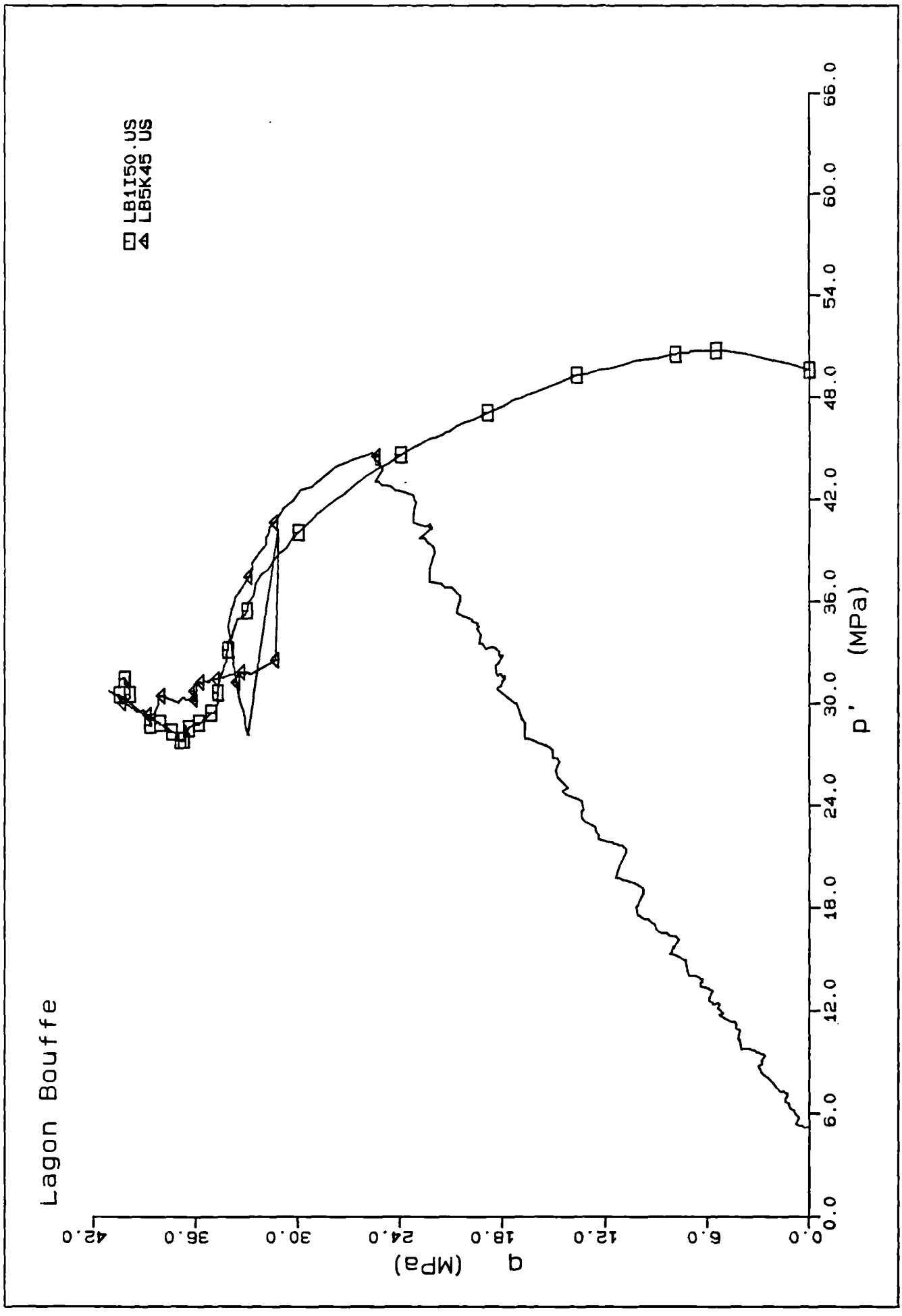

Fig. 7.2 Comparison of the stress paths of LB1I50 and LB5K45.

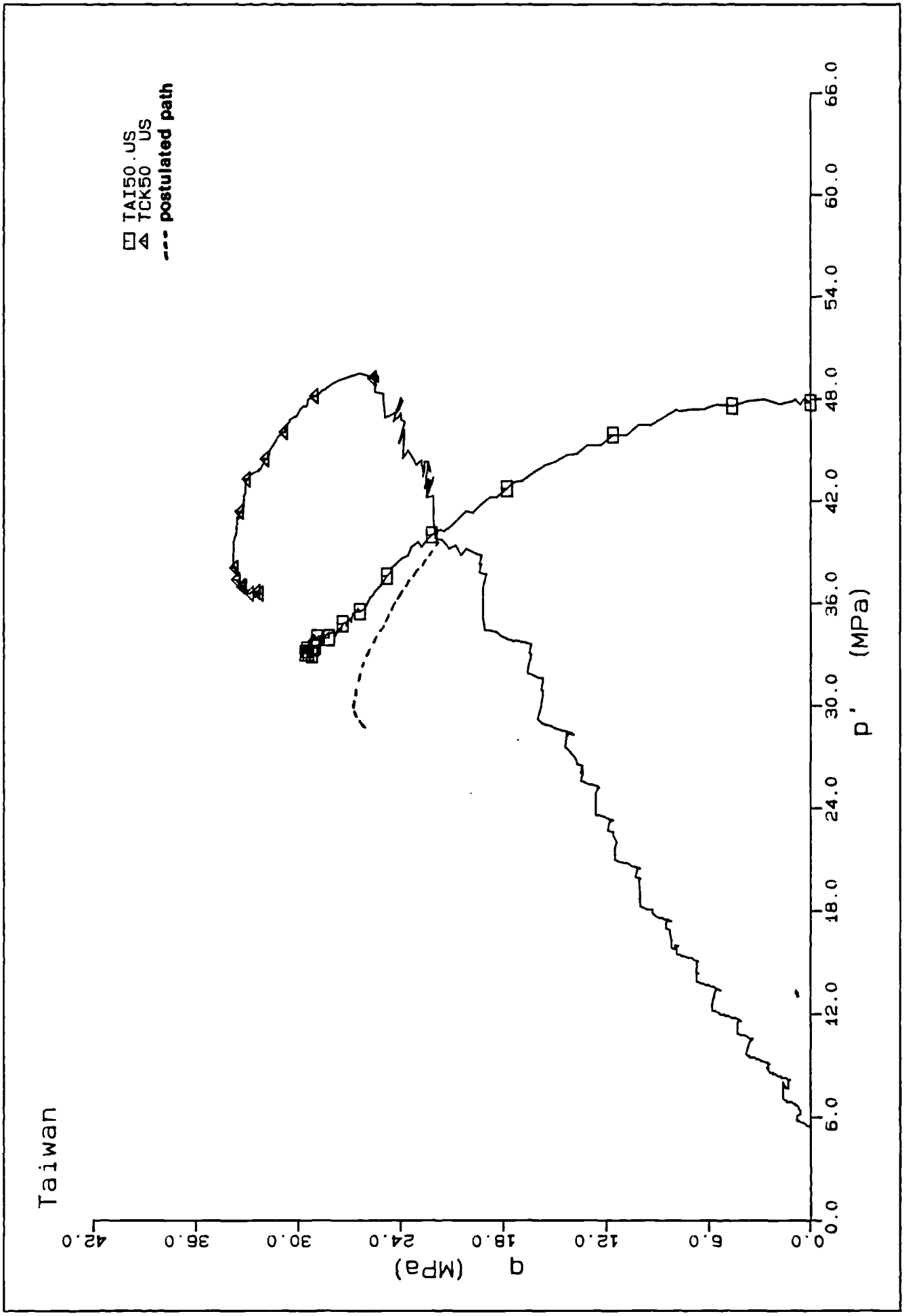

Fig. 7.3 Comparison of the stress paths of TAI50 and TCK50

consolidated beyond the above-mentioned point X. If TC had been consolidated to that point, it would have had a lower strength than sample TA (fig. 7.3), assuming that the undrained shear curve is repeatable at different stresses for the anisotropically consolidated samples (which is shown in section 7.2.3). The reason for the observed difference in behaviour is most likely to be the difference in structure after different types of consolidation, enhanced by the higher clay content of the Taiwan material. This is explored further in the note below.

Note on the effect of sample preparation on the behaviour of the mud volcano clays:

Presumably, the effect of stress path on the Taiwan clays would have been even more pronounced had the samples not been prepared in the small cylinder apparatus (Appendix 4), which is thought to have made the samples very anisotropic before the start of testing. The Taiwan materials show the least sensitivity to stress path in their e - ln p' relationship. Ideally, a normally consolidated clay would be expected to lose more volume with increasing shear stress (Schofield and Wroth, 1968; fig. 7.1). The difference in the compressibility values for the two DW tests (fig. 6.9) may be a good clue as to why this is so. The preparation in the small cylinder apparatus (Appendix 4) seems to decrease the compressibility of the material, which implies that it has an anisotropic structure which cannot then deform isotropically under isotropic consolidation. This is also indicated by the distance the ram has to travel into the pressure vessel before reaching the sample; from calculations of height loss based on volume loss, it is estimated that the height decreases by up to 4 times the diameter (for the Taiwan material) during isotropic consolidation to 5 MPa (see Appendix 6).

If we compare tests TAI50 and TCK50 again, it can be demonstrated that the two samples did not follow the same stress path during undrained shear. If the Taiwan samples were isotropic, they would be expected to have the consolidation paths shown in the e - p' diagram in fig. 7.1. Point X, the intersection between the isotropic undrained shear path and the K-line, would be expected to have the same voids ratio as point I on the isotropic consolidation line before the start of undrained shear. TC, the anisotropically consolidated sample, should therefore plot on point J (fig. 7.1) and should have a lower voids ratio than TA. In fact, TA and TC had similar voids ratios at the start of undrained shear (fig. 6.5). If TA and TC had the same undrained shear behaviour, TA would be expected to have shown a steady increase in q with no change in p' until point J' was reached (fig. 7.4). Clearly, this does not occur, indicating that the two samples are shearing along different surfaces in stress space.

The Lagon Bouffe materials, on the other hand, are slightly less sensitive to the preparation procedure because of their high silt content, so that there is less particle orientation during consolidation, although it was estimated that the samples lost 2.8 times as much height as diameter during isotropic consolidation (Appendix 6).

Stress path dependence has been observed in triaxial tests at low and medium effective stresses, and natural soils are now known to deviate from the predicted models (Skinner, 1975; Gens, 1982; Burland, 1987; Atkinson, *et al* 1987; Leroueil and Vaughan, 1989). Skinner (1975) conducted four undrained shear experiments on Ham River sand samples, one of which was anisotropically consolidated to an s' ($(\sigma_1' + \sigma_3')/2$) of 2000 psi (13.8 MPa). His results (fig. 7.5) suggest that the stress path controls the behaviour of the samples. Gens (1982) compared the effect of stress path on the undrained shear strength of the Lower Cromer Till, a similar material to the Taiwan clays, and produced very similar results to Skinner's (fig. 7.6), although for lower stresses. The behaviour is explained by the greater instability of an anisotropic soil structure (Gens, 1982). This is discussed in the next section. The Lagon Bouffe materials seemed to be less sensitive to consolidation path (although the difficultly with test LB5K45 may have obscured the relationship). The Taiwan material, however, showed considerable sensitivity to consolidation path.

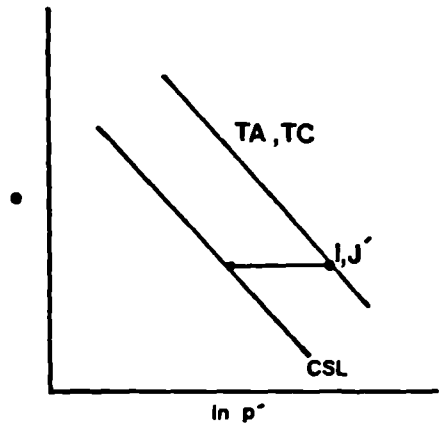

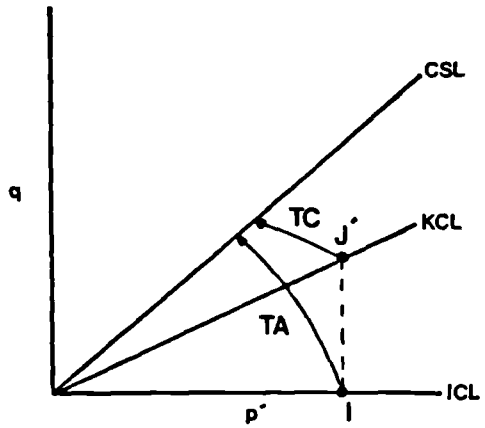

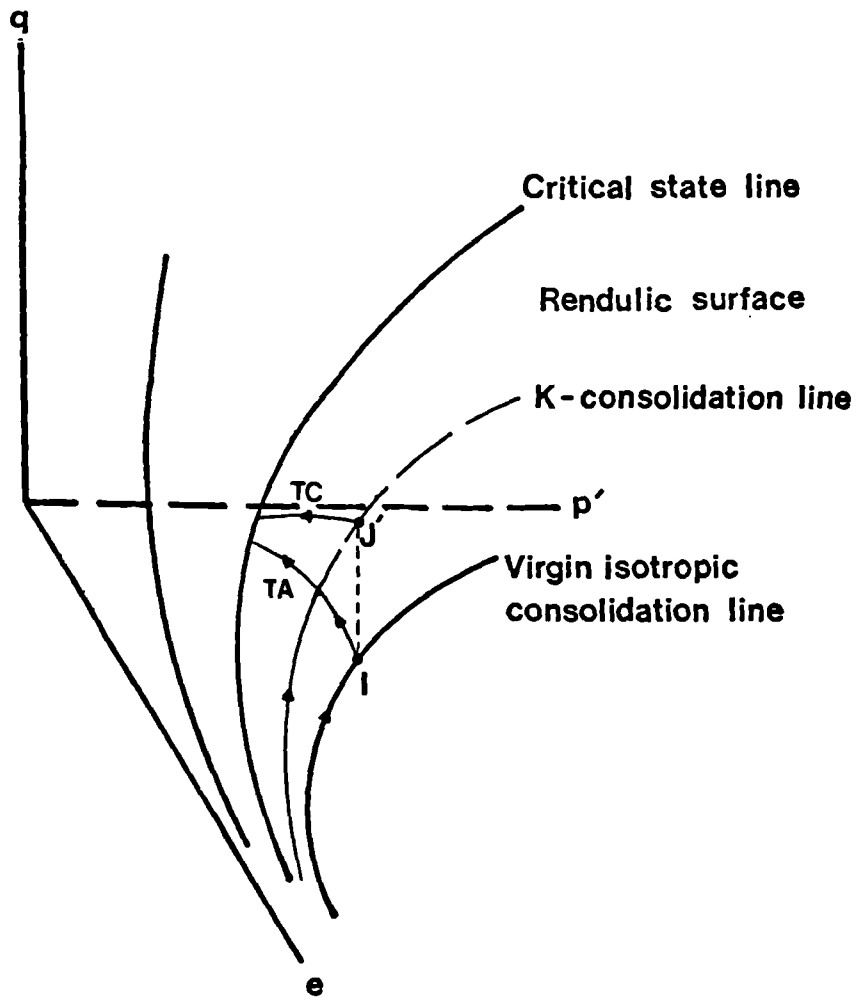

Fig. 7.4 Postulated stress path followed by TAI50 in an ideal critical state soil behaviour

Fig. 7.5 Undrained shear tests on the Ham River Sand, consolidated both isotropically and anisotropically (Bishop et al, 1965)

Fig. 7.6 Normalised stress paths for Lower Cromer Till, consolidated at different stress ratios from K = 1 to K = 0.4 (Gens, 1982); the stresses were normalised with respect to p'_e, the value of p' for the same voids ratio on the isotropic consolidation line.

b) Effect of Anisotropic Consolidation on Pore Pressure Response

The effect of consolidation path on pore pressure generation should be reflected by the ratio between excess pore pressure and shear stress. This was analysed in two ways: a) by dividing the value of excess pore pressure by the corresponding change in q from the value at the start of undrained shear (q_I), $\{A = u_e / (q - q_I)\}$; and b) by calculating the pore pressure-shear stress ratio at increments of 1% axial strain ($A' = du_e / dq$).

The results are very interesting. Calculation method a) showed very strong differences between isotropic and anisotropic tests for the Lagon Bouffe and Taiwan materials (fig. 7.7.a and b). The pore pressure response (A) is higher for the anisotropic tests, especially for the Taiwan results, reaching values far in excess of 1. This was also observed for the Ham River sand (Bishop et al, 1965), (fig. 7.5). An A-value of>1 means that the increase pore pressure is greater than the stress increase. This usually indicates the collapse of a loose structure, in a sensitive clay (Bjerrum, 1954; see section 7.3.3 below), in a chalk (Leddra, 1989), or in a loose sand (Bishop et al, 1965). The stresses acting on the soil skeleton transfer to the pore fluids when the structure breaks down, causing abnormally high pore pressures (Lambe and Whitman, 1979). The only isotropically consolidated material which attains an A-value of>1 is the Devil's Woodyard clay; the two Devil's Woodyard results are inserted in fig. 7.7 for comparison with the other clays.

The A' values (fig. 7.8) show that, incrementally, very large pore pressures are generated with small changes in q, particularly in the anisotropic tests. (The downward-pointing arrows in fig. 7.8 indicate that the pore pressures continue to rise with decreasing q). As expected, the result is particularly dramatic for anisotropic tests where the p' q curve flattened (LB2K25 and LB3K15, fig. 6.10) or moved down the failure line (TCK50 and TEK25, fig. 6.13). The latter type of behaviour is commonly termed "contractant" behaviour.

If the A'-values were compared for LB1I50 and LB5K45, discussed above, it is seen that they are quite similar - so, indeed, is LB4K60 (fig. 7.8.a). This would imply that the Lagon Bouffe material is insensitive to consolidation path; why, therefore, are LB2 and LB3 different to LB5 and LB6? It seems that, not only are there considerable differences in pore pressure response between isotropic and anisotropic tests, there are also differences within samples consolidated in the same manner, and within different materials. This is discussed in the next two sections.

c) Failure

From the limited data available, there are indications that the consolidation path affects the mode of failure for the two materials, but the relationship seems to be also dependent on stress magnitude. For example, although the anisotropically consolidated sample LB5K45 failed in a similar manner to the isotropic sample LB1I50, implying that consolidation path does not affect the Lagon Bouffe materials, its lower pressure equivalents LB2K25 and LB3K15 failed in a completely different manner (fig. 6.10). The failure of the first two was "dilatant", whereas LB2K25 and LB3K15 failed in a "critical state" manner, i.e., the samples continued to deform with no further changes in effective stress. "Dilatant" behaviour at failure under undrained conditions is the opposite of "contractant" behaviour, in that the sample is "trying" to expand, with associated decrease in pore fluid pressures and increase in strength.

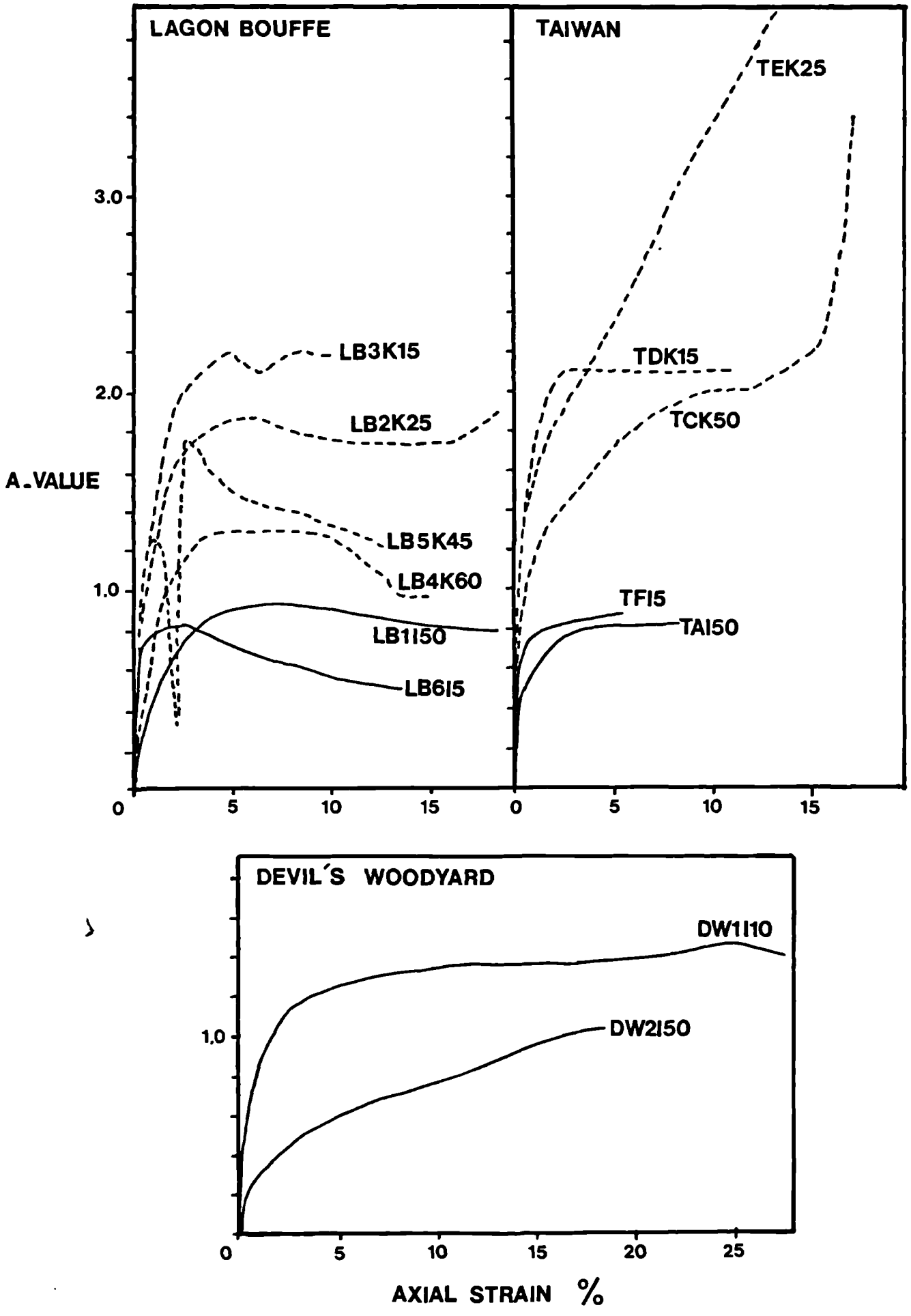

Fig. 7.7 Values of pore pressure response (A) vs. axial strain for all the tests. a. Lagon Bouffe; b. Taiwan; c. Devil's Woodyard

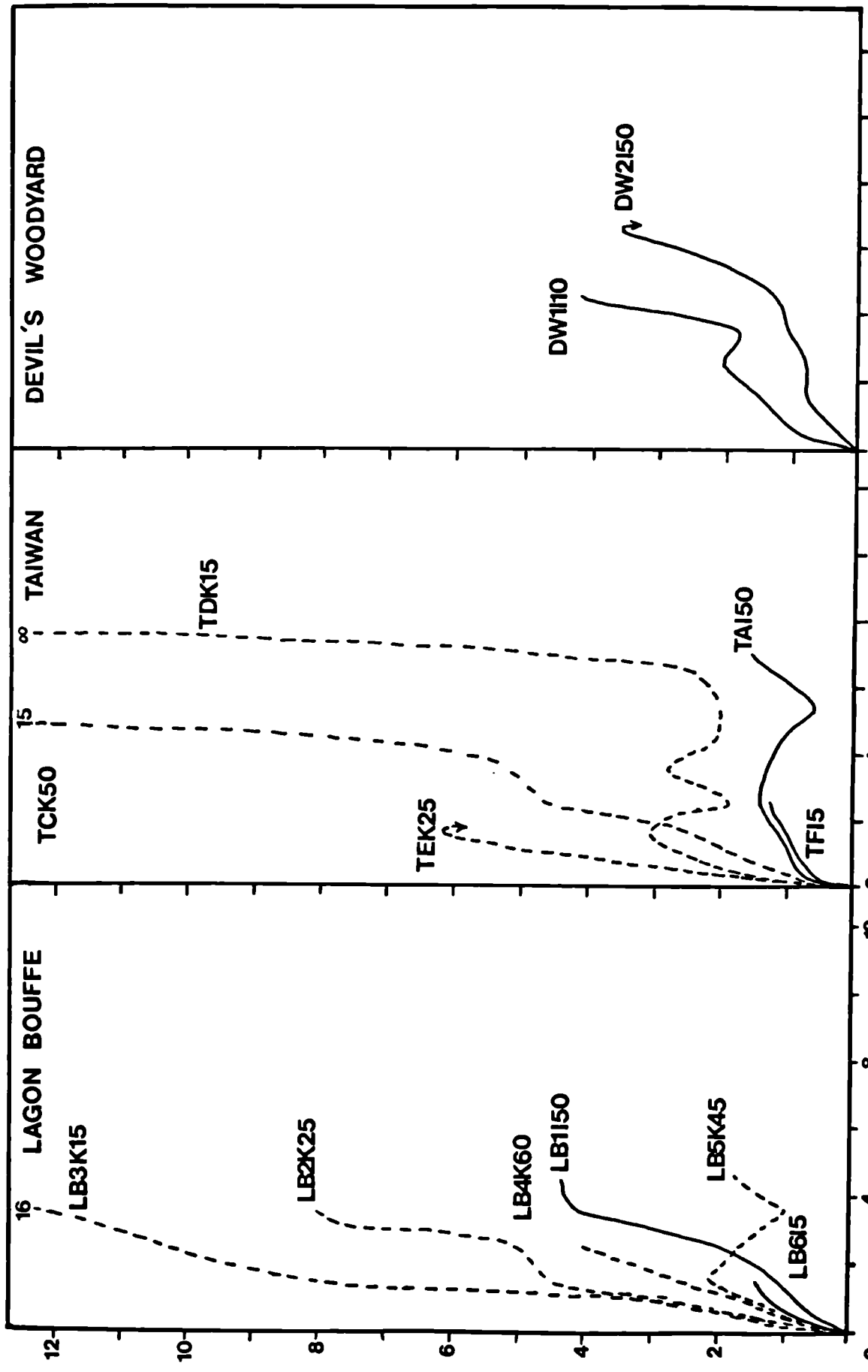

Fig. 7.8 Values of pore pressure response (A') vs. axial strain for all the tests. a. Lagon Bouffe; b. Taiwan; c. Devil's Woodyard

The Taiwan clays show more dependence on stress path in their mode of failure; compare, for example, the failure of TAI50 with TCI50, (fig. 7.3). The former fails in a "critical state" manner, whereas the other fails in a "contractant" manner.

There are several indications that consolidation path affects sediment behaviour considerably. However, it was demonstrated in the previous Chapter that the failure states of all the samples within any test series were defined by a single line in effective stress space. Therefore, although behaviour during undrained shear may vary considerably, the material is bound by predictable stress conditions defining possible states for the material.

7.2.3. Effect of Stress Magnitude on Undrained Shear Behaviour

a) Normalised Stresses and Strains

In order to examine the effect of stress magnitude on the undrained shear behaviour of the three materials, the stresses and strains were normalised with respect to p'_o, the value of p' at the start of undrained shear. This facilitates the direct comparison of tests with similar stress paths consolidated to different stress magnitudes (i.e. it eliminates the parameter of voids ratio or porosity for the same consolidation path). Data for the three materials are discussed separately before the effect of stress magnitude on pore pressure response and failure is studied more closely.

Data for the experiments conducted on the Lagon Bouffe clays do not normalise well (fig. 7.9.a). The two isotropic tests, LB1 and LB6 are similar in stress space, but show different stress- strain relationships (fig. 7.9.b). LB1 tends towards constant effective stresses with increasing strain (critical state) whilst LB6 shows strain hardening.
The Lagon Bouffe anisotropic tests are also not fully normalisable (fig. 7.9.a). As mentioned in Chapter 6, LB4K60 and LB5K45 dilate at failure, whereas LB2K25 and LB3K15 show a steady value of q with decreasing p', until failure is reached. The "critical state" point for the two tests is identical in normalised effective stress space (fig 7.9.a); this deformation at constant effective stresses is also observed in the normalised stress strain curve (fig. 7.9.b). LB4 and LB5 have greater normalised strength than LB2 and LB3 and show slight strain hardening (fig. 7.9.b).

The isotropic tests and the anisotropic tests conducted on the Taiwan clay show normalisable behaviour (fig. 7.10). They therefore seem to show less sensitivity to stress magnitude than the Lagon Bouffe materials. There are, however, some variations in behaviour. TEK25 and TCK50 fail in a "contractant" manner, wheres TDK15 fails in a "critical state" manner.

The Devil's Woodyard clays show significant differences in behaviour as seen in the normalised stress space and stress strain diagrams (fig. 7.11). DW1 fails in a "critical state" manner, with deformation at constant effective stresses, whereas DW2 fails in a "brittle" manner (fig. 7.11.a), with post-peak strain softening. It can be seen, however, that DW2 may have reached a residual strength equivalent to that of DW1 (fig. 7.11.b). As only two tests were performed, it is difficult to say whether the material is dependent on stress magnitude, although this is very likely. The post-peak drop in strength of DW2

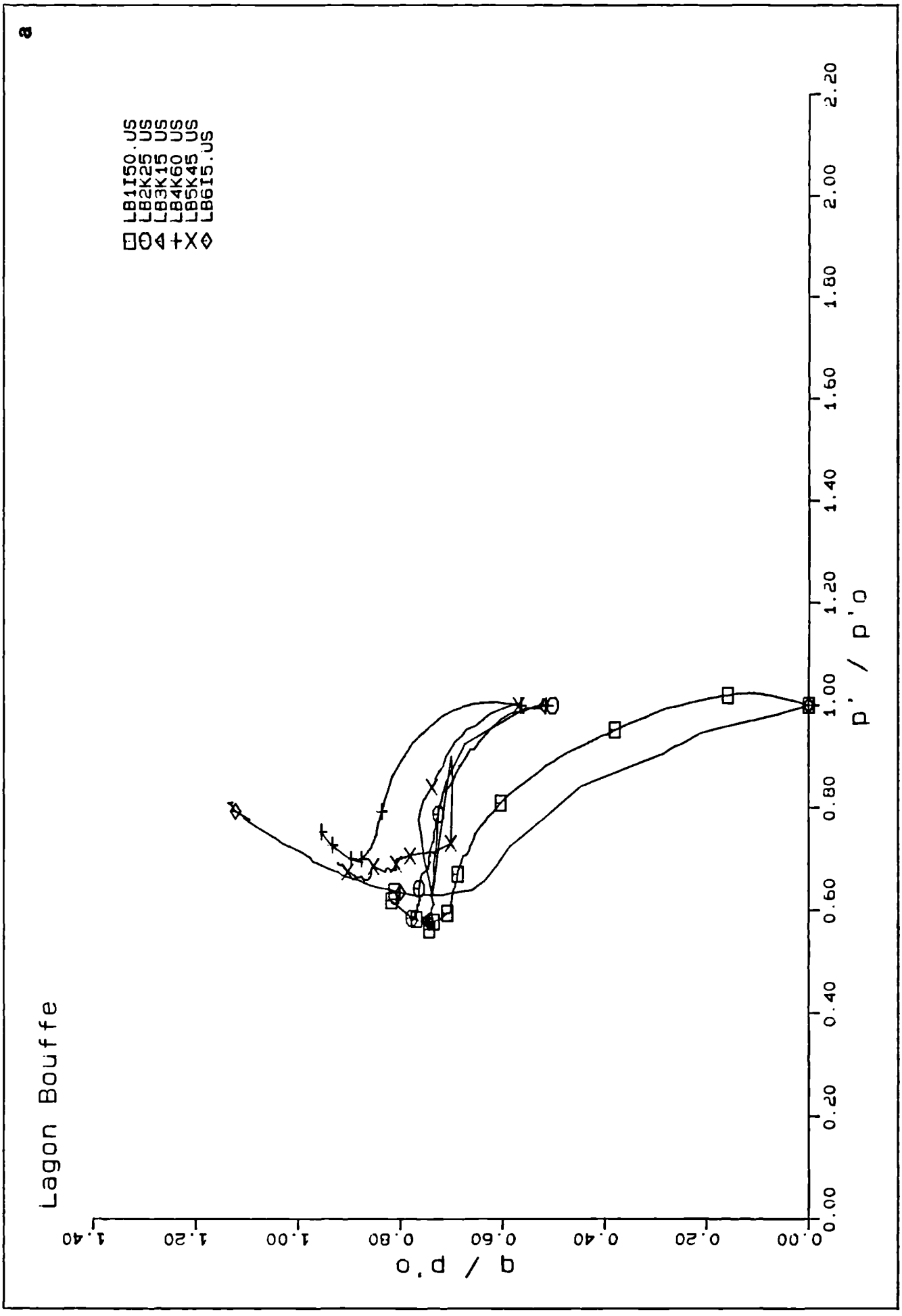

Fig. 7.9 Normalised stresses for the Lagon Bouffe series. a. normalised stress paths; b. normalised stress-strain curves

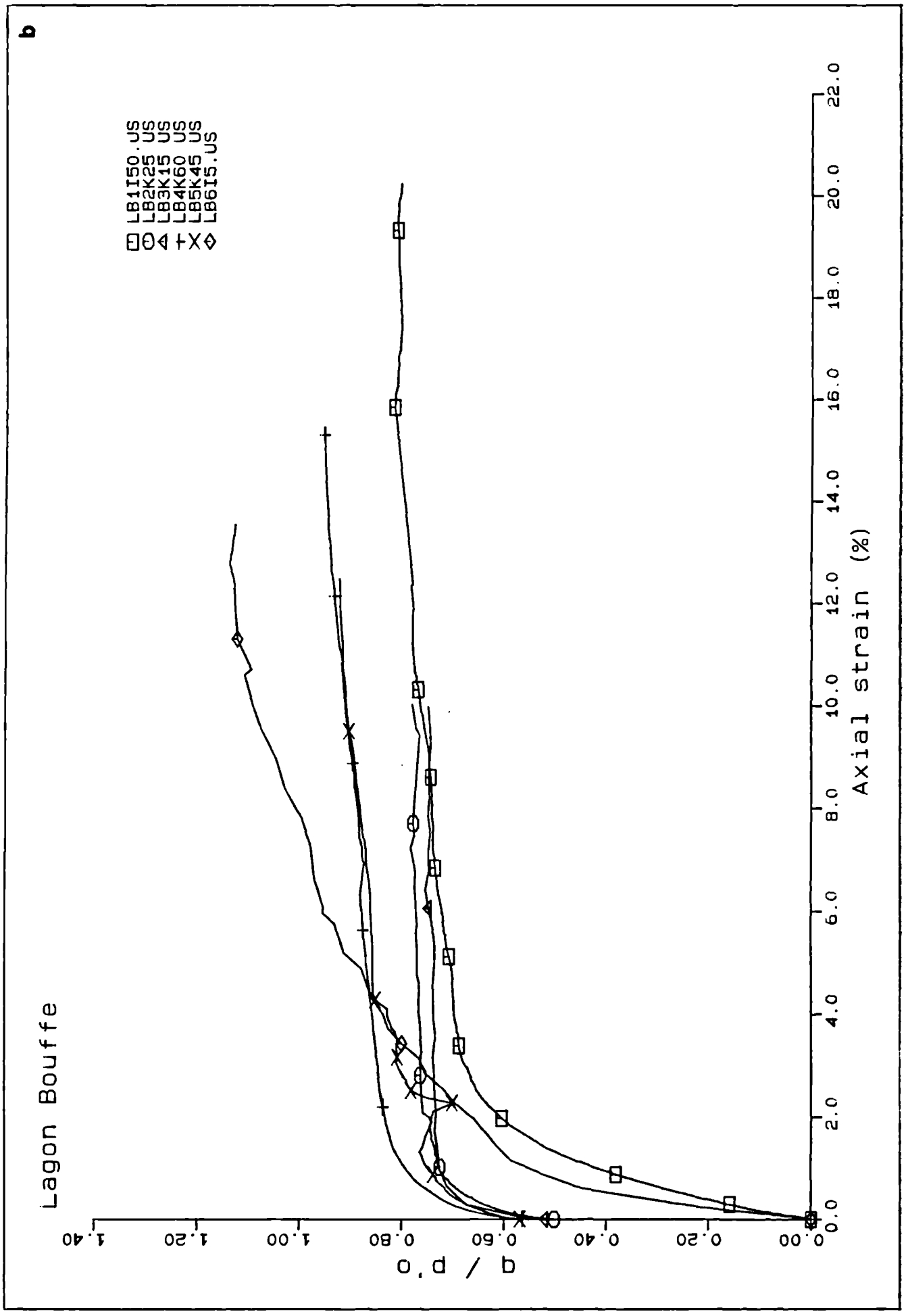
b
LB1I50.US
LB2K25.US
LB3K15.US
LB4K60.US
LB5K45.US
LB6I5.US
Lagon Bouffe
q / p'o
0.00
0.20
0.40
0.60
0.80
1.00
1.20
1.40
Axial strain (%)
0.0
2.0
4.0
6.0
8.0
10.0
12.0
14.0
16.0
18.0
20.0
22.0

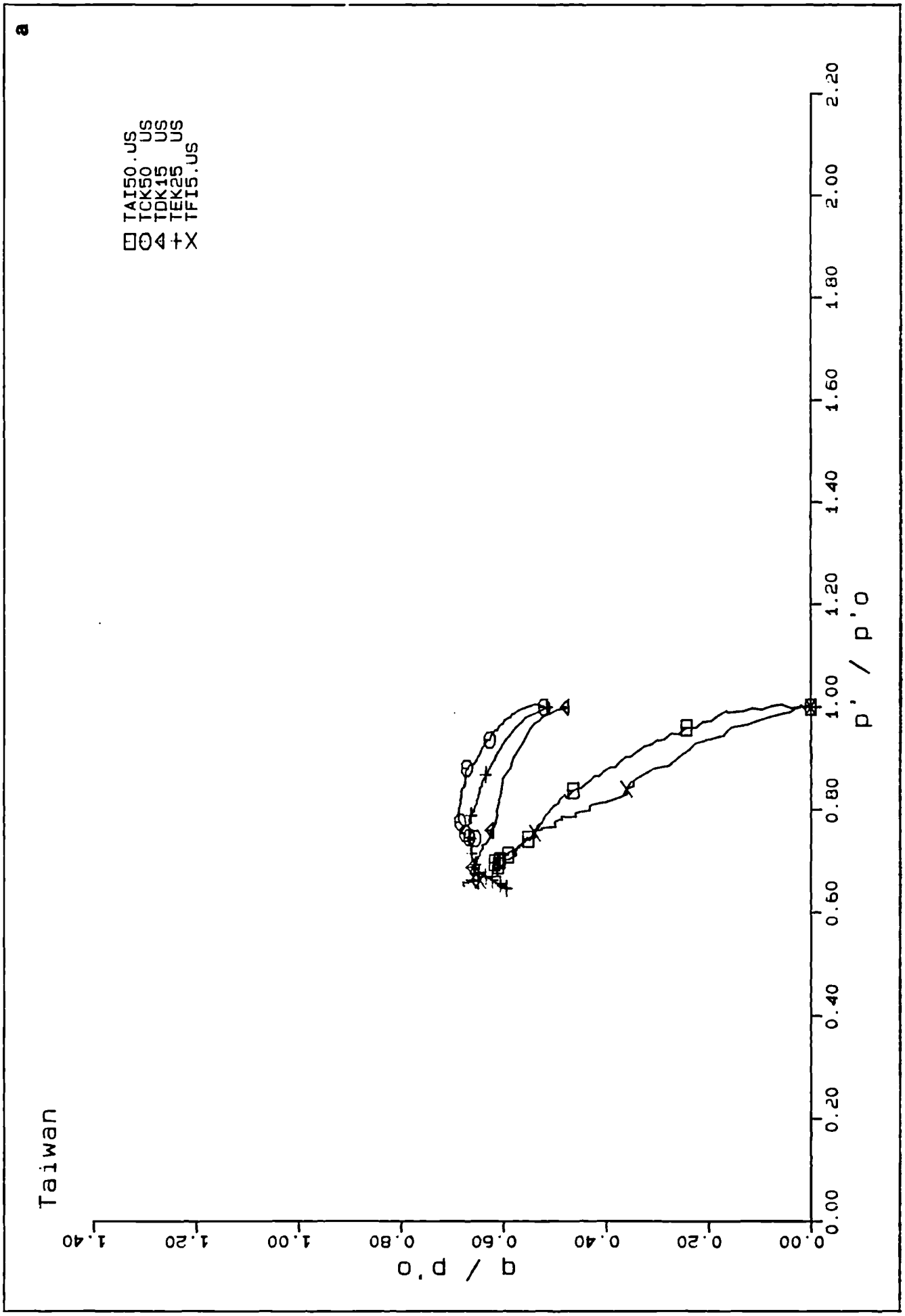

Fig. 7.10 Normalised stresses for the Taiwan series. a. normalised stress paths; b. normalised stress-strain curves

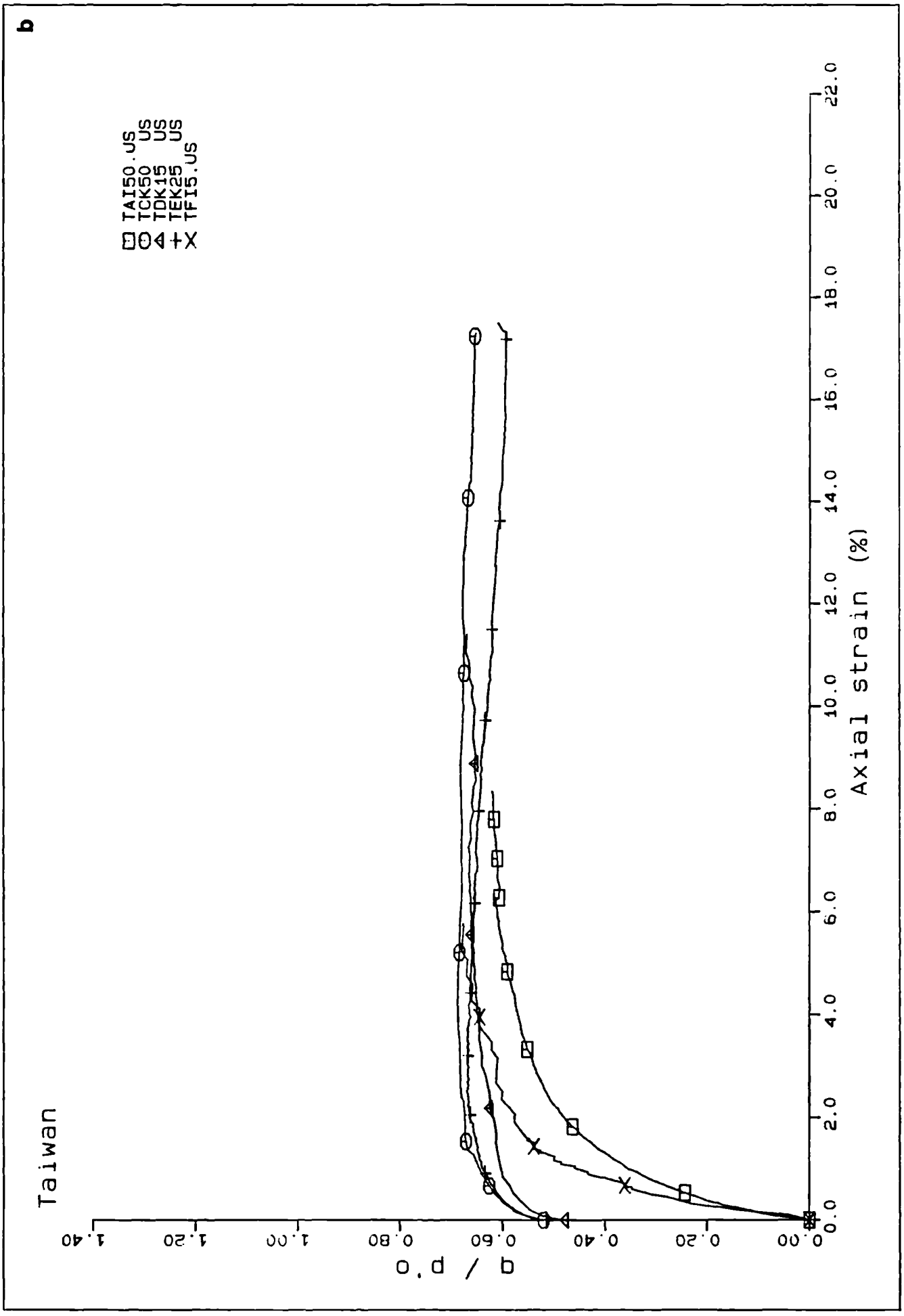
b
TAI50.US
TCK50 US
TDK15 US
TEK25 US
TFI5.US
Taiwan
q / p'o
Axial strain (%)
0.00
0.20
0.40
0.60
0.80
1.00
1.20
1.40
0.0
2.0
4.0
6.0
8.0
10.0
12.0
14.0
16.0
18.0
20.0
22.0

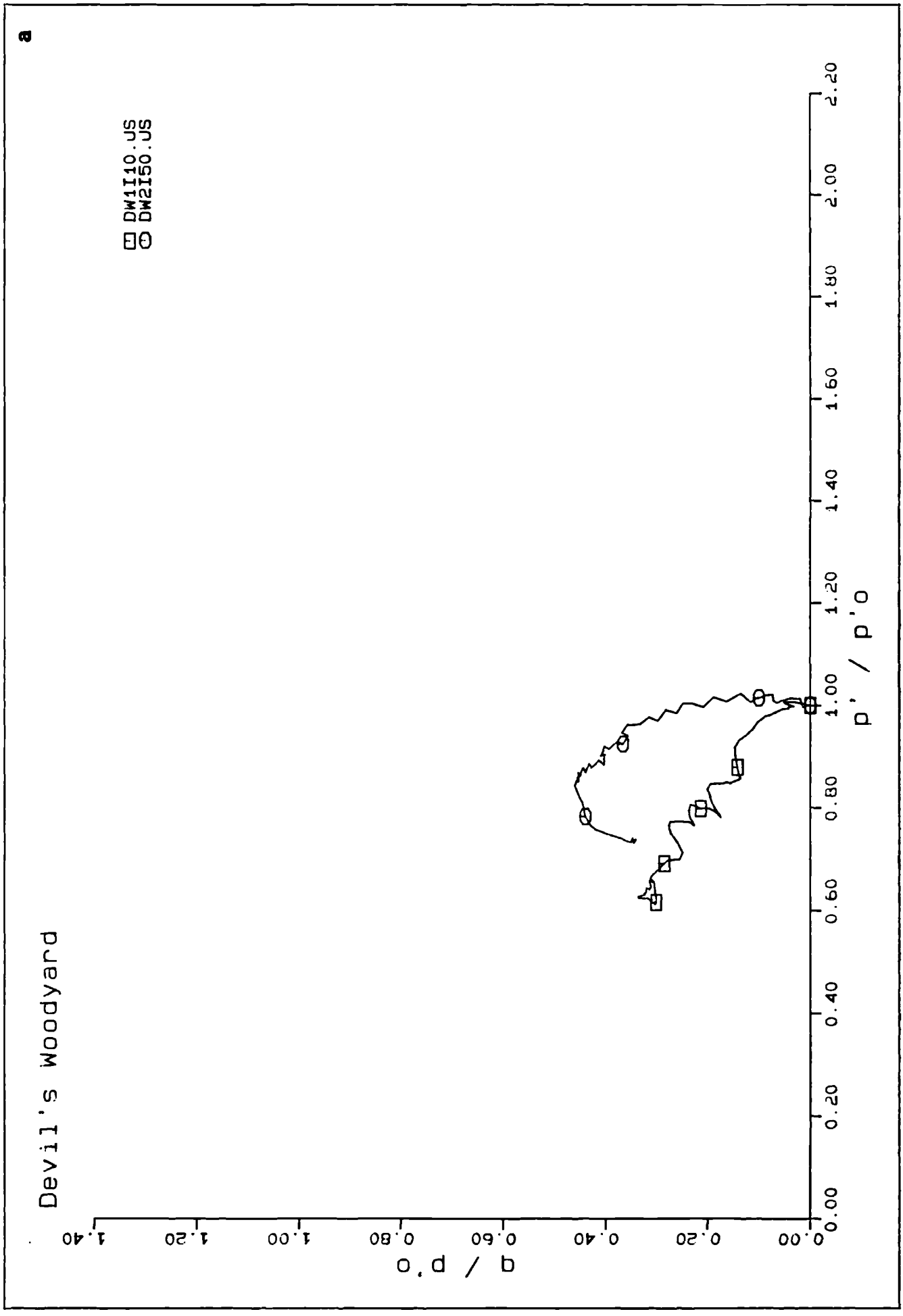

Fig. 7.11 Normalised stresses for the Devil's Woodyard series. a. normalised stress paths; b. normalised stress-strain curves

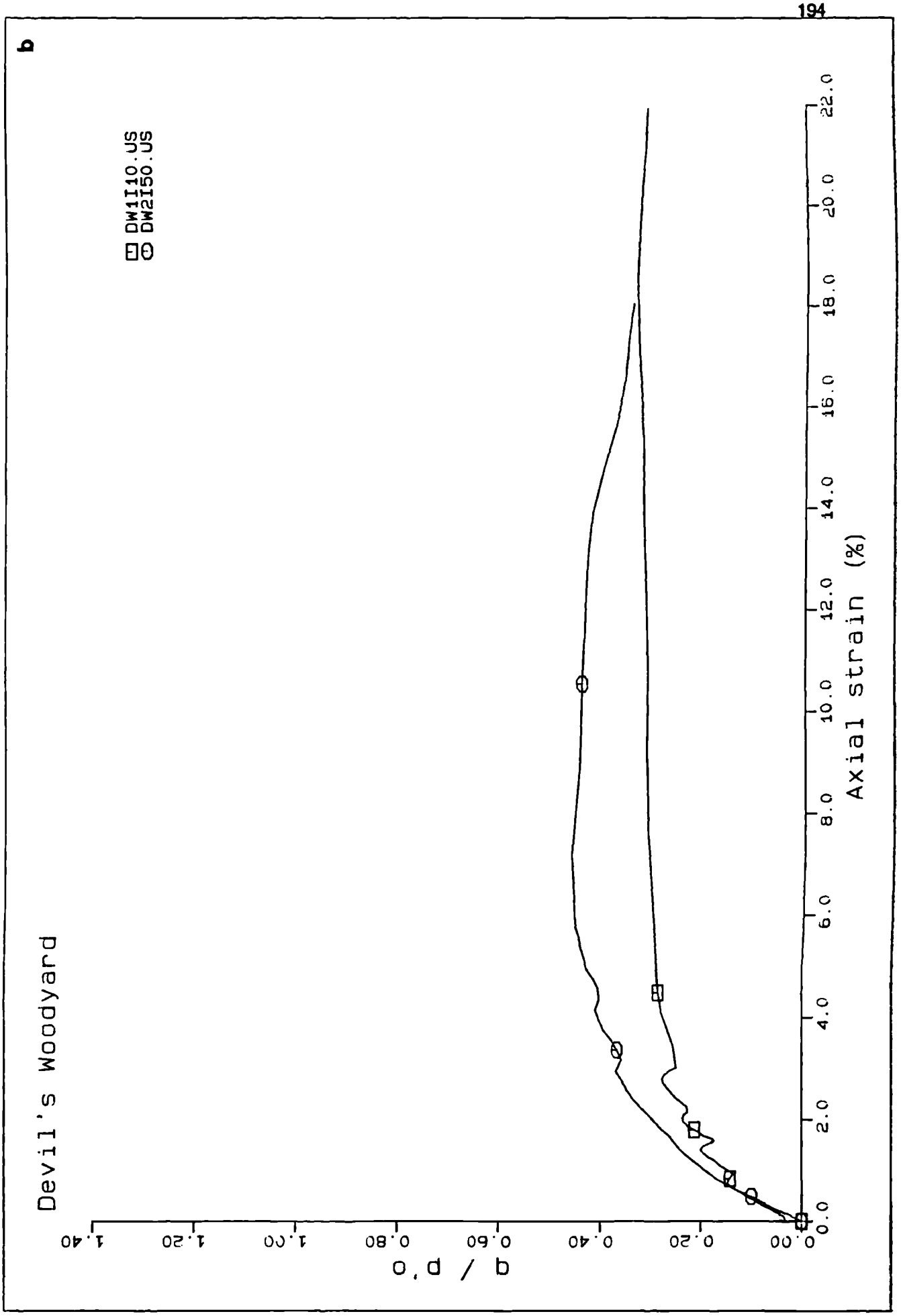
b
DW1I10.US
DW2I50.US
Devil's Woodyard
q / p'o
Axial strain (%)
0.00
0.20
0.40
0.60
0.80
1.00
1.20
1.40
0.0
2.0
4.0
6.0
8.0
10.0
12.0
14.0
16.0
18.0
20.0
22.0

was probably caused by the higher orientation of clay particles with higher stresses (Skempton, 1964; Tchalenko, 1968; Lupini et al, 1981).

There is therefore strong evidence that the behaviour of a sediment changes with increasing consolidation stress. This is further demonstrated in section b), using the pore pressure response data before the possible reasons for changing behaviour with increasing stress are discussed in section c), which concentrates mainly on failure mechanisms.

b) Effect of Stress Magnitude on Pore Pressure Response

As observed in the previous section, stress magnitude seemed to have an influence on pore pressure response. When the pore pressures are normalised with respect to p'_o, it is found that, generally, the higher the consolidation stress, the lower the normalised pore pressure response (fig. 7.12). The Lagon Bouffe series show that LB6I5 initially gives a higher response than LB1I50, although the former subsequently shows a more dramatic drop in pore pressure. LB2K25 and LB3K15 are identical and LB5K45 and LB4K60 give the lowest values respectively (fig. 7.12.a). In the Taiwan series, TFI5 gives the highest response, followed by TAI50, TDK15, TEK25 and TCK50 respectively, i.e. in order of increasing consolidation stress for the two consolidation paths (fig. 7.12.b). TD and TE have a very similar response, as do their respective equivalents in the Lagon Bouffe series, LB3 and LB2. Finally, DW1I10 gives a higher normalised pore pressure response than DW2I50 (fig. 7.12.c).

Values of (u_e / q), fig. 7.13, highlight the effect of stress magnitude on material behaviour, showing much better-defined differences in pore pressure response at different stress magnitudes. Samples consolidated anisotropically to mean effective stresses of 15 and 25 MPa gave distinctly different values of u_e / q to samples consolidated at 45 MPa or above for both the Lagon Bouffe and Taiwan materials. (Note that u_e / q is the same as the A-value for isotropic tests). As seen in figs. 7.7 and 7.8, the A and A' values give even more dramatic results. In the Lagon Bouffe test series, samples anisotropically consolidated to the higher stresses gave similar A' values to the isotropically consolidated sample LBI50 (fig. 7.8.a). In the Taiwan series, there was a less obvious change in A and A' response with increasing stress. The two isotropic tests normalised well, as did the anisotropic tests (fig. 7.8.b). The two Devil's Woodyard samples show similar A' responses (fig. 7.8.c).

This decrease of pore pressure response with stress magnitude is attributed to the dramatic decrease in voids ratio or porosity as the material consolidates. The response was particularly dramatic between 25 and 45 MPa for the silty Lagon Bouffe clay, and the more clay-rich Taiwan material. The relationship between voids ratios and effective stress in natural sediments is discussed in section 7.3.3.

c) Failure

It has been demonstrated that all three clays, particularly the Lagon Bouffe clay, are dependent on stress magnitude in their behaviour during undrained shear. It is therefore to be expected that the mode of failure may show the same trend.

The Lagon Bouffe test series shows the most dramatic effect, where two changes in behaviour are observed with increasing stress. LB6I5, the sample consolidated to the lowest stress "dilates" at failure.

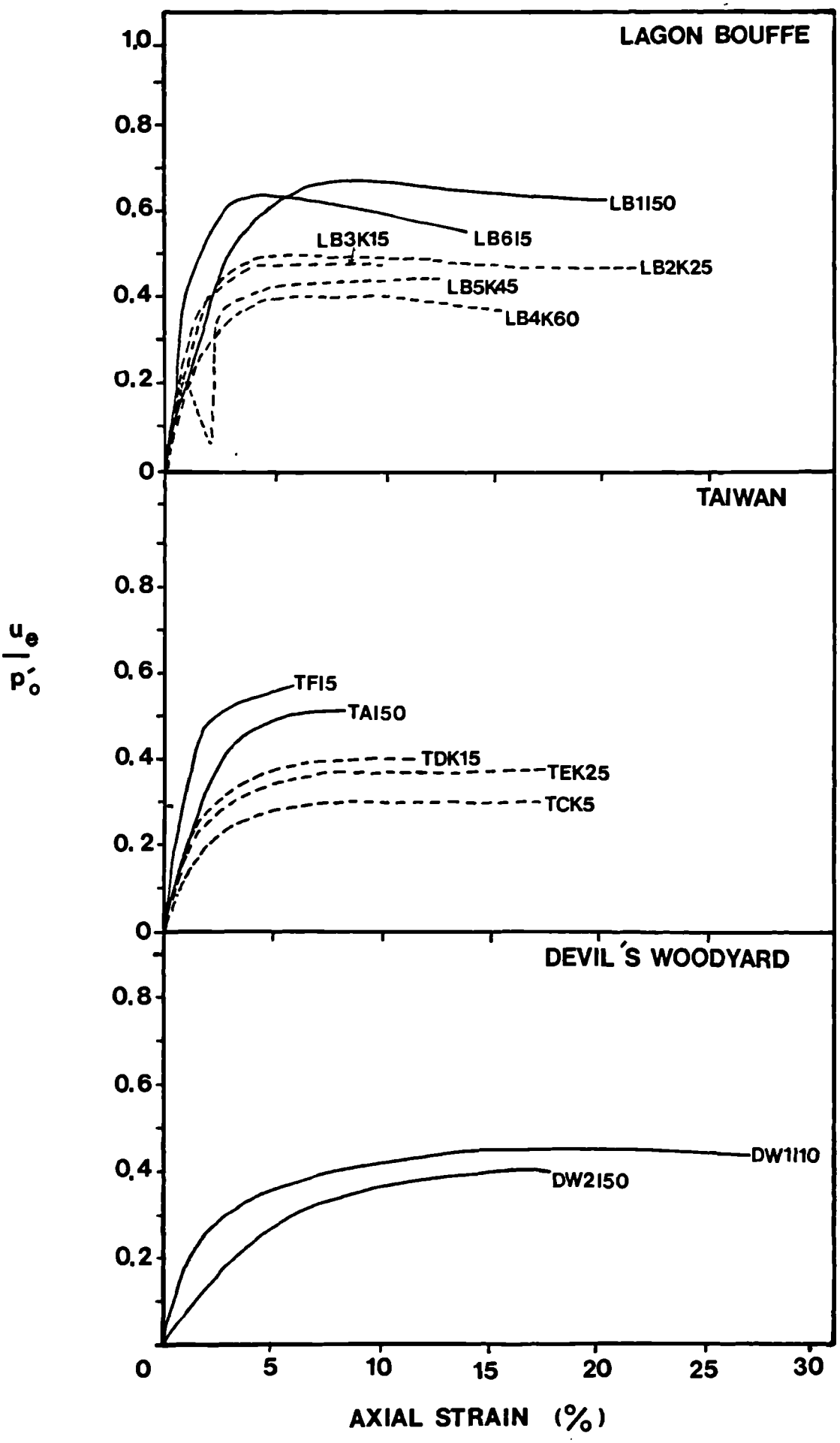

Fig. 7.12 Normalised pore pressure-strain curves for all the tests. a. Lagon Bouffe; b. Taiwan; c. Devil's Woodyard

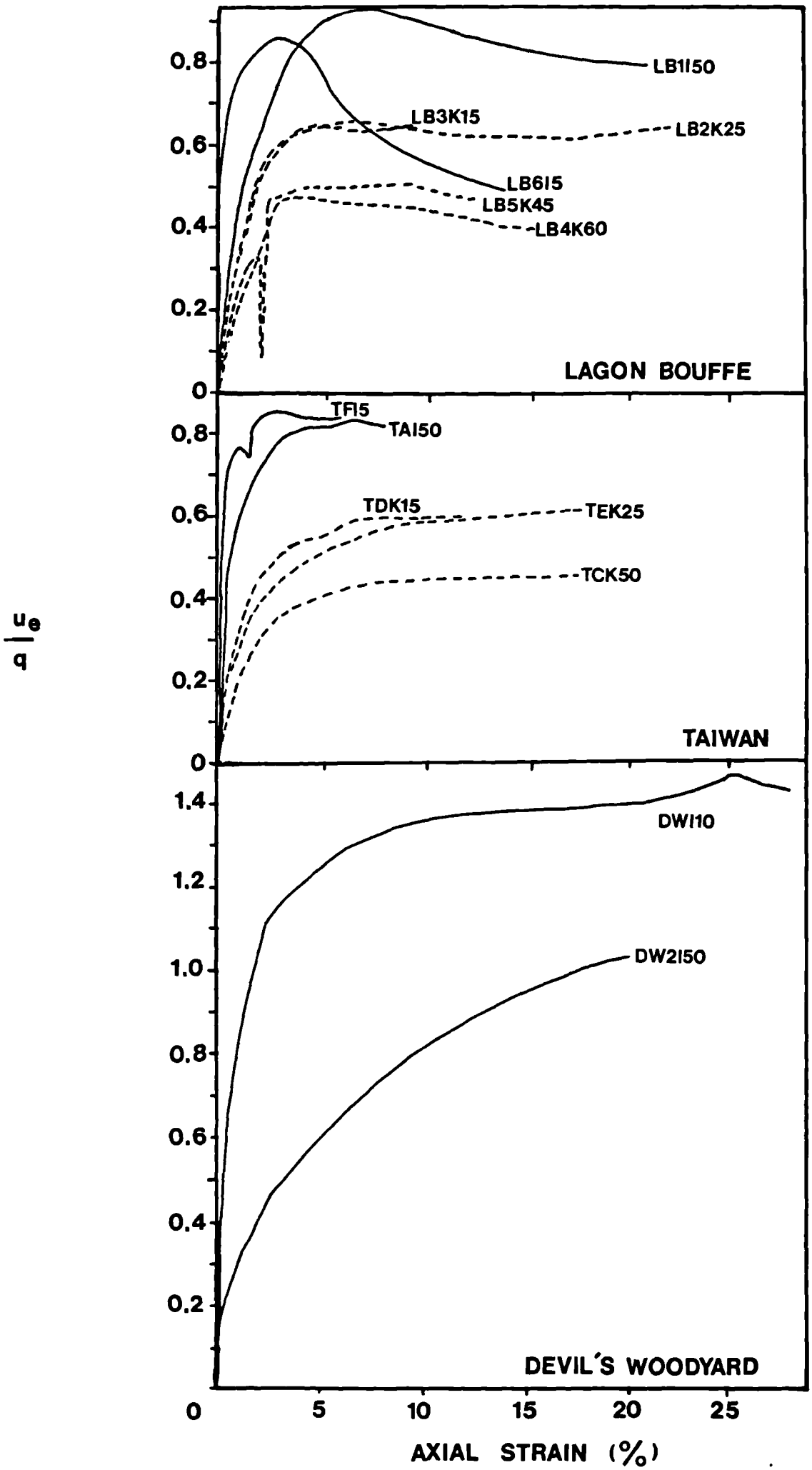

Fig. 7.13 Values of u_e/q vs. axial strain for all the tests. a. Lagon Bouffe; b. Taiwan; c. Devil's Woodyard

LB3K15 and LB2K25 reach "critical state" in that they continue to deform at constant effective stresses, and LB5K45, LB1150 and LB4K60, consolidated to higher stresses, show "dilatant" behaviour again at failure (fig. 6.10). Dilatancy is attributed to the large proportion of granular particles in the Lagon Bouffe material, as it is associated with dense sands at low effective stresses (Lee and Seed, 1967; Lambe and Whitman, 1979). It is thought, however, that with increasing consolidation stress, particle crushing becomes predominant in a granular material (Lee and Farhoomand, 1967), and this crushing overcomes any tendency in the material to dilate (Lee and Seed, 1967; Skinner, 1975). The change in behaviour from dilatant to non- dilatant has been observed by Skinner (1975) on the loose Ham River Sand, consolidated to 500 - 1000 psi (3.5 - 7 MPa), (see also Bishop et al, 1965). Particle crushing generated excess pore fluid pressures, causing the sand to fail in a manner similar to the breakdown of the structure of sensitive clays (Bjerrum, 1954) and chalk (Leddra, 1989). In one test, the A-value at peak deviatoric stress was in excess of 1, increasing to 1.8 by the end of the test (fig. 7.5). LB3K15 and LB2K25 did not seem to be associated with particle crushing (plate 7.1, c-d), but their behaviour may indicate that the collapse of the soil structure during undrained shear overcomes any tendency of the material to dilate, so that failure is more similar to the "contractant" mode observed by Skinner; the same behaviour was also observed by Been and Jeffries (1985), see below.

Particle crushing becomes apparent with increasing consolidation stress in the Lagon Bouffe material (plate 7.1, e-h), and correlates with dilatant behaviour at failure; it therefore seems to be associated with different undrained shear behaviour to that observed by Skinner (1975). The cracks are parallel to the direction of the greatest principal stress, and typically go through several large grains in contact with each other (plate 7.1.h). There is also evidence that the material stiffens considerably with increasing consolidation stress, as shown by the stress-strain curves for the anisotropically consolidated samples (figs. 6.4 and 6.8). Why, then, does this change in mode of failure occur between consolidation stresses of 25 MPa and 45 MPa? Johnston and Novello (1985) suggest that crack propagation causes a decrease in pore fluid pressures. The fracture model proposed by the authors combines critical state concepts with the Griffith crack criterion to explain the dilatant failure of the Melbourne mudstone in the undrained shear triaxial experiments. The experiments were undertaken by Chiu and Johnston (1984). In order to account for the constant volume during the undrained shear test, Johnston and Novello assume that when cracks begin to propagate in the mudstone the "intact material" drains into the cracks which causes a reduction in the volume of the intact material equivalent to that of the cracks, and a corresponding decrease in the pore fluid pressure. It is difficult, however, to see how the material could dissipate excess pore fluids into the cracks. It is more likely that, at high stresses, and with very low voids ratios, materials do not obey the "constant volume" rule, and that crack propagation causes the dense material to expand slightly, thus dissipating some of the excess pore pressures at failure. This effect could not be investigated because of the limitations of the equipment used; internal strain gauges are needed to monitor changes in the sample shape as it deforms.

An interesting point to note here is the effect of particle crushing on the particle size distribution of a sediment. Lee and Farhoomand (1967) and Skinner (1975) found that the action of shear on granular materials caused considerable "flattening" of the particle size distribution curves due to increasing fines. This may partly explain the uniform distributions observed for all the mud volcano clays, particularly from Trinidad (section 4.2). It may also be the reason for the low plasticity indices obtained for all the samples despite the high clay content of most (section 4.5). If the materials extruded by mud volcanoes have undergone crushing, it is very important to understand the state of the parent bed both before and after deformation. Unfortunately, this was could not be investigated further in this work.

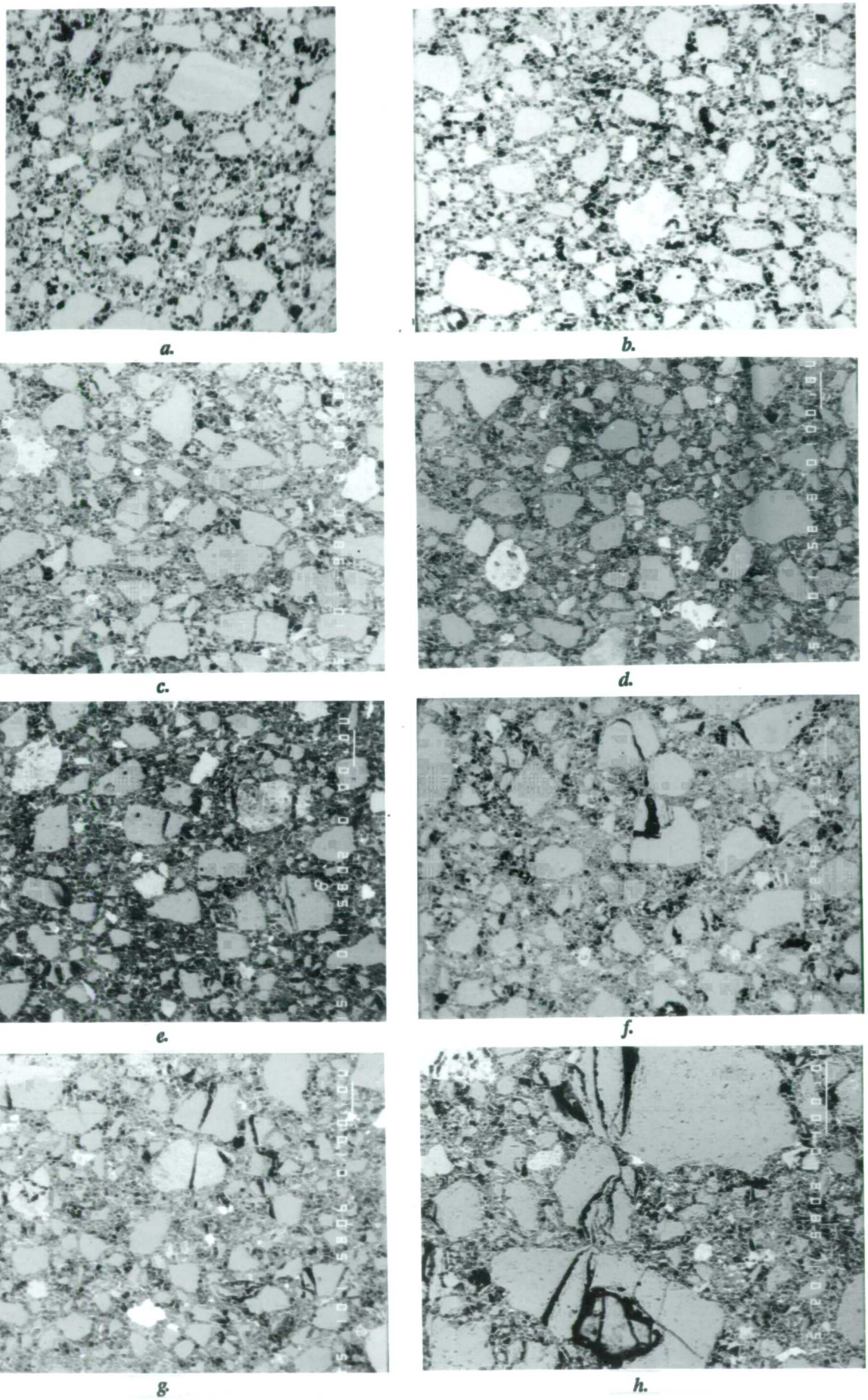

Plate 7.1 Backscatter SEM photographs of the Lagon Bouffe samples before and after testing, showing particle crushing with increasing consolidation stress: a. before testing; b. LB6I5, showing quartz grains in calcite cement (near centre); c. LB3K15; d. LB2K25; e. LB5K45; f. LB1I50; g. LB4K60; h. LB4K60, showing crack going through three grains; (scale bar = 100u).

Addis (1987) and Leddra (1989) conducted undrained shear experiments on chalk consolidated up to a p' of 60 MPa (fig. 7.14.a). The results were combined and they were found to be very compatible, falling on the same failure line (Leddra and Jones, 1989); no distinct failure plane had been observed by Addis (1987). The chalks showed a change from "contractant" to "dilatant" behaviour with increasing stresses. The change in behaviour was attributed to the yield point of the chalk, beyond which the material behaves in a plastic, granular fashion. When the chalk was consolidated to a point within its elastic region, its undrained shear behaviour reflected the breakdown of cement bonds, with associated loss of strength and dramatic pore pressure increase, in a manner very similar to liquefied sands and sensitive clays (see section 7.3), Leddra (pers. comm., 1988). The high pore pressure response associated with the breakdown of the chalk cement was also observed by Addis (1987) in the high pressure oedometer, where the C-value (section 5.2.6) reached a value of 2, i.e. twice the increment of vertical stress.

The changes in behaviour observed in both the Lagon Bouffe test series are very comparable to similar observation for sands at low stress (Been and Jeffries, 1985) and chalk at high stress (Leddra and Jones, 1989). Been and Jeffries conducted experiments on the Kogyuk sand and found that the behaviour changed from dilatant, to contractant, and back to dilatant with increasing stress (fig. 7.14.b).

The Taiwan material is less sensitive to stress magnitude than the Lagon Bouffe material, as shown by the normalised stress paths (fig. 7.10.a), but different modes of failure are again observed with increasing consolidation stress for the anisotropically consolidated samples: TFK15 fails in a "critical state" manner, whereas TEK25 and TCK5 fail in a "contractant" manner. The two isotropically consolidated samples fail in a "critical state" manner. The behaviour at higher pressures could be explained by increased particle orientation, where the material tries to behave in a "brittle" manner, but is prevented from doing so by the presence of the coarser particles (see section 7.2.4).

Again, the two Devil's Woodyard samples fail differently; DW1 attains "critical state", whereas, DW2 fails in a "brittle" manner, showing a drop in strength. The change in behaviour for the two Devil's Woodyard samples could be due partly to stress magnitude and partly to preparation procedure. Because the material is very clay-rich, particle orientation predominated at higher stresses (Skempton, 1964; Tchalenko, 1968; see also section 7.2.4).

The slope of the failure line in stress space decreased slightly with higher stresses for all three materials, as observed in the previous chapter. This is another indication that the behaviour changes with increasing stress.

There is therefore a strong indication that the consolidation stress magnitude, which largely controls the porosity, has a great effect on the manner in which a material behaves. Although the stress paths were found to normalise reasonably well, especially for the Taiwan materials, the pore pressure response decreased noticeably as consolidation stresses increased, with associated changes in failure mechanisms. Behaviour leading to sedimentary volcanism is not seen to be associated with the higher stresses (45 MPa), particularly where materials dilate at failure - rather with the lower range of stresses, where pore pressure response was high and where failure was associated with constant or decreasing effective stresses with continuing strain.

Fig. 7.14 Contractant and dilatant behaviour during undrained shear. a. Chalk results by Leddra (1989) and Addis (1987); b. Kogyuk sand results by Been and Jeffries (1985).

7.2.4. Effect of Clay Plasticity on Undrained Shear Behaviour

The results in Chapter 4 have shown that the Lagon Bouffe clay is the siltiest of the clays, with a plasticity index of 8%. The Devil's Woodyard clay has the highest clay content of the three with a plasticity index of 34%; the Taiwan clay has an average plasticity index of 13% (table 4.7). The results presented in Chapter 6 and discussed above show that there are considerable differences between the three materials.

Equivalent tests have been carried out on the three materials for direct comparison. LB1, TA and DW2 were all consolidated isotropically to a p' of 50 MPa; LB6 and TF were consolidated isotropically to 5 MPa; LB2 and TE were consolidated anisotropically to 25 MPa and LB3 and TD were consolidated anisotropically to 15 MPa. These are compared in figs. 7.15 to 7.18. As observed in Chapter 6, the strongest material is the Lagon Bouffe clay, and the Devil's Woodyard clay is the weakest. The former material also generates higher pore fluid pressure before reaching failure. The undrained stress paths are similar in the initial stages of undrained shear, especially for the isotropically consolidated samples (figs. 7.15.a and 7.18.a). Note the nearly identical behaviour of LB6 and TF before failure (fig. 7.18.a).

This greater strength of the Lagon Bouffe clays is to be expected, as the more silty a material is, the lower the voids ratio for a given effective stress, and the lower the voids ratio, the stronger the material becomes as the grains interlock further. The relationship between voids ratio and mean effective stress established for the three materials has shown that the Lagon Bouffe clays are the least compressible, with the lowest voids ratios for the same effective stress.

The pore pressure response A is highest for the Devil's Woodyard clays (fig. 7.7), exceeding 1 for isotropically consolidated samples. The Lagon Bouffe and Taiwan clays have similar A-values ($\zeta_{<1}$), the latter generally giving slightly higher values.

We have also seen that the three materials showed different modes of failure. The siltiest material, Lagon Bouffe was not very sensitive to stress path, at least, at the higher stresses, but showed great sensitivity to stress magnitude in its behaviour, whereas the Taiwan material was very dependent on stress path, less so on stress magnitude, although changes in pore pressure response and mode of failure were observed at higher stresses. The Devil's Woodyard material was very sensitive to preparation procedure, and the two samples behaved very differently during undrained shear, although they failed on the same point in normalised stress space (fig. 7.11.a) and they both developed polished shear planes (plate 6.1). These differences in behaviour with increasing plasticity are explained by the influence of clay particles. It was observed by Lupini et al (1981) that the drained shear behaviour of a cohesive soil was influenced by decreasing interparticle friction, usually aided by increasing proportions of platy minerals (provided they have low interparticle friction) and decreasing contact of rotund particles. Modes of shearing changed from turbulent shear to sliding shear with decreasing interparticle friction. The Lagon Bouffe material, would be expected to behave in a turbulent fashion, and the Devil's Woodyard clay showed evidence of sliding shear in that preferred orientation of clay minerals became evident on the shear surface at failure (plate 6.1). The Taiwan material probably experienced transitional modes between the two types of shear. It should also be noted that the effect of high stresses will cause grain crushing in addition to these two shear mechanisms and would probably be more influential in sediments with more granular particles (Lee and Farhoomand, 1967).

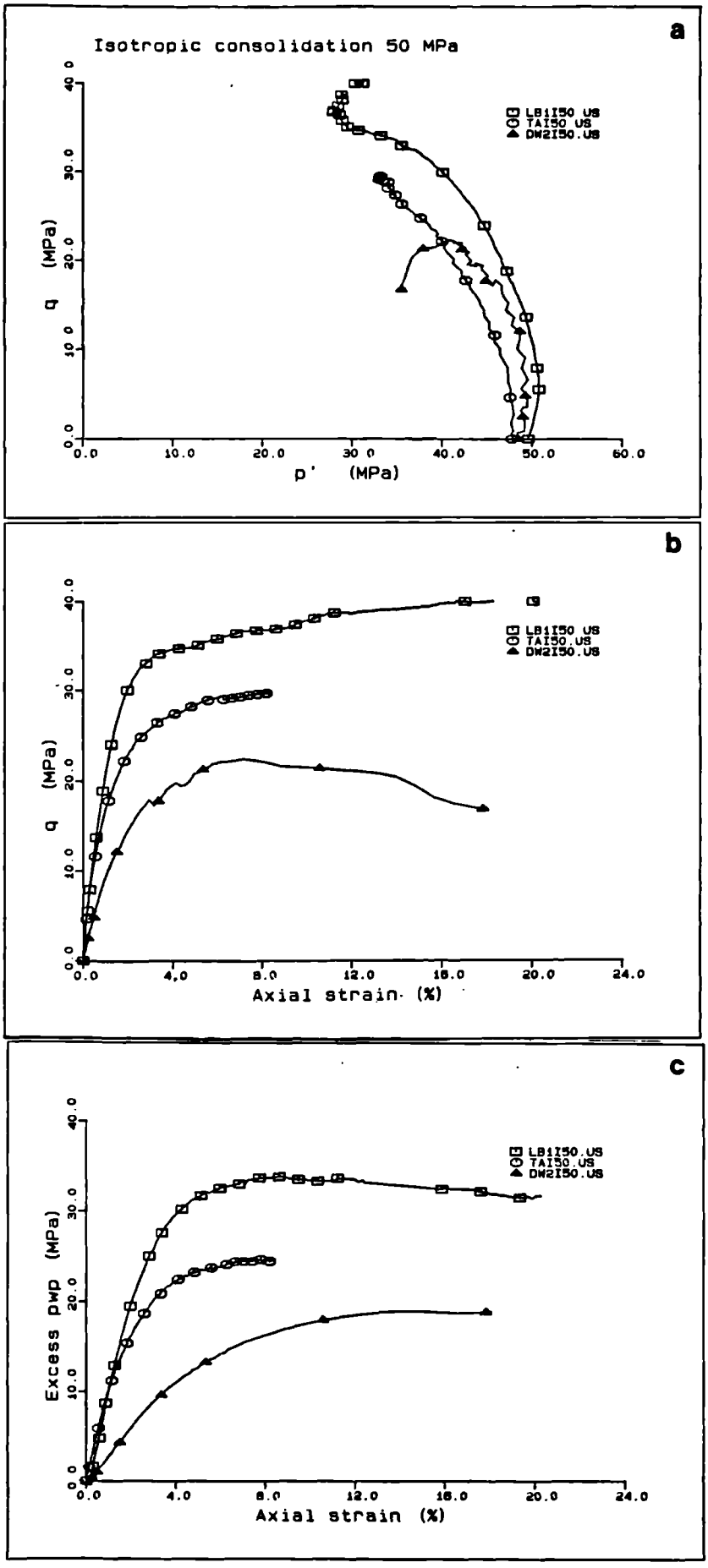

Fig. 7.15 Comparisons between LB1I50, TAI50 and DW2I50. a. stress path; b. stress-strain; c. pore pressure-strain

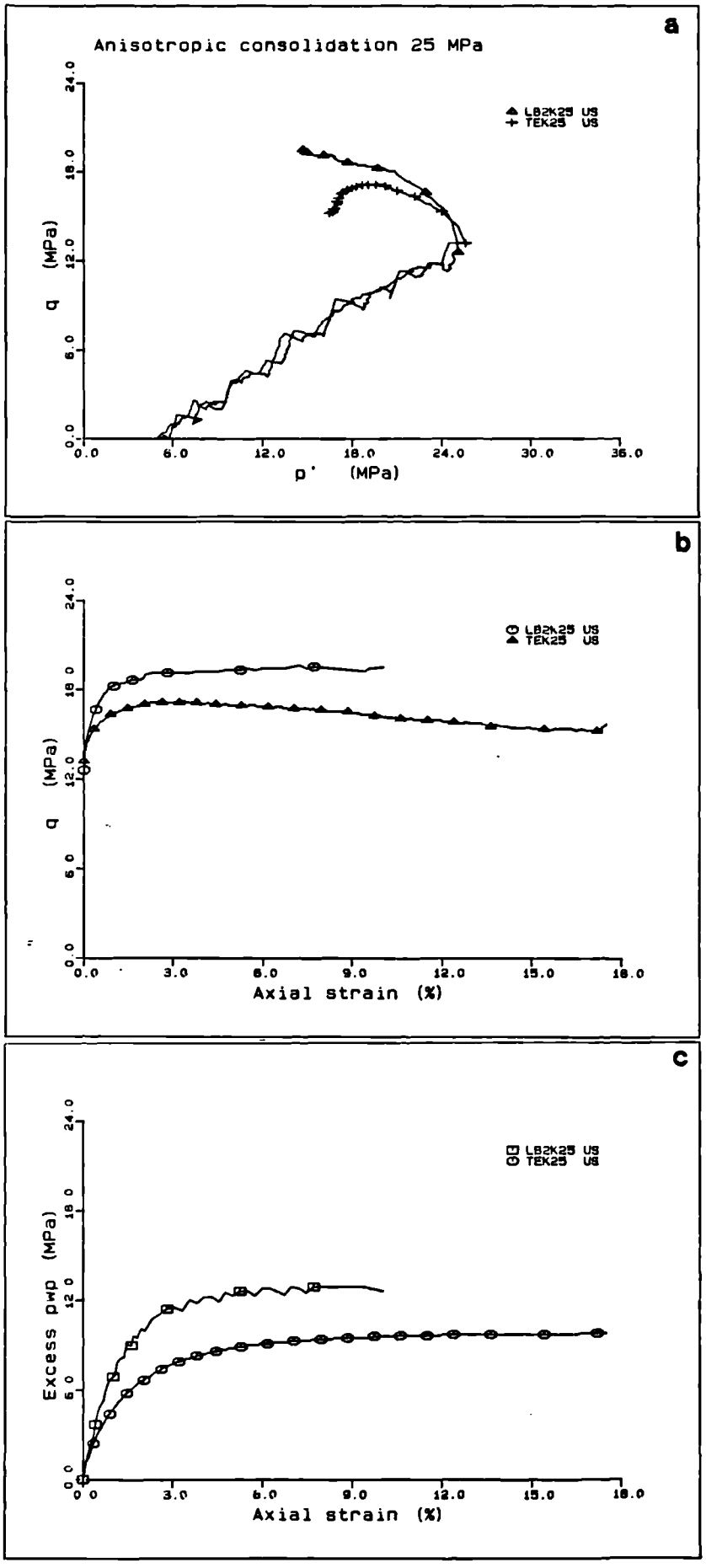

Fig. 7.16 Comparisons between LB2K25 and TEK25. a. stress path; b. stress-strain; c. pore pressure-strain

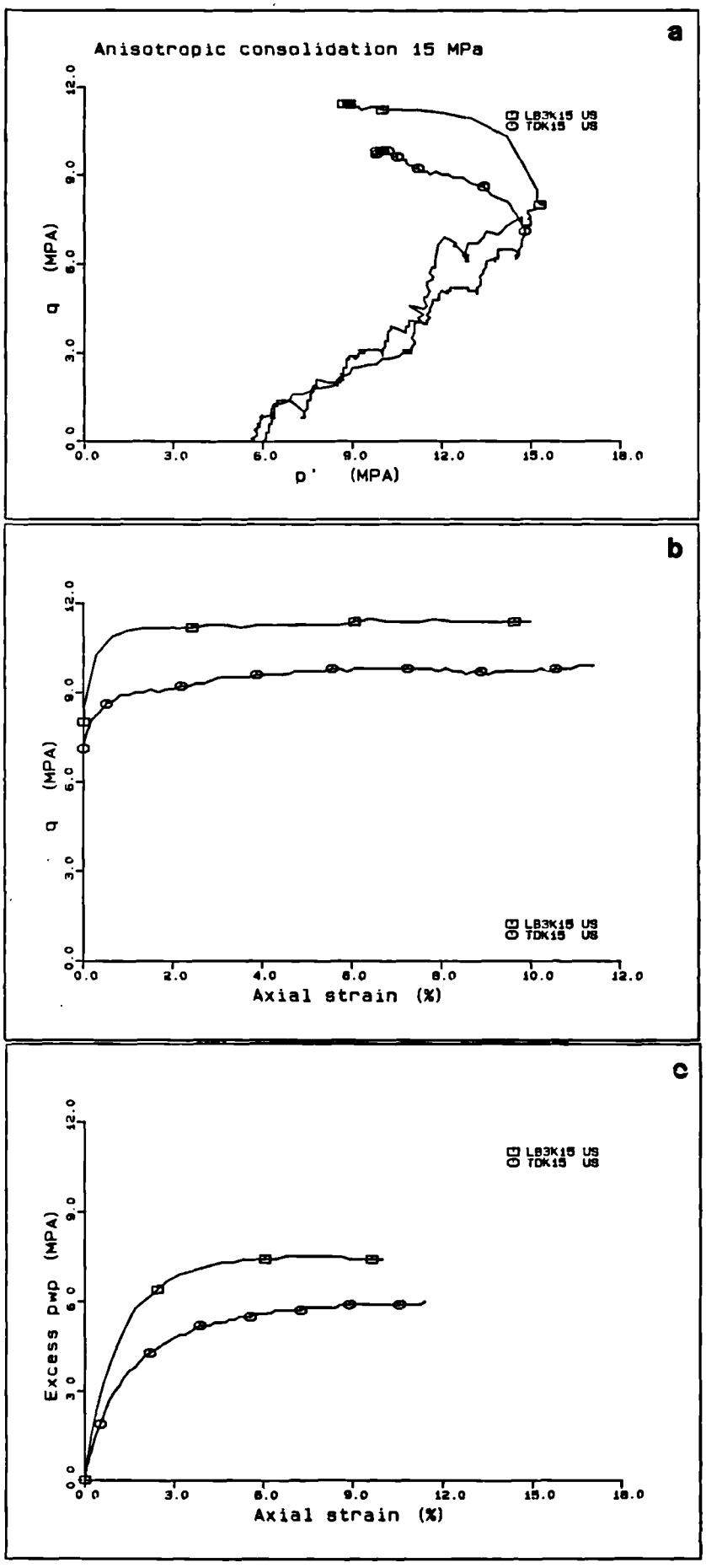

Fig. 7.17 Comparisons between LB3K15 and TDK15. a. stress path; b. stress-strain; c. pore pressure-strain

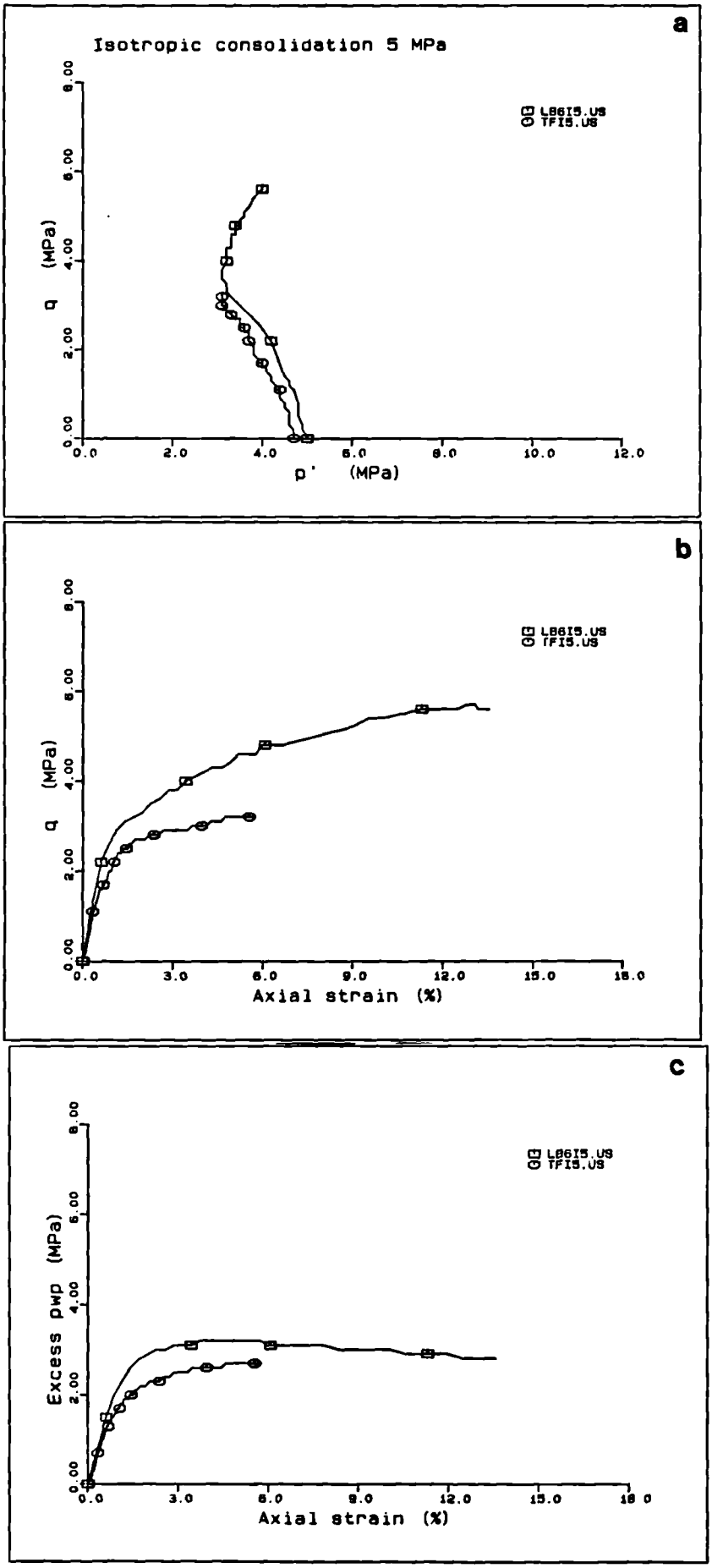

Fig. 7.18 Comparisons between LB6I5 and TFI5. a. stress path; b. stress-strain; c. pore pressure-strain

7.2.5. Summary

The strength of the mud volcano clays subjected to high pressure triaxial compression is therefore found to be affected by,

- **anisotropy in consolidation path. This is particularly reflected by pore pressure response (A and A'); anisotropically consolidated samples had higher responses than isotropically consolidated samples;**

- **stress magnitude; the greater the stress, the stronger the sample, and the lower its pore pressure response A, particularly for anisotropically consolidated samples. Different failure mechanisms were also observed at the higher stresses;**

- **clay plasticity; the higher the plasticity, the higher the pore pressure response and the greater the tendency for particle orientation during shear.**

It has also been demonstrated that shear stresses produce excess pore fluid pressures in an undrained, normally consolidated sediment - even when it is fully consolidated to a high effective stress. This, of course, is a well-known phenomenon in low pressure soil mechanics and is related to volume loss during drained shear (section 5.2.5).

7.3. OTHER FACTORS AFFECTING SEDIMENT BEHAVIOUR IN A MUD VOLCANO ENVIRONMENT

7.3.1. Introduction

It should be appreciated that the experiments carried out on the mud volcano clays were directed at understanding the undrained shear behaviour of clays of different plasticity, normally consolidated to high pressures, rather than modelling sedimentary volcanism. Several conditions in the natural environment were not satisfied by the experiments, four of which are discussed below:

- **The natural burial and consolidation history in the tectonic environment was probably very complex, changing to higher values of stress ratio (K) with depth as tectonic stresses became more felt.**

- **The material was sampled in a naturally remoulded state, but it is highly unlikely that it was in this state at depth. It is suggested that the natural material is very likely to be cemented.**

- **σ_1' in the experiments was vertical, i.e., perpendicular to particle orientation in the sample. In an area of tectonic compression, σ_1' is more likely to be horizontal, i.e., parallel to the "bedding" at the onset of deformation. Also, the sediments are more**

likely to be loaded in an intermittent manner, as opposed to a constant rate of strain, possibly experiencing reversal of principal stresses. This is particularly the case in the presence of earthquake activity.

These aspects are discussed here in the light of this experimental study, and others conducted on similar materials at low pressure.

7.3.2. Consolidation Path in a Mud Volcano Area

It was observed above that consolidation path could have a great effect on undrained shear behaviour. The finding of workers such as Skinner (1975), Gens (1982), Jardine (1985) support the view that greater structural anisotropy causes greater loss in strength, with associated pore pressure increase. Fig. 7.6.b showed experimental results obtained by Gens for samples anisotropically consolidated at different K-ratios, the lowest being 0.4.

It is difficult to judge what the natural consolidation path of mud volcano material is. It is always assumed that, in a stable sedimentary basin, there is little or no lateral deformation during consolidation and therefore the consolidation path follows K_o (Jones and Addis, 1986; Addis, 1987). Karig (1986) models the stress path of sediments deforming in an accretionary complex (favourable for sedimentary volcanism, as discussed in Chapter 2) on this K_o path, consolidation being followed by undrained shear, much in the manner of this study. In an area of tectonic compression, however, it is difficult to see how the sediment could consolidate under K_o conditions. Unfortunately, it was not possible, in the course of this study, to obtain values of horizontal stresses acting on sediments with depth in areas of tectonic compression, but it is felt by the author that the K ratio probably increases with depth until a rotation of the principal stresses occurs (fig. 7.19; also see section 7.3.4 below). This is observed by Hottman et al (1979) in sediments offshore Alaska, where shallow extensional structures gave way to compressional structures with greater depth (section 2.2.2). If consolidation continues at depth, the sediment could experience a type of "unloading" of deviatoric stress (fig. 7.19). In that case, its undrained shear behaviour is different to a sediment normally consolidated at a constant K-ratio to the same stress. This is implied by the results in this study, where the samples showed dependence on stress path in their undrained shear behaviour. Gens (1982) proves this point by an elaborate experimental programme whereby equivalent samples of the Lower Cromer Till are subjected to different stress histories before undrained shear at the same effective stress. In the case of the samples which experienced decreasing deviatoric stresses during consolidation, the samples behaved in a more brittle manner than that expected of samples which had undergone isotropic consolidation (see fig. 7.19.b); this was attributed to the fact that a sediment will "remember" its early burial history, which affects its subsequent undrained shear behaviour, especially when it is unloaded during consolidation (see section 7.2.3 above).

The consolidation history of the sediment is very likely to be further complicated by rapid sedimentation and associated underconsolidation. It was mentioned in Chapter 2 that overpressured clays were usually associated with low densities, and low equivalent depths (z_e), Chapman (1972). The negative gravity anomalies observed in the southeast Taiwan mud volcano area and over some of the Trinidad mud volcanoes, such as Moruga Bouffe (sections 3.2.5) are most likely to be related to low density

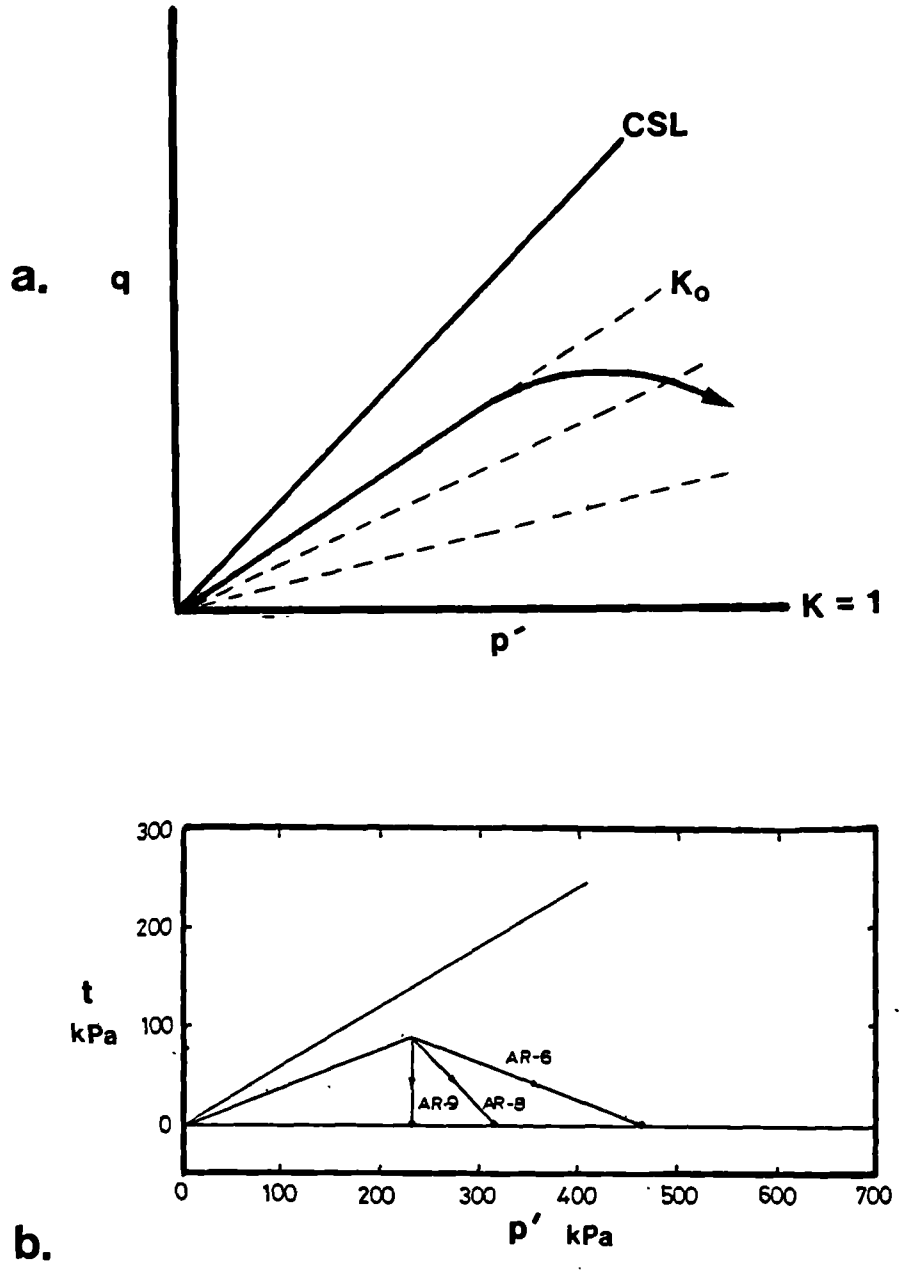

Image removed due to third party copyright

Fig. 7.19 Changing principal stresses during consolidation and burial in an area of tectonic compression. a. schematic illustration; b. results by Gens (1982) showing effect of unloading of deviatoric stresses on the behaviour of the Lower Cromer Till; (p'_e is the value of p' for the same voids ratio on the isotropic consolidation line)

material (section 1.2.11). Low density overpressured clays were also observed in the Trinidad logs published by Higgins, 1959 (section 3.2.4), but it was difficult to quantify in-situ voids ratios without access to detailed log data.

If underconsolidation takes place, and assuming that the principle of effective stress still applies, the sediment will only "remember" its early consolidation history, so that its undrained shear behaviour will be dependent only on its early stress path and the maximum effective stress the sediment had been consolidated to. This is because the porosity of the sediment is too high for its depth of burial and it would be expected to behave in a manner similar to a material fully consolidated to the same value of effective stress. The next section will discuss the importance of the concept of high porosity at depth in terms of possible modes of failure leading to mud volcanoes.

7.3.3. Natural Voids Ratios and Cements

The natural state of the parent bed would be expected to be very different from the "remoulded" state of the extruded muds. As the porosity of a sediment is one of the key factors in governing its behaviour, it is very important to understand the relationship between porosity and effective stress in nature.

Experimental studies on the behaviour of soft sediments can never model the natural behaviour of the sediments, especially if the material is in a "remoulded", slurry state. Section 7.2.3 discussed the volume loss relationship with effective stress as examined in the laboratory. Skempton (1943) recognised that not only are natural voids ratios higher than laboratory-determined voids ratios, but natural materials tested in the laboratory have higher voids ratios than remoulded materials for the same effective stress. The reason given for this is that, in nature, particle arrangement and natural cementation produce an open structure which is destroyed by remoulding and/or fast laboratory consolidation experiments. The open structure can survive considerable effective stresses (Leroueil and Vaughan, 1989).

The destruction of clay cement at shallow depths is known to produce a dramatic collapse of structure and decrease in strength. This is quantified by the term "sensitivity", which is the ratio of undisturbed to remoulded strength (with no change in water content); the stresses initially sustained by the mineral skeleton are transferred to the pore water (Lambe and Whitman, 1979; fig. 7.20). Quick clays, with a sensitivity of 8, collapse completely and liquefy when subjected to loads high enough to destroy the bonds between the particles which then flow with zero strength, causing major failure phenomena, such as landslides (Bjerrum, 1954).

Perhaps more realistically for the stress range expected in a mud volcano environment, Ohtsuki et al (1981) report a silty mudstone from Japan with a voids ratio of 1.4 and a pre- consolidation pressure (maximum effective stress it had undergone) of 5 MPa - this is a very open structure when compared with equivalent values in the laboratory (Leroueil and Vaughan, 1989; see also voids ratios of the three mud volcano clays at 5 MPa). The undrained shear behaviour was very dramatic, showing very "contractant" behaviour (decreasing p' and q at failure). Their results are very similar to those obtained by Leddra (1989) from high pressure undrained shear experiments on chalk (fig. 7.14.a) which show dramatic undrained shear behaviour at the lower stress range, associated with the yield point of the chalk (fig. 7.14). The chalk samples looked like putty at the end of the test (Leddra, pers. comm., 1988).

Fig. 7.20 Schematic representation of transfer of load form the sediment skeleton to the pore fluids during structural breakdown (after Lambe and Whitman, 1979)

This dramatic loss of strength is associated with the breakdown of the cements during shear; naturally, the pore pressures generated were very large. Samples allowed to consolidate to higher effective stresses, to well beyond the yield point of the chalk (Addis, 1987; Leddra, 1989) did not show this type of behaviour, and, in fact, dilated after failure in the manner shown by the Lagon Bouffe samples at higher stresses (see figs. 7.9.a).

It is not suggested here that the sediments responsible for sedimentary volcanism are quick clays, or chalks. However, evidence points to the fact that cementation and consolidation in nature will produce a more open structure than those predicted by laboratory work. SEM work on the Lagon Bouffe samples has, in fact, shown evidence of calcite cementation around the silt particles, which collectively act as larger sand grains (plate 7.1.b). Also, the samples consolidated to the lower stresses produced higher A-values, some showing increasing pore pressures with no increase, or even decreasing q. It is likely, therefore, that a natural sample would be able to sustain higher effective stresses with the same voids ratio, possibly showing more dramatic "contractant" behaviour during undrained shear. Unfortunately, it was not possible to explore this in the experimental work due to unavailability of source bed material. However, it may be deduced that this dramatic loss of strength will not be expected at the high consolidation stresses, where voids ratios become very small and the structure of the sediment very "packed", as discussed in section 7.2.3.

7.3.4. Principal Stress Orientation in Areas of Tectonic Compression

The stress orientation in the experiments does not model that in an area of tectonic compression. The samples are loaded vertically in the experiments, i.e., perpendicular to particle orientation in the sample. In reality, it is expected that the greatest principal stress will be acting parallel to the "bedding" of the sediments. As most materials are far from isotropic, as demonstrated in section 7.2.2, it would be expected that their undrained shear behaviour in extension would be different to that in compression. This has been explored by many workers (eg. Parry, 1971; Roscoe and Burland, 1968; Jardine, 1985; Gens, 1982 and Atkinson et al, 1987). Opinions vary as to whether the failure envelope in compression is similar to that in extension. There is evidence that the strength of a sample anisotropically consolidated to a certain effective stress will, in fact, be weaker in extension, with much higher associated pore fluid pressures (Gens, 1982; Jardine, 1985). The change in deviatoric stress required to reach failure from the K_o state is, however, much greater. Hight et al (1987) showed evidence that the difference in behaviour in extension and compression decreased with increasing plasticity (fig. 7.21).

It is worth noting that diapiric behaviour is observed in deltaic sediments (section 2.2.2), where σ_1 is vertical (or near-vertical), i.e., perpendicular or at angles to particle orientation in the sediments, which is closer to the stress system in the triaxial compression experiments. These sediments are subjected to very high shear stresses due to the geometry of the delta, where differential loading occurs between the thick sediments of the delta and the thinner sediments at the toe (section 2.3.1.b). Again, shear deformations occur in the undrained state because of the rapid deposition of low permeability materials. It is therefore possible to achieve the same type of failure in two different stress regimes.

Fig. 7.21 Comparison of undrained shear strength by compression and extension for different plasticity clays (from Hight et al, 1987)

Another aspect of the stress system in a tectonically active area, briefly explored in the experimental programme, is the influence of earthquake activity, which is common in mud volcano areas (table 1.2). This has been extensively modelled in soil mechanics by means of cyclic loading tests, where the stresses are cyclically decreased and increased to model the effect of earthquake shocks on sediments. Several workers have conducted cyclic loading tests on clays (eg. Andersen et al, 1980; Takahashi, 1981; Lewin, 1985; Kamhawi, 1985). The effect of cyclic loading is to produce a permanent excess pore pressure after each cycle until, eventually, sufficient pore pressures can build up, causing the sediment to fail; the larger the amplitude of the cycles, the fewer the cycles needed to reach failure (Takahashi, 1981). The failure of loose sands is very dramatic, where liquefaction occurs, with associated permanent pore pressures and total loss of strength (Seed and Lee, 1966), similar to the failure of quick clays and to the chalk results in fig. 7.14.a. Skinner (1975) found that undrained unloading of the Ham River sand after failure caused the pore pressures to increase dramatically, and the effective stresses approach zero. Dense clays may not produce the same dramatic results as sand, but they still register permanent pore pressures, as observed in test TGCY30 (sections 6.2.3 and 6.3.3). Undrained cyclic loading of a clay with a relatively open structure would serve to cause the collapse of this structure, with associated pore pressure increase.

Cyclic loading is very likely to occur in areas adjacent to a large active fault, such as the Los Bajos Fault in southern Trinidad (fig. 3.4), even where no major earthquake activity occurs. Movements along the fault would deform adjacent sediments in an intermittent, "slip-stick" manner, which could cause the loading-unloading of the bed.

7.4. THE ORIGIN OF MUD VOLCANOES

7.4.1. Introduction

This study has incorporated a geological field and laboratory investigation of mud volcano clays with an experimental programme aimed at understanding the behaviour of the muds. This section will apply the findings in this study to the geological environment, combining the experimental results with field observations. Particular attention is paid to the origin of overpressuring which will greatly affect the behaviour of the sediment, and to the role of tectonic activity in failing and extruding the materials.

7.4.2. Overpressuring of Mud Volcano Clays

Mud volcanoes are closely associated with geologically dynamic areas, where very rapid sedimentation combines with continuous tectonic activity. It was shown in Chapter 3 that both study areas have experienced periods of structural deformation and associated thick sedimentary deposits. The thickness of the Pliocene sequence in the Tainan area, southwest Taiwan, for example, is 5 km. Such an environment of very rapid sedimentation which continues for long periods of time will enhance

underconsolidation. The slump deposits observed in both areas indicate slides, probably triggered by tectonic activity; these would induce sudden loading of the underlying deposits, so that their pore fluid pressures would increase. If the sediments are trapped and cannot lose their excess pore fluid pressures they would become underconsolidated with burial, even if they had been fully consolidated prior to the sudden loading. The permeability in the drainage boundaries decreases, preserving high voids ratios in the sediment, probably enhanced by cementation.

There is very little evidence of the natural state of the parent bed, but section 3.2.4 described some of the conditions encountered whilst drilling through overpressured clays in Trinidad. One formation oozed out like toothpaste, and another produced high density, but highly overpressured muds. This suggests that the state of the parent bed can vary considerably. It is not very likely that the parent bed can be as "wet" as toothpaste throughout - otherwise the value of λ would not be less than 1, but highly underconsolidated mud may occur as "pockets" within a higher density sequence. It should also be remembered that mud will pick up considerable quantities of water on its way up to the surface, so that its water content will not be representative of the parent bed. This is supported by the findings in the Anglais Point mud volcano. Section 3.2.5 described the presence of small broken mudstone clasts in the matrix which were identical in colour and mineralogy to the matrix (section 4.2.3), implying that the source material was broken up by fluids on its way to the surface. Nevertheless, low density clays are observed, such as those encountered in well Morne Diablo 34, Trinidad (section 3.2.4).

At least some of the overpressured formations in Trinidad are therefore likely to be underconsolidated. As Taiwan shows many similarities to Trinidad, this is probably also true for the former. Other overpressuring mechanisms such as smectite dehydration, hydrocarbon generation and aquathermal pressuring differ from rapid sedimentary loading in that they can only be effective at depth. From the limited data available, there is little evidence of smectite dehydration in the mud volcano areas studied. The presence of smectite in considerable proportions in the Trinidad muds (section 4.3.3) can be considered as evidence against the theory, as do the montmorillonitic clays of the New Zealand mud volcanoes (table 1.2). The Taiwan clays may be argued to have been "dehydrated", so that only illites are present now, but as the stratigraphic studies in the area have shown that the whole sedimentary sequence is free of smectite (section 4.3.4), this argues against the case.

Hydrocarbon generation would have a great effect on the behaviour of the source bed due to the presence of more than one pore fluid (and partial saturation in the presence of gas like methane). An investigation on the effect of gas bubbles on the undrained shear behaviour of soft sediments on the sea-bed has been carried out by Wheeler (1988). Wheeler found that, during undrained shear, the pore water pressures go up to a sufficiently high level that flooding of the bubbles occurs as the gas dissolves. Gas is a highly compressible fluid, and any gas generated in the sediment should dissolve, especially where high pore fluid pressures are being generated by tectonic loading, regardless of whether other mechanisms of overpressuring are taking place. Gas would therefore only be effective in overpressuring the sediment after gas "saturation" has occurred, as observed in some Gulf Coast formations (Swanson, 1984). The presence of hydrocarbons, particularly methane, in almost all reported mud volcano examples (table 1.2) cannot be ignored. Hydrocarbon generation can therefore contribute to overpressuring, but it is difficult to see how it can be a major process of overpressuring in either Taiwan or Trinidad, where sedimentary and tectonic loading play an important role.

Temperature would serve to enhance high pore fluid pressures in an undrained situation, but would also speed up the consolidation process in a permeable material (Daines, 1982). Two conditions can be envisaged whereby temperature would be effective in overpressuring sediment: if the temperature gradient increases suddenly and sharply, which is equivalent to sudden loading, or if the sediment is "undrained" and is being subjected to increasing pressure and temperature with burial. In the latter case, which is more usual in an area of normal geothermal gradients such as Trinidad (Rodrigues, 1985), the sediment would, by virtue of its undrained state, already be overpressured by sedimentary and/or tectonic loading. Temperature too can therefore enhance overpressures in a clay-rich sediment, but it must be operational in conjunction with other mechanisms of overpressuring.

There are further complications to sediment history caused by the generation of excess pore fluid pressures at depth (with no associated normal or shear deformation, as suggested by the above-mentioned hypotheses, see also section 2.2). The principle of effective stress states that, in the absence of shear deformation, changes in effective stress must be accompanied by changes in volume, otherwise, the effective stress does not change (Terzaghi, 1943). Therefore, if the pore fluid pressures in a sediment increase, and the volume of this sediment does not change (as required by the aquathermal pressuring and smectite dehydration hypotheses), the effective stresses do not decrease. If the volume is allowed to change, on the other hand, the sediment will swell in response to the increase in pore pressure. In that case, its subsequent undrained shear behaviour will be different to that of a sediment normally consolidated to the same effective stress. The sediment will be overconsolidated, with associated small, or decreasing pore pressures during undrained shear, depending on the degree of overconsolidation (see section 5.2.7). But this is assuming that no shear deformations occur in response to the generation of overpressures.

Perhaps most importantly, all mud volcanoes occur in areas of neotectonic activity, as do most other examples of sedimentary volcanism. This is particularly obvious for Taiwan, which is the site of a subduction zone with associated uplift and seismicity (fig. 3.11). In the Barbados Ridge complex, just north of Trinidad, the Carribean-North American convergence rates are estimated by modelling to be 2 - 3.6 km per million years (Moore and Biju-Duval, 1984). Trinidad itself occurs at a junction between the North and South American plates and the westward- dipping Atlantic ocean floor (Bertrand and Bertrand, 1985), although the area is less affected by earthquake activity than Taiwan. In both areas, therefore, thick regressive sedimentary sequences are subjected to huge tectonic stresses which are bound to play a vital role in overpressuring and deforming these sediments.

The experimental work conducted in this study has confirmed that shear stresses are an extremely effective process of pore fluid pressure generation in an undrained sediment. This applies to both underconsolidated and normally consolidated materials, i.e., materials which had not experienced higher effective stresses before they are sheared. The degree of pore pressure generation during undrained shear was found to be dependent on factors such as the composition of the material, the consolidation path and consolidation stress magnitude. It was postulated that the effect of undrained shear is particularly dramatic if the clay has an open structure which is destroyed by the action of tectonic shear; this produces pore fluid pressures in excess of the applied stress as stresses are transferred from the sediment "skeleton" to the pore fluids. Other processes of pore pressure generation by undrained loading briefly explored in this study are undrained horizontal compression (experimentally known as undrained extension), which is probably more applicable to sediments in an area of tectonic compression. This produces dramatic pore pressure increases, especially for the coarser-grained

sediments within a formation. Cyclic loading, produced by the action of earthquake activity and movements along faults, was also shown to produce excess pore fluid pressures.

An environment of tectonic compression, can therefore be regarded as the most favourable for generation of abnormally high pore fluid pressures. Rubey and Hubbert (1959) suggest that the overpressures in sediments in compressional areas lower the strength of these sediments, facilitating low angle thrusts and other shear distortions. This discussion has demonstrated that shear stresses themselves cause the generation of abnormally high pore fluid pressures, so that the two processes, shear deformations and pore fluid pressure generation complement each other.

7.4.3. Failure and Extrusion of Mud Volcano Clays

Naturally, as pore pressures increase, the effective stresses in the sediment decrease, and the sediment eventually fails. Failure alone, however, is not the only prerequisite for mud volcano formation. Other factors governing the extrusion of the clay were discussed in Chapter 2, and it was suggested that stress regime, parent bed rheology and the strength of the overburden should be considered.

Let us consider first the state of the sediment at failure. Some of the materials tested dilated at failure, whereas others contracted, sometimes, with continuing pore pressure increase. Some samples in all three materials reached critical state, where the material continued to deform with no further changes in effective stresses. Some evidence of the stress state of the parent bed can be derived from drilling data. Section 3.2.4 described the state of the Karamat formation in Trinidad during drilling. This produced highly pressured and sheared materials which shattered into small pieces upon removal from the core, showing the type of slickensided surface observed in the two Devil's Woodyard samples. This is assumed to be the "scaly clay" fabric observed in fine-grained sediments in compressional forearc environments such as Barbados, southern Mexico and Mariana, east of Japan (Moore et al, 1986) and in Timor (Audley-Charles, 1965); the fabric is often found in association with diapiric clays. The presence of these shear surfaces indicates that the material is at failure.

It is difficult to predict which beds will have the appropriate rheology for mud volcanic activity. It is assumed, however, that sediments consolidated to the very high stresses are less likely to be responsible for this type of phenomenon. This was shown by the lower A-values with increasing consolidation stress magnitude, particularly for the Lagon Bouffe materials, which also dilated at failure. It was suggested earlier in the discussion that the materials most likely to be involved in sedimentary volcanism are those with an open structure which breaks down during undrained shear, displaying "contractant" behaviour, with dramatic loss of strength at failure. The loose state of the sediment as it extrudes to the surface is attributed partly to remoulding during undrained shear, and partly to underconsolidation, which, from the above discussion, seems to be an important factor in preserving high voids ratios. It is also expected that considerable quantities of water are picked up by the muds on their way to the surface, making them softer and less viscous. Naturally, hydrocarbons present in the sediment also contribute to its rheology during extrusion. It was suggested in Chapter 1 that mud volcanoes are probably the surface expression of a more viscous, underlying diapir (Chapman, 1983; Barber et al, 1986). This is very likely to be the case, where the most mobile elements within a diapir, including hydrocarbons, extrude to the surface in the form of mud volcanoes.

The close association of mud volcanoes with folds and faults (table 1.2, Chapter 3) suggests that geological structures control their formation. As mentioned above, movement of the structures will enhance the deformation and overpressuring of the clays, continuously loading and unloading them. The failed clays then use the points of weakness in the overburden to dissipate their excess pore pressures; they can only be actively "intrusive" if their pore fluid pressures exceed the tensile strength of the overburden. It is possible that the size of the extrusion is dependent on the size of the structure, so that the large diapirs are more likely to be associated with major faulting and folding.

Both the geological and geotechnical observations made in this study therefore indicate that shear stresses, particularly in an area of tectonic compression, are a very important process of both overpressuring and extruding mud volcano clays.

CHAPTER 8

CONCLUDING REMARKS

There are very few detailed studies of the origin of sedimentary volcanism, and even fewer studies of the mechanical processes of soft sediment deformation at depth leading to the phenomenon - a field still relatively new to geologists. This work has incorporated geological investigations of mud volcanoes in the field and laboratory, with experimental work on high pressure soft sediment mechanics to provide a better understanding of the origin of overpressures and extrusion in a mud volcano area. Because of the numerous "unknowns" in this work, such as the exact origin of the source bed and its physical nature, many stones have been left unturned. It is hoped, however, that the study has shed some light on the type of phenomenon most likely to be responsible for the formation of mud volcanoes, namely, the application of high shear stresses to a thick layer of clay.

The main conclusions are:

- **Mud volcanoes are the product of sediment overpressuring and deformation. They are closely related to other examples of sedimentary volcanism, like diapirism.**

- **The type of environment most suited to the formation of mud volcanoes is an area of tectonic compression, with associated rapid sedimentation and structural deformation. This has been found to apply to both field areas: Trinidad and Taiwan.**

- **There is no "unique" mud volcano composition. The muds analysed contained variable quantities of silt and clay. It was not known how representative these materials were of the parent bed, but the identical results of the Taiwan mud analyses implied that very little contamination was taking place. It is assumed that the materials involved in sedimentary volcanism must be of fairly low permeability, or sealed in an impermeable sequence, to be able to sustain high pore fluid pressures.**

- **Underconsolidation is probably an important process in a mud volcano area due to the rapid sedimentation of fine-grained sediments. The low permeability of the sediments will encourage very slow consolidation and the preservation of an open structure; cementation would help to preserve this open structure. Overpressuring by rapid sedimentary loading will persist as long as the sediment is underconsolidated.**

- **Other mechanisms, such as hydrocarbon generation and temperature would enhance the high pore fluid pressures, but if they are solely responsible for the overpressures, the parent bed could behave in a dilatant manner during shear, causing the dissipation of these pressures.**

- **A very effective mechanism of overpressuring normally (or under-) consolidated sediments is tectonic compression, provided that the shear stresses are applied in an undrained situation - a condition satisfied by the thickness and low permeability of the sediments. Therefore, not only do high pore fluid pressures enhance tectonic deformations such as low angle thrust faults, tectonic stresses themselves produce high pore fluid pressures.**

- **If failure occurs in a "critical state" manner, the sediment subsequently deforms with no further changes in effective stresses. However, failure is more likely to occur in a non- critical state manner because of sediment inhomogeneity. In cemented, high porosity clays, undrained shear can be associated with dramatic pore pressure generation.**

- Factors affecting the undrained shear behaviour and failure of the sediments include;
- - magnitude of consolidation; the lower the voids ratio, the less likely it is to have the type of failure postulated for a mud volcano clay;
- - stress path during consolidation; the higher the shear stresses during consolidation, the more anisotropic the sediment structure, and the nearer it is to failure conditions.
- - material properties; the higher the plasticity, the weaker the clay;
- - cementation effects are very important. The breakdown of cement bonds in weak sediments is known to generate very high pore fluid pressures leading to failure.

- Once the sediment has failed, it would not necessarily behave "volcanically" unless overburden conditions allow it to do so. The overpressured clays could remain intact until a weakness in the overburden allows them to move. From the evidence presented in this work, structural weaknesses seem to be a prerequisite for mud volcano formation.

Suggestions for Future Research

The following improvements on the research are suggested:

Field Geology:

- individual mud volcano cones should be studied more closely. Their activity should be continuously monitored and they should be sampled seasonally, to explore the changes in mud composition and chemistry.

- well log and core studies in mud volcano areas are essential for a better understanding of the parent bed porosity and pore pressures and its relationship with ejected material.

- it would be of interest to explore fossil examples of sedimentary volcanism for comparison with modern examples.

Experimental:

- undrained shear experiments should be conducted on natural material if possible, or a synthetic material with an introduced cement.

- principal stress orientation should be explored to examine material anisotropy in compression and extension.

- finally, internal strain measurements of axial strain should be taken to be able to accurately determine stress-strain relationships during consolidation and shear. Also, an additional pore pressure probe in the middle of the sample may give a better indication of pore pressure conditions during undrained shear.

BIBLIOGRAPHY

Abikh (1948): From Jakubov et al (1976).

Addis, M. A. (1987): Mechanics of sedimentary compaction responsible for oilfield subsidence. PhD thesis, University of London.

Andersen, K., Pool, J., Brown, S. and Rosenbrand, W. (1980): Cyclic and static laboratory tests on Drammen clay. Proceedings of the American Society for Civil Engineers 106, GT5, p.499-529.

Arnold, R. and Macready G. (1965): Island-forming mud volcanoes in Trinidad. Bulletin of the American Association of Petroleum Geologists 40, p. 2748-2758.

Atkinson, J. and Bransby P. (1978): The Mechanics of Soils: An Introduction to Critical State Soil Mechanics. McGraw-Hill Book Company Ltd., London University Series in Civil Engineering, 375pp.

Atkinson, J., Richardson, D. and Robinson, P. (1987): Compression and extension of K_o normally consolidated kaolin clay. Journal of Geotechnical Engineering 113, p.1468-1480.

Audley-Charles, M. (1968): The geology of Portuguese Timor. Memoir of the Geological Society of London 4, p. 1-76.

Aoyagi K. and Kazama, T. (1969): Mineralogical study of Neogene sedimentary rocks in Taiwan by X-ray diffraction method. Technical Laboratory, Japan Petroleum Development Corporation, 6pp. (from Chou, 1971).

Barber, A., Tjokrosapoetro, S. and Charlton, T. (1986): Mud volcanoes, shale diapirs and melanges in accretionary complexes, Eastern Indonesia. Bulletin of the American Association of Petroleum Geologists 70, p. 1729-1741.

Barker, C. (1972): Aquathermal pressuring - the role of temperature in the development of abnormal pressure zones. Bulletin of the American Association of Petroleum Geologists 56, p. 2068-2071.

Barker, C. and Horsfield, B. (1982): Mechanical versus thermal cause of abnormally high pore pressures in shales. Bulletin of the American Association of Petroleum Geologists 66, p. 99-100.

Barr, K. and Saunders, J. (1965): An outline of the geology of Trinidad. Transactions of the 4th Carribean Geological Conference, Trinidad, published 1968, p. 1-10.

Beeby-Thompson, A. (1910): The Oilfields of Trinidad. The West Indian Committee Rooms, 15 Seething Lane, EC London, pamphlet 12. (From Higgins and Saunders, 1974).

Been, K. and Jeffries, M. (1985): A state parameter for sands. Geotechnique 35, p.99-112.

Bennett, R., Bryant, W. and Keller, G. (1977): Clay fabric and geotechnical properties of selected submarine sediment cores from the Mississippi delta. NOAA Professional Paper 9. (from Isaac and Shaw, 1984).

Berner, H., Ramberg, H. and Stephanson, O. (1972): Diapirism in Theory and Experiment. Tectonophysics 15, p. 197-218.

Berry, F. (1973): High fluid potential in the California Coast Ranges and their tectonic significance. Bulletin of the American Association of Petroleum Geologists 57, p.1219-1249.

Bertrand A., and Bertrand W., (1985): Plate tectonic evolution of the southeast Carribean. Transactions of the First Geological Conference of the Geological Society of Trinidad and Tobago, p. 242-260.

Biju-Duval, B., Le Quellec P., Mascle, A., Renard, V., Valery, P. (1982): Multibeam bathymetric survey and high resolution seismic investigations on the Barbados Ridge Complex (Eastern Carribean): A key to the Knowledge and interpretation of an accretionary wedge. Tectonophysics 86, p. 275-304.

Biot M. and Ode H. (1965): Theory of gravity instability with variable overburden and compaction. Geophysics 30, p. 213-227.

Birchwood, K. (1965): Mud volcanoes in Trinidad. Institute of Petroleum Review 19, p. 164-167.

Bishop, A. (1976): The influence of system compressibility on the observed pore pressure response to an undrained change in stress in saturated rock. Geotechnique 26, p.372-375.

Bishop, A. and Henkel, D. (1962): The measurement of soil properties in the triaxial test. Published Edward Arnold Ltd., 2nd edition, 227pp.

Bishop, A., Kumpaley, N. and El-Ruwayih, A.(1975): The influence of pore water tension on the strength of clay. Philosophical Transactions of the Royal Society of London. A. Mathematical and Physical Sciences 278 (1286), p.511-554.

Bishop, A. and Skinner, A. (1977): The influence of high pore water pressure on the strength of cohesionless soils. Philosophical Transactions of the Royal Society of London 284, p. 97-130.

Bishop, A., Webb, D. and Skinner A. (1965): Triaxial tests on soil at elevated cell pressures. Proceedings of the 6th International Conference on Soil Mechanics and Civil Engineering, p.170-174.

Bishop, R. (1978): Mechanism for emplacement of piercement diapirs. Bulletin of the American Association of Petroleum Geologists 62, p.1561-1581.

Bjerrum L. (1954): Geotechnical properties of Norwegian marine clays. Geotechnique 4, p.49.

Bjerrum, L., Simons, N. and Torblaa, I. (1958): The effect of time on the shear strength of soft marine clays. Proceedings of the Brussels Conference on Earth Pressure Problems 1, p. 148-158. (From Lambe and Whitman, 1979).

Bower, T. (1951): Mudflow Occurrence in Trinidad, BWI. Bulletin of the American Association of Petroleum Geologists 35, p.908- 912.

Bower, T.(1965): Geology of Texaco Forest Reserve Field, Trinidad, W.I. Transactions of the 4th Carribean Geological Conference, Trinidad, p. 75-86.

Bredehoeft, J. and Hanshaw, B. (1968): On the maintenance of anomalous fluid pressures: I. Thick sedimentary sequences. Bulletin of the Geological Society of America 79, p. 1097-1106.

Breen, N. and Silver, E. (1986); Structural styles of an accretionary wedge south of the island of Sumba, Indonesia, revealed by Seamarc 2 side-scan sonar. Bulletin of the Geological Society of America 97, p.1250-1261.

Brindley, G. (1980): X-Ray mineral analysis of clays. In Crystal Structures of Clay Minerals and their X-ray Identification, ed. Brindley, G. and Brown, G., published by the Mineralogical Society, London, p. 411-438.

British Standards BS1377 (1975): Methods of test of soils for civil engineering purposes, BSI.

Brown, G. (1961): The X-Ray identification and crystal structures of clay minerals. Published by Mineralogical Society, London.

Brown, G. and Brindley, G. (1980): X-Ray diffraction procedures for clay mineral identification. In Crystal Structures of Clay Minerals and their X-ray Identification, ed. Brindley, G. and Brown, G., published by the Mineralogical Society, London, p. 305-360.

Brown, K. and Westbrook, G. (1987): The tectonic fabric of the Barbados Ridge Accretionary Complex. Marine and Petroleum Geology 4, p.71-81.

Bruce, C. (1973); Pressured shale and related sediment deformation: mechanism for development of regional contemporaneous faults. Bulletin of the American Association of Petroleum Geologists 57, p.878-886.

Bruce, C. (1984): Smectite dehydration - its relation to structural development and hydrocarbon accumulation in Northern Gulf of Mexico Basin. Bulletin of the American Association of Petroleum Geologists 68, p.673-683.

Burland, J. (1987): MSc. Soil Mechanics course lectures, Imperial College London.

Burst, J. (1969): Diagenesis of Gulf Coast clayey sediments and its possible relation to petroleum migration. Bulletin of the American Association of Petroleum Geologists 53, p.73-93.

Carr-Brown, B. and Frampton, J. (1979): An outline of the stratigraphy of Trinidad. 4th Latin American Geological congress of the Geological Society of Trinidad and Tobago, p.7-20.

Carstens, H. and Dypvik, H. (1981): Abnormal formation pressure and shale porosity. Bulletin of the American Association of Petroleum Geologists 65, p.344-350.

Casagrande A. (1948): Classification and identification of soils. Transactions of the American Society for Civil Engineers 113, p. 901.

Chan, Y. (1964): Preliminary study on the geothermal gradients and formation or reservoir pressures of oil and gas fields in Northern Taiwan. Petroleum Geology of Taiwan 3, p. 127-139.

Chapman, R. (1972): Clays with abnormal interstitial pore fluid pressures. Bulletin of the American Association of Petroleum Geologists 56, p.790-795.

Chapman, R. (1974): Clay diapirism and overthrust faulting. Bulletin of the Geological Society of America 85, p.1597-1602.

Chapman, R. (1980): Mechanical versus thermal cause of abnormally high pore pressures in shales. Bulletin of the American Association of Petroleum Geologists 64, p.2179-2183.

Chapman, R. (1983): Petroleum Geology. Elsevier books.

Chen, H. (1987): The stability and mechanical behaviour of colluvium slopes in Taiwan. PhD thesis, University of London.

Chiu, H. and Johnston, I. (1984): The application of critical state concepts to the Melbourne mudstone. 4th Annual New Zealand Conference on Geomechanics, Perth 1.

Chou, J. (1971): A preliminary study of the stratigraphy and sedimentation of the mudstone formations in the Tainan area, southern Taiwan. Petroleum Geology of Taiwan 8, p.187-219.

Chou, J. (1973): Sedimentology and Palaeogeography of the Upper Cenozoic system of Western Taiwan. Proceedings of the Geological Society of China 16, p.111-143.

Chou, J. (1980): Stratigraphy and Sedimentology of the Miocene in Western Taiwan. Petroleum Geology of Taiwan 17, p.33-52.

Coward, M. (1981): Diapirism and gravity tectonics: report f a tectonic studies group conferences held at Leeds University 25-26 March, 1980. Journal of Structural Geology 3, p.89-95.

Cunningham-Craig, E. (1905); General report on the oilfields of the Southern Anticline, Trinidad. Council Paper 119. (From Higgins and Saunders, 1974).

Dailly, G. (1976): A possible mechanism relating progradation, growth faulting, clay diapirism and overthrusting in a regressive sequence of sediments. Bulletin of Canadian Petroleum Geology 24, p.92-116.

Daines, S. (1982): Aquathermal pressuring and geopressure evaluation. Bulletin of the American Association of Petroleum Geologists 66, p.931-939.

Dickey, P., Shiram, C. and Paine, W. (1968): Abnormal pressures in deep wells in Southwestern Louisiana. Science 160, p.609-615.

Dickinson, G. (1953): Geological Aspects of abnormal reservoir pressures in the Gulf Coast of Louisiana. Bulletin of the American Association of Petroleum Geologists 37, p.410-432.

Dixon, J. (1975): Finite strain and progressive deformation in models of diapiric structures. Tectonophysics 28, p.89-124.

Freeman, P. (1968): Exposed Middle Tertiary mud diapirs and related features in South Texas. Memoir of the American Association of Petroleum Geologists 8 (Diapirism and Diapirs), p. 162-182.

Fertl, W. (1971): A look at abnormally pressured formations in the USSR. Society of Petroleum Engineers paper 3613.

Fertl, W. (1972); Worldwide occurrence of abnormal formation pressures, Part I. Society of Petroleum Engineers paper 3844.

Fertl, W. (1973): Significance of shale gas as an indicator of abnormal pressures. Society of Petroleum Engineers paper 4230.

Fertl, W. (1976): Abnormal Formation Pressures: implications to exploration, drilling and production of oil and gas reservoirs. Development in Petroleum Science 2. Elsevier Scientific Publications Company, 382 pp.

Gansser, A. (1960): Uber sclammvulkane und salzdome. Vierteljahrsschrift Naturf. Ges. Zurich 105, p. 1-46.

Gens, A. (1982): Stress-strain and strength characteristics of a low plasticity clay. PhD thesis, University of London.

Gibbs, R. (1965): Error due to segregation in quantitative clay mineral X-ray diffraction mounting techniques. American Mineralogist 50, p.714-751.

Gibson, R. (1958): The progress of consolidation in a clay layer increasing in thickness with time. Geotechnique 8, p.171-182.

Gill, J. (1972): Shale mineralogy and overpressure: some case histories of pressure detection worldwide utilising consistent shale mineralogy parameters. Society of Petroleum Engineers paper 3890.

Gilreath, J. (1968): Electric log characteristics of diapiric shale. Memoir of the American Association of Petroleum Geologists 8 (Diapirism and Diapirs), p.137-144.

Goff, J.(1983): Hydrocarbon generation and migration from Jurassic source rocks in the E. Shetland Basin and Viking Graben of the northern North Sea. Journal of the Geological Society of London 140, p. 445-474.

Gretener, P. (1985): The National Conference on Earth Science, Banff, November 5-9, 1984: Geopressures and hydrocarbon occurrences. Bulletin of Canadian Petroleum Geology 33, p.269- 273.

Hall, P., Astill, D. and McConnell, J. (1985): Thermodynamic and structural aspects of the dehydration of smectites in sedimentary rocks. Presented at conference on: Features and Problems of Mineral Diagenesis in Hydrocarbon Reservoirs, organised by the Clay Minerals Group of the Mineralogical Society, London and the Petroleum Exploration Society of Great Britain.

Hanshaw, B. and Bredehoeft, J. (1968): On the maintenance of anomalous fluid pressures, II; source layer at depth. Bulletin of the Geological Society of America 79, p.1107-1122.

Hanshaw, B. and Zen, E. (1965): Osmotic equilibrium and overthrust faulting. Bulletin of the Geological Society of America 76, p.1379-1387.

Harkins, K. and Baugher, J. (1969): Geological significance of abnormal formation pressures. Journal of Petroleum Technology 21, p.961-968.

Harrison, J. (1944): Mud volcanoes on the Makran Coast. Geographical Journal 103, p.180-181.

Hedberg, H. (1974): Relation of methane generation to undercompacted shales, shale diapirs and mud volcanoes. Bulletin of the American Association of Petroleum Geologists 58, p.661- 673.

Henderson, G. (1976): Petroleum geology. In: The Geology of Greenland, ed. Escher, A. and Wall, W., p. 489-506.

Herring, E. (1973): Estimating abnormal pressures from log data in the North Sea. Society of Petroleum Engineers paper 4301.

Higgins, G. (1959): Seismic velocity data from Trinidad, B.W.I. and comparison with the Carribean area. Geophysics 24, p.580-597.

Higgins, G. and Saunders, J. (1964): Geological notes on the newly-formed island in Erin Bay off Chatham, August 1964. Geological Report 478, Geological Department, Texaco Trinidad, Inc., Pointe-a-Pierre, 18pp.

Higgins, G. and Saunders, J. (1967): Report on 1964 Chatham Mud Island, Erin Bay, Trinidad, W.I. Bulletin of the American Association of Petroleum Geologists 51, p. 55-64.

Higgins, G. and Saunders, J. (1974): Mud volcanoes - their nature and origin. Contributions to the Geology and Palaeobiology of the Carribean and Adjacent Areas. Verh. Naturfosch. Ges. Basel 84, p. 101-152.

Hight, D., Jardine, R. and Gens, A. (1987): The behaviour of soft clays. In: Embankments on Soft Clays, Special Publication Bulletin of the Public Works Research Centre, Ministry of Environment, Physical Planning and Public Works, Athens, Chapter 2, p. 33-159.

Ho, C. (1975): an introduction to the geology of Taiwan, explanatory text of the geologic map of Taiwan. Published by the Ministry of Economic Affairs, Republic of China, Taipei, Taiwan, 153 pp.

Ho, C. (1982): Tectonic evolution of Taiwan, explanatory text for the tectonic evolution of Taiwan. Published by the Ministry of Economic Affairs, Republic of China, Taipei, Taiwan, 126 pp.

Hofman (1949): Southern Trinidad Bouger Anomaly Map (scale 1:100,000).

Hottman, C., Smith, J. and Purcell, W. (1979): Relationship among earth stresses, pore pressure and drilling problems offshore Gulf of Alaska. Journal of Petroleum Technology 31, p.1477-1484.

Hower, J. (1981): Shale diagenesis. In: Clays and the reservoir geologist - short course notes, ed. Longstaffe, F., Mineralogical Association of Canada, p.60-77. (From Shaw, 1987).

Hsieh, S. (1972): Subsurface geology and gravity anomalies of the Tainan and Chungchan structures of the coastal Plain of southwestern Taiwan. Petroleum Geology of Taiwan 10, p.323-338.

Hubbert, M. and Rubey, W. (1959): Role of fluid pressure in mechanisms of overthrust faulting: I. Mechanics of fluid-filled porous solids and its application to overthrust faulting. Bulletin of the Geological Society of America 70, p.115-166.

Humphrey, W. (1963): Sedimentary volcanism in Eastern Mexico and Northern Colombia. Bulletin of the Geological Society of America 74, p.125-128.

Isaac, K. and Shaw, H. (1984): Overpressuring in mudrocks: an introduction and review with special reference to mudrock petrology. A report for Schlumberger Cambridge Research Ltd., 39pp.

Jakubov, A., Ali-Zade, A. and Zeinalov M. (1971): Mud volcanoes of the Azerbaijan SSR. Publishing House of the Academy of Sciences of the Azerbaijan SSR, Baku, 256pp.

Jardine, R. (1985): Investigations of pile-soil behaviour, with special reference to the foundations of offshore structures. PhD thesis, University of London.

Johnston, I. and Novello, E. (1985): Cracking and critical state concepts for soft rocks. Proceedings of the 11th International Conference on Soil Mechanics and Foundation Engineering, San Francisco, p.515-518.

Jones, M. and Addis, M. (1985): On changes in porosity and volume during burial of argillaceous sediments. Marine and Petroleum Geology 2, p.247-253.

Jones, M. and Addis, M. (1986): The application of stress path and critical state analysis to sediment deformation. Journal of Structural Geology 8, p.575-580.

Jones, P. (1980): Role of geopressure in the hydrocarbon and water system. American Association of Petroleum Geologists Studies in Petroleum Geology 10, p.207-216.

Kalinko, M. (1967): Mud volcanoes as a source of information on the composition of hydrocarbons, their quantity, and conditions of occurrence. Soviet Geology 7, p.86-96.

Kamhawi, K. (1986): The effective stress behaviour of a clay under undrained cyclic loading. MSc thesis, University of Manchester.

Karig, D. (1986): Effects of physical properties and mechanical state on the deformation of porous sediments. Private report.

Kerr, P., Drew, J. and Richardson, D. (1970): Mud volcano clay, Trinidad, W.I. Bulletin of the American Association of Petroleum Geologists 54, p. 2101-2110.

Kidwell, A. and Hunt, J. (1958): Migration of oil in recent sediments at Pedernales, Venezuela. In Habitat of Oil, ed. Weeks, L., p.790-817. (From Skempton, 1972).

Kugler, H. (1933): Contribution to the knowledge of sedimentary volcanism in Trinidad. Journal of the Institute of Petroleum Technology of Trinidad 19, p.743-772.

Kugler, H. (1938): Nature and significance of sedimentary volcanism. Science of Petroleum (Oxford University Press), p.297-299.

Kugler, H. (1959): Geological Map of Trinidad (scale 1:100,000).

Kugler, H. (1965): Sedimentary volcanism. transactions of the 4th Carribean Geological Conference, Trinidad, p.11-13.

Kugler, H. (1978): Volcanism, sedimentary. Encyclopaedia of Sedimentology (ed. Fairbridge and Bourgeas), p.854-857.

Kvenvolden, K. (1985): Comparison of marine gas hydrates in sediments of active and passive continental margins. Marine and Petroleum Geology 2, p.65-71.

Lambe T. and Whitman, R. (1979): Soil Mechanics, SI version. series in soil engineering (John Wiley and Sons, Inc.), 553pp.

Langseth, M., Westbrook, G. and Hobart, M. (1988): Geophysical survey of a mud volcano seaward of the Barbados Ridge accretionary complex. Journal of Geophysical Research 93, p.1049-1061.

Lavayssee, D. (1813): Voyage aux iles de la Trinite, Tobago et Margarita; et en diverses parties de Venezuela en Amerique de Sud. Paris 2tt 8 vol. (From Higgins and Saunders, 1974).

Leddra, M. (1989): PhD thesis on the behaviour of chalk at high pressure, to be submitted to the University of London.

Leddra, M. and Jones, M. (1989): Steady state flow during undrained loading of the chalk. To be presented at the International Chalk Symposium, Brighton, September, 1989.

Lee, K. and Farhoomand, I. (1967): Compressibility and crushing of granular soil in anisotropic triaxial compression. Canadian Geotechnical Journal 4, p.68-86.

Lee, K. and Seed, H. (1967): Drained strength characteristics of sands. Proceedings of the American Society for Civil Engineers, SM6, p. 117-141.

Leonard, R. (1983): Geology and hydrocarbon accumulations, Columbus Basin, offshore Trinidad. Bulletin of the American Association of Petroleum Geologists 67, p.1081-1093.

Leroueil, S., Tavenas, F. and Le-Bihan, J. (1983): Proprietes caracteristiques des argiles de l'est du Canada. Canadian Geotechnical Journal 20, p.681-705.

Leroueil, S. and Vaughan, P. (1989): The importance of structure in natural soil. In press.

Lewin, P. (1985): Reversible behaviour in cyclic undrained triaxial tests on clay till. Proceedings of the Conference on Clay Tills, Edinburgh, p. 99-101.

Lin, C. (1965): The naming of the Akungtein Formation with discussion of the origin of the fossils in the mud ejected from the Kunshuiping mud volcanoes near Ch'iao, Kaohsiunghsien, Taiwan. Petroleum Geology of Taiwan 4, p.107-145.

Lindberg, P., Riise, R. and Fertl, W. (1980): Occurrence and distribution of overpressures in the Northern North Sea area. Society of Petroleum Engineers paper 9339.

Liu, K (1969): Preliminary report on the study of petroleum exploration of the mudstone area in Tainan-Kaohsiung. Unpublished report to Chinese Petroleum Company. (From Chou, 1971).

Lupini, J., Skinner, A. and Vaughan, P. (1981): The drained residual strength of cohesive soils. Geotechnique 31, p.181-213.

Magara, K. (1968): Compaction and migration of fluids of Miocene mudstone, Nagaoka Plain, Japan. Bulletin of the American Association of Petroleum Geologists 52, p. 2466-2501.

Magara, K. (1971): Permeability considerations in generation of abnormal pressures. Journal of the Society of Petroleum Engineers paper 11, p.236-242.

Magara, K. (1975): Re-evaluation of montmorillonite dehydration as the cause of abnormal pressures and hydrocarbon migration. Bulletin of the American Association of Petroleum Geologists 59, p.212 -302.

Magara, K. (1975): Importance of the aquathermal pressuring effect in the Gulf Coast. Bulletin of the American Association of Petroleum Geologists 59, p.2037-2045.

Magara, K. (1978): The significance of the expulsion of water in oil-phase primary migration. Bulletin of Canadian Petroleum Geology 26, p. 123-131.

Martin, G. (1972): Abnormal high pressure and environment of deposition. Society of Petroleum Engineers paper 3846.

Mascle, A., Bonhold, B. and Renard, V. (1973); Diapiric structures off the Niger Delta. Bulletin of the American Association of Petroleum Geologists 57, p.1672-1678.

Mascle, A., Lajat, D. and Nely, G. (1979): Sediment deformation linked to subduction and to argiliokinesis in the southern Barbados Ridge from multi-channel seismic surveys. 4th Latin-American Geological Congress, Trinidad and Tobago, p. 837-882.

McClelland, B. (1967): Progress of consolidation in delta front and pro-delta clays of the Mississippi River. Marine Geotechnique, ed. Richards, A., University of Illinois Press, p. 22-40. (From Skempton, 1970).

McIver, R. (1982): Role of naturally-occurring gas hydrates in sediment transport. Bulletin of the American Association of Petroleum Geologists 66, p.789-792.

McManus, J. and Tate, A. (1986): Mud volcanoes and the origin of certain chaotic deposits in Sabah, East Malaysia. Proceedings of the Geological Society of Malaysia Bulletin 19, p.193-205.

Meissner, F. (1980): Examples of abnormal fluid pressures produced by hydrocarbon generation (Abstract). Bulletin of the American Association of Petroleum Geologists 64, p.7-49.

Meissner, F. (1982): Abnormal pressures produced by hydrocarbon generation and maturation and their relation to migration and accumulation. Bulletin of the Corpus Christi Geological Society 1982, p.4-6. (From Isaac and Shaw, 1984).

Mesri, G., Adachi, K. and Ullrich, C. (1976): Pore pressure response in rock to undrained change in all-round stress. Geotechnique 26, p. 317-330.

Milliken, K., Land, L and Loucks, R. (1981): History of burial diagenesis from isotopic geochemistry, Frio formation, Brazoria County, Texas. Bulletin of the American Association of Petroleum Geologists 65, p.1397-1413.

Moore, J. and Biju-Duval, B. (1984): Tectonic synthesis, deep sea drilling project leg 78A: Structural evolution of offscraped and underthrust sediment, Northern Barbados Ridge complex. Initial Reports of the Deep Sea Drilling Project, Volume LXXVII, p. 601- 621.

Moore, J., Roeske, S., Lundberg, N., Schoonmaker, J., Cowan, D., Gonzales, E. and Lucas, S. (1986): Scaly fabrics from deep sea drilling project cores from forearcs. Geological Society of America Memoir 166, p.55-73.

Morgan, J. (1961): Genesis and palaeontology of the Mississippi River mudlumps, Part I: Mudlumps at the mouths of the Mississippi River. Geological Bulletin no. 35, published by the Department of Conservation, Louisiana Geological Survey, 116pp.

Morgan, J., Coleman, J. and Gagliano, S. (1968): Mudlumps: Diapiric structures in Mississippi river sediments. Memoir of the American Association of Petroleum Geologists 8 (Diapirism and Diapirs), p.145-161.

Musgrave, A. and Hicks, W (1968): Outlining shale masses by geophysical methods. Memoir of the American Association of Petroleum Geologists 8 (Diapirism and Diapirs), p. 122-136.

Nadeau, P., Wilson, M., McHardy, W. and Tait, J. (1984): Interparticle diffraction: a new concept of interstratified clays. Clay Mineralogy 19, p. 751-769.

Nettleton, L. (1949): Geophysics and geology of oil finding. Geophysics 14, p.273-289.

O'Brien, G. (1968): Survey of Diapirs and Diapirism. Memoir of the American Association of Petroleum Geologists 8 (Diapirism and Diapirs), p.1-9.

Ohtsuki, H., Nishi, K., Okamoto, T. and Tanaka, S. (1981): Time- dependent characteristics of strength and deformation of a mudstone. Proceedings of the Symposium on Weak Rock, Tokyo, 1, p.119-124.

Ovnatanov, S. and Tamarazyan, G. (1970): Thermal studies in subsurface structural investigations, Apsheron Peninsula, Azerbaijan, USSR. Bulletin of the American Association of Petroleum Geologists 54, p.1677-1685.

Parry, R. (1971): Undrained shear strength in clays. Proceedings of the 1st Australian-New Zealand Conference on Geomechanics, p.11-15.

Persad, K. (1985): Presentation of a new tectonic map of Trinidad and Tobago. Transactions of the 1st Geological Conference of the Geological Society of Trinidad and Tobago, p. 217-226.

Pierce, J. and Siegel, F. (1969): Quantification of clay mineral studies of sediments and sedimentary rocks. Journal of Sedimentary Petrology 39, p.187-193.

Plumley, W. (1980): Abnormally high fluid pressure - survey of some basic principles. Bulletin of the American Association of Petroleum Geologists 64, p.414-422.

Powers, M (1967): Fluid release mechanisms in compacting marine mudrocks and their importance in oil exploration. Bulletin of the American Association of Petroleum Geologists 51, p.1240-1254.

Pritchett, W. (1978): Physical properties of shales and possible origin of high pressures. Society of Petroleum Engineers paper 7506.

Ramberg, H. (1972): Theoretical models of density stratification and diapirism in the earth. Journal of Geophysical Research 77, p.877-889.

Rehm, B. (1972): Worldwide occurrence of abnormal formation pressures II. Society of Petroleum Engineers paper 3845.

Ridd, M. (1970): Mud volcanism in New Zealand. Bulletin of the American Association of Petroleum Geologists 54, p.601-616.

Rieke, H. and Chilingarian, G. (1974): Compaction of Argillaceous Sediments. Developments in Sedimentology 16. Elsevier scientific Publishing Co., 424pp.

Rodrigues, K. (1985): Thermal history modelling in petroleum exploration: examples from Southern Trinidad. 1st Geological Conference of the Geological Society of Trinidad and Tobago, p.217-226.

Roscoe, K. and Burland, J. (1968): On the generalised stress- strain behaviour of 'wet' clay. Engineering Plasticity, eds. Heyman, J. and Leckie, F., Cambridge University Press, p.535-609.

Rubey, W. and Hubbert, M. (1959): Role of fluid pressure in overthrust faulting: II. Overthrust belt in a geosynclinal area of Western Wyoming in the light of the fluid pressure hypothesis. Bulletin of the Geological Society of America 70, p.167-206.

Santoso, M. (1976): Inventarisasi kenampkan geyala panasbumi: Daerah Husatenggara Timur (Portugese Timor). Report to Subdirektorat Volkanologi Seksi Penyelielikan Panasbutri.

Saunders, J. (1974): Trinidad. Special Publication of the Geological Society of London 4 (Mesozoic-Cenozoic orogenic belts, ed. Spencer, A.), p.671-682.

Schofield, A. and Wroth, C. (1968): Critical state soil mechanics. McGraw-Hill Book Co. Ltd.

Schwerdtner, W. and Troeng, B. (1978): Strain distribution within arcuate diapiric ridges of silicone putty. Tectonophysics 50, p.13-28.

Seed, H. and Lee, K. (1966): Liquefaction of saturated sands during cyclic loading. Proceedings of the American Society for Civil Engineers 92, SM6, p.105-134.

Sharp, J. (1983): Permeability controls on aquathermal pressuring. Bulletin of the American Association of Petroleum Geologists 67, p.2057-2061.

Shaw, H. (1987): Clays and their effects on source and reservoir rocks. Joint Association for Petroleum Exploration Courses (UK), course notes 61.

Shih, T. (1963): Types of the active mud volcanoes in Taiwan: graduation thesis of the MC of the Tokyo University of Education, 83pp.

Shih, T. (1967): A survey of the active mud volcanoes in Taiwan and a study of their types and the character of the mud. Petroleum Geology of Taiwan 5, p.259-311.

Shouldice, D. (1971): Geology of the Western Canadian continental shelf. Bulletin of Canadian Petroleum Geology 19, p.405-436.

Skempton, A. (1943): Notes on the compressibility of clays. Quarterly Journal of the Geological Society of London 100, p. 119-135.

Skempton, A. (1953): Soil mechanics in relation to geology. Proceedings of the Yorkshire Geological Society 29, p.33-62.

Skempton, A. (1954): The pore pressure coefficients A and B, Geotechnique 4, p. 143-147.

Skempton, A. (1964): Long term stability of clay slopes. Geotechnique 14, p.77.

Skempton, A. (1970): The consolidation of clays by gravitational compaction. Quarterly Journal of the Geological Society of London 125, p.373-411.

Skempton, A. and Bjerrum, L. (1957): A contribution to the settlement analysis of foundations on clay. Geotechnique 7, p.168.

Skinner, A. (1975): The effect of high pore water pressure on the mechanical behaviour of sediments. PhD thesis, University of London.

Snead, R. (1964): Active mud volcanoes in Baluchistan, West Pakistan. Geographical Review 4, p.546-560.

Smith, J. (1973): Shale compaction. Society of Petroleum Engineers paper Journal 12 (Transactions vol. 253), p.12-22.

Spinks, R. (1970): Offshore drilling operations in the Gulf of Papua. Australian Petroleum Exploration Association Journal 10, p. 108-114. (From Chapman, 1972).

Stiffe, A. (1874): On the mud craters and geological structure of the Makran Coast. Quarterly Journal of the Geological Society 30, p.50-53.

Stride, A., Belderson, R. and Kenyon, N. (1982): Structural grain, mud volcanoes and other features on the Barbados Ridge Complex revealed by Gloria side-scan sonar. Marine Geology 49, p.189-196.

Strong, S. (1931): Ejection of fault breccia in the Waimata Survey District, Gisborne, New Zealand. New Zealand Journal of Science and Technology 12, p.257-267. (From Ridd, 1970)

Suter, H. (1954): The general and economic geology of Trinidad, BWI. Colonial Geology and Mineral Resources (Her Majesty's Stationary Office, London).

Swanson, R. (1984): Gulf Coast geopressure: Old questions, new answers. Society of Petroleum Engineers paper 13090.

Takahashi, M. (1981): Transient and cyclic behaviour of a sandy clay. PhD thesis, University of London

Tanner, W. and Williams, G. (1968): Model diapirs, plasticity and tension. Memoir of the American Association of Petroleum Geologists 8 (Diapirism and Diapirs), p.10-15.

Tavenas, F., and Leroueil, S. (1977): Effects of stresses and time on yielding of clays. Proceedings of the 9th International Conference on Soil Mechanics and Foundation Engineering, I, p.319-326.

Tchalenko, J. (1968): The evolution of kink bands and the development of compression textures in sheared clays. Tectonophysics 6, p. 159-174

Terzaghi, K. (1943): Theoretical Soil Mechanics, John Wiley and Sons, New York.

Tkhostov, B. (1963): Initial rock pressures in oil and gas deposits. Translated by Ledward, R. Pergamon Press, 118 pp.

Wall, G. and Sawkins, J. (1860): Report on the geology of Trinidad; or part I of West Indian Survey. Memoirs of the Geological Survey, Longman, Green-Longman and Roberts. (From Higgins and Saunders, 1974).

Ward, Penman and Gibson, (1955): Stability of a bank on a thin peat layer. Geotechnique 5, p.154-163.

Westbrook, G. and Smith, M. (1983): Long decollements and mud volcanoes: Evidence from the Barbados Ridge Complex for the role of high pore fluid pressure in the development of an accretionary complex. Geology 11, p.279-283.

Westbrook, G., Mascle, A. and Biju-Duval, B. (1984): Geophysics and structure of the Lesser Antilles forearc. In: Initial Reports of DSDP 78A, Biju-Duval, B. and Moore, J..

White, D. 91955): Violent mud volcano eruption of Lake City Hot Springs, North-east California. Bulletin of the Geological Society of America 66, p.1109-1130.

Williams, P., Pigram, C. and Dow, D. (1984): Melange production and the importance of shale diapirism in accretionary terrains. Nature 309, p.145-146.

Wilson, C. (1965): The Los Bajos Fault. Transactions of the 4th Carribean Geological Conference, p. 87-89.

Wilson, C. and Birchwood, K. (1965): The Trinidad mud volcano island of 1964. Proceedings of the Geological Society of London 1626, p.169-174.

Yefremova, A. and Zhizhchenko B. (1975): Occurrence of crystal hydrates of gases in the sediments of modern marine basins. Academy of Science USSR Dollady, Earth Science Section 214, p. 219-220. (From McIver, 1982).

Young, A. and Low, P. (1965): Osmosis in argillaceous rocks. Bulletin of the American Association of Petroleum Geologists 49, p.1005-1007.

Zelikson, A. (1987): Large centrifuge models for video monitoring of diapirs growth. 28th US Symposium on Rock Mechanics, Tuscon, p. 763-770.

APPENDICES

APPENDIX 1. PARTICLE SIZE DISTRIBUTION METHODOLOGY

The method employed for calculating the particle size distribution of the mud volcano clays is the hydrometer method (Test 7(D) in BS1377, 1975). This is briefly described below:

An air-dried sample weighing 75g was treated with 150 ma of 20% solution of hydrogen peroxide. When the frothing was over the sample was heated gently until the solution reduced to 50 ml. The mud contained considerable quantities of oil which was difficult to remove completely. It was sometimes necessary to add more hydrogen peroxide during heating until the frothing subsided.

The sample was then filtered through Whatman 50 filter paper on a Hirsch funnel under a vacuum. Distilled water was added until the soil was cleared of the peroxide. The sample was oven-dried and weighed, placed in a stoppered bottle with 100 ml of sodium hexametaphosphate solution and placed in a mechanical shaking device for at least 4 hours. It was then wet-sieved through a 63 micron sieve with distilled water; the material passing through was transferred to a 1000 ml cylinder and made up to 1000 ml with distilled water.

The cylinder was shaken and the sedimentation analysis initiated using a calibrated hydrometer which measures the settlement of the particles using Stoke's Law (BS1377). Readings were taken after 30 sec., 1 min., 2 min., 4 min., 30 min., 1 hour, 2 hour, 4 hour, then twice daily.

Material retained on the 63 micron sieve was oven-dried and weighed, then dry sieved using the 425, 300 and 150 micron sieves. The sieves were shaken by hand for 10 minutes. The percentages of the total sample were calculated according to BS1377.

The original sample was sieved through the 425 micron sieve to remove the coarse fragments which appeared to be chips from exotic blocks. This was the maximum size recommended for Atterberg limits tests (Appendix 3) and it is also used for the samples tested in the high pressure triaxial cell. The possible inaccuracy introduced is minimal as the >425 micron fraction constituted a small percentage of the total sample (see section 4.2).

APPENDIX 2. X-RAY DIFFRACTION OF THE CLAY

A2.1. Separation and Pretreatment

25g of clay was placed in a beaker containing 250cc of distilled water. The beaker was placed in an ultrasonic bath for 15 minutes to allow dispersion of the clays. No calgon was used for this procedure (nor any type of chemical pretreatment) for minimum chemical disturbance. The water-clay mixture was placed in a 1000cc cylinder which was topped up with distilled water. This was shaken a few times and left to settle for 3 hours and 50 minutes at a room temperature of 20° C. The top 5cm, comprising the < 2u fraction, was then carefully removed with a pipette and placed in a bottle.

A2.2. Mounting Technique

The centrifugation method involved placing 2ml of the clay-water mixture in a water-filled centrifuge tube with a ceramic plate at its base. This was centrifuged for 5 minutes at 1000 r.p.m. and the plate was then removed and dried in a desiccator. The suction method was that used by Shaw (1987). The water-clay mixture was shaken thoroughly and poured over a ceramic plate fixed onto a beaker under a vacuum. There can never be exact control over the amount of clay mounted, but with experience, just enough clay was poured to ensure that the ceramic plate is totally covered.

A2.3. Pretreatment of Slides

Four runs were performed on each sample; these included oriented (untreated), glycolated and two heated runs. The same slide was used by the author to ensure repeatability of the results. After the oriented run, the ceramic plate was placed in a desiccator with ethylene glycol; this was left in a 60°C oven overnight (Brown, pers. comm., 1987). The two heats chosen were 335°C and 550°C (Shaw, 1987). The heat was applied for 1 hour (no difference was detected between 1 hour and 6 hours by the author).

A2.4. X-Ray Diffraction Run

The runs were performed at 40 kV and 20 mA. The speed was 1°/ minute, at 1000 CPS (but sometimes 400 CPS were necessary to enhance the peaks). The range covered was 2 - 45° 2O.

A2.5. Equipment Specifications

The X-ray diffraction machine used was a Phillips PW 1050/25, with a Cu K alpha radiation tube. The goniometer was model PW 1965/40. The radiation was directed through a 1 degree slit.

A2.6. Calculation Methods

Two calculation methods were used to estimate the clay mineral percentages. These are methods 2 and 3 in Pierce and Siegel (1969). Method 2 involved measuring the areas under the 17A (smectite), 10A (illite) and 7A (kaolinite + chlorite) reflections on the glycolated trace. The area of the 10A peak is multiplied by four and the 7A peak by two. The relative proportions are then calculated. Method 3 involved comparing the height of the 10A peak before and after heat-treatment. Illite and smectite are assumed to reflect X-rays with equal intensity at 10A. The 10A and 7A peaks were compared directly to calculate the percentages of illite and kaolinite + chlorite.

APPENDIX 3. ATTERBERG LIMITS METHODOLOGY

A3.1. Liquid Limit

The fall-cone test (2(A) in BS1377) was employed. This is briefly described below:

After wet sieving through a 425 micron sieve and air drying, a sample weighing 200g was mixed with water until it formed a paste. It was left to stand in a sealed plastic bag overnight. It was then remixed for 10 minutes and water was added. The soil was packed in the cup, ensuring that no air bubbles were trapped, then the cone (specifications in BS1377) was lowered until it touched the flat surface of the soil. The cone was released for 5 seconds and a reading of the penetration taken. This was repeated after remixing and adding more of the soil; if the two readings are within 0.1 mm of each other, a moisture content was taken. More water was added and the process repeated 5-6 times within the 15-25 mm penetration range. The penetration reading was plotted against moisture content; the moisture content corresponding to 20 mm penetration is the liquid limit.

A3.2. Plastic Limit

A sample weighing 20g from material passing through the 425 micron sieve (as above) was mixed with distilled water until plastic enough to shape into a ball. This was divided into 8 equal parts. Each part was threaded into 6 mm diameter and rolled with the hand 10 times to a diameter of 3 mm. This was repeated until the soil lost enough moisture for longitudinal and transverse cracks to appear when the thread was 3 mm in diameter. The thread was quickly transferred to an air-tight container and a moisture content was taken of 4 threads together. If the two moisture contents were within 0.5% of each other, the result was accepted.

APPENDIX 4. SAMPLE PREPARATION FOR TRIAXIAL TESTING

The muds collected were already in a remoulded state (i.e. they had no cements or bonds). They had to be consolidated to a strength which would withstand high pressure testing. The following procedure was followed:

A4.1. Sieving

The clay was wet sieved with distilled water using the 425 micron sieve used in the Atterberg Limits tests (Appendix 3). This sieve separated out the coarse fragments in the clay which constituted only a small percentage (see table 4.1).

A4.2. Mixing Under Vacuum

The clay was mixed with more distilled water to a Liquidity Index value of 2 (see section 4.5). This was placed in a simple mixer with two slowly rotating blades; a vacuum was then applied. The clay was allowed to mix for 3-4 days to ensure full saturation.

A4.3. Consolidation 1

The clay was scooped out and placed into a large 25 cm diameter oedometer (used by Gens, 1982). It was distributed evenly on the base of the oedometer under water to ensure that no air bubbles are trapped in the clay. It was then loaded with a small weight which was doubled at the end of each consolidation stage; drainage was allowed from both ends. After consolidation to a maximum of 1 MPa, the "cake" of clay was removed and sealed. (The Devil's Woodyard clay was consolidated to 300 kPa, and the Lagon Bouffe an Taiwan clays to 1 MPa).

A4.4. Consolidation 2

Further consolidation of the samples was necessary for two main reasons:

a) It was found that the clays were still too soft after consolidation at 1 MPa. Volume loss with consolidation during the test would have led to membrane failure (Appendix 5) at the higher stresses.

b) The material was not always enough to produce a "cake" of sufficient thickness to provide samples with the right height for triaxial testing (76 mm, Bishop and Henkl, 1962). It was possible to superimpose plugs and consolidate them further into one sample.

A simple cylindrical oedometer was therefore designed to produce the samples for triaxial testing. It was driven by air pressure on a piston. A diameter of 42 mm was chosen to be able to trim the sample down to the required diameter of 38 mm (Bishop and Henkl, 1962). Again, the consolidation increment was doubled until the maximum stress was reached (2.45 MPa); drainage was allowed from both ends. The sample was left in the cylinder for two weeks.

(In both oedometers, porous stones were used at the top and bottom, separated from the sample by filter paper; the porous stones were de-aired by boiling in distilled water. The sides of the oedometers were greased to reduce friction during settlement).

A4.5. Preparation for a Triaxial Test

The sample was trimmed using the standard trimming apparatus described in Bishop and Henkl (1962). The heights and diameters were deliberately made slightly above the standard 38 mm x 76 mm when the sample was going to undergo considerable volumetric strains before it was sheared. It was measured and weighed and moisture contents were taken. A wet filter strip was wrapped around the sample (to speed up consolidation - Bishop and Henkl, 1962); this touched the de-aired porous stones (separated by filter paper on either end of the sample). Two pieces of membrane were placed on both ends to ensure that the outer membranes were not pierced by the joins between porous stones and the sample. Two 130 by 38 mm neopreme membranes were tested for leaks, then placed on the sample using the techniques described by Addis (1987). It was found that two membranes were necessary to prevent membrane failure during the test. The membranes were sealed at the top and bottom caps of the triaxial machine by O-rings (fig. A5.1).

APPENDIX 5. THE HIGH PRESSURE TRIAXIAL APPARATUS

Two high pressure triaxial machines were used during the course of the testing programme: the triaxial cell in the Imperial College Soils Laboratory, described in Addis (1987), and the Wyckeham Farrance design in the Reservoir Dynamics Laboratory at University College London (fig. A5.1). The two machines are very similar. As the former was only used for 2 out of the 14 tests performed, the reader is referred to Addis (1987) for its precise specifications. The Wyckeham Farrance apparatus is described here.

The testing apparatus is divided into the following components (fig. A5.2; plate A5.1):

1) A Wyckeham Farrance 250 kN stepless compression machine (WF 10080) capable of displacement rates between 5 and 0.00001 mm/min.

2) A Wyckeham Farrance high pressure (0-70 MPa) steel cell (WF 40030) with a counterbalanced ram to prevent the upward thrust of cell pressure. This has two bottom inlet/outlet ports for the pressurising fluid and two top ports for complete de-airing of the cell and ram chamber. It is pressure sealed by a steel ring secured to the base by 8 steel bolts (fig. A5.1). The inside of the cell consists of a pedestal and top cap - both of which are 38 mm in diameter. These were modified to allow pore pressure measurements by making fine (1 mm diameter) central holes connecting to high pressure steel tubes leading to two pressure transducers (plate A5.1). The base of the cell contains 8 ports allowing transducer connections for internal measurements of the sample.

3) The cell is pressurised using a Wyckeham Farrance automatic pressure controller (WF 40070) capable of maintaining pressures of up to 70 MPa with an accuracy of +/- 0.25%. This is made up of a self-balancing hydraulic system which runs on castor oil. The cell pressure is measured using a pressure transducer at the base of the cell and checked with the dial at the front of the pressure controller.

4) The drainage system (plate A5.1) was designed by Tony Goldsmith, Reservoir Dynamics Laboratory, University College, based on the system used by Addis (1987). It has the facility of draining both ends of the sample into separate volume gauges which can be pressured by the same or separate back pressures. It also has two Wyckeham Farrance hand rams used to de-air the system with distilled, de-aired water. The drainage path used in the tests is depicted in fig. A5.2.

The back pressure is supplied by British Oxygen Company nitrogen cylinders and regulated by Air Products valves. High pressure valves on either side of the pore pressure transducers were supplied by Nova Swiss, and the low pressure ball valves in the drainage system were supplied by Tescom.

Six measurements were taken during the tests:

i) Load, measured by an external Tedea load cell (model 100) with a maximum capacity of 250 kN and an accuracy of +/- 0.075%.

ii) Cell pressure, measured by a Shape Instruments pressure transducer (model no. SP 1082), with a range of 0-70 MPa and an accuracy of +/- 0.1%.

iii), iv) Top and bottom pore pressures, measured by Maywood Instruments pressure steel transducers (model no. P-102), with a range of 0-70 MPa and an accuracy of +/- 0.1%.

v) Volume change, measured with an LSC axial displacement transducer with a range of 0-26.9 mm. It is attached to the 50 cc I.C. volume gauge with an accuracy of +/- 0.01 cc (see Addis, 1987 for further details).

vi) Axial displacement of the ram, measured by an MPE axial displacement transducer (type HS). This is externally fixed on the ram (plate A5.1). It has a range of 0-26 mm and an accuracy of +/- 0.1%.

The gauges were energised with 5 volts, using an RS Components bench power supply (model 611-420). This maintained a constant power within +/- 0.002 volts.

The datalogging system used a CIL unit and a BBC master micro- computer. It was capable of any logging intervals above 5 seconds. The software was written by Dave Toll at the Imperial College Soil Mechanics Laboratory where the system is in use by some of the researchers.

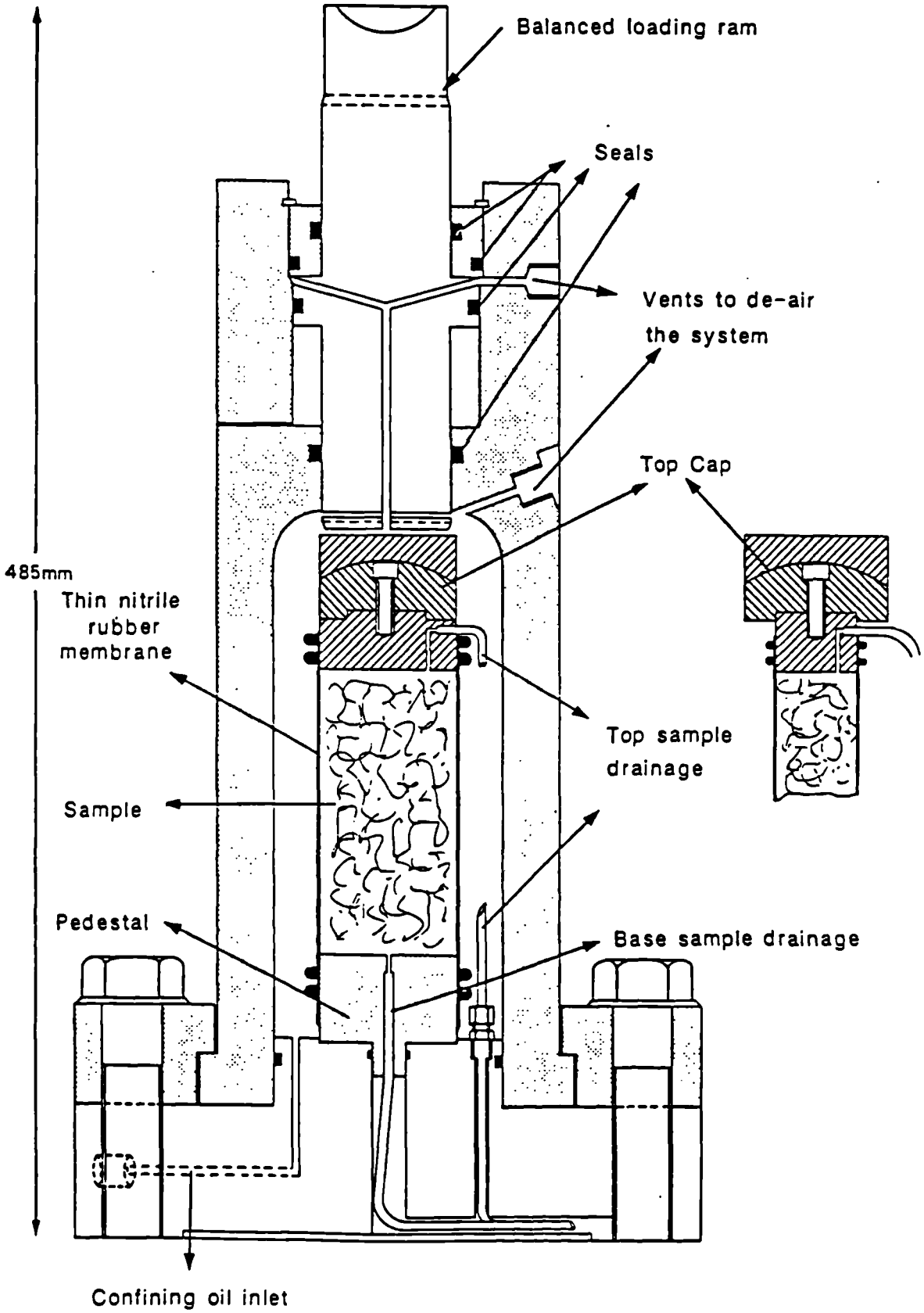

Fig. A 5.1 The high pressure triaxial cell

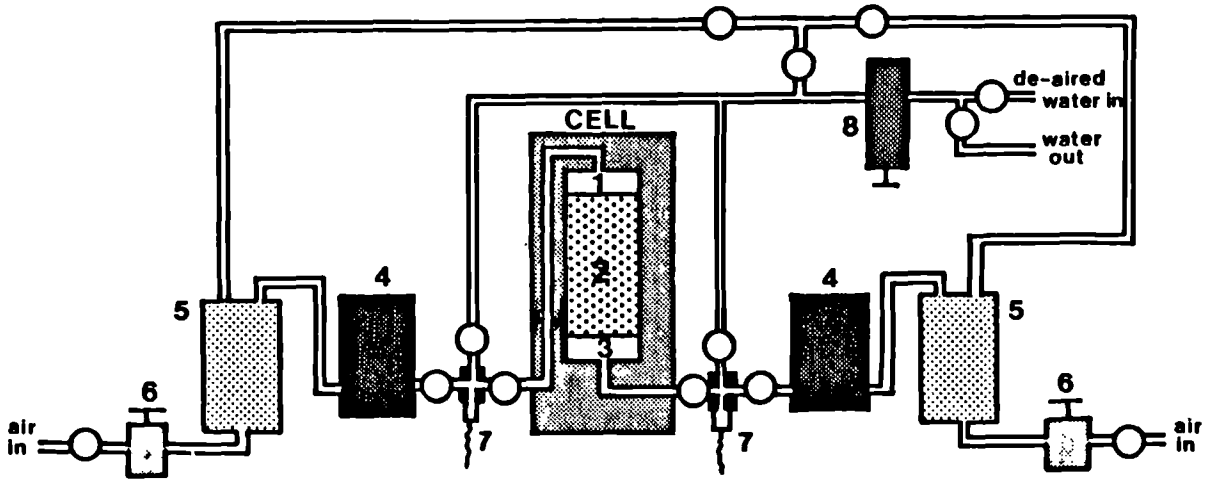

1 Top cap
2 Sample
3 Bottom drainage line
4 Back pressure regulator
5 Volume gauge
6 Air pressure regulator
7 Transducer block
8 Hand ram

Fig. A5.2 The components of the high pressure triaxial apparatus

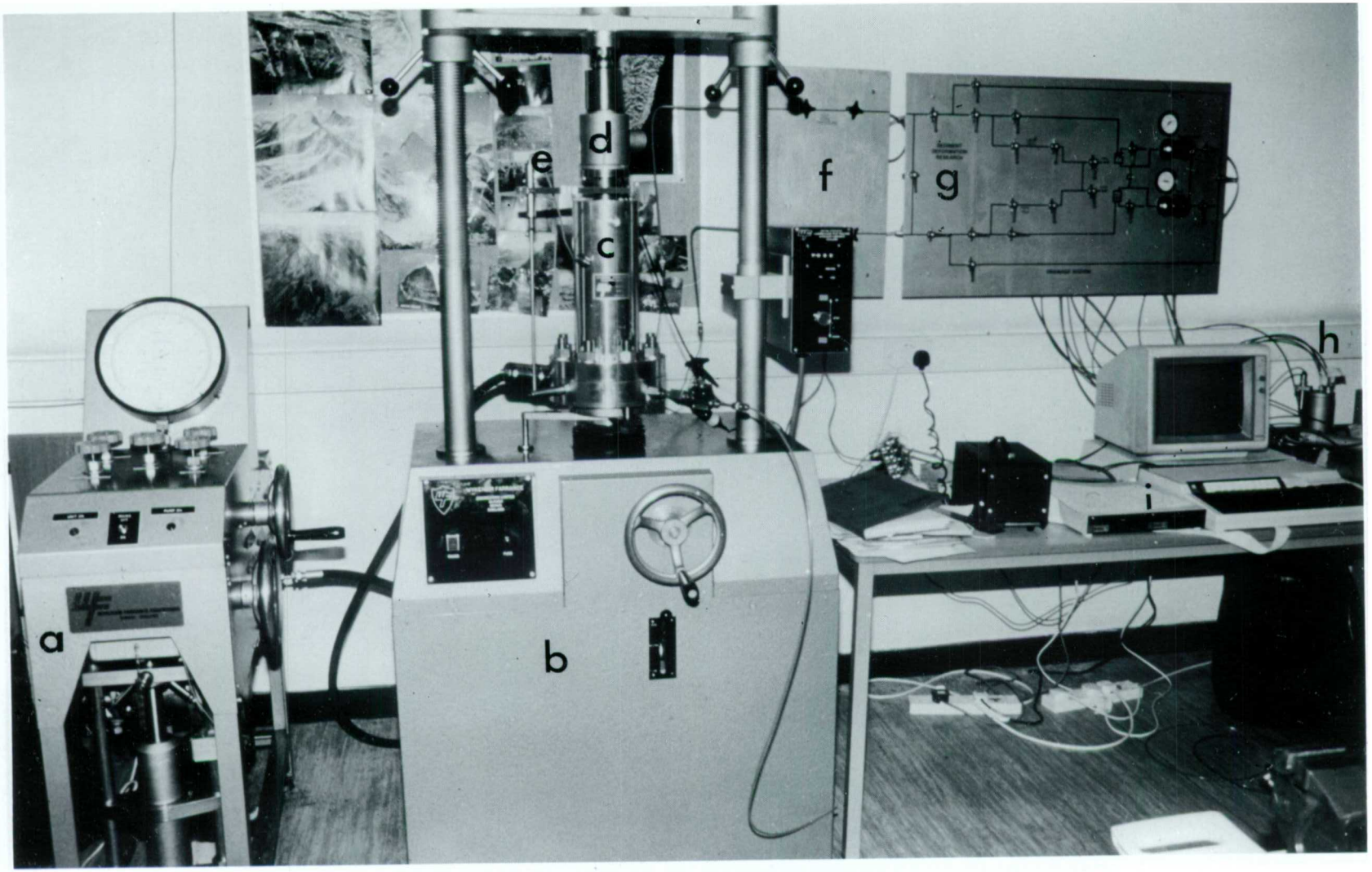

Plate A5.1 The high pressure triaxial apparatus: a. constant cell pressure control system; b. load frame; c. high pressure triaxial cell; d. load cell; e. axial displacement transducer; f. drainage board with top and bottom pore pressure transducers; g. drainage board with de-airing system and back pressure control valves leading to the volume gauge; h. volume gauge; i. data-logging system.

APPENDIX 6. EXPERIMENTAL METHODOLOGY

The samples were assumed to be fully saturated, although some evaporation would have been expected to occur whilst trimming the sample to the desired size. The samples were consolidated in the triaxial cell at 0.3 MPa upwards in double increments up to 5 MPa mean effective stress; the back pressure used was 1 MPa. 5 MPa was chosen as it was double the pre-consolidation pressure in the piston (2.45 MPa) to minimise the effects of unloading on the behaviour of the sample and ensure that the sample is normally consolidated (as opposed to overconsolidated).

Two stress paths were chosen after isotropic consolidation at a mean effective stress of 5 MPa:

1) further isotropic consolidation at different effective stresses, followed by undrained shear.

2) anisotropic consolidation at a stress ratio K of 0.6. This had to be achieved in two stages as the stress path was beginning from 5 MPa on the isotropic line. The stress ratio was initially 0.55 until the K-line was intersected. The sample was then allowed to consolidate at a stress ratio of 0.6 to the required mean effective stress, then sheared undrained.

Filter paper was placed around all the samples to speed up the consolidation. Drainage was allowed from the bottom in the Trinidad samples to facilitate monitoring of the pore pressure gradient across the sample throughout the test, but the author was obliged to drain the sample from both ends for the Taiwan samples to speed up the tests, which were particularly slow during K-consolidation due to the high clay content of the material.

Axial displacement rates used were slow enough to ensure that no pore pressure gradient above 2% of the cell pressure was created in the sample. In the K-consolidation stage, they varied between 0.0001 and 0.0005 mm/min., according to the permeability of the material. During the undrained shear stage, axial displacement rate of 0.002 mm/min. was used, with the exception of LB3 and LB6, which were sheared at 0.004 mm/min.

A Note on Height Loss During Isotropic Consolidation

The axial displacement transducer is external (plate A5.1) and can only measure sample height changes when the ram is in contact with the sample. Height loss during isotropic consolidation (with no shear component) was therefore estimated by comparing the distance between the ram and the sample before and after isotropic consolidation. In an isotropic sample, height loss would be expected to be twice diameter loss; in fact, the samples lost 3-4 times as much height as diameter. The average diameter to height loss ratio was 0.24 for the Taiwan clays, whereas for Lagon Bouffe clays, it was 0.36.